

การประเมินเสถียรภาพความลาดและผลกระทบต่อ การออกแบบบ่อเหมืองดินขาว จังหวัด
ระนอง ประเทศไทย



บทคัดย่อและแฟ้มข้อมูลฉบับเต็มของวิทยานิพนธ์ตั้งแต่ปีการศึกษา 2554 ที่ให้บริการในคลังปัญญาจุฬาฯ (CUIR)
เป็นแฟ้มข้อมูลของนิสิตเจ้าของวิทยานิพนธ์ ที่ส่งผ่านทางบัณฑิตวิทยาลัย

The abstract and full text of theses from the academic year 2011 in Chulalongkorn University Intellectual Repository (CUIR)
are the thesis authors' files submitted through the University Graduate School.

วิทยานิพนธ์นี้เป็นส่วนหนึ่งของการศึกษาตามหลักสูตรปริญญาวิศวกรรมศาสตรมหาบัณฑิต

สาขาวิชาวิศวกรรมทรัพยากรธรณี ภาควิชาวิศวกรรมเหมืองแร่และปิโตรเลียม

คณะวิศวกรรมศาสตร์ จุฬาลงกรณ์มหาวิทยาลัย

ปีการศึกษา 2558

ลิขสิทธิ์ของจุฬาลงกรณ์มหาวิทยาลัย

SLOPE STABILITY ASSESSMENT AND ITS EFFECT ON PIT DESIGN AT KAOLIN MINE,
RANONG PROVINCE, THAILAND

Mr. Somboun Vang



A Thesis Submitted in Partial Fulfillment of the Requirements
for the Degree of Master of Engineering Program in Georesources Engineering

Department of Mining and Petroleum Engineering

Faculty of Engineering

Chulalongkorn University

Academic Year 2015

Copyright of Chulalongkorn University

Thesis Title SLOPE STABILITY ASSESSMENT AND ITS EFFECT
 ON PIT DESIGN AT KAOLIN MINE, RANONG
 PROVINCE, THAILAND

By Mr. Somboun Vang

Field of Study Georesources Engineering

Thesis Advisor Pipat Laowattanabandit, Ph.D.

Accepted by the Faculty of Engineering, Chulalongkorn University in Partial
Fulfillment of the Requirements for the Master's Degree

..... Dean of the Faculty of Engineering
(Associate Professor Supot Teachavorasinskun, D.Eng.)

THESIS COMMITTEE

..... Chairman
(Associate Professor Dawan Wiwattanadate, Ph.D.)

..... Thesis Advisor
(Pipat Laowattanabandit, Ph.D.)

..... Examiner
(Assistant Professor Tanate Srisirojanakorn, Ph.D.)

..... External Examiner
(Associate Professor Pornkasem Jongpradist, Ph.D.)

สมบุญ หวัง : การประเมินเสถียรภาพความลาดและผลกระทบต่อารออกแบบบ่อเหมืองดินขาว จังหวัดระนอง ประเทศไทย (SLOPE STABILITY ASSESSMENT AND ITS EFFECT ON PIT DESIGN AT KAOLIN MINE, RANONG PROVINCE, THAILAND)
 อ.ที่ปรึกษาวิทยานิพนธ์หลัก: ดร. พิชิตน์ เหล่าวัฒนบัณฑิต, 183 หน้า.

วิทยานิพนธ์ฉบับนี้นำเสนอการวิเคราะห์เสถียรภาพของความลาดด้วยวิธีแบบจำลองเชิงตัวเลขรูปทรงหลายโมเดลของความลาดได้ถูกสร้างขึ้นและทำการวิเคราะห์ด้วยโปรแกรมไฟไนต์ดิฟเฟอเรนซ์ (FLAC3D) ในขั้นตอนของการวิเคราะห์เสถียรภาพความลาดนั้น ปัจจัยที่สำคัญบางอย่างเป็นที่ต้องการที่เพิ่มเติมในการสร้างโมเดล ได้แก่ คุณสมบัติของวัสดุธรณี รวมไปถึงขนาดและรูปร่างของความลาด เพื่อหาค่าคุณสมบัติของวัสดุธรณี จึงได้มีการดำเนินการทดสอบต่างๆ ในห้องปฏิบัติการธรณีกลศาสตร์หลายตัวอย่าง ซึ่งเป็นการค่อนข้างยากที่จะทำการทดสอบกับหินผุเหล่านี้อย่างถูกต้อง ความแข็งแรงของวัสดุในพื้นที่ทำการศึกษานั้นมีค่าต่างกันค่อนข้างสูง ค่าของแรงยึดเหนี่ยว มีค่าเปลี่ยนแปลงตั้งแต่ 13.7 ไปจนถึง 178.1 kPa และค่าของมุมเสียดทานภายใน เริ่มจาก 3 องศา ไปจนถึง 57.6 องศา

สำหรับการเปรียบเทียบ บ่อเหมืองจำนวน 3 รูปแบบที่มีความแตกต่างกันในแง่ของมุมชันหน้าลาดและมุมชันโดยรวมได้ถูกออกแบบและวิเคราะห์ หลังการวิเคราะห์อย่างละเอียดพบว่า บ่อเหมืองรูปแบบที่หนึ่ง ที่มีความสูงของหน้าพักเท่ากับ 4 เมตร มุมชันหน้าลาดเท่า 40 องศา และมุมชันโดยรวมเท่ากับ 28 องศา เป็นบ่อเหมืองที่เหมาะสมที่สุดที่แนะนำให้เป็บบ่อเหมืองสุดท้ายของบ่อย่อย MF-10 ถึงแม้ว่าจะได้ปริมาณแร่สำรองต่ำที่สุดสำหรับการทำเหมือง แต่รูปแบบนี้จะประกันความปลอดภัยสำหรับการดำเนินงานทั้งในระยะสั้นและระยะยาว อย่างไรก็ตามยังคงมีแง่มุมอื่นๆ ที่สำคัญจะต้องมีการศึกษาเพิ่มเติม และนั่นคือผลกระทบของกระบวนการกัดกร่อนที่มีต่อเสถียรภาพความลาดของบ่อเหมือง ซึ่งเห็นได้ชัดในบ่อเหมืองเหมืองอื่นๆในพื้นที่

ภาควิชา วิศวกรรมเหมืองแร่และปิโตรเลียม ลายมือชื่อนิสิต

สาขาวิชา วิศวกรรมทรัพยากรธรณี ลายมือชื่อ อ.ที่ปรึกษาหลัก

ปีการศึกษา 2558

ACKNOWLEDGEMENTS

I would like to express my acknowledgement to the financial support provided by the ASEAN University Network Southeast Asia Engineering Education Development Network Scholarship (AUN-SEED/Net) of the Japan International Cooperation Agency.

I am also greatly indebted to my advisors, Dr. Pipat Laowattanabandit, for the guidance, his helpful, and valuable suggestions and especially for his patience, and the moral support he has given to me throughout this research.

I wish to express my gratitude towards Assoc. Prof. Dr. Dawan Wiwattanadate, Assist. Prof. Dr. Tanate Sririrojanakorn, and Assoc. Prof. Dr. Pornkasem Jongpradist the thesis committee, for their encouragement, useful suggestion and advice.

I am grateful to Mr. Yuthakarn Suwanawate, Mr. Ngo Tan Phong and Mr. Chunla Cheng at the Department of Civil Engineering, Faculty of Engineering, Chulalongkorn University, for helping me on the Geotechnical Laboratory testing and advice the calculation process of result from the testing.

I am appreciative to my friends in Thailand for their insight and ideas during our discussions.

At last, I would like to acknowledgement my beloved parents from the bottom of my heart for their encouragement, advice and mental support. Thank you for always being on my side.

CONTENTS

	Page
THAI ABSTRACT	iv
ENGLISH ABSTRACT	v
ACKNOWLEDGEMENTS.....	vi
CONTENTS.....	vii
LIST OF FIGURES	xi
LIST OF TABLES.....	xv
CHAPTER I INTRODUCTION	1
1.1 Background.....	1
1.2 Location of study.....	2
1.3 Local climate	2
1.4 General geology of research area	2
1.5 Objectives	2
CHAPTER II LITERATURE REVIEW.....	7
2.1 Deterministic method	7
2.2 Numerical modeling	8
2.3 Finite difference computer software	9
2.3 Mohr-Coulomb Model	11
2.4 Open pit slope design	12
2.5 Basic bench geometry.....	15
2.6 Pit design by 3D block model method	17
2.7 Inverse distance weighting technique.....	18
2.8 Stripping ratio.....	20

	Page
2.9 Related research.....	20
CHAPTER III RESEARCH METHODOLOGY	23
3.1 The procedure flowchart of this research.....	23
3.2 Desk data collection	24
3.3 Site investigation	24
3.4 Geotechnical laboratory testing.....	25
3.4.1 Natural moisture content (ASTM D 2216)	25
3.4.2 Particle size grading by sieve analysis (ASTM D 422)	28
3.4.3 Direct shear test (ASTM D 3080)	28
3.4.4 Unconfined compression test (ASTM D 2166)	29
3.4.5 Unconsolidated Undrained Triaxial Test (ASTM D 2664).....	29
3.5 Pit slope and open pit design.....	31
3.5.1 Topo map and drill holes data preparation	33
3.5.2 Loading and creation of data base.....	36
3.5.3 Creation of solid zone.....	37
3.5.4 Creation the 3D block model	39
3.5.5 Block grade estimation.....	39
3.5.6 Pit design.....	40
3.6 Pit slope stability analysis	42
3.6.1 Creation SGM, and assigning GMP for the final Pit slope design Ver.1, 2, and 3	43
3.6.2 Creation SGM, and assigning GMP for the cross-section of Pit Ver. 1, 2, and 3.	47

	Page
3.6.3 Creation SGM, and assigning GMP for the assuming bench of trial pit slope (Short term mining slope).....	48
CHAPTER IV RESULTS AND DISCUSSIONS	50
4.1 Results of site investigation and Laboratory testing.....	50
4.2 Results of open pit design	53
4.2.1 Drill-hole data analysis	53
4.2.2 Geological model	55
4.2.3 3D block model, its grade, and resource estimation.....	58
4.2.4 Open pit design and reserves estimation	61
4.3 Results of pit slope stability analysis	68
4.3.1 Pit slope stability analysis for the final Pit slope design Ver.1, 2, and 3	69
4.3.2 Pit slope stability analysis for the cross-section model of Pit Ver.1, 2, and 3.....	71
4.3.3 Pit slope stability analysis for the assuming bench height and face slope angle of trial pit slope (Short term mining slope).....	85
CHAPTER V CONCLUSIONS AND RECOMMENDATIONS	88
5.1 Conclusions.....	88
5.2 Recommendations	89
REFERENCES.....	91
APPENDIX I Drill-hole data and its analysis.....	94
APPENDIX II Slope stability analysis for the final Pit design Ver.1, 2, and 3	108
APPENDIX III Slope stability analysis for the cross-section model	118
APPENDIX IV Slope stability analysis for the assuming model	126

	Page
APPENDIX V Geotechnical laboratory testing results	140
APPENDIX VI Command used in FLAC3D for solved FOS	177
VITA	183



LIST OF FIGURES

Figure 1. 1 The kaolin mine location	3
Figure 1. 2 Research target area and the sub-pit in this kaolin mine.....	4
Figure 1. 3 Geological map of MRD mine (GDP, 2010a)	5
Figure 1. 4 Some Quartz veins at Pit MF-10	6
Figure 2. 1 Example of acceptable FOS value (Priest & Brown, 1983).....	7
Figure 2. 2 Minimum dimension for slope analysis model.....	10
Figure 2. 3 Mohr-Coulomb failure criterion (Soltani, 2015).....	12
Figure 2. 4 Potential impacts of slope steepening (Read & Stacey, 2009).....	14
Figure 2. 5 Geometry change in pit creation (Hustrulid, Kuchta, & Martin, 2013)	15
Figure 2. 6 Pit wall terminology (Read & Stacey, 2009)	16
Figure 2. 7 Cumulative frequency distribution of measured bench face angles (call, 1986)	17
Figure 2. 8 Diagrammatic view of a 3D block matrix (Crawford & Davey, 1979).....	18
Figure 2. 9 Block estimation by extending the grade computed in its center	19
Figure 2. 10 Summary the slopes of stability analysis method (Wenbing, 2008)	21
Figure 2. 11 Roughly summary the pit design steps (Appianing & Mireku-Gyimah, 2015)	22
Figure 3. 1 The procedure flowchart of this research.....	23
Figure 3. 2 Topo map show an expect the pit boundary to extend	26
Figure 3. 3 The southwestern slope at Pit MF-10, photo on May 2015	27
Figure 3. 4 Circular slope failure due to the erosional process in the rainy season at Pit MF-10, Photo on September 2015.	27
Figure 3. 5 Apparatus used for direct shear test.....	28

Figure 3. 6 Apparatus used for unconfined compression test	29
Figure 3. 7 Apparatus used for UU Triaxial test.....	30
Figure 3. 8 Remolded specimens used in unconfined compression and UU triaxial test.	30
Figure 3. 9 A benches design of Pit Ver.1 (unit is metre and deg.)	31
Figure 3. 10 A benches design of Pit Ver.2 (unit is metre and deg.)	32
Figure 3. 11 A benches design of Pit Ver.3 (unit is metre and deg.)	32
Figure 3. 12 Top view the topo map of Pit MF-10 used for pit design	35
Figure 3. 13 Flowchart of the steps for creation necessary files in MS software.	37
Figure 3. 14 Digitized zone section in 2D (Grid set EW, Plane No. North1100046)	38
Figure 3. 15 Solid model of other rocks and ore body	38
Figure 3. 16 Size of 3DBM used in pits design (10 m x 10 m x 4 m)	41
Figure 3. 17 3DBM of three solid zones.....	41
Figure 3. 18 Top view of Pit design Ver. 1	42
Figure 3. 19 Comparison the different benches design SGM of Pit Ver.1, 2, and 3 (unit is metre)	43
Figure 3. 20 Example of analysis while SGM's width = 1 m, $C = 21.2$ kPa, $\phi = 26.2^\circ$, and obtained of FOS = 1.75	45
Figure 3. 21 Example of analysis while SGM's width = 75 m, $C = 21.2$ kPa, $\phi =$ 26.2°, and obtained of FOS = 1.75	45
Figure 3. 22 The SGM dimension shape of analysis for final Pit design Ver.1	46
Figure 3. 23 The SGM dimension shape of analysis for final Pit design Ver.2.....	46
Figure 3. 24 The SGM dimension shape of analysis for final Pit design Ver.3.....	47
Figure 4. 1 Typical plane failure on kaolin slope at pit MF-2C. (May 2, 2015).....	51

Figure 4. 2 Experience of erosional on kaolin slope due the affected from rain-flow.	51
Figure 4. 3 Particle size distribution of block sample no. BMRD-03	52
Figure 4. 4 Coarse-grained size of quartz in kaolin mine, photo at the floor of Pit MF- 10	52
Figure 4. 5 Histogram plotting show the distribution grade of kaolin.....	54
Figure 4. 6 Cumulative curve plotting the distribution grade of kaolin.....	54
Figure 4. 7 2D view a comparison DH data assay and composited grade of kaolin	55
Figure 4. 8 Overview of drill-hole and topography in 3D model.....	56
Figure 4. 9 Top view of drill-hole location	57
Figure 4. 10 Top view the results of estimated block from IDW method for kaolin	59
Figure 4. 11 3D view the results of estimated block from IDW method for kaolin	60
Figure 4. 12 3D view of final Pit designed Ver.1	62
Figure 4. 13 Top view of Pit Ver.1 and its 3D blocks distribution grade	62
Figure 4. 14 3D view of final Pit designed Ver.2	63
Figure 4. 15 Top view of Pit Ver.2 and its 3D blocks grade distribution	63
Figure 4. 16 3D view of final Pit designed Ver.3.....	64
Figure 4. 17 Top view of Pit Ver.3 and its 3D block grade distribution	64
Figure 4. 18 Cross-section 1-1 of Pit Ver.1 and its vertical 3D block grade distribution, Plane_N 1099966.....	65
Figure 4. 19 Cross-section 2-2 of Pit Ver.2 and its vertical 3D block grade distribution, Plane_N 1099966.....	66
Figure 4. 20 Cross-section 3-3 of Pit Ver.3 and its vertical 3D block grade distribution, Plane_N 1099966.....	67
Figure 4. 21 Distribution curve of FOS value on the final Pit design	70

Figure 4. 22 Pit MF-10 before mining and its cross-section line	72
Figure 4. 23 Pit MF-10 after mining by Pit design Ver.1 and its cross-section line.....	72
Figure 4. 24 Cross-section along A-A' before mining.....	73
Figure 4. 25 Cross-section along A-A' after mining by Pit Ver.1	73
Figure 4. 26 Cross-section along B-B' before mining.....	74
Figure 4. 27 Cross-section along B-B' after mining by Pit Ver.1	74
Figure 4. 28 Cross-section along C-C' before mining	75
Figure 4. 29 Cross-section along C-C' after mining by Pit Ver.1	75
Figure 4. 30 Pit MF-10 after mining by Pit design Ver.2 and its cross-section line.....	76
Figure 4. 31 Cross-section along D-D' of Pit Ver.2	76
Figure 4. 32 Cross-section along E-E' of Pit Ver.2	77
Figure 4. 33 Cross-section along F-F' of Pit Ver.2	77
Figure 4. 34 Pit MF-10 after mining by Pit design Ver.3 and its cross-section line.....	78
Figure 4. 35 Cross-section along G-G' of Pit Ver.3.....	78
Figure 4. 36 Cross-section along H-H' of Pit Ver.3	79
Figure 4. 37 Cross-section along I-I' of Pit Ver.3	79
Figure 4. 38 Distribution curves of FOS value on cross-section model	81
Figure 4. 39 The results of cross-section model analysis for Pit Ver.1	82
Figure 4. 40 The results of cross-section model analysis for Pit Ver.2.....	83
Figure 4. 41 The results of cross-section model analysis for Pit Ver.3.....	84
Figure 4. 42 The plotting curve of FOS versus slope angle	87

LIST OF TABLES

Table 3. 1 Summary of block samples collection	25
Table 3. 2 Summary the benches parameter used in pit design	33
Table 3. 3 Part of the Collar file (collar.csv)	34
Table 3. 4 Part of the Survey file (survey.csv).....	34
Table 3. 5 Part of the Assay file (assay.csv)	34
Table 3. 6 Part of the Lithology file (litho.csv)	35
Table 3. 7 Summary the analytical cases for SGM of final Pit design Ver.1, 2, and 3	47
Table 3. 8 Summary the analytical cases for cross-section model of Pit Ver.1, 2, and 3	48
Table 3. 9 Summary the analytical cases for assuming bench model of trial pit slope ...	49
Table 4. 1 Summary the results of kaolin strength testing.....	50
Table 4. 2 Information of Drill-hole data	53
Table 4. 3 Cumulative frequency of kaolin grade	53
Table 4. 4 Summary the ore reserve and overburden of Pit design Ver.1, 2, and 3.....	61
Table 4. 5 Summary of geomaterials properties of the study area	68
Table 4. 6 Summary the results of slope stability analysis for SGM of final Pit design Ver.1, 2, and 3	70
Table 4. 7 Summary the results of slope stability analysis of cross-section model of Pit Ver.1, 2, and 3	80
Table 4. 8 Summary the results of analysis for the models with various bench height ...	85

CHAPTER I INTRODUCTION

1.1 Background

One of the most safety problems in the open-pit mining is to maintain the stability of pit slope throughout the mine life. A proper solution to this slope stability problem will certainly improve the working; thus, enhance the economic efficiency of the mining operation.

There is a case problem occurred in the kaolin mine at Ranong province, southern Thailand (Figure 1.1). This kaolin mine is operated by the company Minerals Resources Development (MRD). The kaolin mine has been excavated by open cut mining method. The whole area of this mine has been separated into many sub-pits as shown in Figure 1.2.

This research target area is at the sub-pit MF-10, which is located in the northwestern part of the kaolin mine. This sub-pit covers a small area for mining, but the company would like to maximize the kaolin reserves on this pit. In order to maximize ore reserves, the pit has to be designed with slope as steep as possible as well as pit boundary has to expand as far as possible. However, the southwestern slope of pit MF-10 is located next to the public creek and the buffer area has to be at least 50 metres from the creek. According to the MRD's plan, the pit MF-10 was designed only 20 metres between pit boundary and the creek. Respected to Thailand's minerals law, "The Mineral Act B.E 2510" has some important main points in the "chapter 4" and "section 62". Those words written are "The holder of a Prathanabat shall not mine within fifty metres of a highway or public waterway, unless the Prathanabat allows him to do so or he has obtained a license from the Local Mineral Industry Official, however, he must comply with the conditions prescribed in such a license". To get the permission, it is necessary to do the research in terms of slope stability assessment for a guarantee. So it becomes to be a part of this research for doing the slope stability assessment and design an acceptable pit slope that have safety and suitable for this pit.

1.2 Location of study

The MRD's kaolin mine is at Haad Sompan sub-district, Muang district, Ranong province in the southern part of Thailand. The mine concession area is about 3 km³. Mine site is located at the north-eastern area of Ranong town by road distance on rout No. 4005 about 13.3 km and far from Bangkok about 563 km by Phetchakasem highway.

1.3 Local climate

- Ranong province has a tropical monsoonal climate with short dry season and long wet season.
- The mean temperature is 25 degree Celsius.
- Total annual precipitation is 4,185 mm on average, for the detail of rainfall and groundwater level were followed GDP reported (GDP, 2010b);(GDP, 2013).

1.4 General geology of research area

MRD mine is located in granite terrain as illustrated in Figure 1.3. The intrusion of granite occurred during the late Cretaceous. The rock is biotite-muscovite granite, white, equi-granular, fine to coarse-grained. A number of quartz veins are exposed in the pit as demonstrated in Figure 1.4. The rocks in the mine have been passed through several degree of weathering processes. In fact, some rocks are completely changed to residual soils (Pipat, 2016).

1.5 Objectives

The objectives of the study are as following:

- 1) Firstly, to investigate the characteristics of geomaterials in Pit MF-10.
- 2) The second objective is to evaluate the stability of all slope faces in Pit MF-10 during both dry and wet seasons.
- 3) Third, to analyze the slope stability by using different numbers of bench height and overall slope angle (OSA). Then, observe the effects slope stability (factor of safety) and the tonnage of kaolin reserve at Pit MF-10.

- 4) Lastly, to choose a suitable overall slope angle (OSA) and slope face angle (FSA), which are safety and optimum to design Pit MF-10.



Figure 1. 1 The kaolin mine location

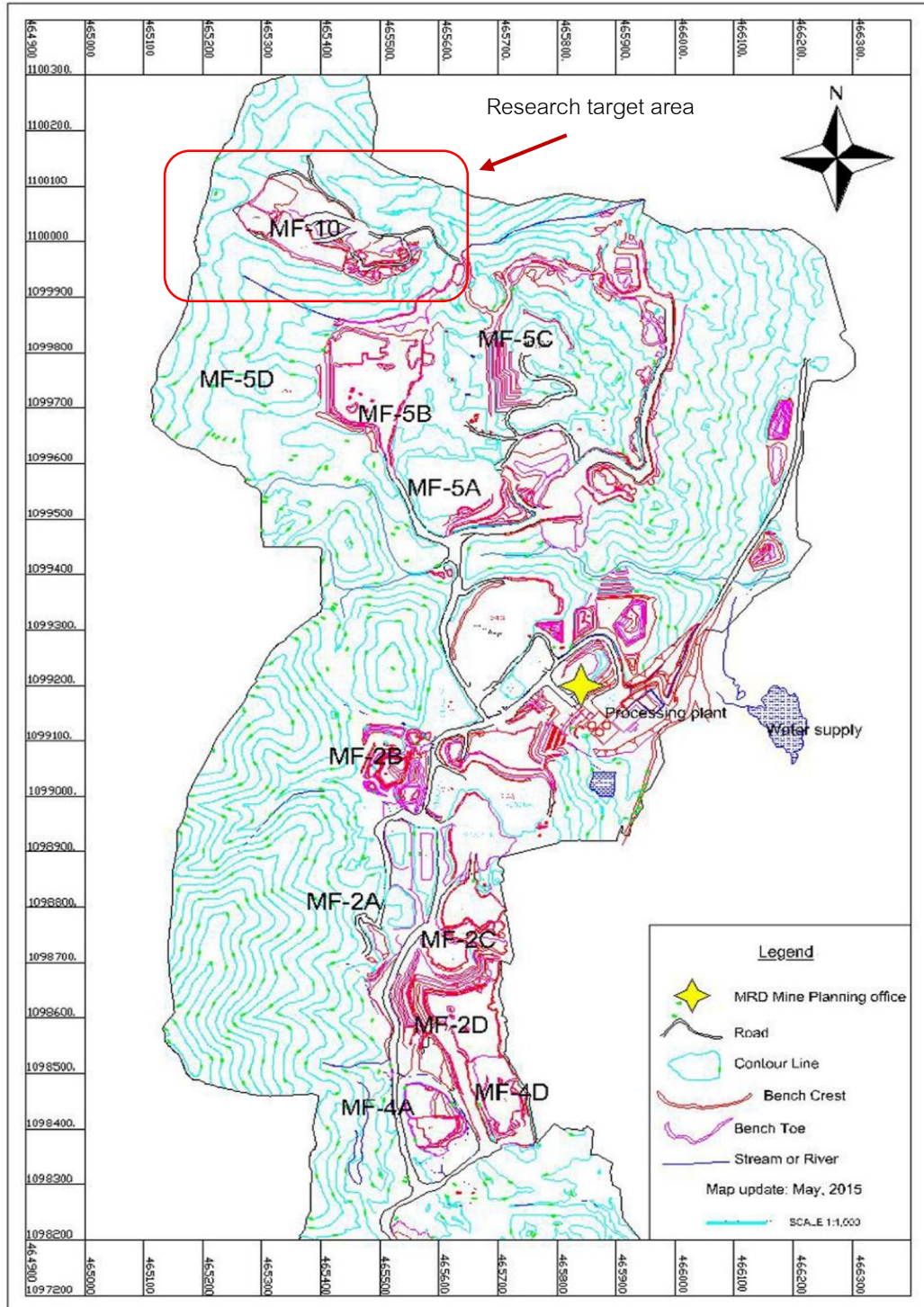


Figure 1. 2 Research target area and the sub-pit in this kaolin mine

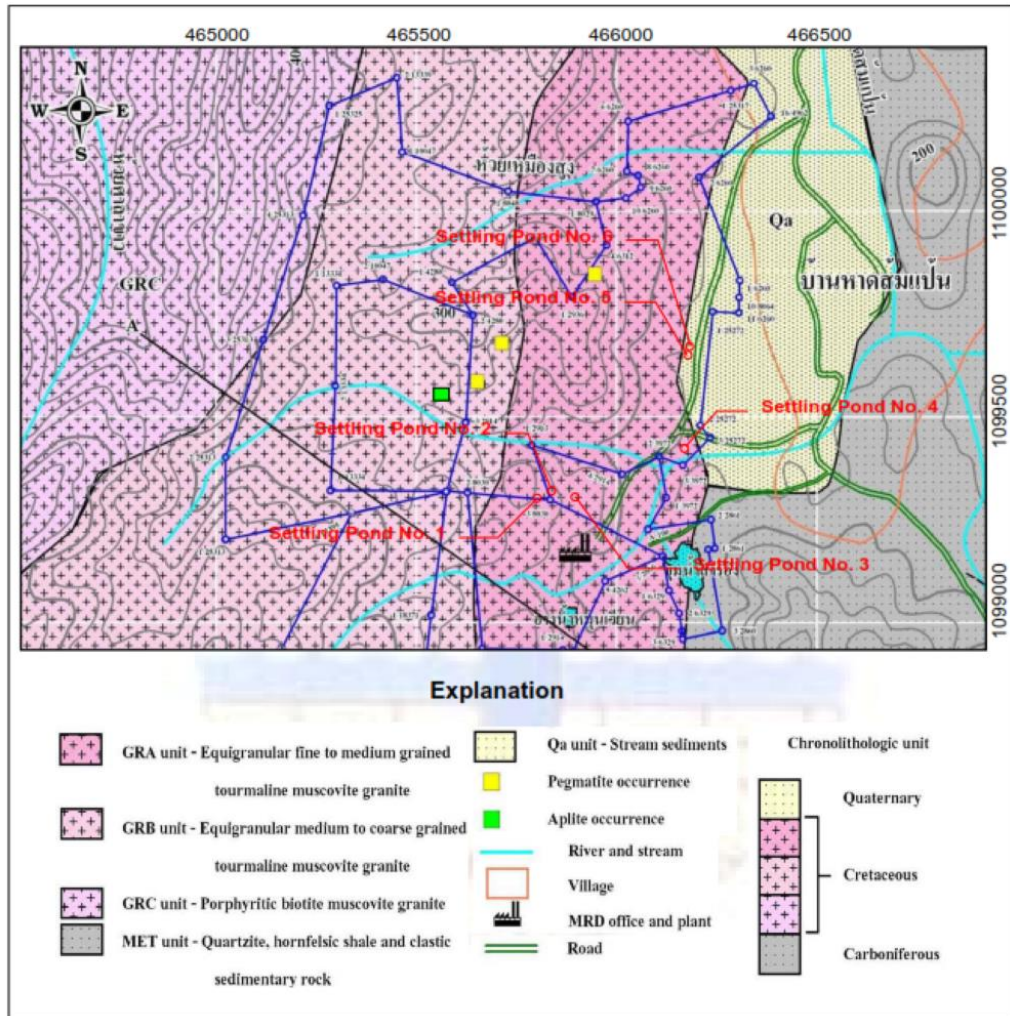


Figure 1. 3 Geological map of MRD mine (GDP, 2010a)

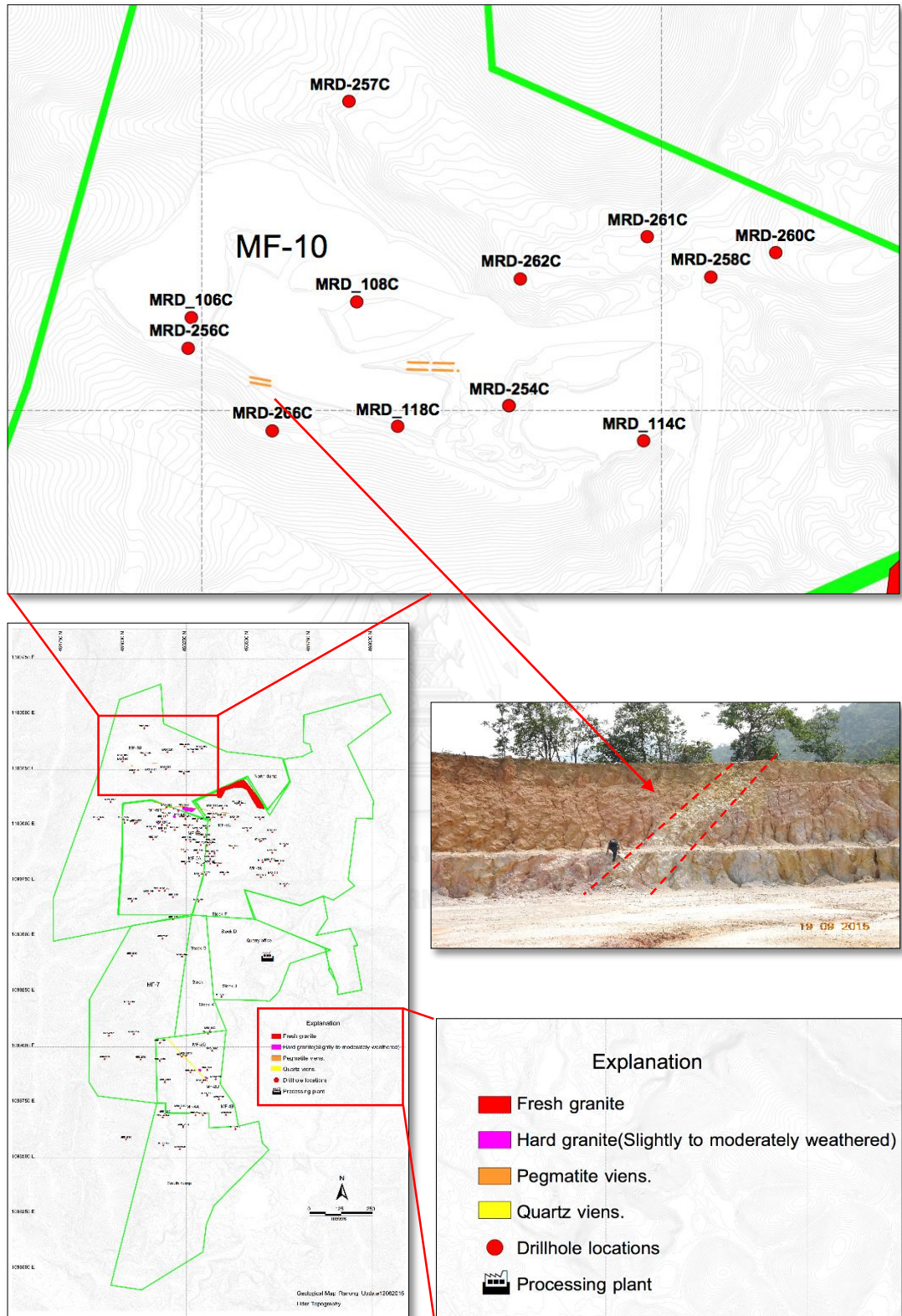


Figure 1. 4 Some Quartz veins at Pit MF-10

CHAPTER II

LITERATURE REVIEW

2.1 Deterministic method

According to its definition, a factor of safety (FOS) > 1.0 means stabilizing forces are greater than sliding forces and hence the slope should be stable. As there is always some degrees of uncertainty connected to the input parameters, however, this may not necessarily be the case. To take the uncertainty into account and in order to allow for the different stability requirements of different types of structures, the following criteria for stability are often used: short-term stability (e.g. temporary slopes in an open pit mine), FOS ≥ 1.3; long-term stability (e.g. permanent mine slopes or road cuts), FOS ≥ 1.5. In addition, Figure 2.1 shows acceptable FOS for different engineering works.

The FOS is a deterministic measure of the ratio between the resisting forces (capacity) and driving force (demand) of the system in its considered environment:

$$FOS = \frac{\text{Total force available to resist sliding}}{\text{Force tending to induce sliding}} \quad (2.1)$$

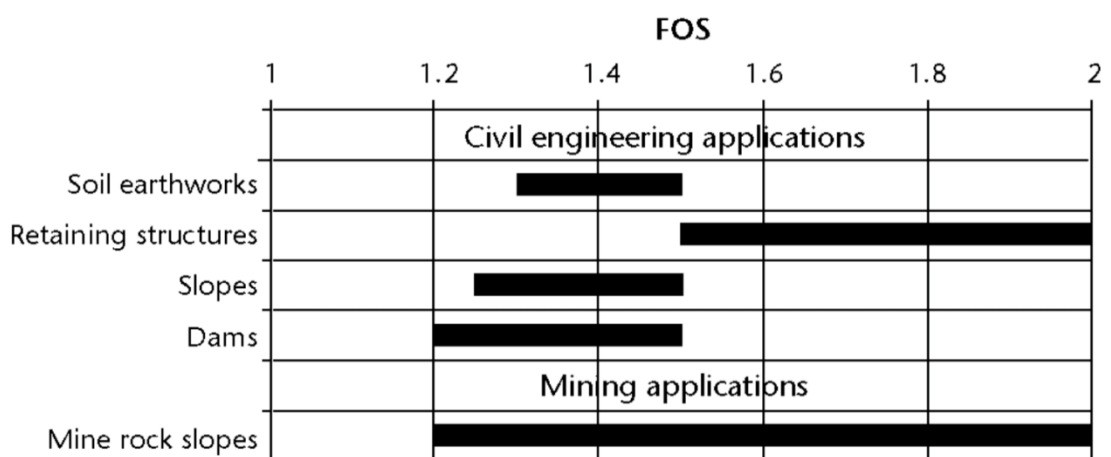


Figure 2. 1 Example of acceptable FOS value (Priest & Brown, 1983)

2.2 Numerical modeling

According to (Soren, 2010), Numerical models are computer programs that attempt to represent the mechanical response of a rock mass subjected to a set of initial condition (e.g., in situ stress, water level), boundary conditions, and induced change (e.g., slope excavation). The result of a numerical model simulation is typically either equilibrium or collapse. If an equilibrium result is obtained, the resultant stresses and displacements at any point in the rock mass or soils can be compared with measured values. If a collapse result is obtained, the predicted mode of failure is demonstrated. In either case, the factor of safety can be calculated.

Numerical models divide the rocks mass or soils into elements. Each element is assigned a material model and properties. The material models are idealized stress/strain relations that describe how material behaves. The simplest model is a linear elastic model, which uses the elastic properties (Young's modulus and Poisson's ratio) of the material. Elastic-plastic models use strength parameters to limit the shear stress that an element may sustain. The elements may be connected together (a continuum model) or separated by discontinuities (a discontinuum model). Discontinuum model allow slip and separation at explicitly located surfaces within the model.

Numerical models tend to be general purpose in nature, i.e., they are capable of solving a variety of problems. While it is often desirable to have a general-purpose tool available, each problem must be constructed individually. The elements must be arranged by the user to fit the limits of the geomechanical units and/or the slope geometry. Hence, numerical models often require more time to set up and run than special-purpose tools (such as limit equilibrium methods).

Numerical model are used for slope stability studies for a variety of reasons, including:

- Empirical methods cannot confidently be extrapolated outside their databases.
- Other methods (e.g., analysis, physical, limit equilibrium) are not available or tend to oversimplify the problem, possibly leading to overly conservative solutions.

- Key geologic features, groundwater, etc. can be incorporated into numerical models, providing more realistic approximations of real slope behavior.
- Observed physical behavior can be explained.
- Multiple possibilities (e.g., hypotheses, design options) can be evaluated (Hustrulid, McCarter, & Van Zyl, 2000).

2.3 Finite difference computer software

FLAC3D (Fast Lagrangian Analysis of Continua Three Dimensional) is a three-dimensional explicit finite-difference program for engineering, mechanics and computation, simulating the behavior of three-dimensional structures built of soil, rock or other materials, FLAC3D was developed primarily for geotechnical engineering applications, mainly problems in the fields of mining, underground engineering, rock mechanics and research (Itasca, 2005).

Finite Difference Method (FDM) numerical program like FLAC3D differ from Finite Element programs in their use of an explicit solution scheme, coupled with their use of the full dynamic equations of motion, even for static problems. The FDM produces a direct approximation of the governing partial differential equations of the objective functions (e.g. displacement), by replacing them with finite differences spread over the area of interest (Jing & Hudson, 2002).

(Carter, Desai, Potts, Schweiger, & Sloan, 2000) list the advantages and disadvantages of using the explicit solution technique:

Advantages:

- Simple problems are very easy to prepare within the model.
- Structural features in the rock mass, such as closely spaced parallel sets of joints can be modeled.
- Time-dependent material behavior may be introduced.
- The method has been applied to solve practical problems and thus a lot of experience is already available.

- Unlike FEM, the explicit solution method avoids the solution of large sets of equations and therefore reduce processing time, and memory rudiments.

Disadvantages:

- The method is less efficient than FEM for linear or moderately nonlinear problems.
- Due to the requirement of FDM analysis to generate large matrices that must be stored in the computer's memory, the analysis duration and memory requirements may be very high.
- Because FDM is based on Newton's law of motion the solution cycle does not have a defined converge point (it's an infinite loop) even the static problems, therefore judgment of the user as to define whether a sufficient number of time steps have been run, effect the output.
- If the mechanical behavior of the medium in question is dominated by randomly oriented joint or fracture sets, then FDM analysis is generally not suitable.

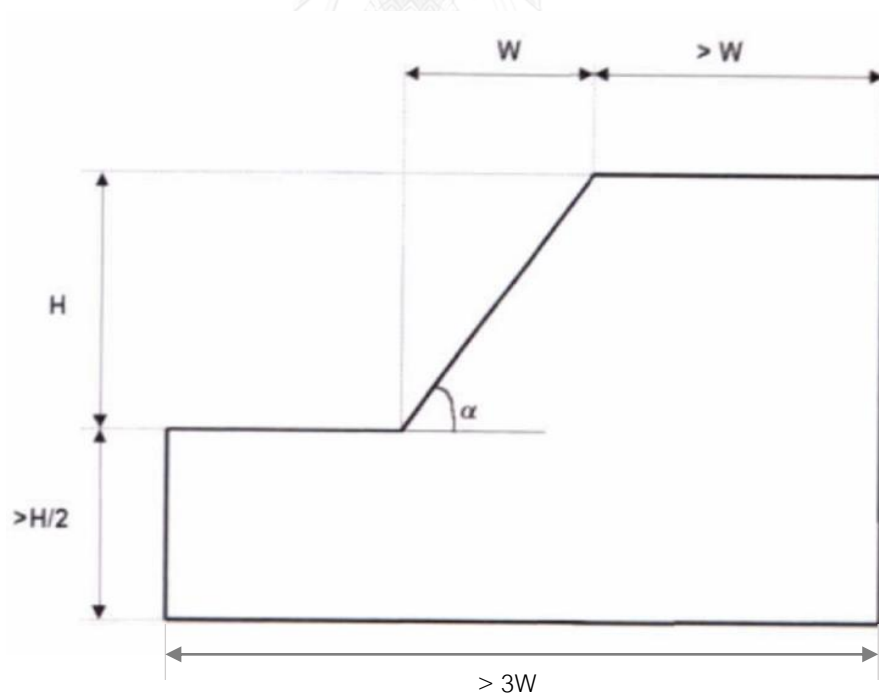


Figure 2. 2 Minimum dimension for slope analysis model

2.3 Mohr-Coulomb Model

The Mohr-Coulomb is the conventional model used to represent shear failure in soil and rock (Vermeer & De Borst, 1984). The Mohr-Coulomb model is useful when yielding or failure is possible in a model but post failure behavior of the material is not important. The following are required properties for the Mohr-Coulomb plasticity model:

- 1) Bulk modulus (K) used consistently for each material.
- 2) Shear modulus (G) used consistently for each material.
- 3) Young's modulus (E) used consistently for each material.
- 4) Poisson's ratio (ν) used consistently for each material.
- 5) Friction (ϕ) changed upon the sample's value.
- 6) Cohesion (c) changed upon the sample's value.
- 7) Tensile strength (T) used consistently for each material.

For Bulk modulus (K), and shear modulus (G) are related to Young's modulus (E), and Poisson's ratio (ν), by following equations bellow:

$$K = \frac{E}{3(1 - 2\nu)} \quad (2.2)$$

$$G = \frac{E}{2(1 - \nu)} \quad (2.3)$$

And

$$E = \frac{9KG}{3K + G} \quad (2.4)$$

$$\nu = \frac{3K - 2G}{2(3K + G)} \quad (2.5)$$

The Mohr-Coulomb failure criterion represents the linear envelope that is obtained from a plot of the shear strength of a material versus the applied normal stress. The failure criterion can be expressed in the following form:

$$f_s = \sigma_1 - \sigma_3 N_\phi + 2c\sqrt{N_\phi} \quad (2.6)$$

Where: $N_\phi = (1 + \sin\phi)/(1 - \sin\phi)$;

σ_1 = major principal stress (kPa);

σ_3 = minor principal stress (kPa);

C = cohesion strength constant (the intercept of the failure envelope with the axis) (kPa);

ϕ = angle of internal friction (slope of the failure envelope) (degree); and

Shear yield is detected if $f_s < 0$ (Itasca, 2005).

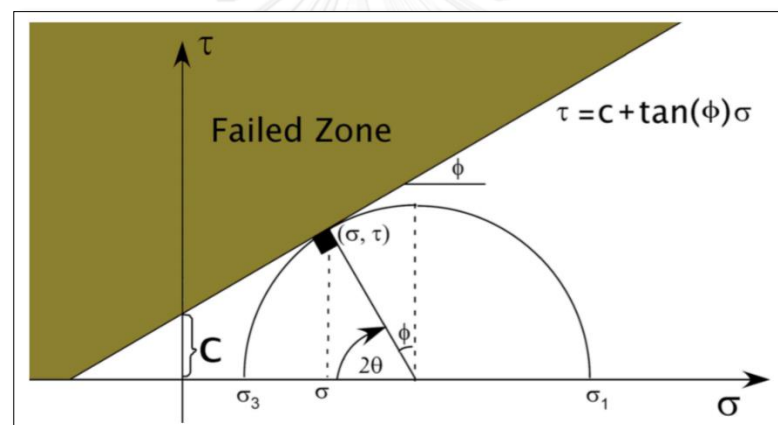


Figure 2. 3 Mohr-Coulomb failure criterion (Soltani, 2015)

Where τ is Shear stress (kPa);

σ is Normal stress (kPa);

C is Cohesion (kPa); and

ϕ is Friction angle (degree).

2.4 Open pit slope design

For an open pit mine, the design of the slopes is one of the major challenges at every stage of planning and operation. It requires specialized knowledge of the geology, which is often complex in the vicinity of orebodies where structure and/or alteration may

be key factors, and of the material properties, which are frequently highly variable. It also requires an understanding of the practical aspects of design implementation.

The aim of any open pit mine design is to provide an optimal excavation configuration in the context of safety, ore recovery and financial return. Investors and operators expect the slope design to establish walls that will be stable for the life of the open pit, which may extend beyond closure. At the very least, any instability must be manageable. This applies at every scale of the walls, from the individual benches to the overall slopes.

It is essential that a degree of stability is ensured for the slopes in large open pit mines to minimize the risks related to the safety of operating personnel and equipment, and economic risks to the reserves. At the same time, to address the economic needs of the owner's ore recovery must be maximized and waste stripping kept to a minimum throughout the mine life. The resulting compromise is typically a balance between formulating designs that can be safely and practicably implemented in the operating environment and establishing slope angles that are as steep as possible.

Unlike civil slopes, where the emphasis is on reliability and the performance of the design and cost/benefit is less of an issue, open pit slopes are normally constructed to lower levels of stability, recognizing the shorter operating life spans involved and the high level of monitoring, both in terms of accuracy and frequency, that is typically available in the mine. Although this approach is fully recognized both by the mining industry and by the regulatory authorities, risk tolerance may vary between companies and between mining jurisdictions.

In a large open pit, steepening a wall by only a few degrees can have a major impact on the return of the operation through increased ore recovery and/or reduced stripping (Figure 2.4).

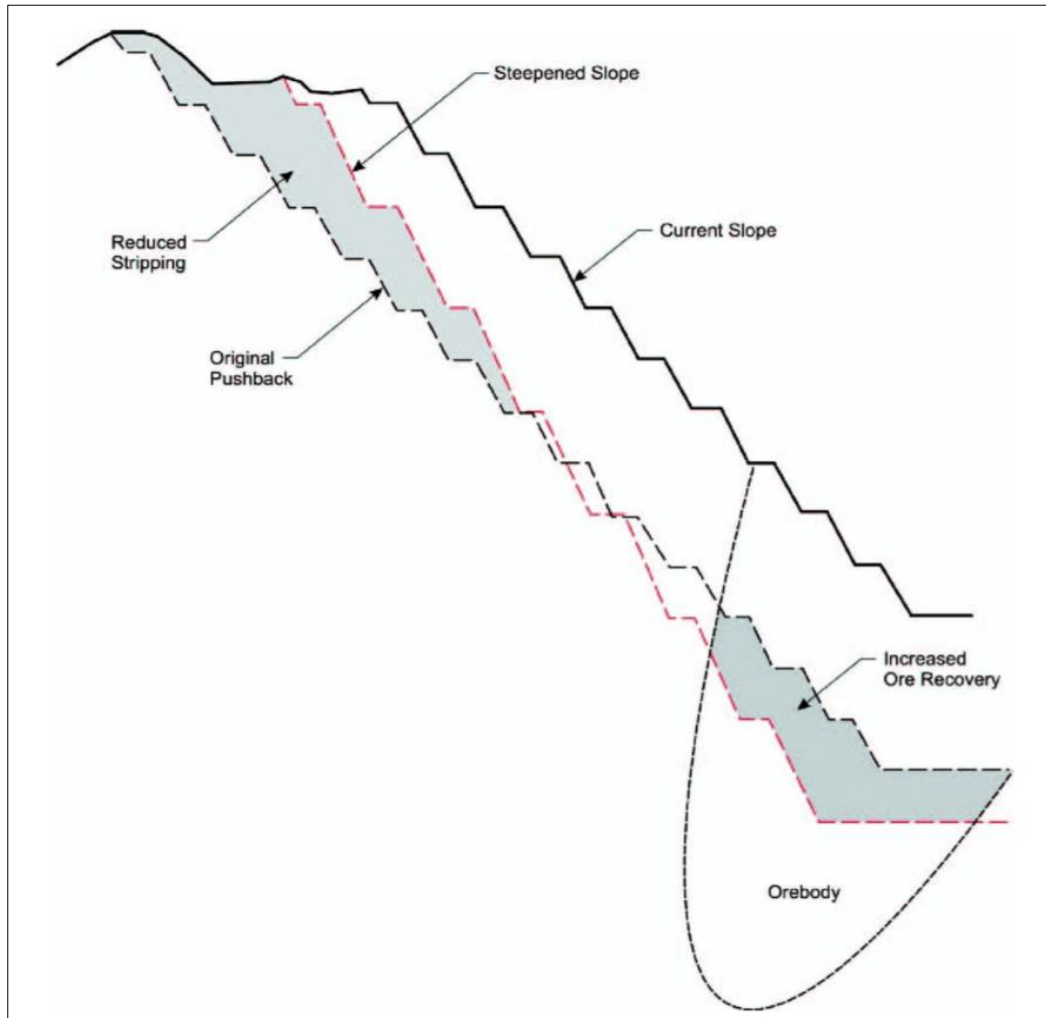


Figure 2. 4 Potential impacts of slope steepening (Read & Stacey, 2009)

2.5 Basic bench geometry

The basic extraction component in an open pit mine is bench. Bench nomenclature is shown in figure 2.5.

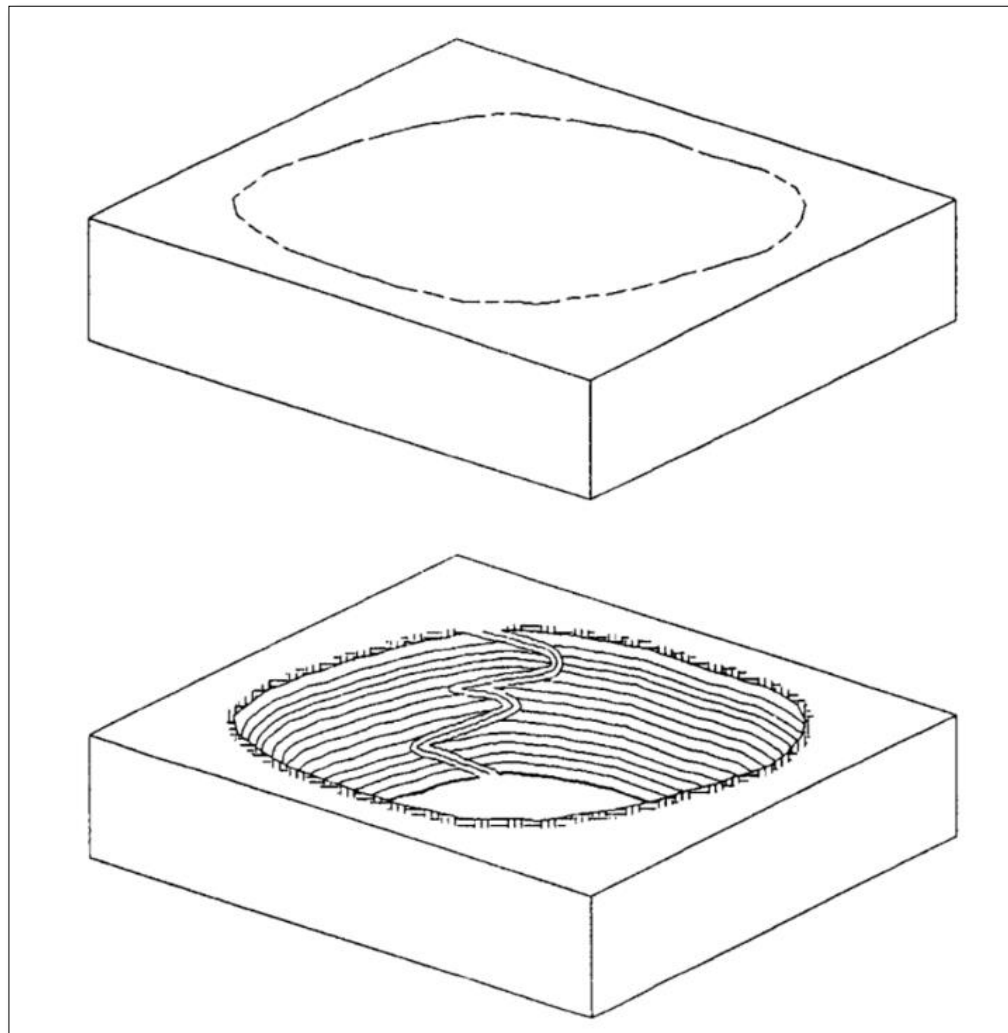


Figure 2. 5 Geometry change in pit creation (Hustrulid, Kuchta, & Martin, 2013)

Each bench has upper and lower surface separated by distance H equal to the bench height. The exposed sub-vertical surface are called the bench faces. They are described by the toe, the crest and face angle α (the average angle the face makes with the horizontal). The bench face angle can vary considerably with rock characteristics, face orientation and blasting practices. In most hard rock pits it varies from about 55° to

80°. A typical initial design value might be 65°. This should be used with care since the bench face angle can have a major effect on the overall slope angle.

Normally bench faces are mined as steeply as possible. However, due to variety of causes there is a certain amount of back break. This is defined as the distance the actual bench crest is back of the designed crest. A cumulative frequency distribution plot of measured average bench face angle is shown in Figure 2.7.

The exposed bench lower surface is called the bench floor. The bench width is the distance between the crest and the toe measured along the upper surface. The bank width is the horizontal projection of the bench face (Hustrulid et al., 2013).

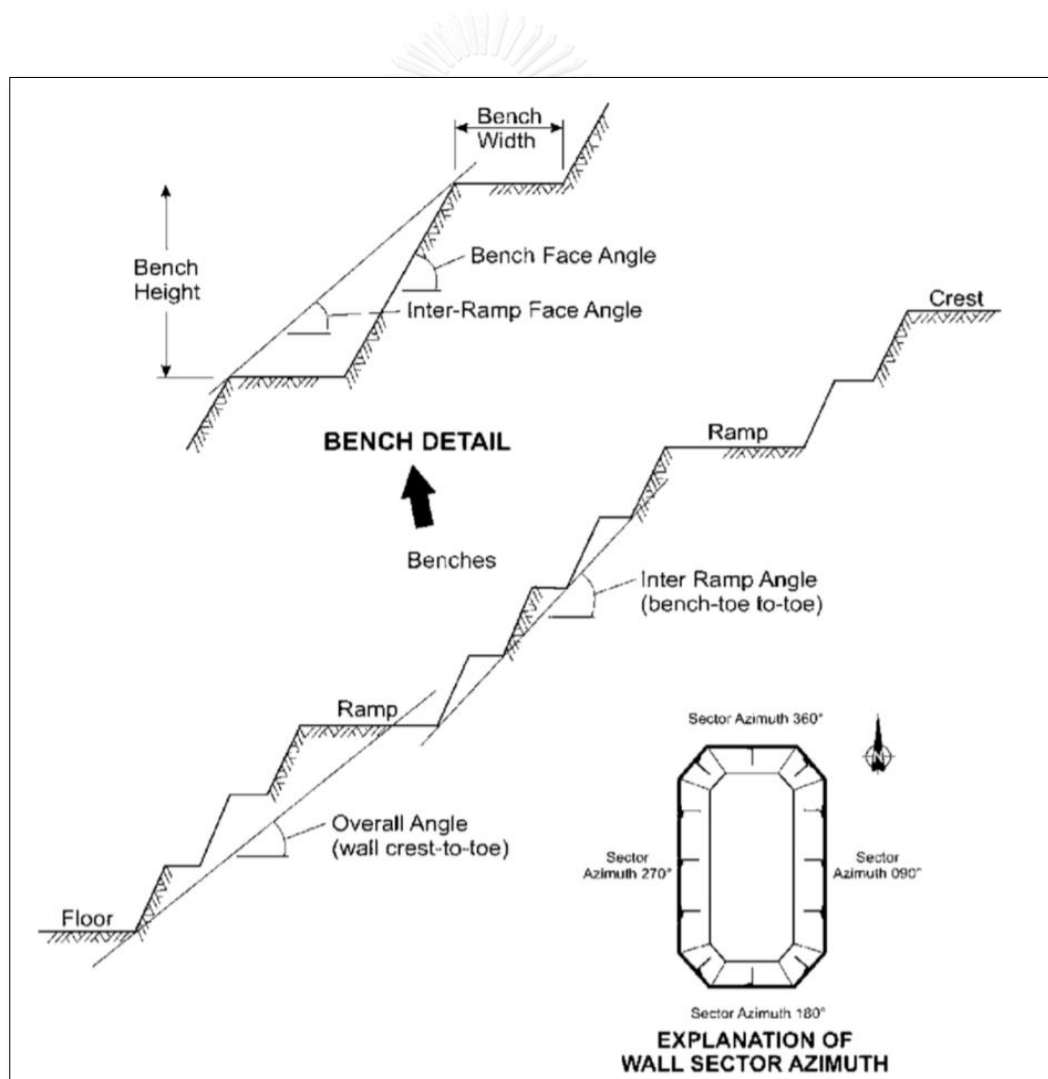


Figure 2. 6 Pit wall terminology (Read & Stacey, 2009)

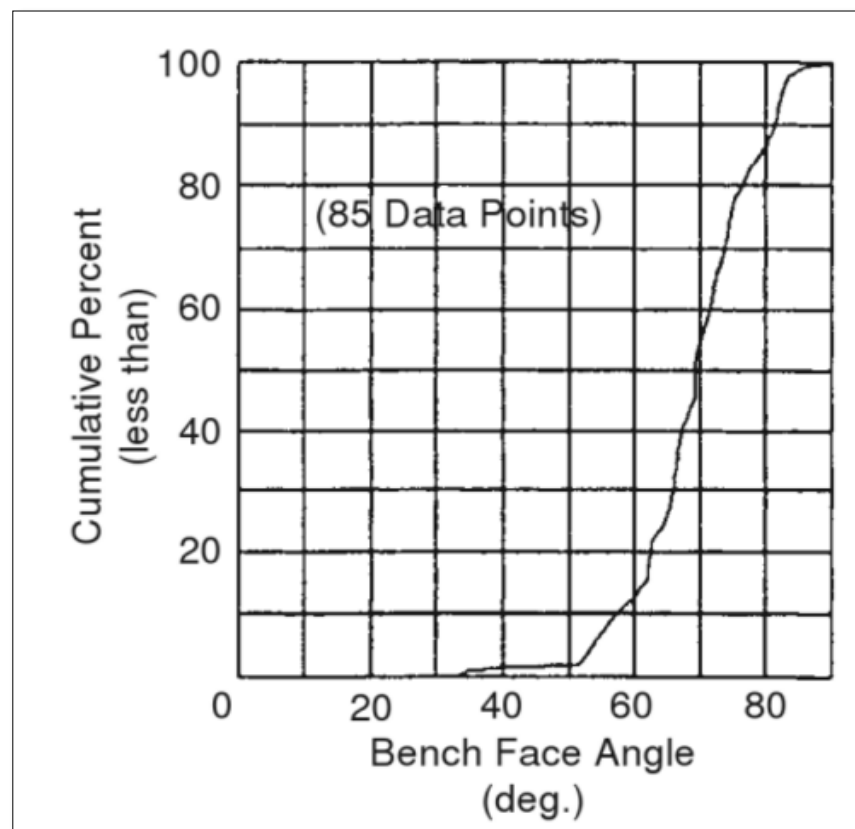


Figure 2. 7 Cumulative frequency distribution of measured bench face angles (call,
1986)

2.6 Pit design by 3D block model method

Currently, most of activities in exploration and mining operation revolve around the 3D block model. In this model, all relevant deposit characteristics are organized in a transparent and manageable way. The quality of the productivity and efficiency of activities are controlled by the 3D block model. Generally speaking, 3D block model is a simplified mathematical description of a deposit. The deposit is subdivided into small blocks that each block represents a planning unit which contains information about raw material properties such as chemical grade, rock type, geology, geological structure condition, etc. The model of 3D block is illustrated in Figure 2.8 (Hustrulid et al., 2013).

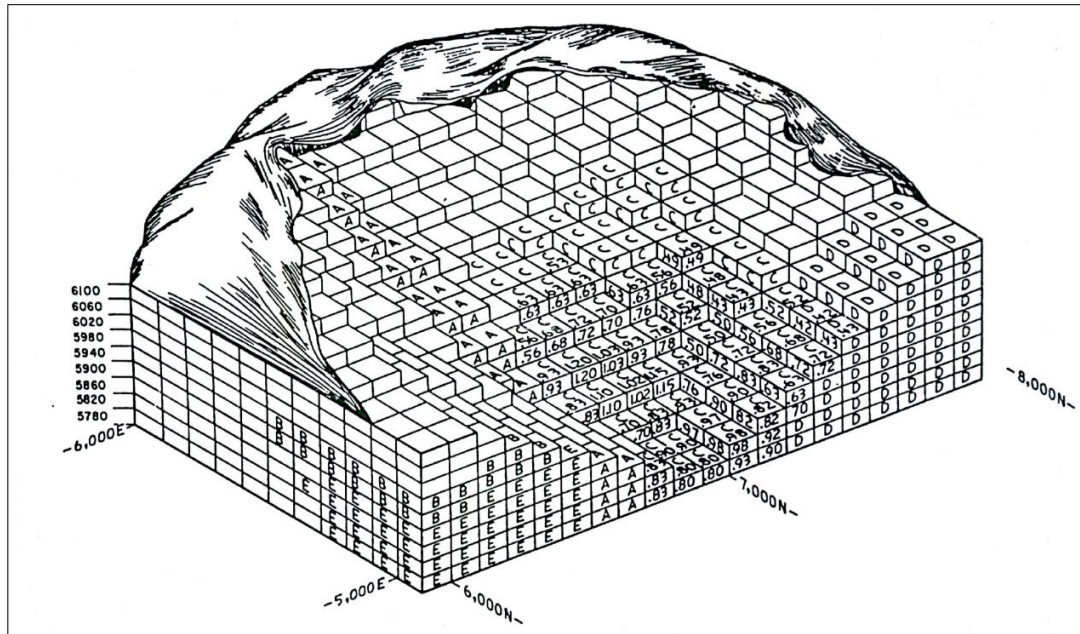


Figure 2. 8 Diagrammatic view of a 3D block matrix (Crawford & Davey, 1979)

In practice, the estimation for the grade and tonnage is carried out by interpolating the ore grades into the block where the overall statistics of the deposit can be made.

To choosing the right kind of block size. As a rule of thumb, the minimum size of block should not be less than 1/4 of the average drill-hole (DH) interval. Let say 50 metres of block dimension for 200 metres DH spacing grid (David, 2012). For the height of block should be equal to the bench height when mining operation (Hustrulid et al., 2013).

2.7 Inverse distance weighting technique

The inverse distance weighting (IDW) is an interpolation technique for estimating value of vocationally department variables by forming a linear combination of a set of measurements. The non-negative weights sum up to one and are inversely related to the distance to data point (Philip & Watson, 1987). The grade or any other variable at unsampled points can be estimated by using the inverse distance weighting as:

$$g_B = \frac{\sum_{i=1}^n \frac{g_i}{d_i^m}}{\sum_{i=1}^n \frac{1}{d_i^m}} \quad (2.7)$$

Where g_B is the estimated grade of a block;

g_i is the grade of sample i ;

d_i is the distance from the center of the block to the nearby block; and

m is the power function (This power function has varied in response to the variation of ore grade).

For ore reserve estimation this technique was used for interpolating a point in the center of an evaluation block (Figure 2.9). The resulting grade was extended to the whole block with an associated error proportional to the block size.

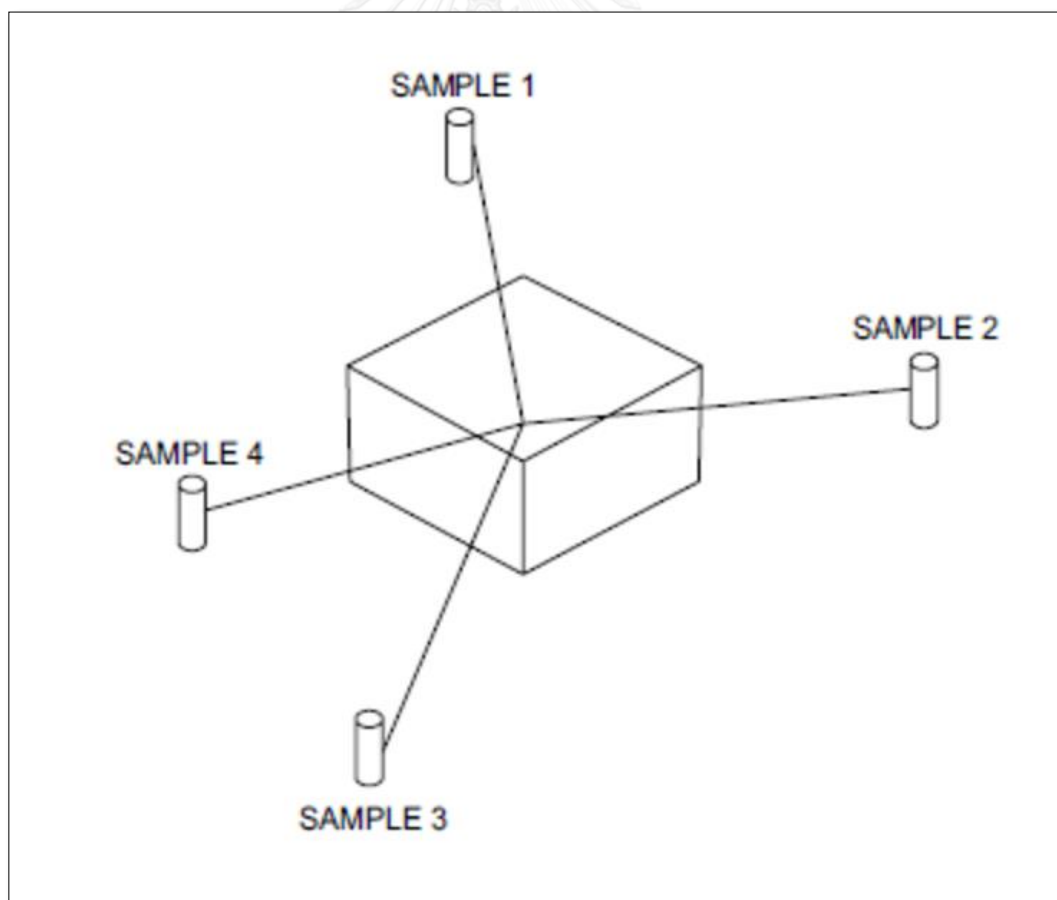


Figure 2. 9 Block estimation by extending the grade computed in its center

2.8 Stripping ratio

The stripping ratio (SR) refers to the amount of waste rock vs. ore (as opposed to mineralization) or, more precisely, how much worthless rock you have to move to get at the ore you plan to mine. If over the life of an open-pit mine you have to move three tons of barren dirt or rock to extract one ton of ore you run through your plant, your stripping ratio is 3:1.

$$SR = \frac{Waste (ton)}{Ore (ton)} \quad (2.9)$$

Or

$$SR = \frac{Waste (volume)}{Ore (volume)} \quad (2.9)$$

2.9 Related research

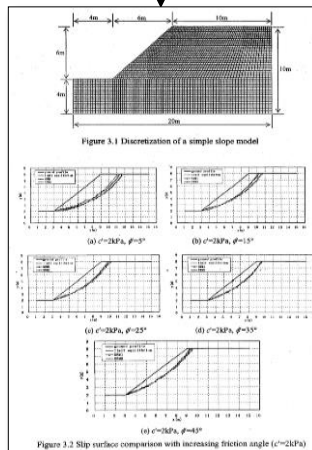
Wei, Wenbing (2008) has a researched about “Three dimensional slope stability analysis and failure mechanism” published by The Hong Kong Polytechnic University. This research aims to conduct an extensive three-dimensional slope stability analysis and to investigate the failure mechanism under different situations by 3D limit equilibrium method (LEM) and 3D strength reduction method (SRM). In the research process have a few computer software like PLAXIS, Phase2, FLAC2D and FLAC3D used to simulation the slope stability analysis. Data base of materials on some cases example of slope stability analysis that attached within the software. Those examples have analyzed and described.

E. J. A. Appianing and D. Mireku-Gyimah (2015) has a researched of “Open pit optimization and design”. The case study area in the gold deposit at the western part of Ghana. The method of 3D block modeling technique used to estimate pit optimization and design. The necessary data is ore grade (assay), DH located (collar), DH direction (survey) and the information of rocks or soils structure at the ore area (lithology). Other data considered are the topography (topo contour map) of the area need to excavate, and some economic cost about the mining activities. The pit design using computer software (Surpac). The roughly process on pit design is import all data necessary into the software - create rock zone and 3D block model – estimate the grade of block – assigned the economic parameters into block - estimate the block value – calculate the final pit boundary – pit design - estimate the ore and waste volume.

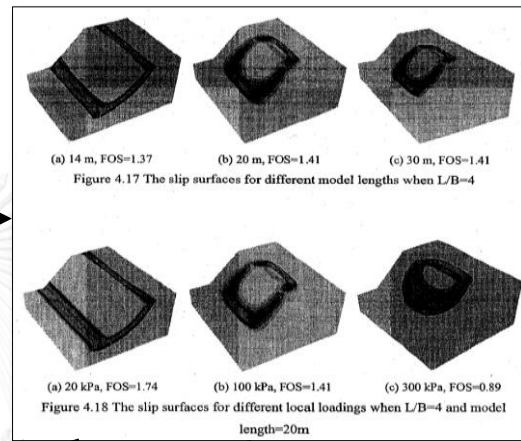
Table 3.2 Soil properties for Figure 3.6

Soil name	Cohesion (kPa)	Friction angle (degree)	Density (kN/m ³)	Elastic modulus (MPa)	Poisson ratio
Soil1	20	35	19	14	0.3
Soil2	0	25	19	14	0.3
Soil3	10	35	19	14	0.3

Assigned the material properties into the geometry model of LEM and SRM



Run the software slope analysis and got the results



Comparison the results from each method of slope stability analysis

Table 3.1 Factors of safety by LEM and SRM

case	c' (kPa)	φ (°)	FOS (LEM)	FOS (SRM1, non-associated)	FOS (SRM2, associated)	FOS difference with LEM (SRM1, %)	FOS difference with LEM (SRM2, %)	FOS difference between SRM1 and SRM2 (%)
1	2	5	0.25	0.25	0.26	0	4.0	4.0
2	2	15	0.50	0.51	0.52	2	4.0	2.0
3	2	25	0.74	0.77	0.78	4.0	5.4	1.3
4	2	35	1.01	1.07	1.07	5.9	5.9	0
5	2	45	1.35	1.42	1.44	5.2	6.7	1.4
6	5	5	0.41	0.43	0.43	4.9	4.9	0
7	5	15	0.70	0.73	0.73	4.3	4.3	0
8	5	25	0.98	1.03	1.03	5.1	5.1	0
9	5	35	1.28	1.34	1.35	4.7	5.5	0.7
10	5	45	1.65	1.68	1.74	1.8	5.5	3.6
11	10	5	0.65	0.69	0.69	6.2	6.2	0
12	10	15	0.98	1.04	1.04	6.1	6.1	0
13	10	25	1.30	1.36	1.37	4.6	5.4	0.7
14	10	35	1.63	1.69	1.71	3.7	4.9	1.2
15	10	45	2.04	2.05	2.15	0.5	5.4	4.9
16	20	5	1.06	1.20	1.20	13.2	13.2	0
17	20	15	1.48	1.59	1.59	7.4	7.4	0
18	20	25	1.85	1.95	1.96	5.4	5.9	0.5
19	20	35	2.24	2.28	2.35	1.8	4.9	3.1
20	20	45	2.69	2.67	2.83	0.7	5.2	6.0
21	5	0	0.20		0.23		15	
22	10	0	0.40		0.45		12.5	
23	20	0	0.80		0.91		13.8	

Table 3.6 Comparison of factor of safety for Figure 3.14

case	c' (kPa)	φ (°)	Density (kN/m ³)	Poisson ratio	Elastic modulus of soil1 (kN/m ²)	Elastic modulus of soil2 (kN/m ²)	FOS (LEM)	FOS (SRM1)	FOS (SRM2)
1	10	15	20	0.3	1.4e5	1.4e2	0.9826	0.954	0.983
2	10	15	20	0.3	1.4e2	1.4e5	0.9826	0.966	0.989
3	10	25	20	0.3	1.4e5	1.4e2	1.2951	1.235	1.297
4	10	25	20	0.3	1.4e2	1.4e5	1.2951	1.259	1.320

Table 3.7 Comparison of factor of safety for Figure 3.15

case	c' (kPa)	φ (°)	Density (kN/m ³)	Poisson ratio	Elastic modulus of soil1 (kN/m ²)	Elastic modulus of soil2 (kN/m ²)	FOS (LEM)	FOS (SRM1)	FOS (SRM2)
1	10	15	20	0.3	1.4e5	1.4e2	0.982	0.964	0.985
2	10	15	20	0.3	1.4e2	1.4e5	0.982	0.963	0.976
3	10	25	20	0.3	1.4e5	1.4e2	1.295	1.288	1.304
4	10	25	20	0.3	1.4e2	1.4e5	1.295	1.282	1.273

Table 3.8 Comparison of factor of safety for Figure 3.16

case	c' (kPa)	φ (°)	Density (kN/m ³)	Poisson ratio	Elastic modulus of soil1 (kN/m ²)	Elastic modulus of soil2 (kN/m ²)	FOS (LEM)	FOS (SRM1)	FOS (SRM2)
1	10	15	20	0.3	1.4e5	1.4e2	0.9826	0.951	0.980
2	10	15	20	0.3	1.4e2	1.4e5	0.9826	0.975	0.980
3	10	25	20	0.3	1.4e5	1.4e2	1.2951	1.240	1.292
4	10	25	20	0.3	1.4e2	1.4e5	1.2951	1.240	1.275

Table 3.9 Comparison of factor of safety for Figure 3.17

case	c' (kPa)	φ (°)	Density (kN/m ³)	ν	Elastic modulus of soil1 (kN/m ²)	Elastic modulus of soil2 (kN/m ²)	Elastic modulus of soil3 (kN/m ²)	FOS (LEM)	FOS (SRM1)	FOS (SRM2)
1	10	15	20	0.3	1.4e5	1.4e2	1.4e5	0.940	0.932	0.951
2	10	15	20	0.3	1.4e2	1.4e5	1.4e2	0.940	0.903	0.947
3	10	25	20	0.3	1.4e5	1.4e2	1.4e5	1.261	1.210	1.275
4	10	25	20	0.3	1.4e2	1.4e5	1.4e2	1.261	1.211	1.268

Figure 2. 10 Summary the slopes of stability analysis method (Wenbing, 2008)

Table 1 Part of the Collar Text File (Collar.txt)

Hole Id	Y (m)	X (m)	Z (m)	Maximum Depth (m)
A01	31797.38	129893.50	78.0	23.1
A02	31752.82	129860.41	78.0	23.1
A03	31698.17	129808.78	77.0	23.1
A04	31645.00	129752.00	78.0	23.1
A05	31564.00	129693.00	78.0	23.1

Table 3 Part of the Assay Text File (Assay.txt)

Hole Id	Sample Id	Depth From (m)	Depth To (m)	Assay Values (g)
A01	A0116	13.4	14.4	0.12
A02	A0211	8.6	9.6	1.32
A02	A0212	9.6	10.5	1.39
A02	A0213	10.5	11.6	2.08
A03	A0317	15.4	16.5	1.05

Table 7 Cost Figures and Parameters used for Optimisation

Mining cost per tonne	\$4.68
Processing cost per tonne	\$19.44
Price of gold	\$40.6/g (\$1134.00/oz)
Selling cost	\$0.90/g (\$25.70/oz)
Capital cost	\$64 000 000
Discount rate	10 %
Mining recovery	95 %
Mining dilution	5 %
Revenue factor range	0.3 to 2 at 0.02 steps
Overall pit slope angle	45°

Table 2 Part of the Survey Text File (Survey.txt)

Hole Id	Depth (m)	Dip (°)	Azimuth (°)
A01	23.1	-70	90
A02	23.1	-70	90
A03	23.1	-70	90
A04	23.1	-70	90
A05	23.1	-70	90

Table 4 Part of the Geology Text File (Geology.txt)

Hole Id	Sample Id	Depth From (m)	Depth To (m)	Rock Type
A01	A0114	11.8	12.6	PH
A01	A0115	12.6	13.4	PH
A01	A0116	13.4	14.4	GQTZ
A01	A0117	14.4	15.5	GQTZ
A01	A0118	15.5	16.3	GQTZ

Import the drill-hole data file into the software and create the rock zones

Assigned the economic parameters into the rock zone

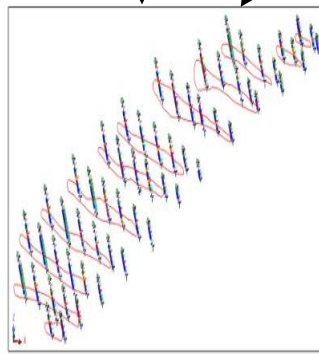


Fig. 1 Digitized Core Zone Sections

Create solid rock zone

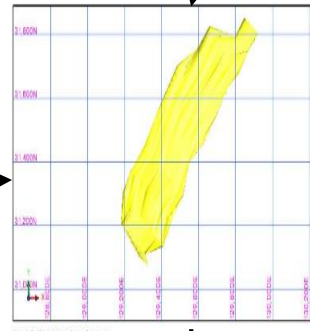


Fig. 2 Solid Model of the Orebody

Calculate the grade of each block

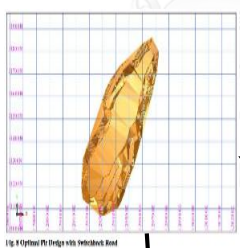


Fig. 4 Optimized Pit Design with Interblock Area

Estimate the ore and waste volume

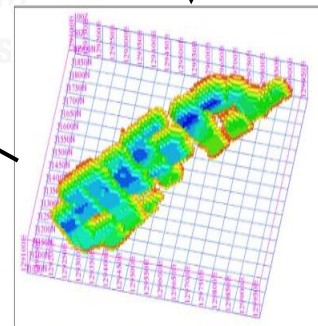


Fig. 7 Expected White Optimal Pit Outline

Export the results

Table 11 Results From Final Pit Design In Surpac

	Volume (m ³)	Tonnage (t)	Gold (g/t)
Ore	1844000	5034120	1.7063
Waste	4097000	11184810	0.08
Total	5941000	16218930	
Stripping Ratio:	2.22:1		
Expected Revenue:	\$331 305 460.10		

Figure 2. 11 Roughly summary the pit design steps (Appianing & Mireku-Gyimah, 2015)

CHAPTER III RESEARCH METHODOLOGY

3.1 The procedure flowchart of this research

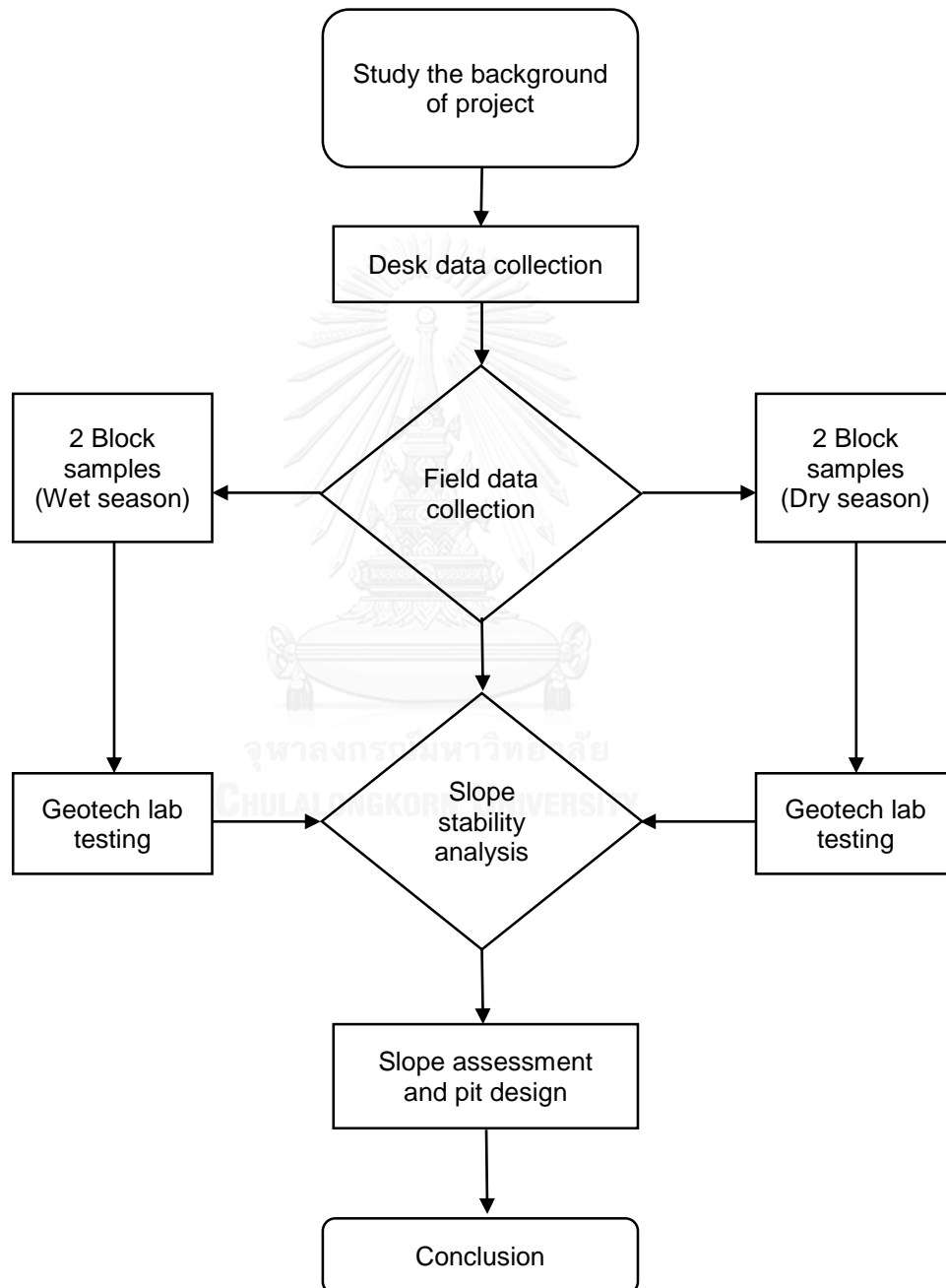


Figure 3. 1 The procedure flowchart of this research

3.2 Desk data collection

Some previous works of slope stability study at MRD's kaolin mine has been carried out by Ground Data Probe Co., LTD (GDP).

There are 2 cases studied of slope stability analysis by GDP. *Case one*, the final report of geotechnical investigation at existing tailings ponds has submitted to the MRD on the date 8 March 2010, and *case two*, the final report of geotechnical investigation works and slope stability analysis of settling pond Nos. 1 and 6, submitted to MRD on 24 December 2013.

3.3 Site investigation

In this study, site investigation and field data collection has been set up at 2 times during both dry and wet seasons. The first visit on May 02, 2015. At that time, the investigators gained more understanding of current state of MRD's kaolin mine. In addition, the investigators learned to realize the important of southwest slope face of Pit MF-10. MRD would like to have this southwest slope face as steep as possible but it is also located next to a small creek (Figure 3.2). The mining law of Thailand indicates that the boundary of the pit shall be at least 50 meters away from any creeks (streams). If the pit boundary is to be less 50 meters from the creek, a proof of mine plan has to be studied and consent by the pertinent government agency. It has been also observed that slope faces at several existing pits experienced a certain degree of slope failures but mainly in erosional fashion, not catastrophic events. During first visit, a few surface samples have been collected for soil classification.

The second attempt was made during Sep 17-19, 2015. During this visit, the mine experienced several small to intense rainfalls resulted in a number of slope failures at Pit MF-10 as shown in Figure 3.4. The failures are obviously triggered by erosional processes.

For the current site investigation, 4 block samples (Table 3.1) have been collected by Block sampling method. These 4 block samples have collection for the soil mechanics laboratory testing. As well as a direct shear test, triaxial test, and some soil basic tests by following the ASTM standard. Block sample no. BMRD-01 and BMRD-02 have been taken

in the dry season while Block Sample No. BMRD-03 and BMRD-04 have been taken in the rainy season. Using block sampling method for minimize the disturbance to the soil samples during the sampling process and transportation. Consequently, the Geotechnical laboratory testing will give rise to the properties as close as to the natural property's condition of the samples.

Table 3. 1 Summary of block samples collection

Sample No.	N (m)	E (m)	Z (m MSL)	Date taken
BMRD-01	1,100,272.47	465,027.42	277.27	17/5/2015
BMDR-02	1,100,253.80	465,063.59	275.71	17/5/2015
BMRD-03	1,100,233.00	465,168.50	252.01	6/10/2015
BMRD-04	1,100,240.62	465,100.58	272.43	7/10/2015

3.4 Geotechnical laboratory testing

Two (2) block samples have been transported to Chulalongkorn University and done lab testing at soil mechanics laboratory of Department of Civil Engineering and some basic soil test at Mining engineering laboratory. The detail of geotechnical laboratory testing as following:

3.4.1 Natural moisture content (ASTM D 2216)

The practical application in determining the water content in material is to determine the mass of water removed by drying the moist material (test specimen) to a constant mass in a drying oven controlled at $110 \pm 5^\circ\text{C}$ and to use this value as the mass of water in the test specimen. The mass of material remaining after oven-drying is used as the mass of the solid particles.

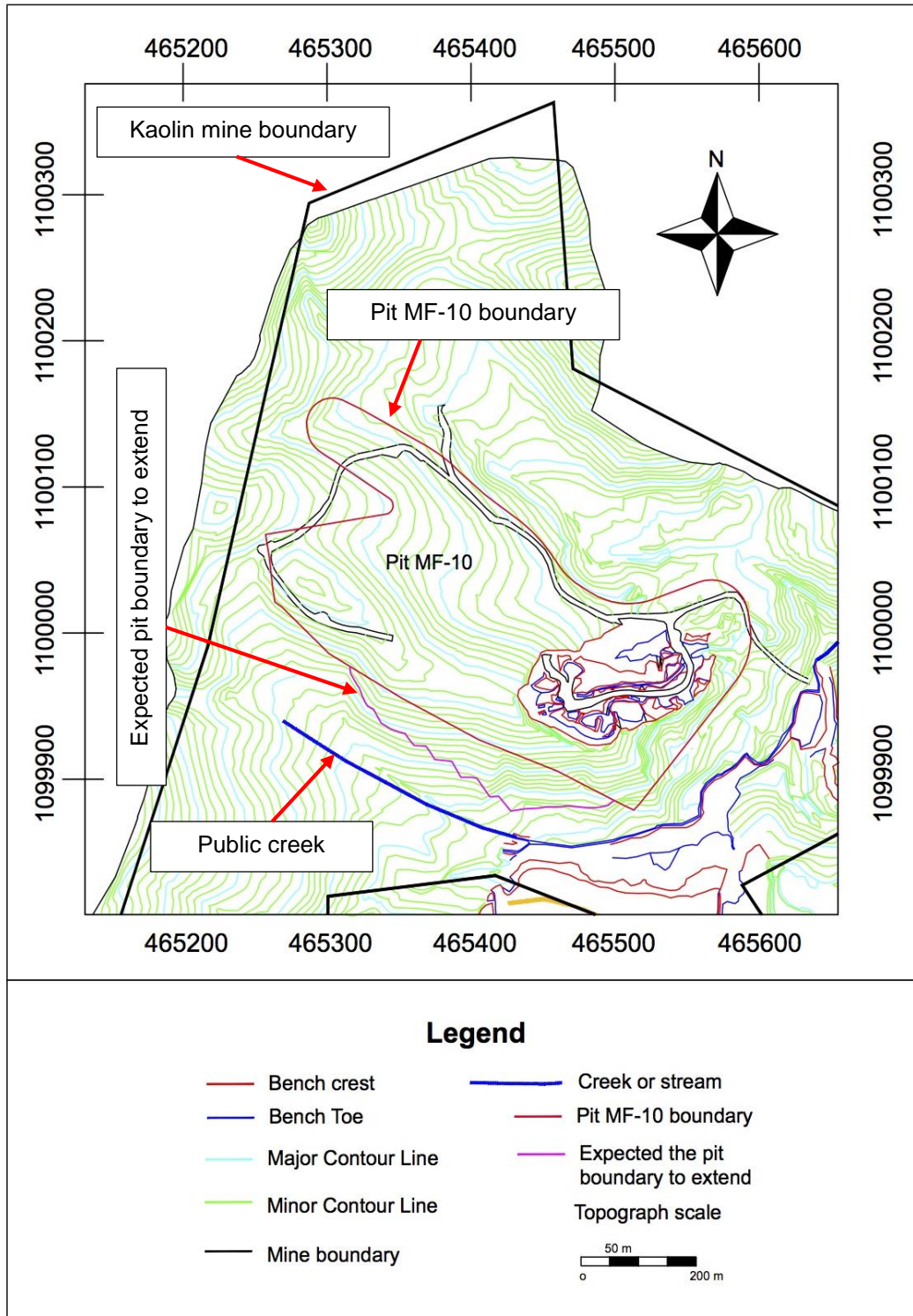


Figure 3. 2 Topo map show an expect the pit boundary to extend

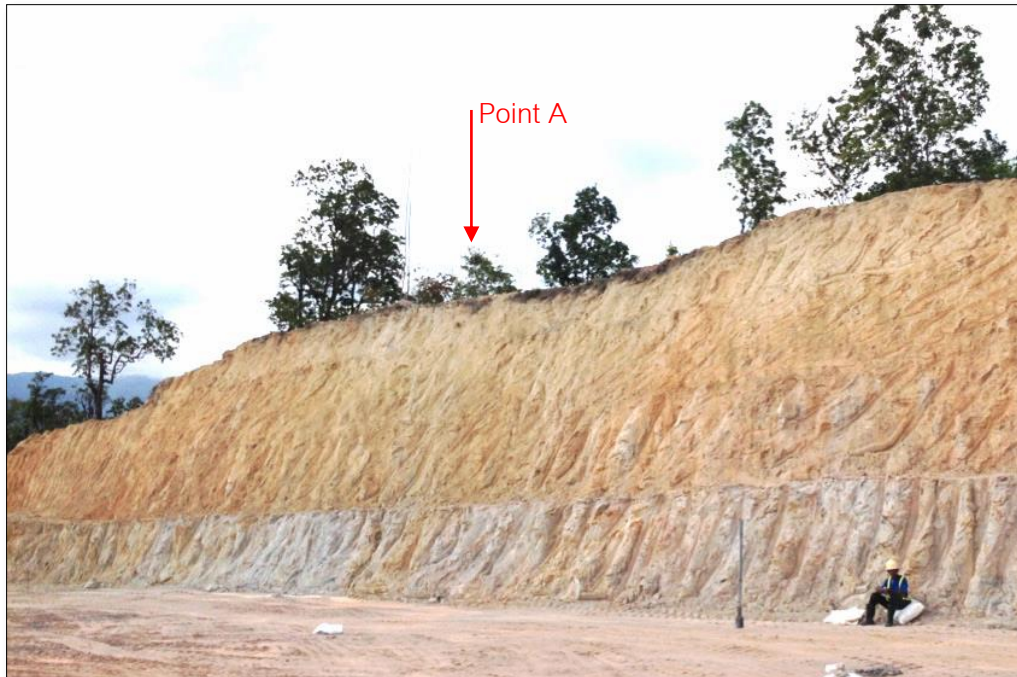


Figure 3. 3 The southwestern slope at Pit MF-10, photo on May 2015

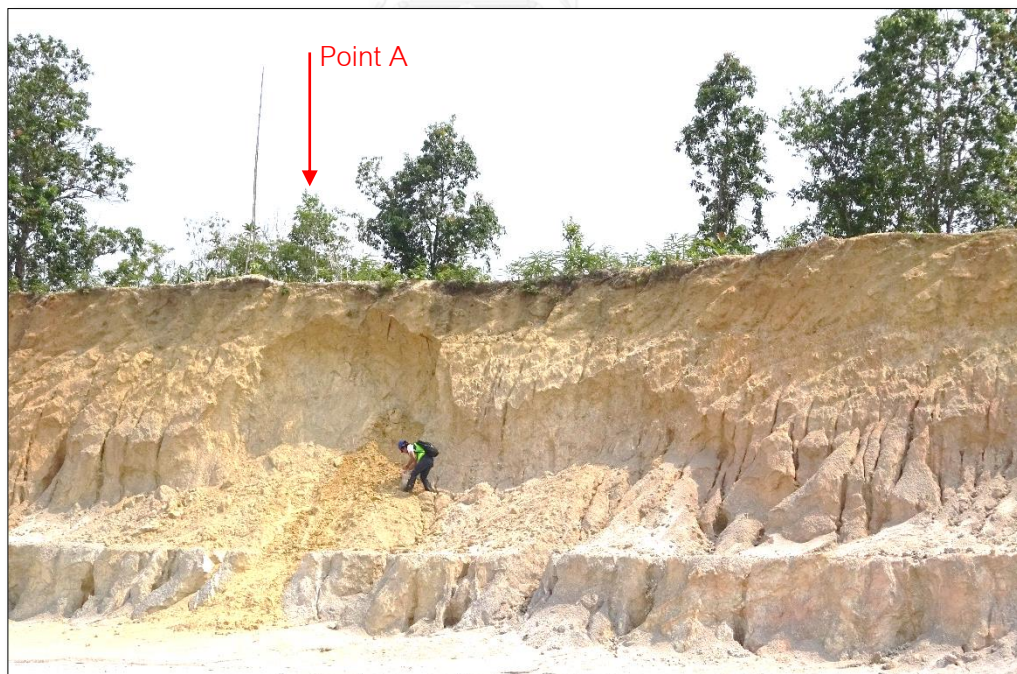


Figure 3. 4 Circular slope failure due to the erosional process in the rainy season at Pit MF-10, Photo on September 2015.

3.4.2 Particle size grading by sieve analysis (ASTM D 422)

This method covers the quantitative determination of the distribution of particle sizes in soils. The distribution of particle sizes larger than $75\ \mu\text{m}$ is determined by sieving. A dry sample of soil is passed through a series of sieves and the weight retained on each sieve is recorded.

3.4.3 Direct shear test (ASTM D 3080)

The shear strength of a specimen depends on the soil type, normal consolidation stress, time of consolidation, rate of strain, and prior stress history of the soil. In this test, the shear strength is measured under constant volume conditions that are equivalent to undrained conditions for a saturated specimen; hence, the test is applicable to field conditions wherein soils have fully consolidated under one set of stresses, and then are subjected to changes in stress without time for further drainage to take place. Three specimens per test on a block soil sample are carried out at different normal stress.



Figure 3. 5 Apparatus used for direct shear test

3.4.4 Unconfined compression test (ASTM D 2166)

The primary purpose of the unconfined compression test is to quickly obtain the approximate compressive strength of soils that sufficient cohesion to permit testing in the unconfined state. In this method, unconfined compressive strength is taken as the maximum load attained per unit area or the load per unit area at 15% axial strain, whichever is secured first during performance of a test. In addition, the undrained shear strength is also use in the design foe stability in practice.



Figure 3. 6 Apparatus used for unconfined compression test

3.4.5 Unconsolidated Undrained Triaxial Test (ASTM D 2664)

The UU triaxial test is performed on intact cylindrical rock samples. The test provides the data for determination of rock strength in an undrained state under 3-D loading. Data from the test can provide, by calculation, the strength and elastic properties of rock sample at various confining pressure, the angle of internal friction, the cohesion intercept and the deformation modulus.



Figure 3. 7 Apparatus used for UU Triaxial test



Figure 3. 8 Remolded specimens used in unconfined compression and UU triaxial test.

3.5 Pit slope and open pit design

The open pit is designed by using a software MineSight (MS). It is for simulating the shape and size of the pit, to visualize the pit boundary and estimate the volumes or tonnage of kaolin that can be excavated.

There are three (3) pits slope design (Figure 3.9, 3.10 and 3.11) for the comparison. The first pit is a base pit or given a name "Pit Version 1" is a final pit design for mining operation at Pit MF-10. It has designed by MRD Company. The distance between this southwestern pit slope and a public creek is about 20 metres.

For second and third pits are the assuming two pits design, names as "Pit Version 2" and "Pit Version 3", respectively. These two pits have a different number of face slope angle (FSA) and overall slope angle (OSA). The pit slope angle of these two pits is steepened than Pit Ver.1 as tabulated in Table 3.2.

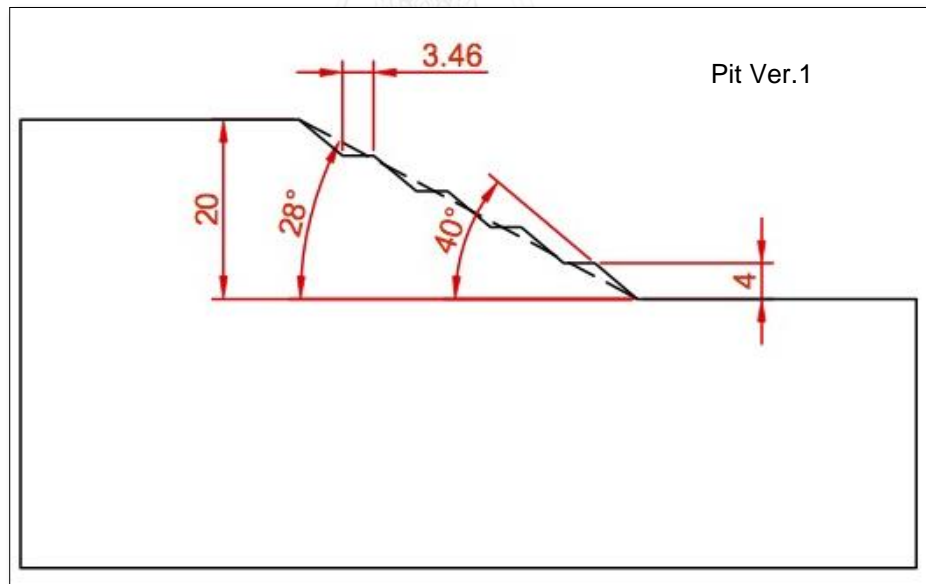


Figure 3. 9 A benches design of Pit Ver.1 (unit is metre and deg.)

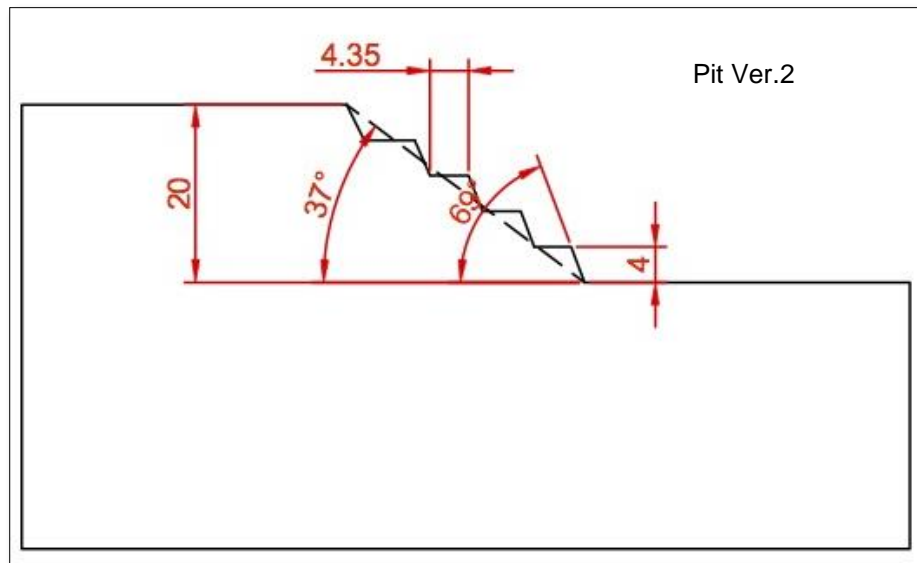


Figure 3. 10 A benches design of Pit Ver.2 (unit is metre and deg.)

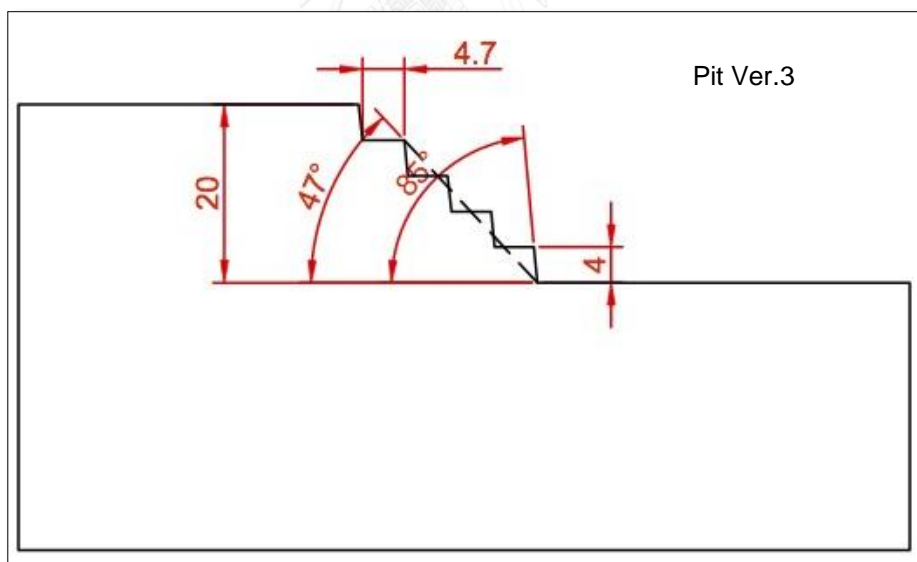


Figure 3. 11 A benches design of Pit Ver.3 (unit is metre and deg.)

Table 3. 2 Summary the benches parameter used in pit design

No.	Face slope angle (°)	Overall slope angle (°)	Bench height (m)	Bench width (m)
Pit Ver.1	40	28	4	3.5
Pit Ver.2	69	37	4	4.3
Pit Ver.3	85	45	4	4.7

In this study, the open pit design will not include the calculation in terms of economic because the researcher cannot get any data related to the economic factor. The design just needs to know the volume and tonnage of kaolin that can calculate by multiplied the obtained kaolin volume from designed with density.

Pit design in this study, the work is based on data gathered from the exploration drilling programs executed by MRD. A total of 205 samples data from 12 drill holes were used for the analysis. The drill holes fell within 1099956 and 1100161 Northing, and 465297 and 465616 Easting of local coordinates system. The work of pit design was divided into some essential steps as bellow:

- Topo map and drill holes data preparation.
- Loading and creation of database.
- Creation of solid 3D model.
- Creation the block model.
- Block grade estimation.
- Pit design.

The detail of each steps will separate describe in a minor topics bellow.

3.5.1 Topo map and drill holes data preparation

Topo map (Figure 3.12) is the contour lines of the area Pit MF-10. The topo map file in this study is a file exported from AutoCAD software. The format of this file is .dxf (Drawing eXchange Format). It is contained the polyline of contour line, and the located

coordinate is 465070 and 465810 Easting, and 1099696 and 1100416 Northing, approximated the total areas of this study is 532,800 square metres.

For drill-hole (DH) data files are obtained from the core drilling log, and laboratory testing. There are four files in terms of numerical data file, such as Assay, Collar, Survey, and Lithology, the format of these files are .csv (Comma-Separate Value). They have edited and exported from the Microsoft Excel. Some example as tabulate in Table 3.3 – 3.6.

Table 3. 3 Part of the Collar file (collar.csv)

Hole_id	X (m)	Y (m)	Z (m_MSL)	Max_Depth (m)
MRD-106C	465298.34	1100030.12	293.68	33
MRD-108C	465388.27	1100039.65	269.06	43.5
MRD-114C	465544.22	1099955.52	251.36	40

Table 3. 4 Part of the Survey file (survey.csv)

Hole id.	From (m)	To (m)	Azimuth (°)	Dip (°)
MRD-106C	0	33	0	-90
MRD-108C	0	43.5	0	-90
MRD-114C	0	40	0	-90

Table 3. 5 Part of the Assay file (assay.csv)

Hole_id	From (m)	To (m)	Interval (m)	% whiteness KLN
MRD-106C	5.5	8	2.5	77.41
MRD-108C	4.5	7.2	2.7	90.79
MRD-114C	3	5.5	2.5	61.28

*Remark: KLN is Kaolinite and GRA is hard Granite.

Table 3. 6 Part of the Lithology file (litho.csv)

Hole_id	From (m)	To (m)	Rock_Code	Rock_Type
MRD-106C	0	2.5	1	SAND
MRD-108C	4.5	42.9	2	KLN
MRD-114C	38.7	40	3	GRA

For all detail of these DH data files will demonstrate in Appendix I.

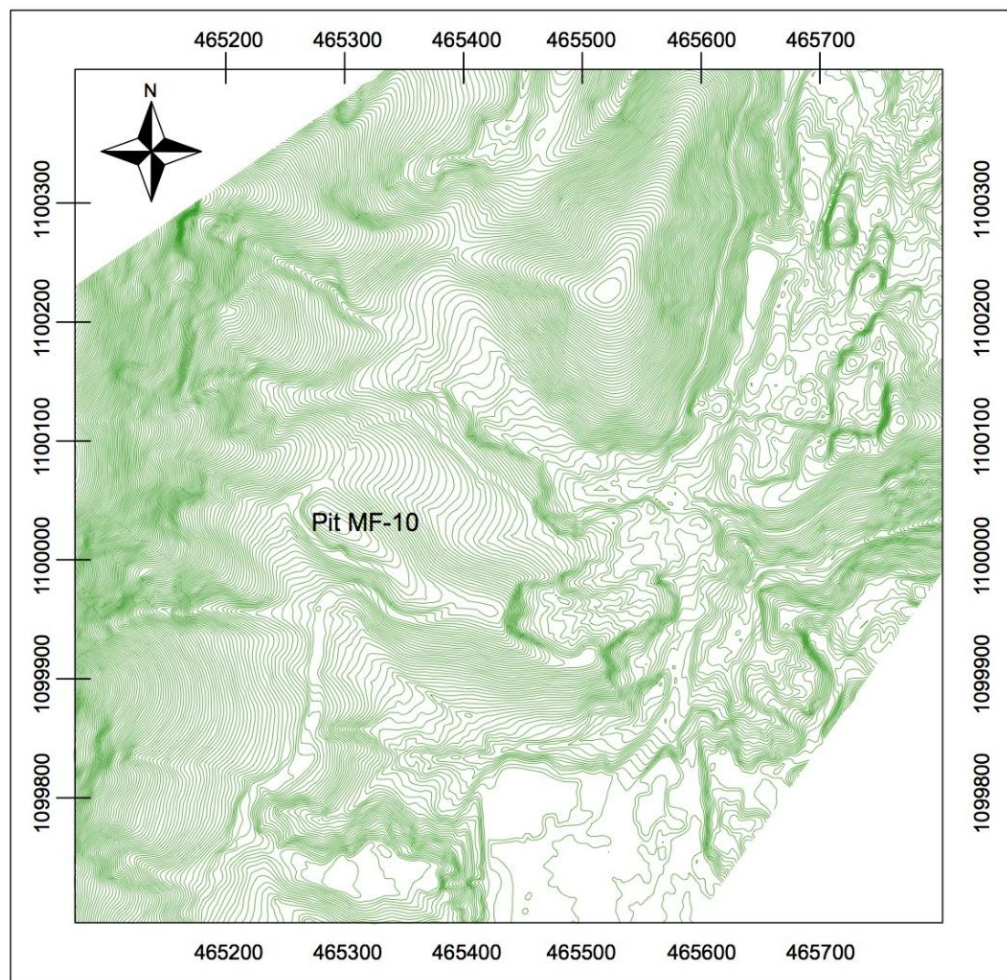


Figure 3. 12 Top view the topo map of Pit MF-10 used for pit design

3.5.2 Loading and creation of data base

This is a prerequisite for database processing and also constitutes a data validation procedure whereby any data input whose description or structure is inconsistent with the definitions made at the database creation stage is rejected. When the database is loaded, it is then ready for data processing, extraction, plotting and reporting. There is also room for data update.

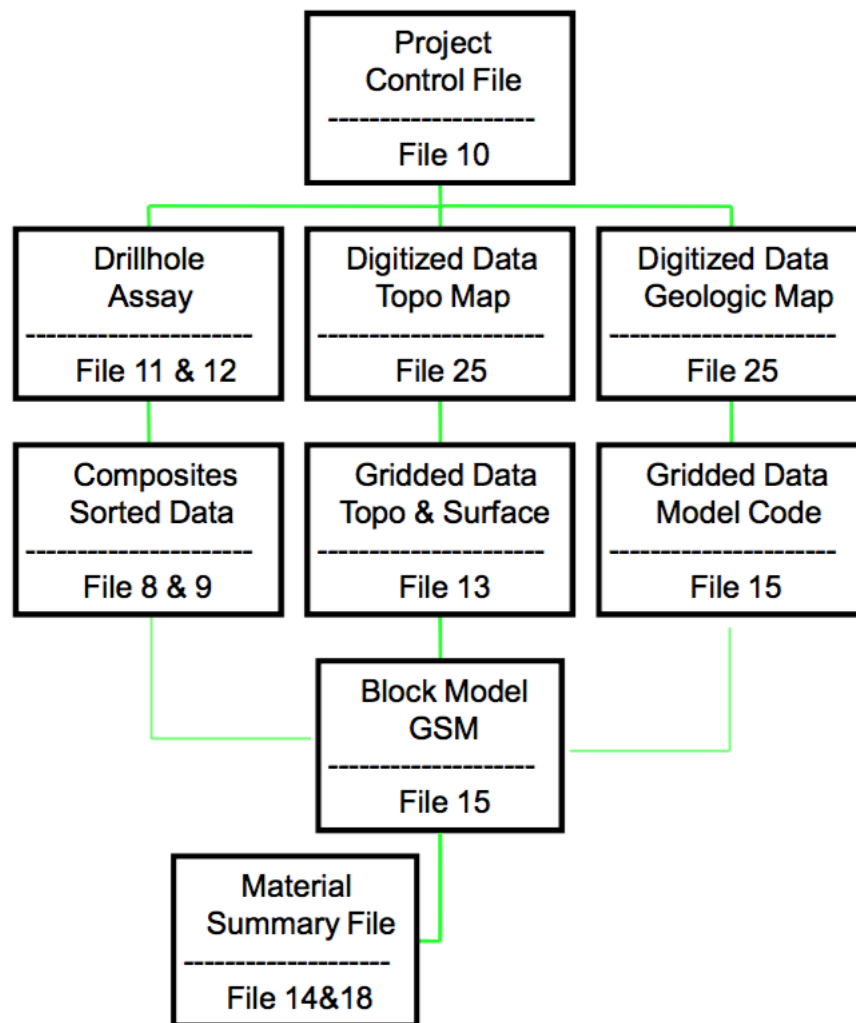
After loading the database, DH layout and sections of the deposit were extracted from the database for plotting and display. The DH layout serves two significant functions:

- 1) It assists mining engineers and geologists to know the pattern of the drill holes and decide as to which planes to take the sections through; and
- 2) It assists mining engineers and geologists to check DH collar coordinates against manually prepared maps as a way of verifying the data (Appianing & Mireku-Gyimah, 2015).

In the MS software, for a completely one project it is necessary to creation some files as described and illustrated in the flowchart (Figure 3.13) bellow:

- File 10 is a MS main data file or a project control file. It is contained all information about the project such as project control area and others minor creation files.
- File 11 is a MS assay file. It is contained the detail of DH assay which are imported.
- File 12 is a MS survey file. It is contained the DH survey information which are imported.
- File 8 and 9 are MS DH composites and sorted data file. These files are contained the compositing grade of ore.
- File 25 is a MS digital file. It is contained the topo map information.
- File 13 is a MS gridded surface file (GSF) or surface model. Used to store elevation data for surface or other types of 2D gridded data.

File 15 is a MS 3D block model (3DBM) file. Used to store the information of 3DBM such as size of block, specific gravity of the material. Etc.



CHULALONGKORN UNIVERSITY

Figure 3. 13 Flowchart of the steps for creation necessary files in MS software.

3.5.3 Creation of solid zone

The demarcated solid zones in the sections were digitized on-screen in clockwise direction to form closed segments that were stitched together to form a wireframe model. This wireframe model was then validated to form a solid model (Figure 3.14). The output files formed at the end of digitizing became ore zone string files which were saved and given a location name and ID range (Figure 3.15)

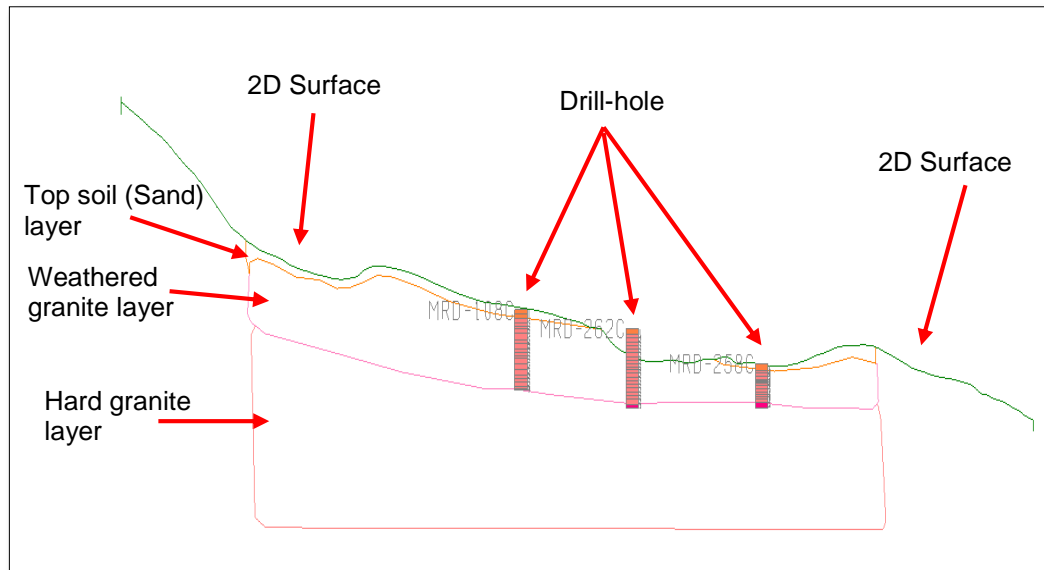


Figure 3. 14 Digitized zone section in 2D (Grid set EW, Plane No. North1100046)

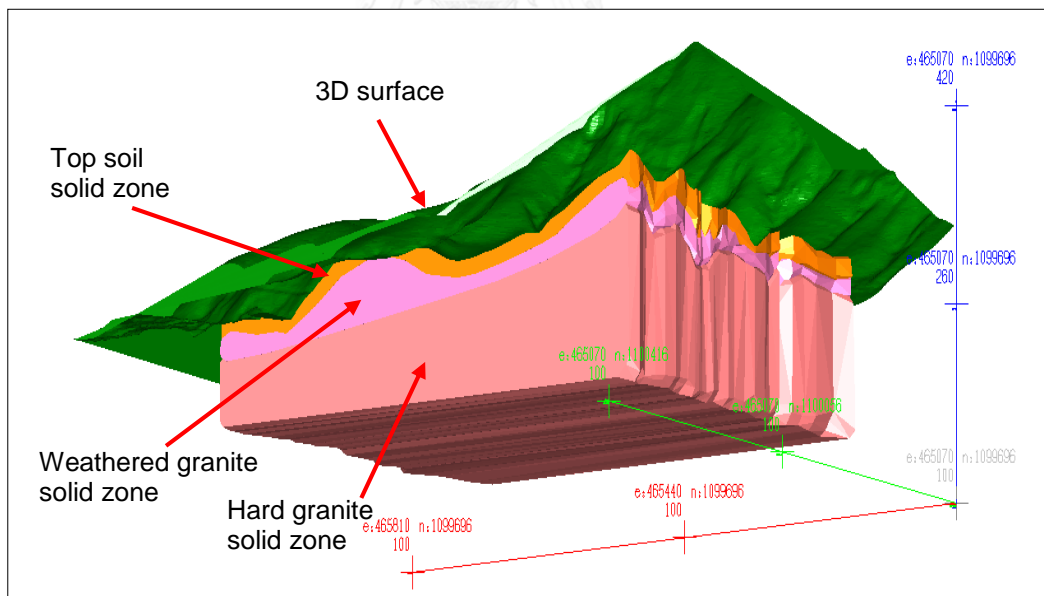


Figure 3. 15 Solid model of other rocks and ore body

From Figure 3.14, it is one of the many sections 2D view for digitized. The spacing of each section in this study equal to 5 metres.

3.5.4 Creation the 3D block model

The following steps were taken to create the block model:

- Empty block model:

An empty block model was created with the following information: block model identification name, origin, extent, and block size (Fig. 3.16). A user block size of 10 m × 10 m × 4 m was used to conform with mining bench width and height.

- Adding constraints:

The addition of constraints was primarily to control the selection of blocks from which interpolations were made or from which information was obtained. Blocks falling within the solid model were ore and waste while blocks falling outside the topography were air blocks.

- Filling the model with attribute values:

At this stage, the empty block model (Figure 3.17) was fill with attribute values. The attributes are the properties to be employed during the pit design. These were % whiteness of kaolin, specific gravity (rock density equal to 2.65), and rock code (code No. 1 stand for Sand, No. 2 stand for Weathered granite, and No. 3 stand for Hard granite).

3.5.5 Block grade estimation

The grade of each block in the block model was estimated using Inverse Distance Weighting (IDW) method, expressed in Equation (2.7), which is available as a module in MS software.

$$g_B = \frac{\sum_{i=1}^n \frac{g_i}{d_i^m}}{\sum_{i=1}^n \frac{1}{d_i^m}} \quad (2.7)$$

In this study, a power index of +2 was considered to used, because this +2 power is an acceptable and widely used in many researches of mine feasibility study. Other assuming parameters are an approximate search distance equal to 100 metres for X

(Easting) and Y (Northing) direction, and search distance for Z (Height or elevation) equal to 15 metres.

3.5.6 Pit design

In this study, pit design for Pit Ver.2 and 3 have to be followed an overall bench height and boundary of Pit design Ver.1 (Figure 3.18) (Pit Ver.1 designed by MRD). The benches parameter used in the pit design was tabulated in Table 3.2.

In this step, a module Pit expansion tool in MS software used for drawing the polyline, and design the pit haul road. A first drawing polyline of every pit is a toe or a bottom of the pit, it was started from the elevation 228 m. MSL and the highest crest of final pit elevation is about 318 m. MSL.

For pit design, a bottom of the pit was beneath under the Pit MF-10 area. A pit bottom has been drawing and edited in the horizontal plane section. Then, expand this bottom outward to the vertical direction by spacing up within 4 metres. For example, the pit bottom started from elevation 228 m. MSL and used pit expansion tool to expand the bench outward in the vertical direction up by 4 metres, next bench from this step was located in the elevation 232 m. MSL. Do like this until the pit expand up on the surface.

The pit haul road design, it was started from elevation 230 m. MSL, Road's width equal to 11 metres, and Road's grade is 10%. A pit haul road in this study was designed by spiral system, it means a haul road is arranged spirally along the perimeter wall of the pit.

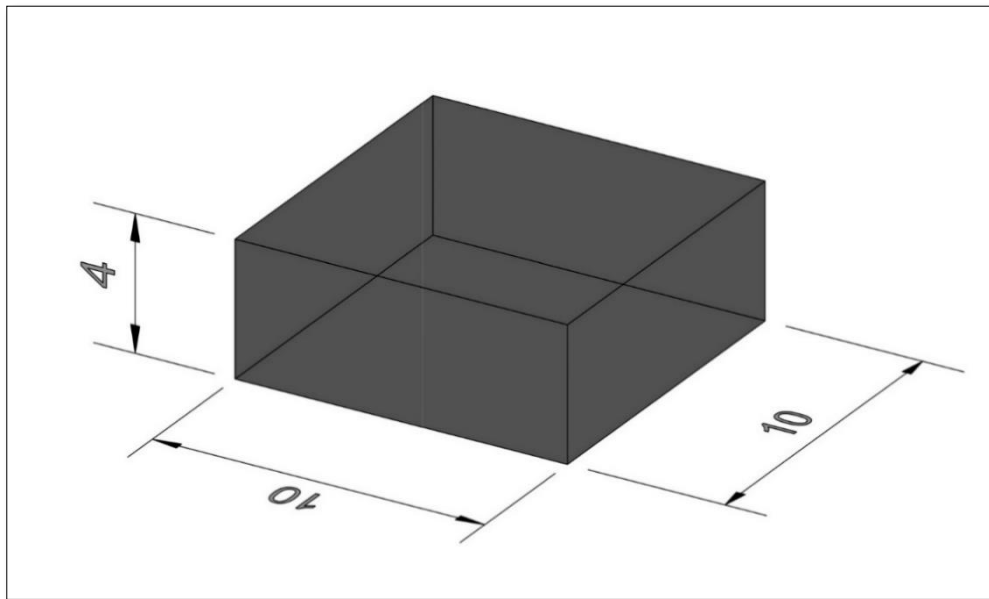


Figure 3. 16 Size of 3DBM used in pits design (10 m x 10 m x 4 m)

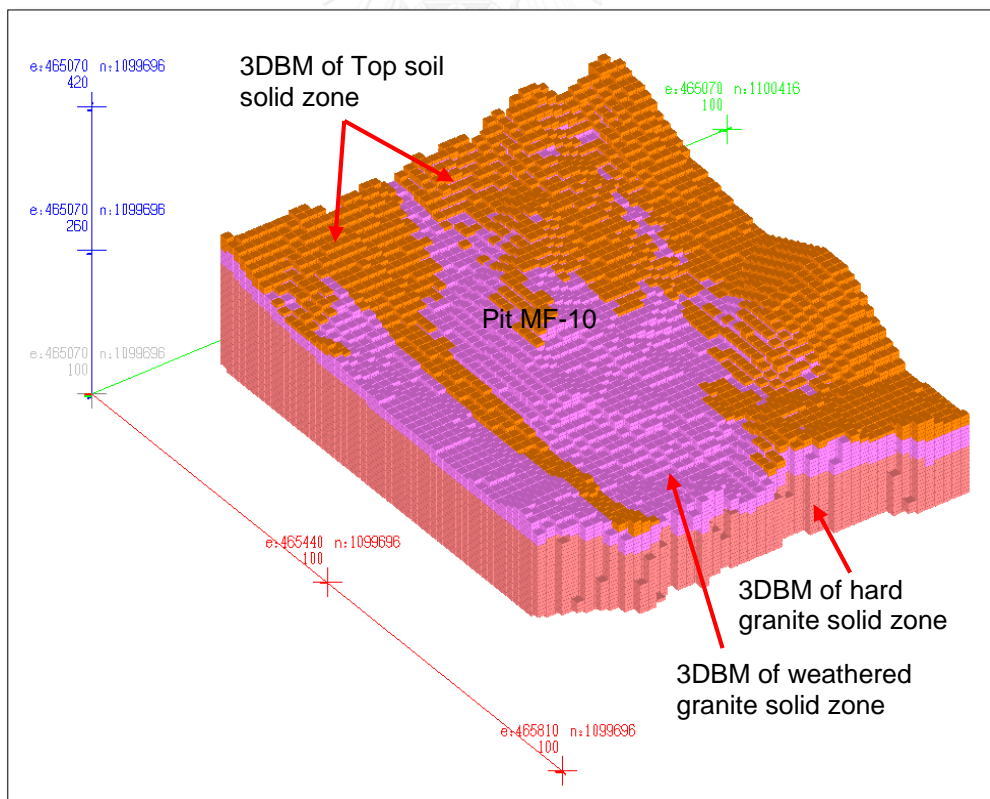


Figure 3. 17 3DBM of three solid zones

3.6 Pit slope stability analysis

Numerical modeling analysis method was used in this study for pit slope stability analysis. A different slope models of analysis have established in FLAC3D. The shape of the slope has obtained from the pit design. In this study, three (3) pits design (Figure 3.9, 3.10 and 3.11) is containing different FSA and OSA (comparison as illustrated in Figure 3.19) have to be analyzed, and compared the FOS results. The purpose of compared FOS is for observing the changing of slope stability behavior when increased the value of FSA and OSA.

For the slope failure criteria on pit design, it has followed to the regulations of the Department of Primary Industries and Mines, Thailand. The “Safety Manual for Mining Activities” (Phairat, 2014) has written some criteria about the open pit mining design. The OSA should be less than 45 degrees and the FOS must more than 1.50 (for long term mining slope) and $FOS \geq 1.3$ (for short term mining slope). The detail of creation slope geometry model (SGM) for analysis, and assigning the geomaterials properties (GMP) were describe in a sub topics bellow.

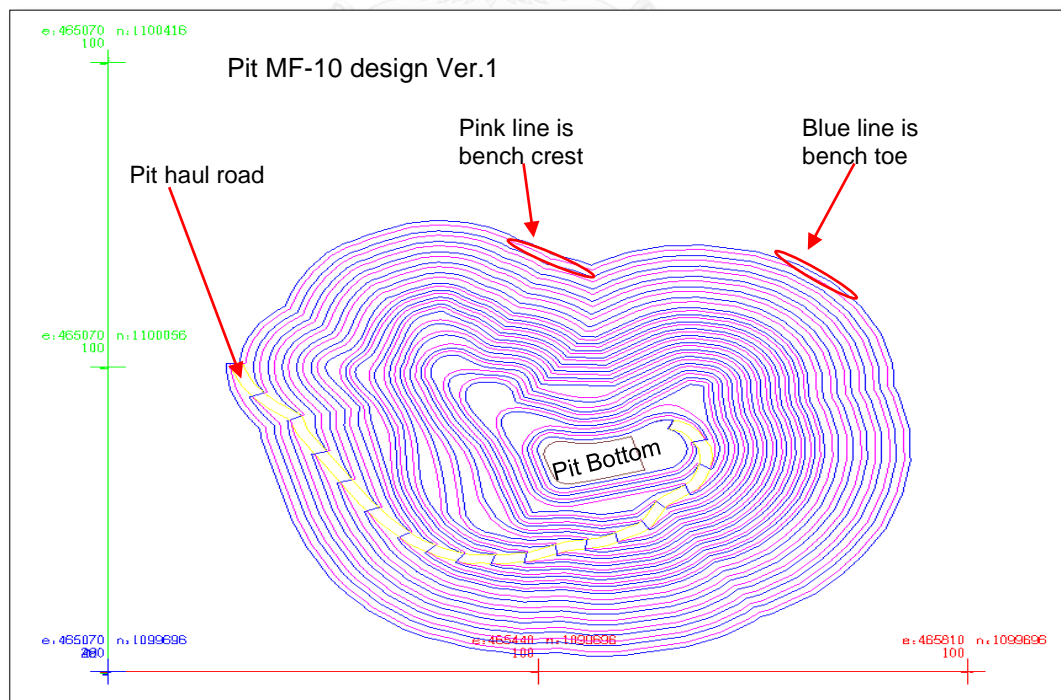


Figure 3. 18 Top view of Pit design Ver. 1

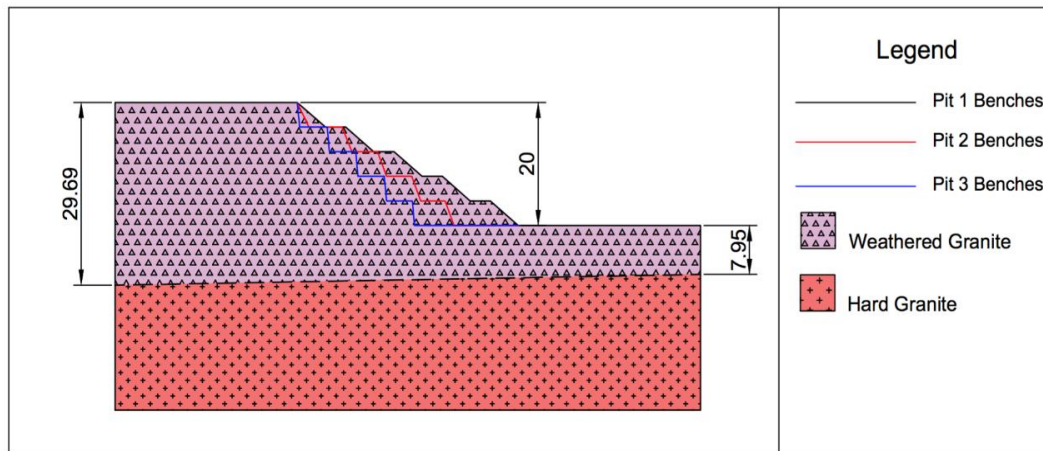


Figure 3. 19 Comparison the different benches design SGM of Pit Ver.1, 2, and 3 (unit is metre)

3.6.1 Creation SGM, and assigning GMP for the final Pit slope design Ver.1, 2, and 3

Using AutoCAD software for drawing and designed the SGM in 2D mode (Figure 3.9, 3.10, and 3.11). Then, exported those SGMs in the format file .dxf, and imported those files individually into the FLAC3D software. In FLAC3D, there are two ways to build the SGM as following:

- 1) Used an Extrusion tool to drawing and digitized follow the SGM edges line and shape.
- 2) Used the Generate command to input the points located of SGM.

These two methods, there are different advantages and disadvantages. For an extrusion method, it is suitable for using with a small project, because this method analysis case by case or only one geometry per case in FLAC3D. Another one method is using Generate command, this method suitable for a project needs an analysis more than two models because this method can use the Call command to operate a many generate zone, and it can automatic running the slope stability analysis when we setting everything in completely.

The dimension of geometry model (in X and Z-axis), it was followed by a minimum of dimension shape in Figure 2.2. For an SGM's width (Y-axis) in this study, using the

dimension of Y-axis equal to one (1) unit, because it can save time in analysis process more than a widely SGM. Less width of SGM is not a problem, the FOS results of less width and widely width SGM is also obtained as the same value when assigning the same value of GMP and zones size. The examples (Figure 3.20 and 3.21) of two cases will show us to prove this sentences.

GMP parameter requires as describe in the topic No. 2.3 Mohr coulomb model:

- 1) Bulk modulus (K) used consistently for each material.
- 2) Shear modulus (G) used consistently for each material.
- 3) Young's modulus (E) used consistently for each material.
- 4) Poisson's ratio (ν) used consistently for each material.
- 5) Friction (ϕ) changed up on the sample's value.
- 6) Cohesion (c) changed up on the sample's value.
- 7) Tensile strength (T) used consistently for each material.

For creation SGM of Pit design Ver.1, 2, and 3 were followed the method above.

The detail of each model as describe bellow:

- SGM of analysis for Pit Ver.1 in this topic was obtained from a final pit design. The assigning GMP, using the results from laboratory testing of four block samples. There are 12 cases of the total test results (Table 4.1). Consequently, slope stability analysis for the final pit of Pit Ver.1 has to be running in 12 cases as tabulated in Table 3.7. The SGM dimension of analysis for this pit as illustrated in Figure 3.22.
- SGM of analysis for Pit Ver.2 is also obtained from the final pit design. For the assigning GMP was using the same value like GMP used in Pit Ver.1. There are also 12 cases of analysis for this model (Table 3.7). The dimension as illustrated in Figure 3.23.
- SGM of analysis for Pit Ver.3 is also followed two pits above (Table 3.7). This SGM dimension is illustrated in Figure 3.24.

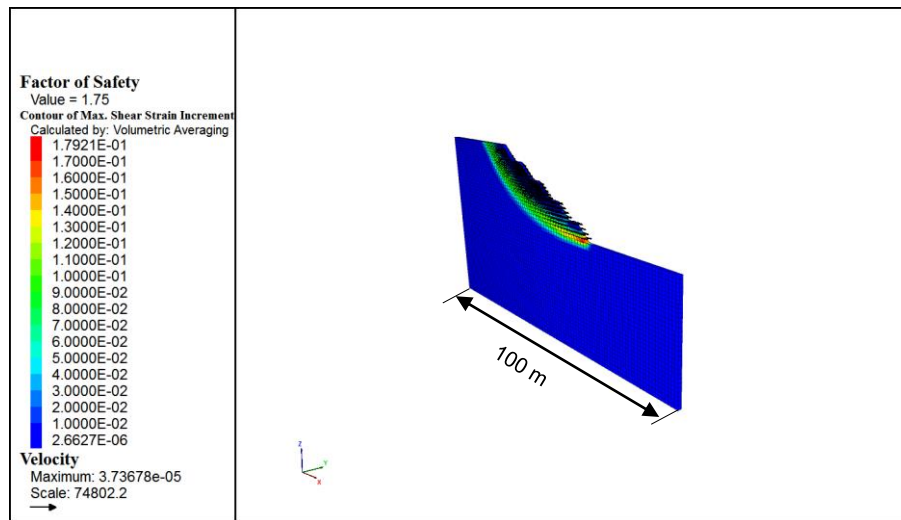


Figure 3. 20 Example of analysis while SGM's width = 1 m, $C = 21.2$ kPa, $\phi = 26.2^\circ$, and obtained of FOS = 1.75

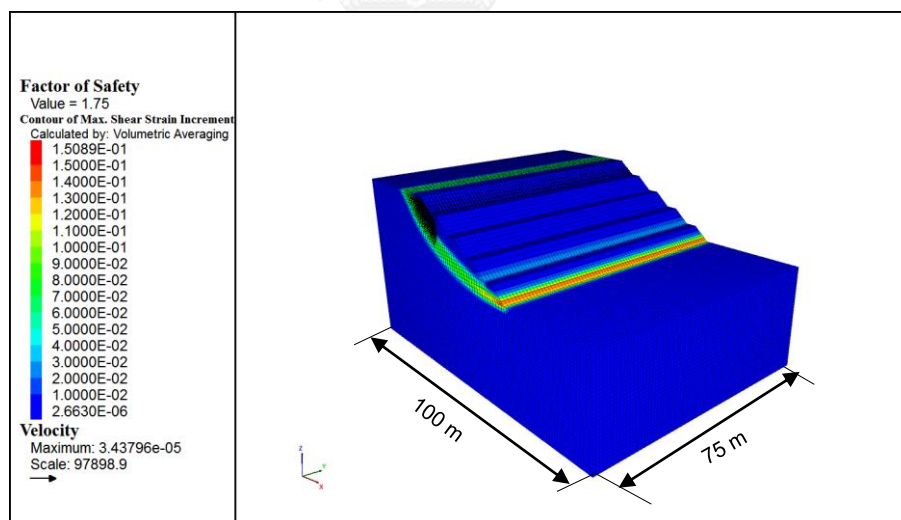


Figure 3. 21 Example of analysis while SGM's width = 75 m, $C = 21.2$ kPa, $\phi = 26.2^\circ$, and obtained of FOS = 1.75

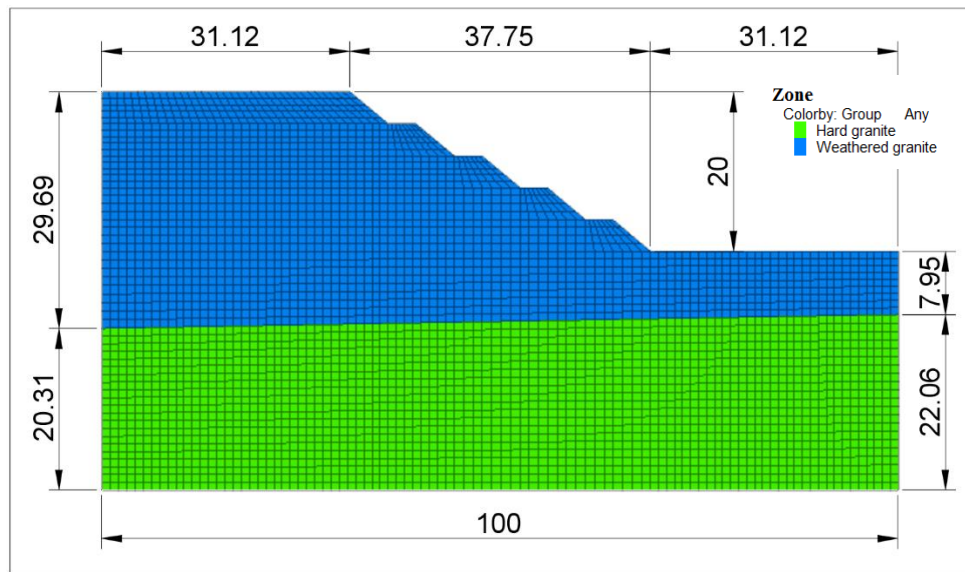


Figure 3. 22 The SGM dimension shape of analysis for final Pit design Ver.1

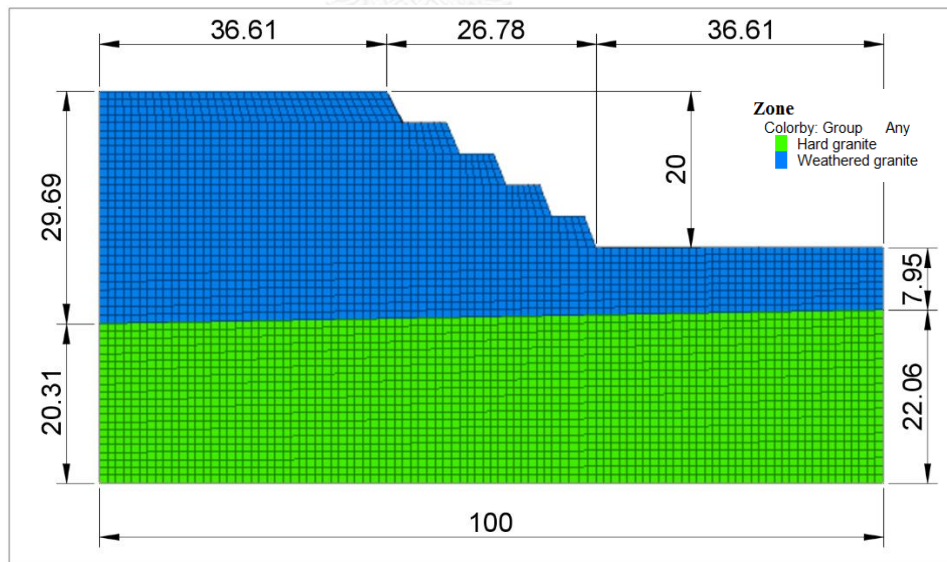


Figure 3. 23 The SGM dimension shape of analysis for final Pit design Ver.2

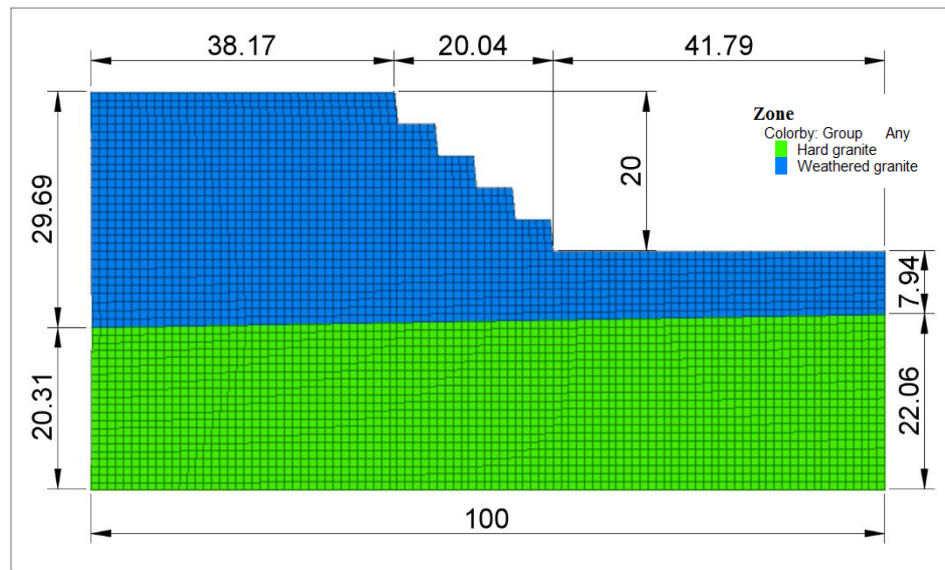


Figure 3. 24 The SGM dimension shape of analysis for final Pit design Ver.3

Table 3. 7 Summary the analytical cases for SGM of final Pit design Ver.1, 2, and 3

No.	Final pit design	Number of SGM	GMP Parameters, c & ϕ (case)	Analytical Case (case)
1	Pit Ver.1	1	12	12
2	Pit Ver.2	1	12	12
3	Pit Ver.3	1	12	12
Total		3		36

*Remark: in this step, there are totally 36 analytical cases for 3 final pit slope design of Pit Ver.1, 2, and 3.

For the results of analysis from FLAC3D are demonstrated in Appendix II.

3.6.2 Creation SGM, and assigning GMP for the cross-section of Pit Ver. 1, 2, and 3.

After pit design completely, this step was used for checking those slope benches stability. The cross-section of those pits have been created. The SGM dimension is obtained from the cross-section line. There are three (3) cross-section models for each

pit, and four (4) SGMs per pit need to analyzed in FLAC3D (summary in Table 3.8). Consequently, there are totally 12 SGMs of analysis in this step.

The assigned GMP in this step were chosen the cohesion and frictional angle that are making a minimum FOS of slope stability analysis in the topic 3.6.1. There is cohesion = 13.9 kPa, and Frictional angle = 28.5 deg. The SGMs of analysis in this topic are demonstrated in Appendix III.

Table 3. 8 Summary the analytical cases for cross-section model of Pit Ver.1, 2, and 3

No.	Final pit design	Number of cross-section (model)	Number of SGM (model)	GMP Parameters, c & ϕ (case)	Analytical Case (case)
1	Pit Ver.1	3	4	1	4
2	Pit Ver.2	3	4	1	4
3	Pit Ver.3	3	4	1	4
Total		9	12		12

3.6.3 Creation SGM, and assigning GMP for the assuming bench of trial pit slope (Short term mining slope)

In this step, SGM was created by assuming face slope angle and bench height for simulated a condition of trial pit slope. The SGM dimension as tabulated in Table 3.7. The method of design SGM is paring a different number of bench height with α_{20} , α_{30} , α_{40} ,..., α_{90} ; (α is a face slope angle).

The assigned GMP in this step were chosen the cohesion and frictional angle that are making a minimum FOS of slope stability analysis in the topic 3.6.1. Chosen cohesion = 13.9 kPa, and Frictional angle = 28.5 deg.

The detail of SGMs of analysis are demonstrated in Appendix IV.

Table 3. 9 Summary the analytical cases for assuming bench model of trial pit slope

No.	Bench height (m)	Face slope angle (°)								Number of SGM (model)	Analytical Case (case)
		α_{20}	α_{30}	α_{40}	α_{50}	α_{60}	α_{70}	α_{80}	α_{90}		
1	4	20	30	40	50	60	70	80	90	8	8
2	8	20	30	40	50	60	70	80	90	8	8
3	12	20	30	40	50	60	70	80	90	8	8
4	16	20	30	40	50	60	70	80	90	8	8
5	20	20	30	40	50	60	70	80	90	8	8
Total										40	40

*Remark: Bench height paring with each number of Face slope angle. It has 8 SGMs per each number of bench height. There are total 40 SGMs of analysis in this step

CHAPTER IV

RESULTS AND DISCUSSIONS

4.1 Results of site investigation and Laboratory testing

According to previous studies (GDP, 2010b); (GDP, 2013) of site investigation and the results from laboratory testing, it can make more understanding about the properties of kaolin's deposit materials. The kaolin is weathered granite with a very low permeability. When the rainy season arrived, the pit slopes always have some small failures (experiencing slope failure in Figure 4.1) because the water cannot infiltrate fast enough, forming big runoff flowing from the crest to toe of the slope. Rapid runoff can erode these weak materials easily and then trigger slope failure (Figure 4.2).

For the geotechnical laboratory testing, it is impossible to prepare the natural condition of kaolin specimens used in Unconfined Compression test and Triaxial test. So the specimens have to be prepared by the remold method. In this case however, there is a problem that the kaolin block samples contained both the coarse-grained size of quartz and kaolin clay. They are having a very different grain size distribution, so when we tried to split or build the specimens shape and size, it always collapses. Even though the remold specimens cannot simulate the actual condition of geomaterials in the pit, it still simulates the closest condition for strength testing and get some data to support the slope stability analysis. Some testing data results show in Table 4.1. For the detail of geotechnical laboratory testing are demonstrated in Appendix V.

Table 4. 1 Summary the results of kaolin strength testing

Sample ID	Direct Shear		UU Triaxial		CU Triaxial			
	c (kPa)	ϕ (°)	c (kPa)	ϕ (°)	c (kPa)	ϕ (°)	c' (kPa)	ϕ' (°)
BMRD-01	21.2	26.2	116.0	4.0	37.0	21.0	50.0	27.0
BMRD-02	31.1	24.8	124.0	3.0	43.0	25.0	54.0	30.0
BMRD-03	13.9	28.5	134.9	8.0				
BMRD-04	13.7	57.6	178.1	6.0				



Figure 4. 1 Typical plane failure on kaolin slope at pit MF-2C. (May 2, 2015)



Figure 4. 2 Experience of erosional on kaolin slope due the affected from rain-flow.

Photo slope at pit MF-2C. (May 2, 2015)

From the results of strength testing in Table 4.1, we can see that strength of material is quite high and not certain. The reasons of this matter maybe those kaolin samples are weathered granite, and there are still some old properties of granite rock. As can see the curve of particle size distribution in Figure 4.3, there is a big portion of coarse grains which are belong to size Quartz (Figure 4.4).

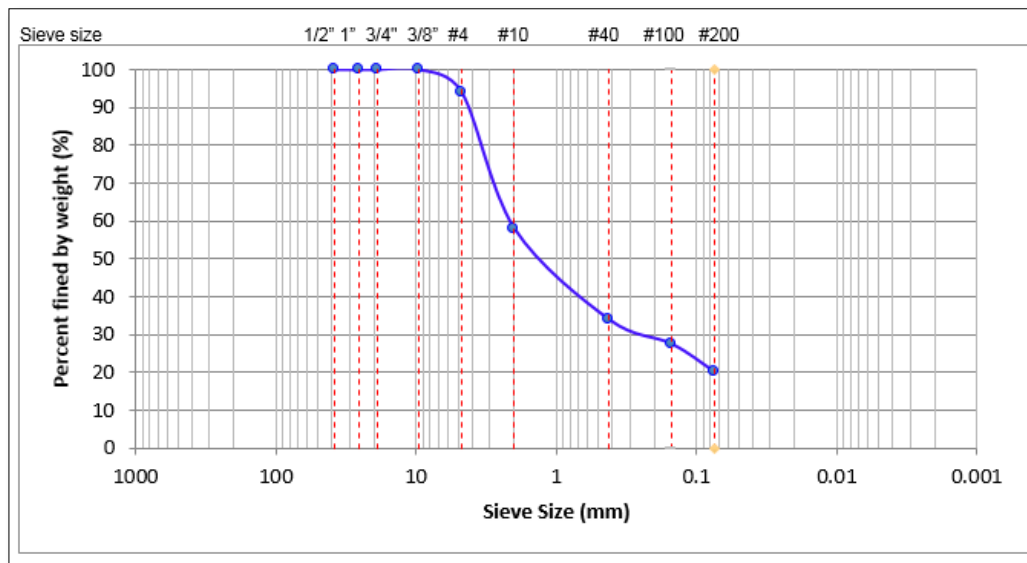


Figure 4. 3 Particle size distribution of block sample no. BMRD-03



Figure 4. 4 Coarse-grained size of quartz in kaolin mine, photo at the floor of Pit MF-10

4.2 Results of open pit design

4.2.1 Drill-hole data analysis

In the processing plant of MRD's kaolin mine, they were using combination of a few parameters to be criteria cutoff grade for kaolin such as %Yield, Casting rate, and %Whiteness. In this study, the researcher cannot get the data of %Yield, and Casting rate. Consequently, this study used %Whiteness of kaolin to be a grade cutoff. %Whiteness of kaolin has been obtained from the measurement of kaolin's whiteness before and after burned. To see the grade or %whiteness of kaolin distribution, they need to be plotted by histogram, and cumulative distribution curve as tabulated in Table 4.3 and illustrated in Figure 4.5.

Table 4. 2 Information of Drill-hole data

Unit	Min	Max	Average	Number of DH samples
Easting (m)	465297	465616	-	-
Northing (m)	1099956	1100161	-	-
Elevation (m. MSL)	211	291	-	-
%Whiteness of kaolin	0	93.9	68.7	205

Table 4. 3 Cumulative frequency of kaolin grade

Grade Interval %	Bin %	Frequency (No.)	Cumulative %
45 - 50	49	0	0.00%
50 - 55	54	8	4.68%
55 - 60	59	2	5.85%
60 - 65	64	7	9.94%
65 - 70	69	4	12.28%
70 - 75	74	2	13.45%
75 - 80	79	23	26.90%
80 - 85	84	29	43.86%
85 - 90	89	54	75.44%
90 - 95	94	42	100.00%
95 - 100	99	0	100.00%

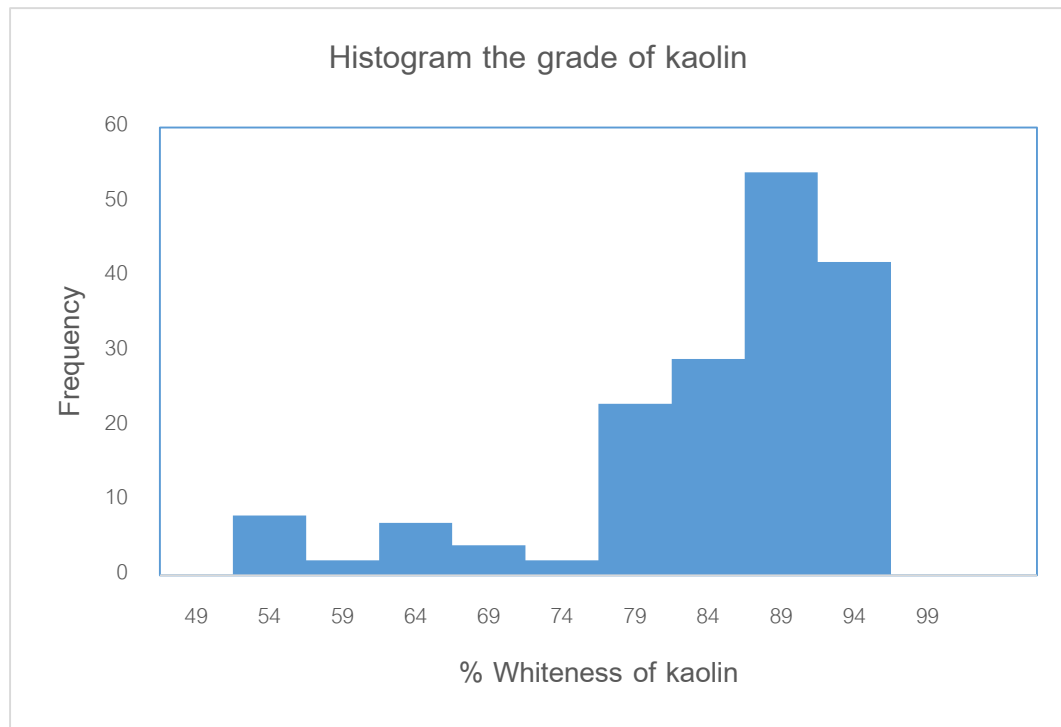


Figure 4. 5 Histogram plotting show the distribution grade of kaolin

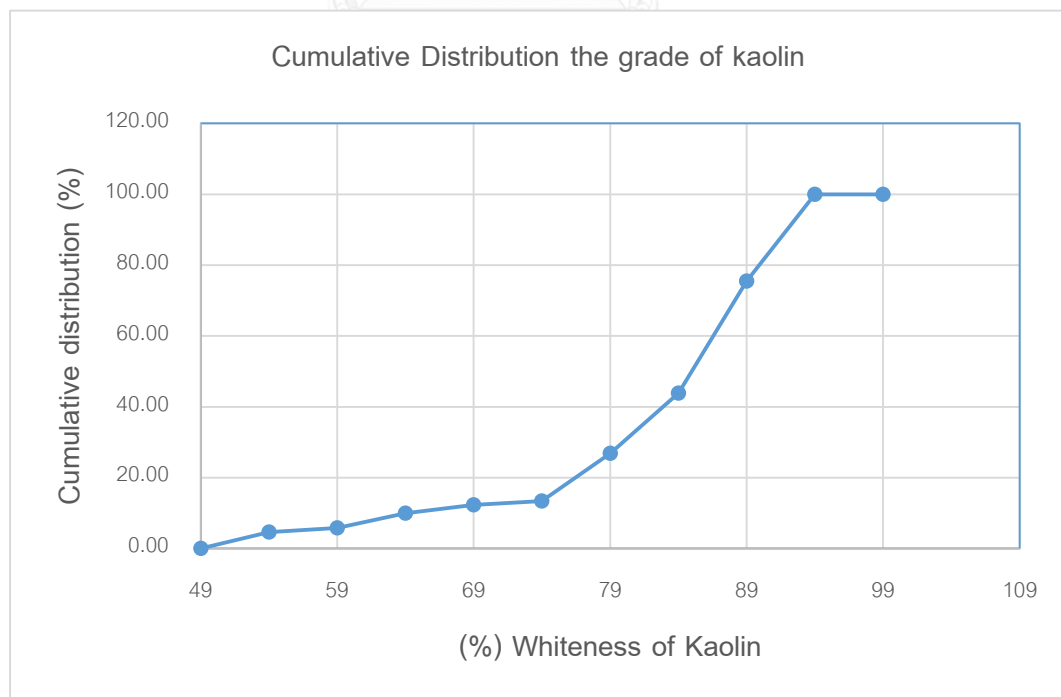


Figure 4. 6 Cumulative curve plotting the distribution grade of kaolin

As observed the frequency grade of kaolin in Table 4.3 and some plotting graph above, high frequency are located in the interval 85-90 (54 samples), and 90-95 (42 samples). That mean the quality of kaolin in these drill-hole (DH) data are quite high.

According to DH data, the distance interval grade of kaolin is varied from 1.5 to 3 metres. For open pit design, the grade of kaolin has to be compositing. In this study, the grade of kaolin was composited by Benches Compositing Method. The interval level of Benches compositing equals to 4 metres. As we see a comparison between DH assay and grade after compositing in Figure 4.7. Those numbers at the right hand side is DH assay, and numbers on the left is composited grade.

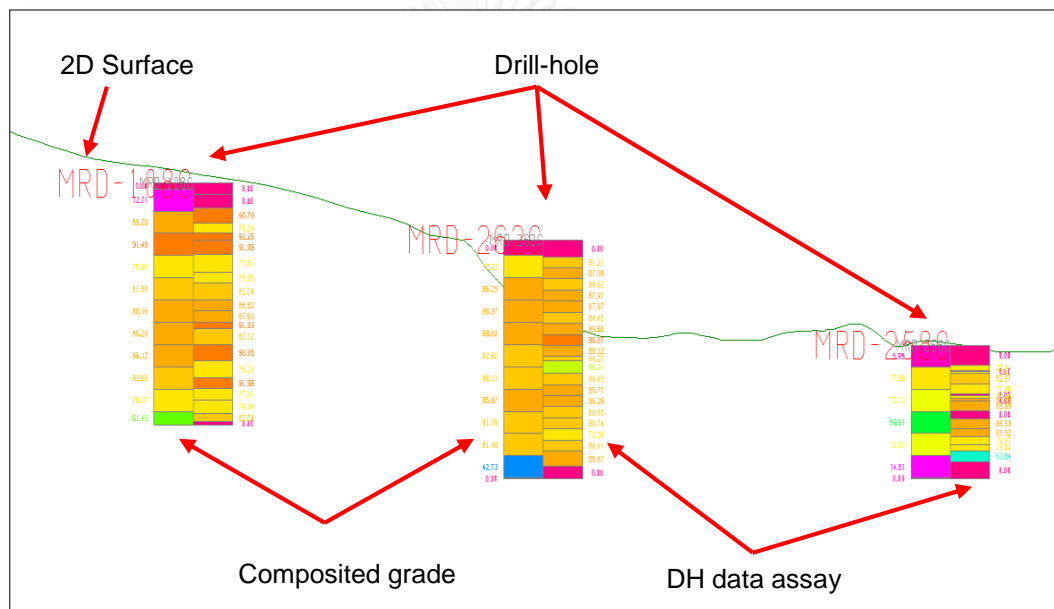


Figure 4. 7 2D view a comparison DH data assay and composited grade of kaolin
The detail of bench compositing grade are demonstrated in Appendix I.

4.2.2 Geological model

Four (4) data files are containing the detail of twelve (12) DHs, and one (1) topo map have been loaded to be a data base of this project in MineSight. The geological model boundary is delineated within the study area, grid coordinates 465070 to 465810 Easting, and 1099696 to 1100416 Northing. Locations of 12 DHs are superimposed with the topography represented by the contour lines and DH ID (red color) as seen in Figure

4.8 and 4.9. In Figure 4.8, it shows the boundary of 3D model encompassing study volume and DH data, the top view of topographic and DH data are shown in Figure 4.9.

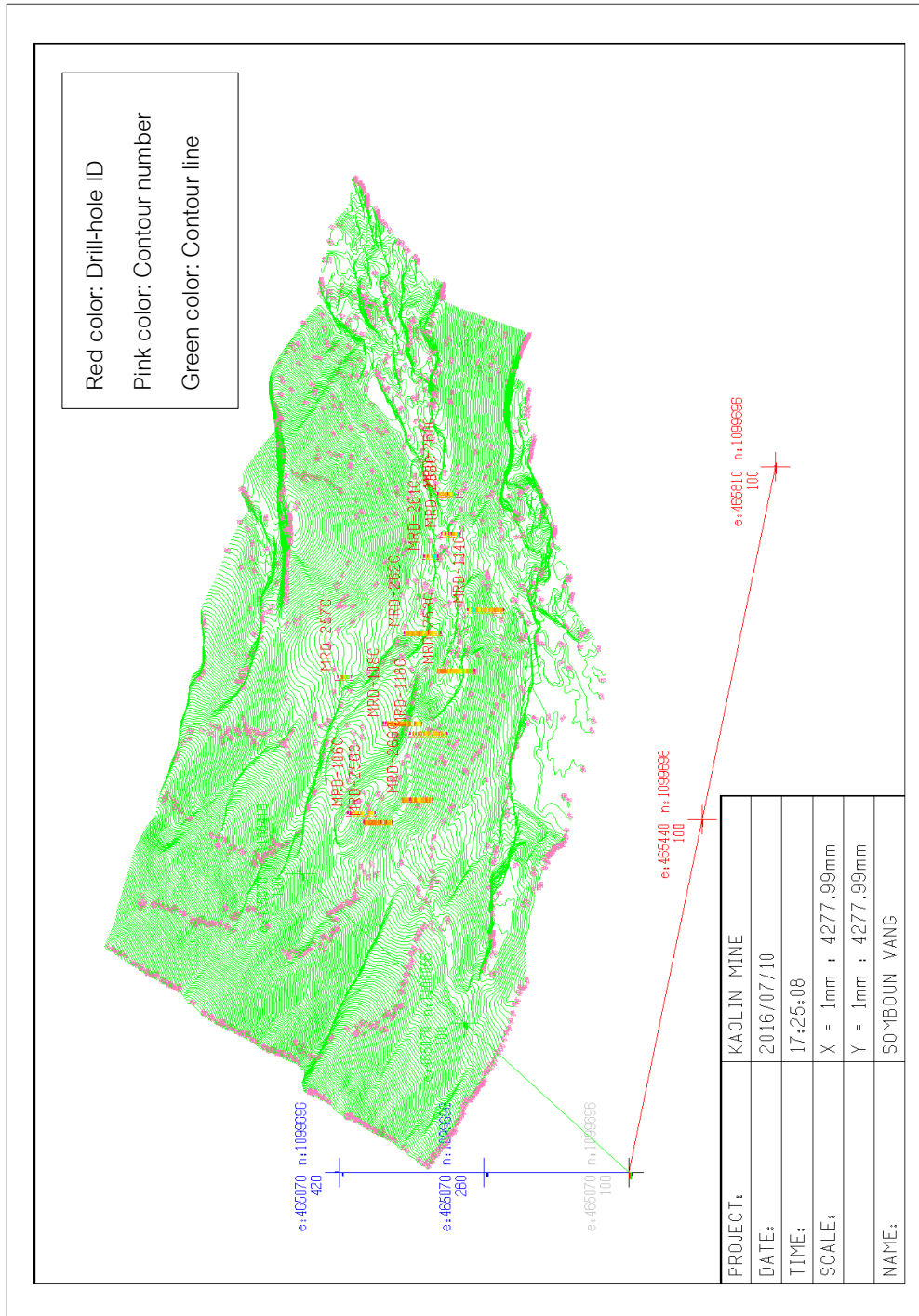


Figure 4. 8 Overview of drill-hole and topography in 3D model

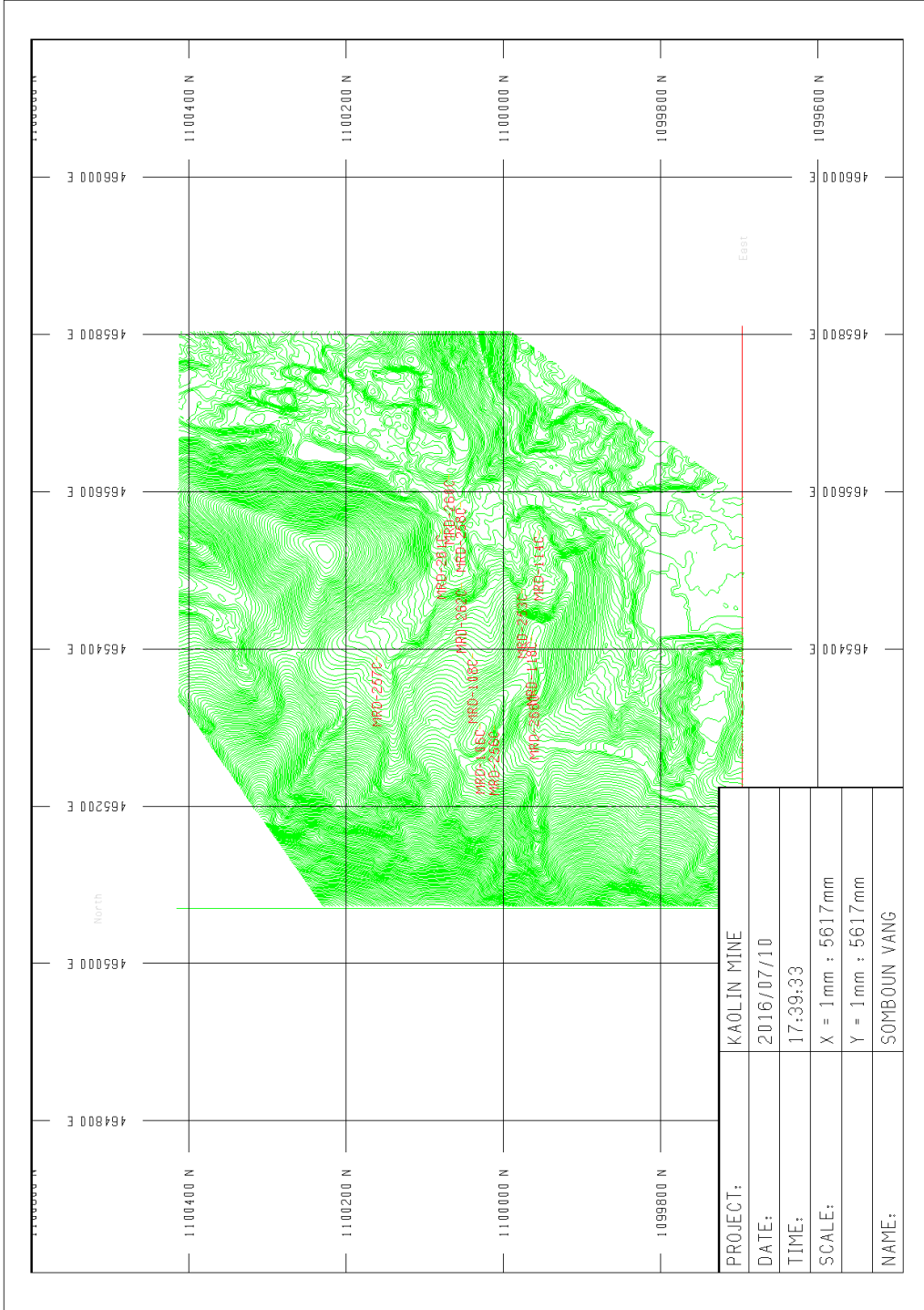


Figure 4. 9 Top view of drill-hole location

4.2.3 3D block model, its grade, and resource estimation

3D block model has been developed from the creation solid zone of each type of rock. The solid zone was created by digitized following the rock code are contained in DH data. In this study, there are three (3) zones or three layers of soil and rock. Zone No.1 is Topsoil or silty sand, Zone no.2 is weathered granite or ore zone. And zone no.3 is hard rock granite (Figure 3.17).

Inverse Distance Squared Weighting method (IDW) was used for calculating the block grade. In this study, the dimension of searching distance of all blocks is selected equal to 100 m x 100 m x (-15 m) (X, Y, and Z- Axis), respectively. The 3D block dimension size is set as 10 m x 10 m x 4 m (X, Y, and Z) as illustrated in Figure 3.16. Resulting from IDW searching, the total numbers of estimated block is 19,527 blocks. Each block contained 400 cubic metres, and given the density of kaolin equal to 1.8 metric tons per cubic metre. Then, resource estimation is calculated by the equation (4.1) below:

$$\text{Resource} = \text{Numbers of estimated block} \times \text{Block volume} \times \text{Density} \quad (4.1)$$

$$\rightarrow \text{Resource} = (19,527 \text{ Blocks}) \times (400 \text{ m}^3/\text{block}) \times (1.8 \text{ tons/m}^3) \approx 14 \text{ Million metric tons}$$

* Remark: This resource estimate is not yet included or multiplied the grade of kaolin. So, after multiply by grade of kaolin, it may reflect the real resource tonnage.

Generally, the estimated blocks are gathered around the DH, distance extending 100 metres from the center of DH as seen in Figure 4.10. Hence, the numbers of estimated blocks is depended upon the searching distance of IDW. It is true that the more of searching distance has been defined the more numbers of estimated blocks obtained, but in terms of quality, the blocks are located very far from DH center, the block grade is might not correct. Finally, kaolin grade distribution of each block was presented by range color in Figure 4.11.

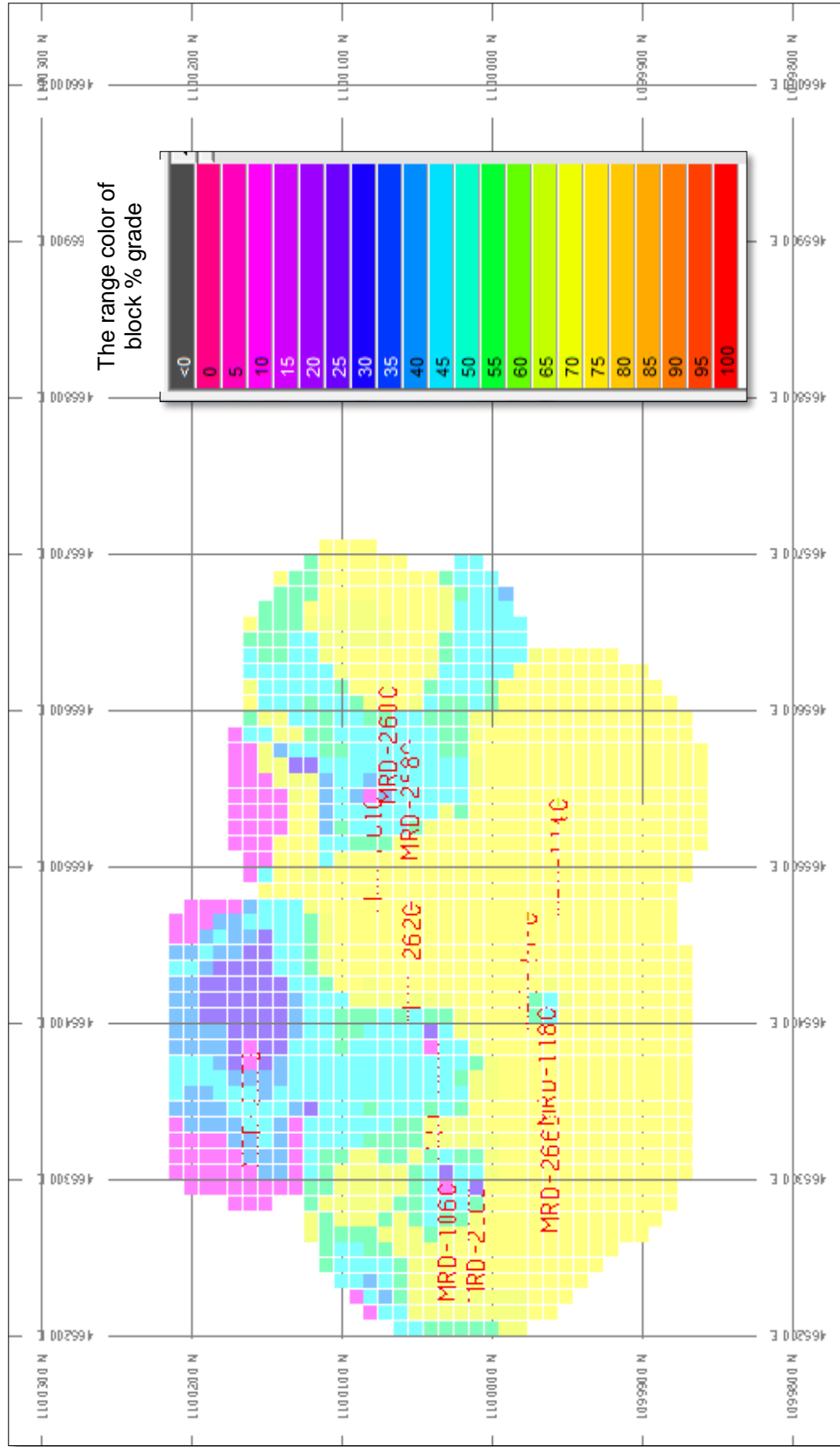


Figure 4. 10 Top view the results of estimated block from IDW method for kaolin

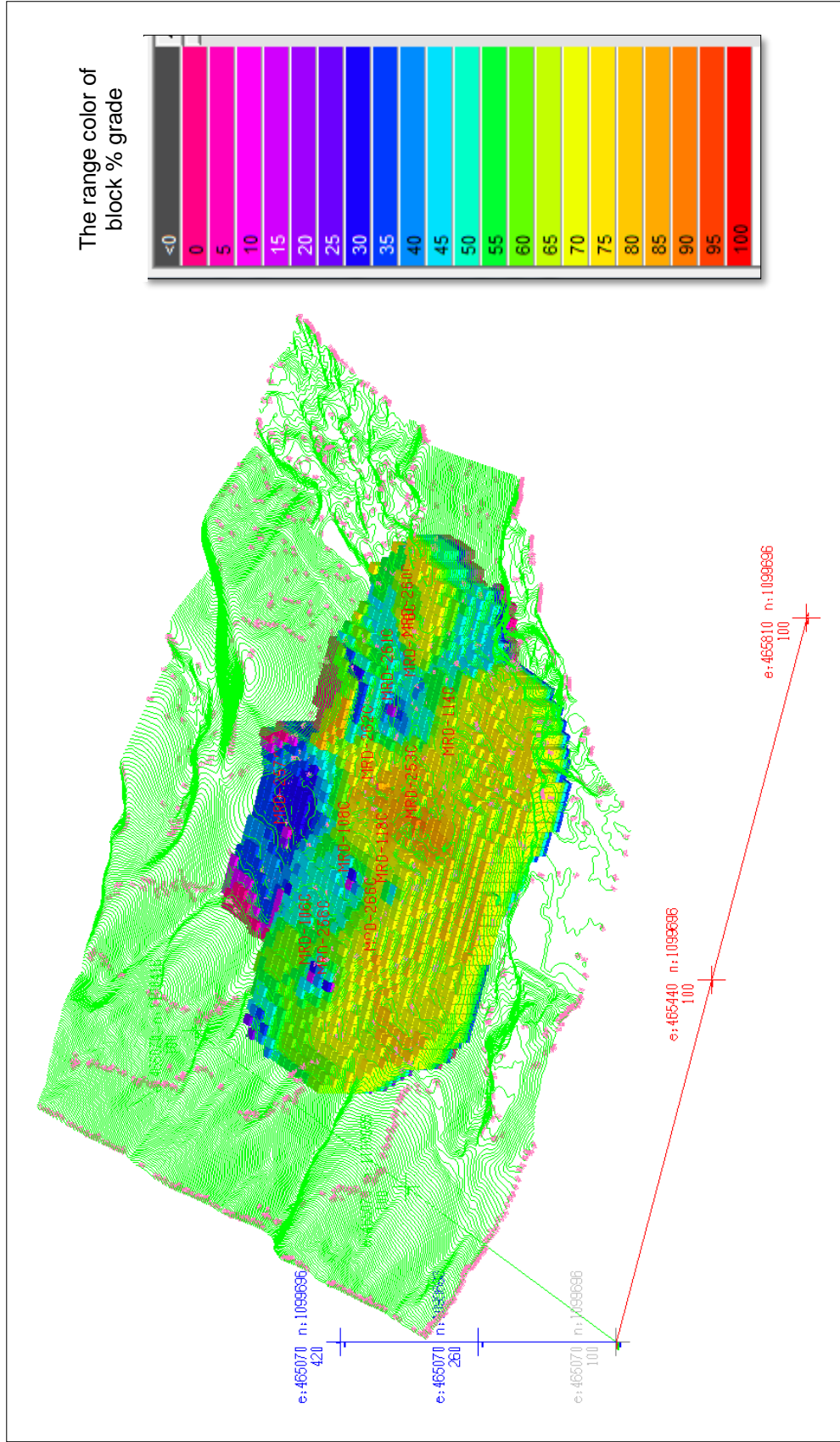


Figure 4. 11 3D view the results of estimated block from IDW method for kaolin

4.2.4 Open pit design and reserves estimation

As described in sub-topic on “3.5.6 Pit design”. The Pit design Ver.2 and 3 were followed by the designing of Pit Ver.1. After pit designed, we can see the shape and pit boundary (Figure 4.12, 4.14, and 4.16). Then, it is able to know the volumes or tonnages of kaolin and waste (Table 4.4). It is also able to see the distribution grade of kaolin in estimated block as demonstrated in Figure 4.13, 4.15 and 4.17 respectively. In the figures of pit design (Figure 4.12, 4.14 and 4.16), the shape of Pit Ver.1, 2, and 3 are quite similar, but actually, those pits are very different in terms of benches face slope angle (FSA) and overall slope angle (OSA). As we already knew the more steep the benches slope angle, the resulting with more ore reserve will be, as tabulate in Table 4.4.

For Pit designed Ver.1, the ore reserve (OR_1) estimation equal to 1.4 million metric tons, overburden (OB_1) is 144,000 metric tons, and the stripping ratio (SR_1) is 0.10; Pit Ver.2 has been obtained OR_2 equal to 1.7 million metric tons, $OB_2 = 145,500$ metric tons, and $SR_2 = 0.08$; and Pit Ver.3, the OR_3 equals to 1.8 million tons, $OB_3 = 148,500$ metric tons and last one is $SR_3 = 0.08$. Following the open pit designed in this study, we can see the stripping ratio is very small, because the top-soil of this area are very thin thickness, thus, it can minimize the mining cost and increase of benefits.

It is desired to have boundary of pit design covering the area of high grade estimated blocks. The grade of estimated 3D blocks is separated by the range color as demonstrated in Figure 4.13, 4.15 and 4.17. For the vertical direction of pit design, it can distinguish the 3D block grade distribution in the cross-section at Figure 4.18, 4.19 and 4.20.

Table 4. 4 Summary the ore reserve and overburden of Pit design Ver.1, 2, and 3

Pit No.	Identify	Volume (m ³)	Density (t/m ³)	Reserves Tonnage & Overburden (Metric ton)	Stripping ratio
Pit Ver.1	Waste	96,000	1.5	144,000	0.10
	Weathered granite	818,889	1.8	1,474,000	
Pit Ver.2	Waste	97,000	1.5	145,500	0.08
	Weathered granite	974,824	1.8	1,754,683	
Pit Ver.3	Waste	99,000	1.5	148,500	0.08
	Weathered granite	1,011,819	1.8	1,821,274	

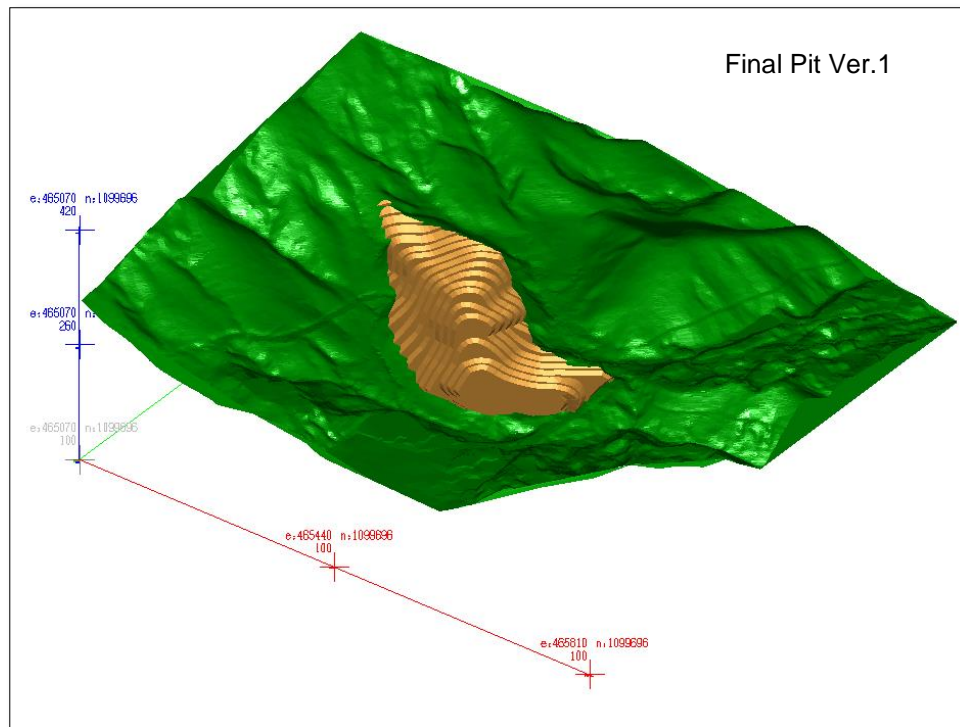


Figure 4. 12 3D view of final Pit designed Ver.1

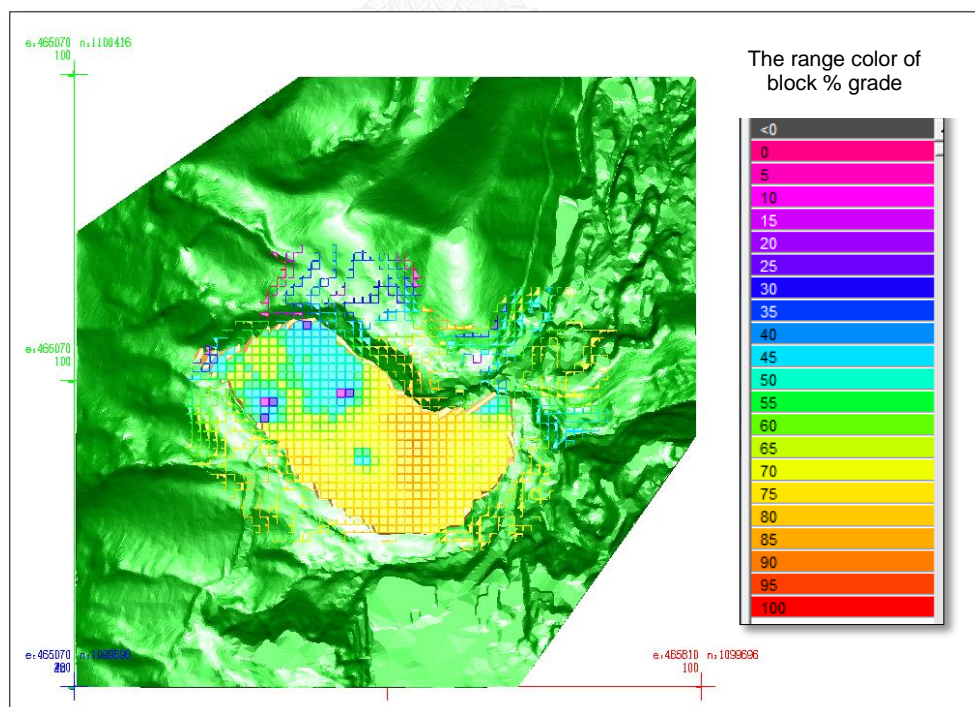


Figure 4. 13 Top view of Pit Ver.1 and its 3D blocks distribution grade

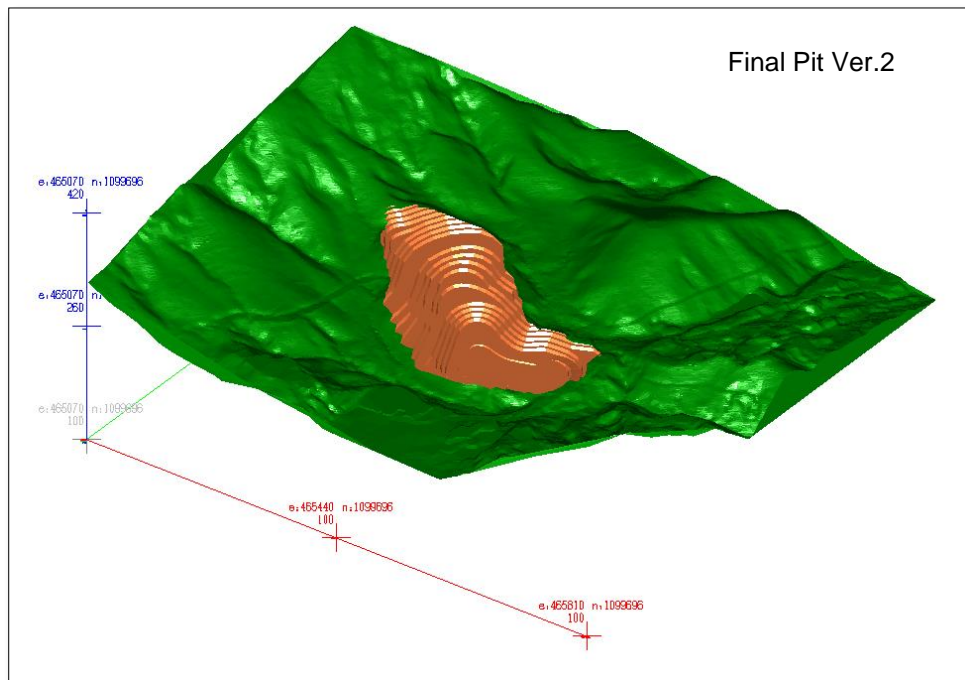


Figure 4. 14 3D view of final Pit designed Ver.2

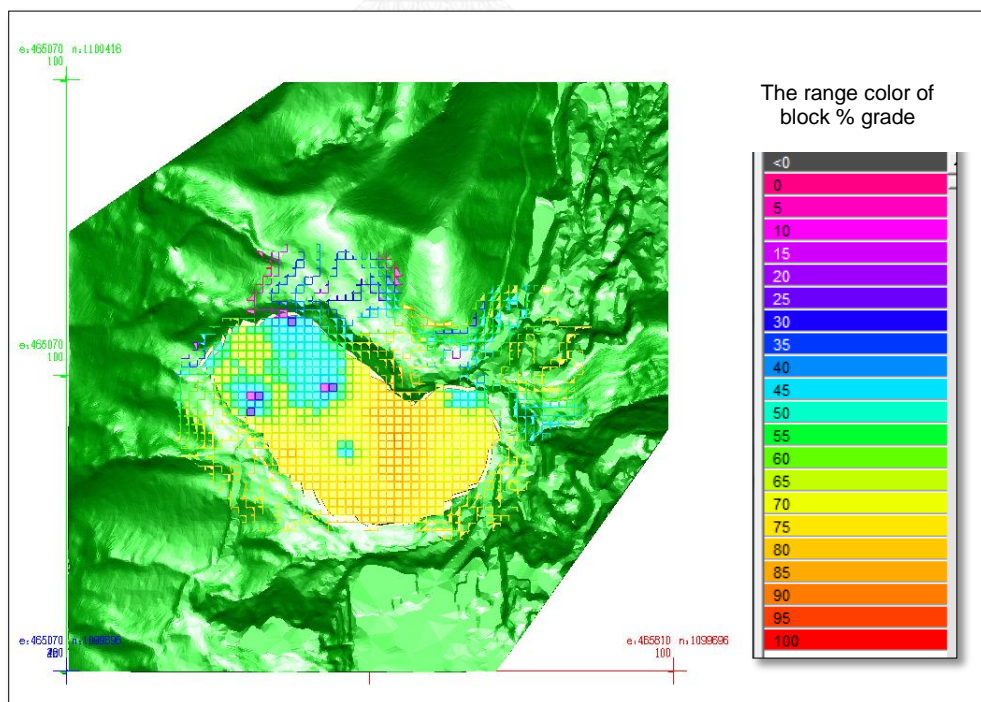


Figure 4. 15 Top view of Pit Ver.2 and its 3D blocks grade distribution

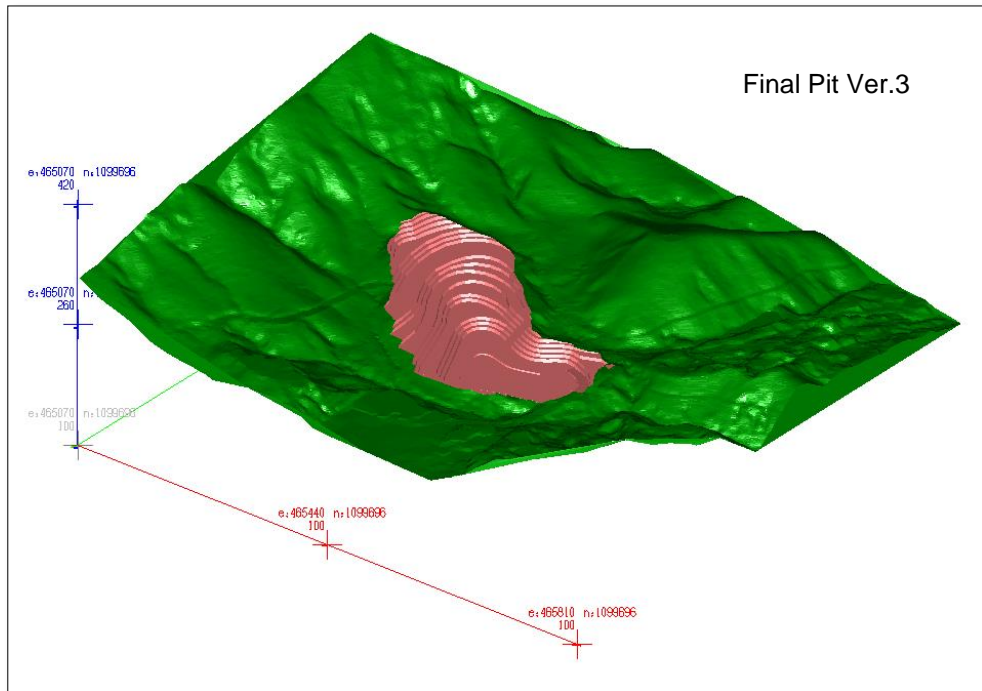


Figure 4. 16 3D view of final Pit designed Ver.3

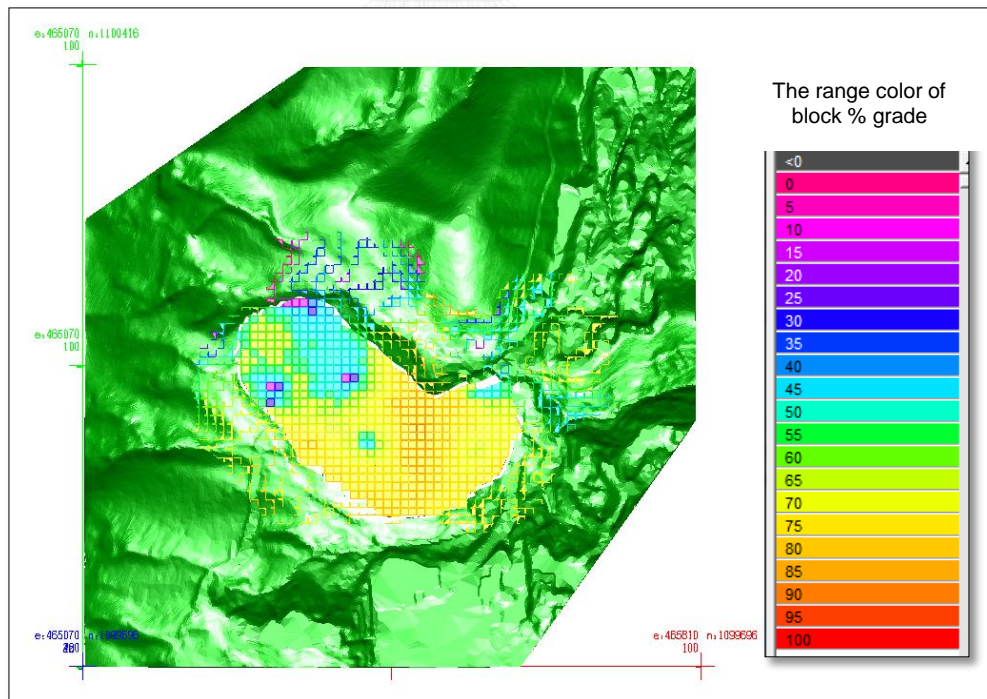


Figure 4. 17 Top view of Pit Ver.3 and its 3D block grade distribution

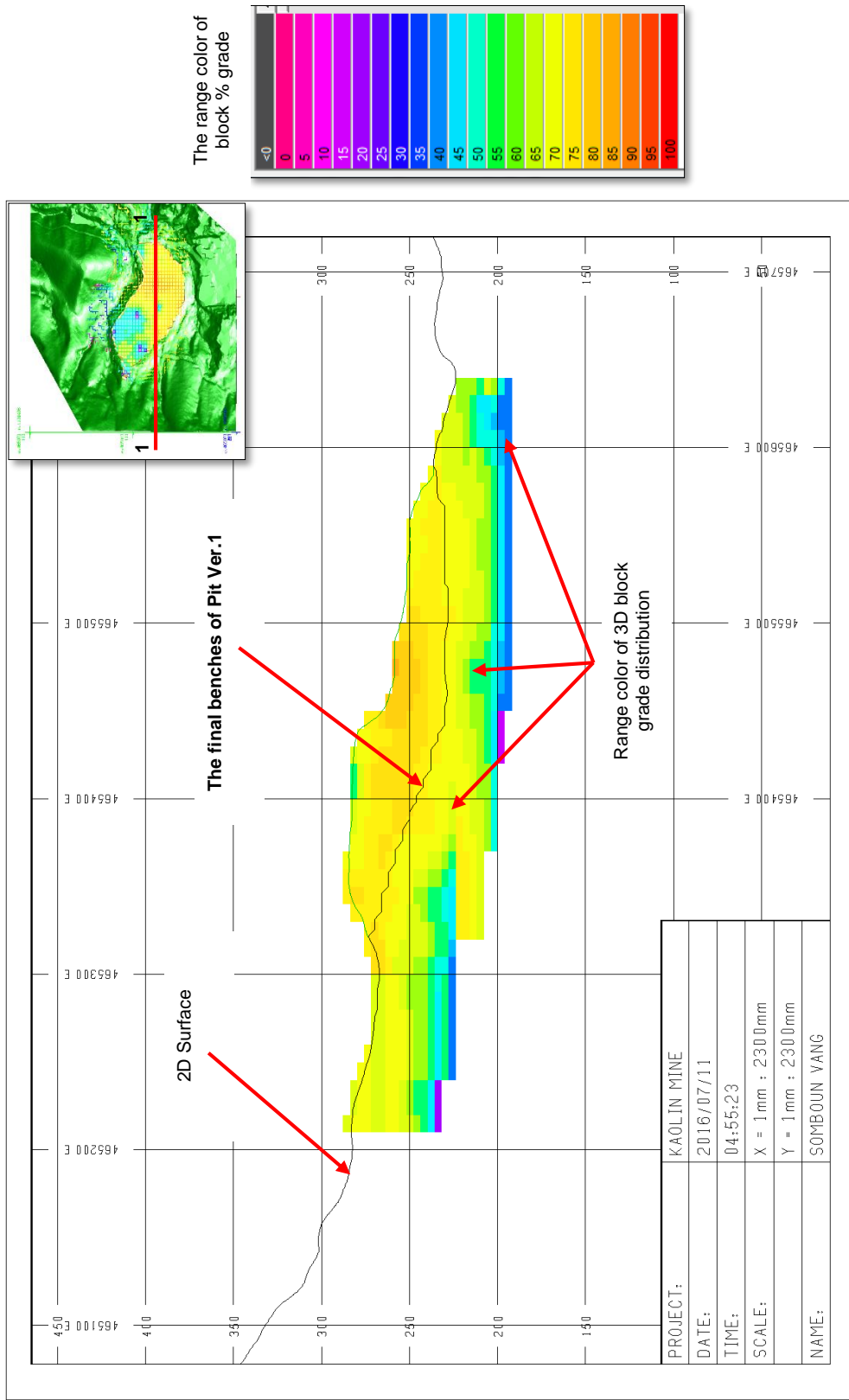


Figure 4. 18 Cross-section 1-1 of Pit Ver.1 and its vertical 3D block grade distribution, Plane_N 1099966

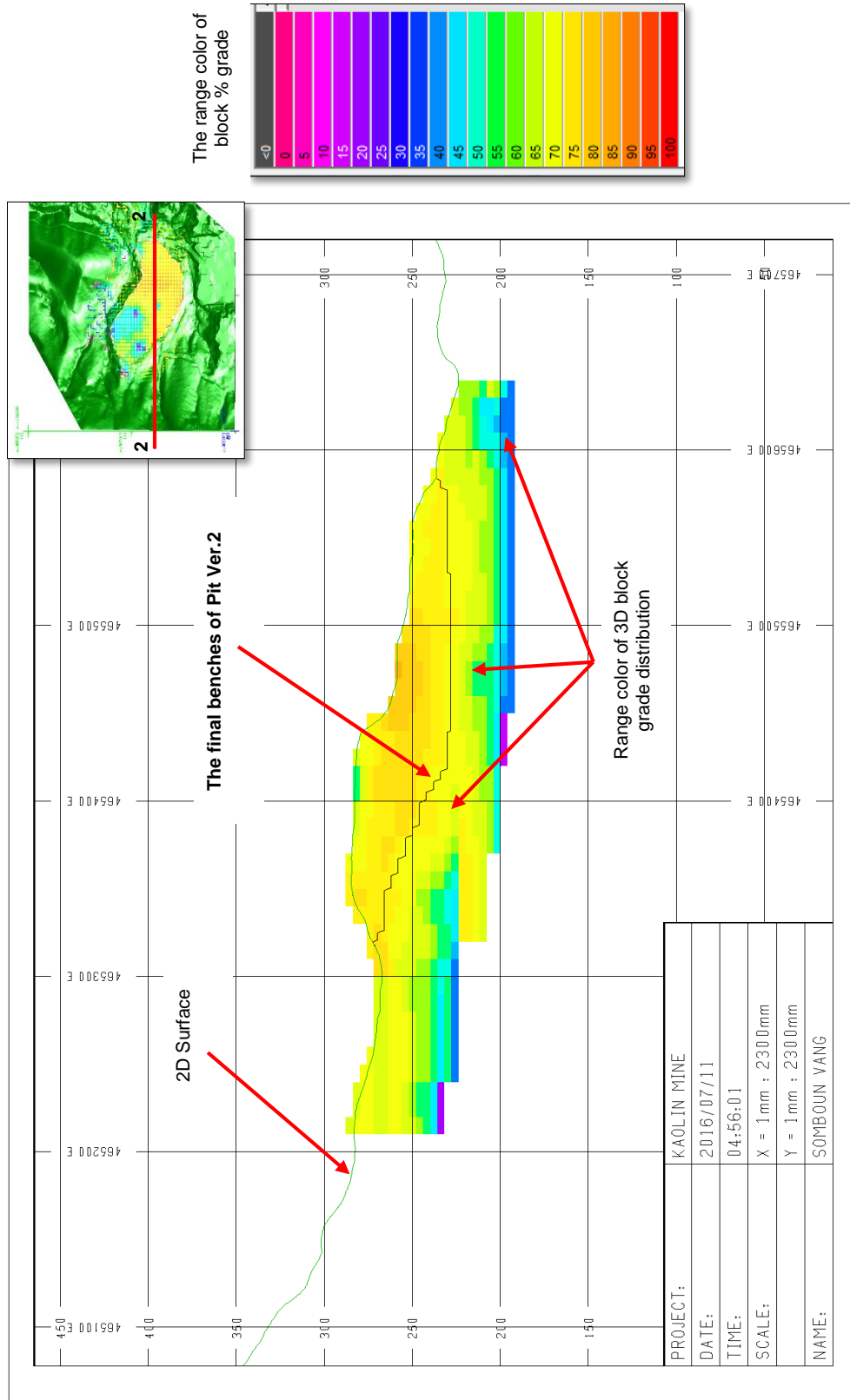


Figure 4. 19 Cross-section 2-2 of Pit Ver.2 and its vertical 3D block grade distribution, Plane_N 1099966

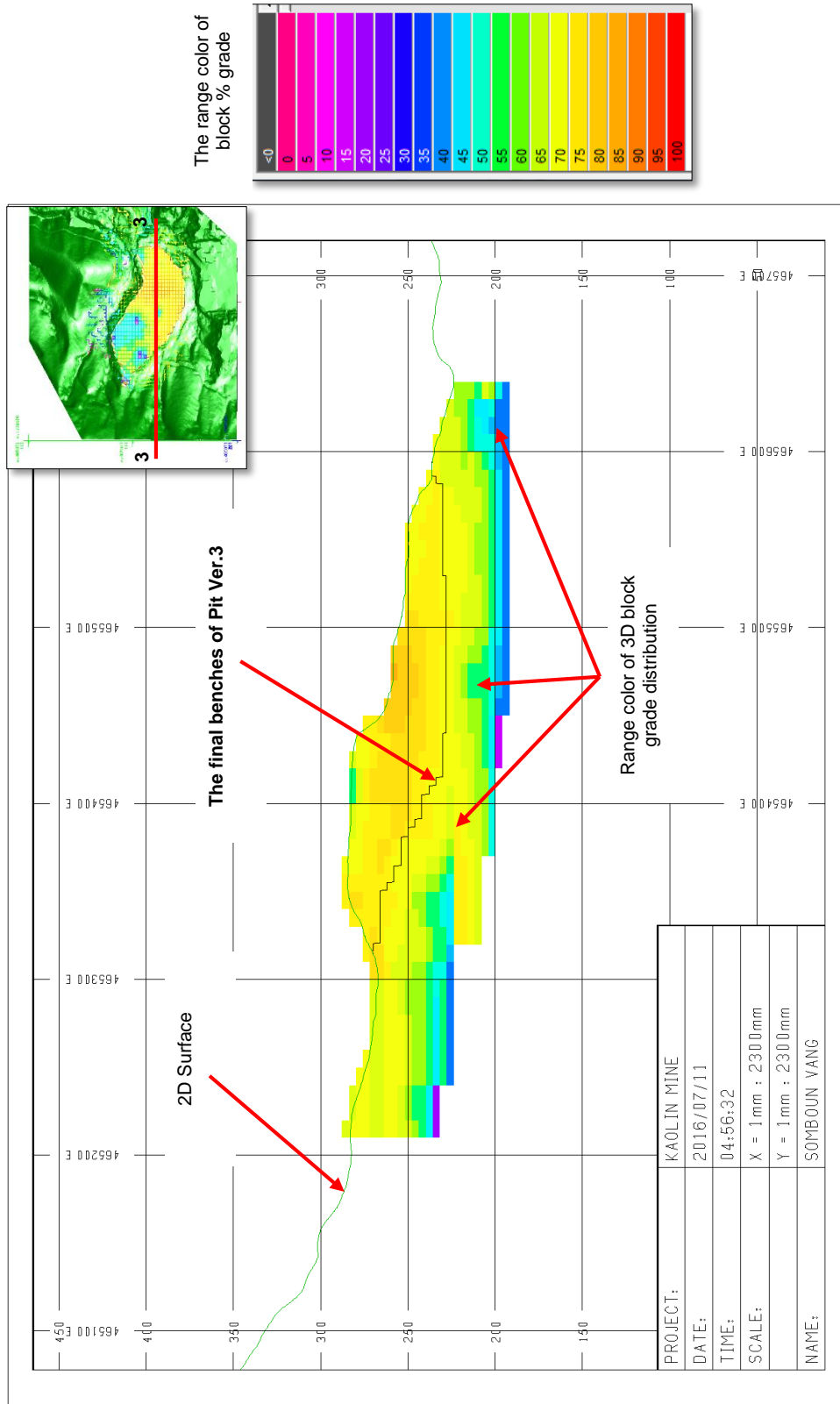


Figure 4. 20 Cross-section 3-3 of Pit Ver.3 and its vertical 3D block grade distribution, Plane_N 1099966

4.3 Results of pit slope stability analysis

In this study, pit slope stability analysis has separated into three (3) major mode as described the detail of those creation slopes geometry model (SGM) and its assigning geomaterials properties (GMP) in the sub-topic 3.6.1, 3.6.2, and 3.6.3.

For the assigning GMP of those SGM are summary in Table 4.5.

Table 4. 5 Summary of geomaterials properties of the study area

Properties	Top soil (SC-SM)	Weathered granite (SC-SM)	Hard granite
Material	Clayey to silty sand (Finer-grained)	Clayey to silty sand (Coarser-grained)	Rock
Thickness (m)	0 – 2	10 – 30	unknown
Density (kg/m ³)	1,500	1,800	2,650
Tensile strength (MPa)	-	0.2	20
Cohesion (kPa)	18.3	13.7 – 178.1	10,000
Friction angle (°)	36.8	3 – 57.6	52 – 65
Young's modulus (GPa)	-	0.5	70
Poisson's ratio	0.35	0.32	0.25
Bulk modulus (GPa)	-	0.06	11.7
Shear modulus (GPa)	-	0.33	43.8

For the detail and resulting of each mode slope stability analysis were separated describe in sub-topic below:

4.3.1 Pit slope stability analysis for the final Pit slope design Ver.1, 2, and 3

In this stages, there are 36 cases of slope stability analysis, as shown the detail in Table 3.7. This analysis is for checking the stability of pit slope designed, and measurement which cohesion and frictional angle are effects to making a minimum value of factor of safety (FOS).

After running FLAC3D to calculate the slope stability analysis, we can discovered a minimum FOS of each pit in the Table 4.6. Some FOS of them are less than 1.50 (a minimum acceptable FOS for long term mining slope), occurring on the Pit Ver.2 and 3. The minimum FOS in Pit Ver.1 = 1.75, Pit Ver.2 = 1.41, and Pit Ver.3 = 1.20, those FOS has obtained from the block sample BMRD-03 (case no. 9) taken during the rainy season and its strength tested by Direct shear test method.

In terms of slope failure criteria, the acceptable pit slope design must have FOS more than 1.50 (for long term slope) and 1.30 (for short term slope) in every condition properties of soils and rocks. However, Pit Ver.1 is an acceptable final pit design for kaolin mine. Whereas, to make decision of selected a pit design is upon the mine owner.

To see the distribution of FOS value, it has to be plotting by versus a value of FOS and numbers of the analytical case as illustrated in Figure 4.21. From this figure, all value FOS of Pit Ver.1 is always located above the criteria line. For Pit Ver.2, has only one point or one case (Case No.9) is located under the criteria line. Another one is Pit Ver.3, this pit's FOS value have a few points (Case No.1, 3 and 9) are located under the criteria line.

The resulting of slope geometry models analysis are obtained from FLAC3D in this stages will attachment within the Appendix II.

Table 4. 6 Summary the results of slope stability analysis for SGM of final Pit design
Ver.1, 2, and 3

Case No.	Block sample	C (kPa)	ϕ (°)	Factor of safety			Condition
				Pit V.1	Pit V.2	Pit V.3	
1	BMRD-01	21.20	26.20	1.84	1.52	1.32	dry season
2		116.00	4.00	2.42	2.24	2.13	dry season
3		37.00	21.00	1.95	1.66	1.48	dry season
4		50.00	27.00	2.61	2.23	1.98	dry season
5	BMRD-02	31.10	24.80	2.03	1.70	1.50	dry season
6		124.00	3.00	2.49	2.31	2.21	dry season
7		43.00	25.00	2.33	1.97	1.75	dry season
8		54.00	30.00	2.89	2.46	2.19	dry season
9	BMRD-03	13.90	28.50	1.75	1.41	1.20	wet season
10		134.90	8.00	3.05	2.81	2.66	wet season
11	BMRD-04	13.70	57.60	4.14	3.15	2.58	wet season
12		178.10	6.00	3.70	3.43	3.27	wet season

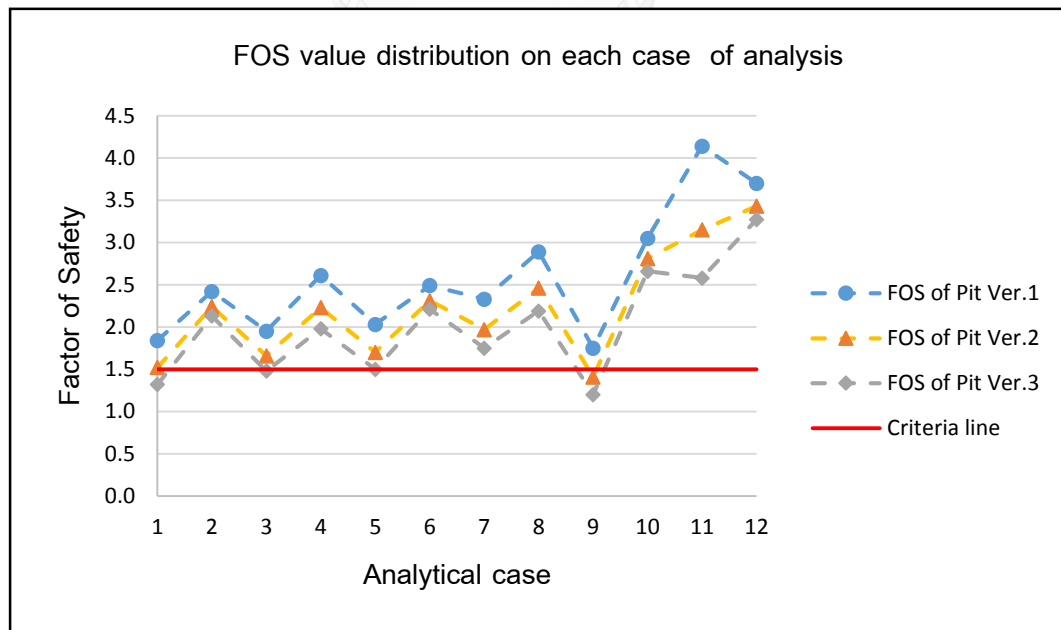


Figure 4. 21 Distribution curve of FOS value on the final Pit design

4.3.2 Pit slope stability analysis for the cross-section model of Pit Ver.1, 2, and 3

The complete pit design may have some dimension of benches slope changed from the original expected final slope. To measurement or prediction the side of slope may occur failure, it has to be created a cross-section line on those pits. The purpose of cross-section is for simulated the actual shape of pit slope. In this stages, there are three (3) cross-section lines for each pit and the total is 9 cross-section model as described the detail of SGM analysis and assigning GMP in sub-topic 3.6.2.

Cross-section in the Pit MF-10 has been created during the period of before and after mining to see a changing of the surface level. The cross-section model of each pit are demonstrated in the figures below:

- The cross-section of Pit design Ver.1 are illustrated in Figure 4.25 (A-A'), 4.27 (B-B'), and 4.29 (C-C'). Those cross-section shown the layers of soil and rock are located around the pit.
- Figure 4.31 (D-D'), 4.32 (E-E'), and 4.33 (F-F') are the cross-section of Pit Ver.2. Can see this benches slope are steeper than the slope of Pit Ver.1.
- According to the cross-section model of Pit Ver.3, it was a steepest slope as indicated in Figure 4.35 (G-G'), 4.36 (H-H'), and 4.37 (I-I').

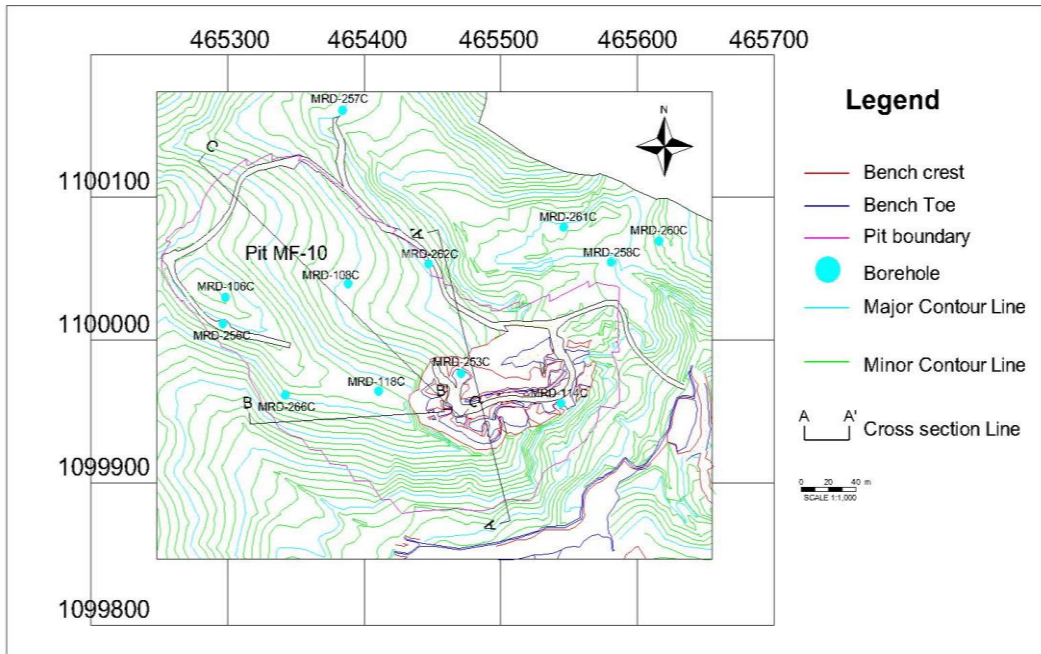


Figure 4. 22 Pit MF-10 before mining and its cross-section line

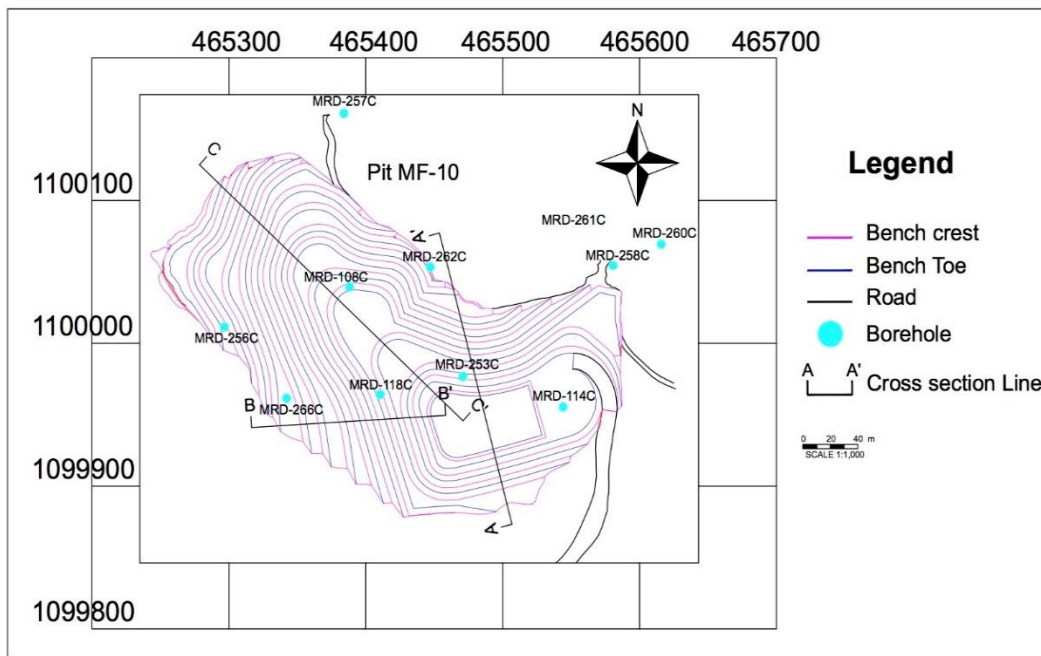


Figure 4. 23 Pit MF-10 after mining by Pit design Ver.1 and its cross-section line

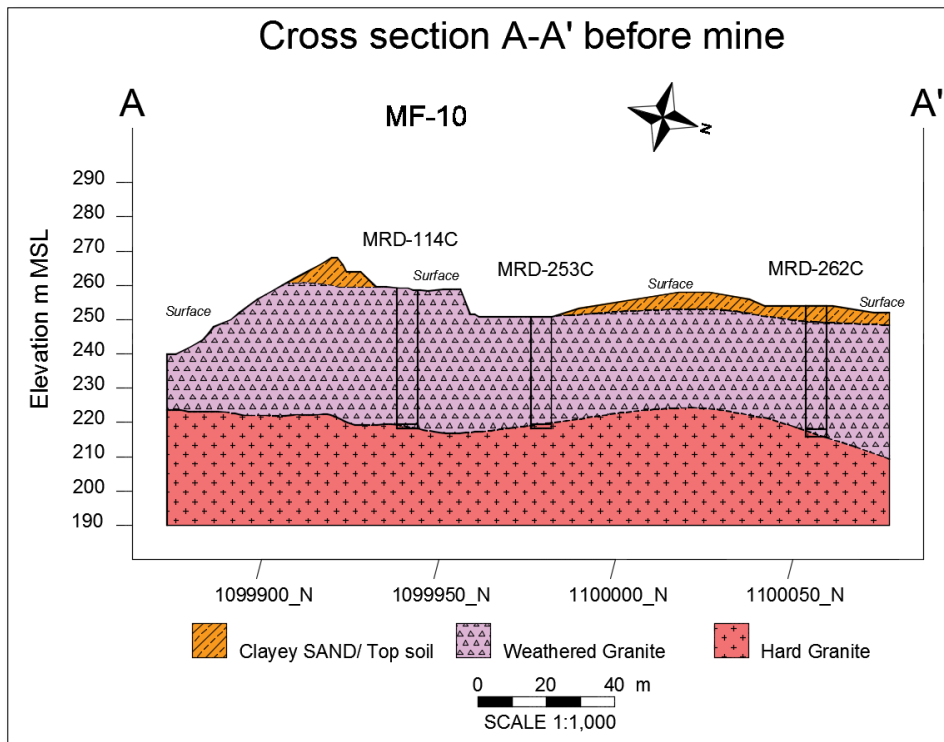


Figure 4. 24 Cross-section along A-A' before mining

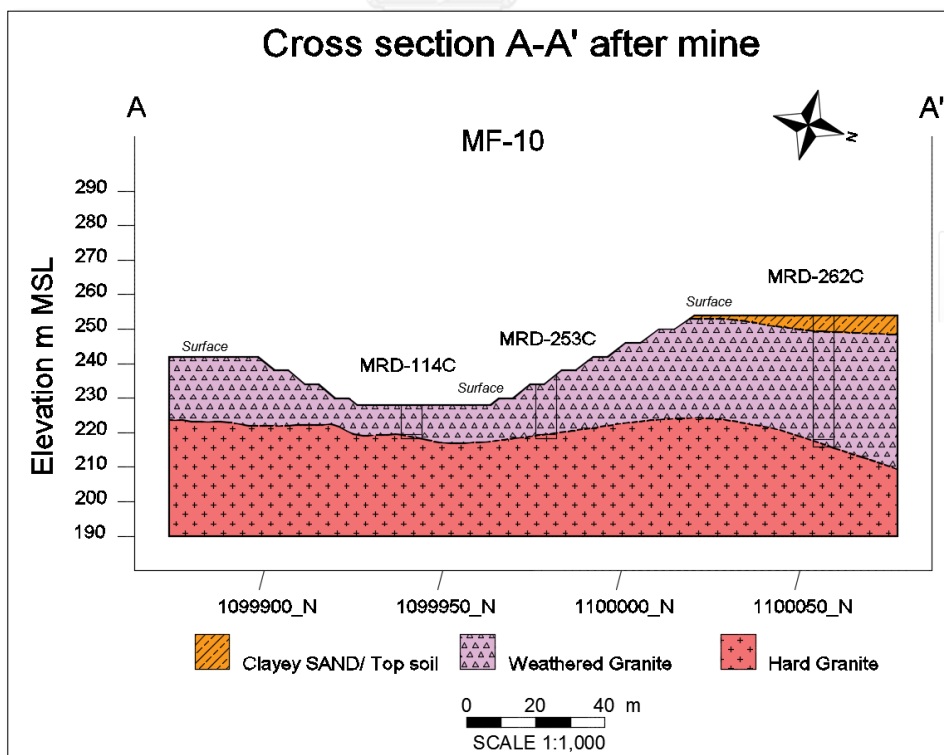


Figure 4. 25 Cross-section along A-A' after mining by Pit Ver.1

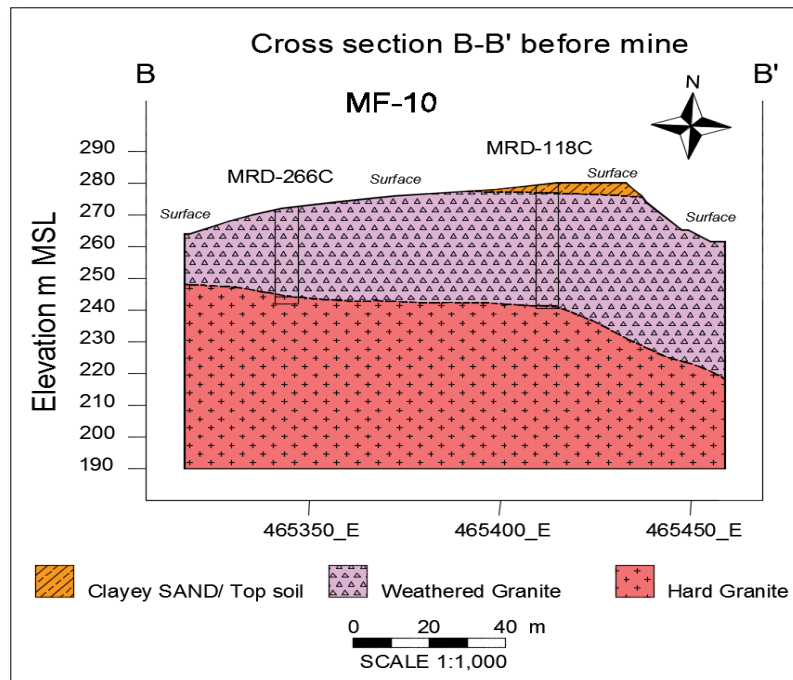


Figure 4. 26 Cross-section along B-B' before mining

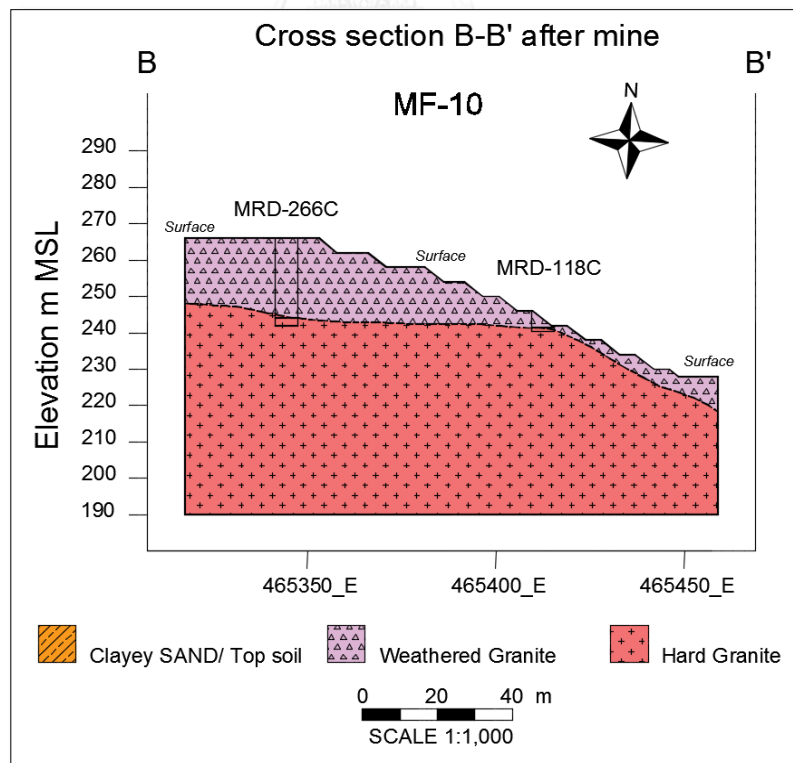


Figure 4. 27 Cross-section along B-B' after mining by Pit Ver.1

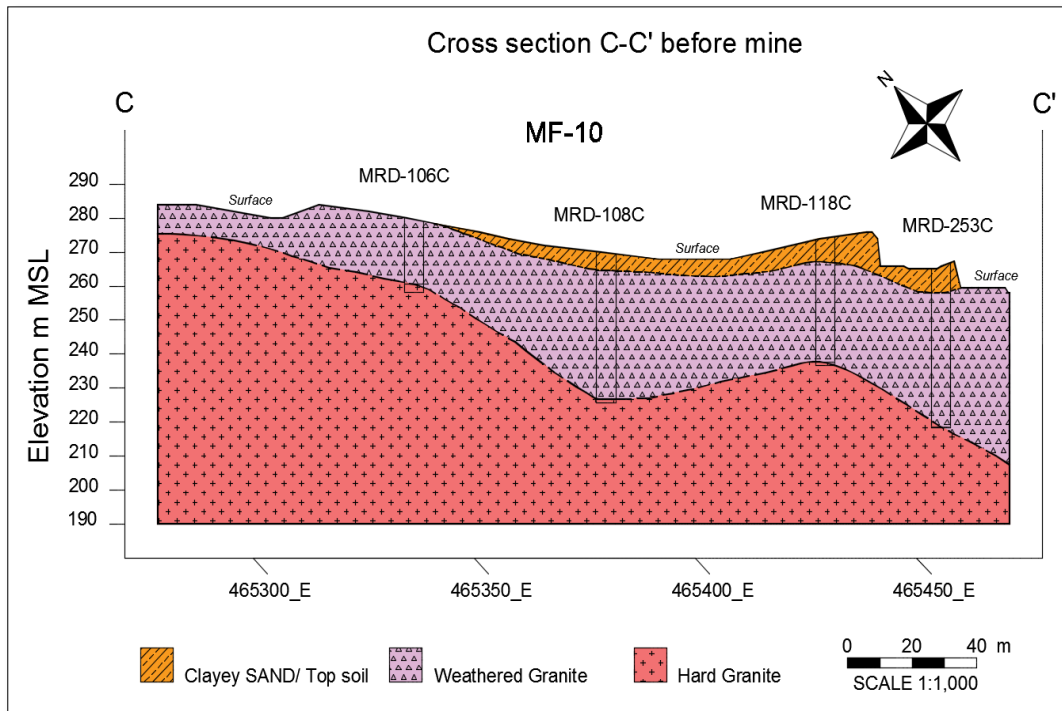


Figure 4. 28 Cross-section along C-C' before mining

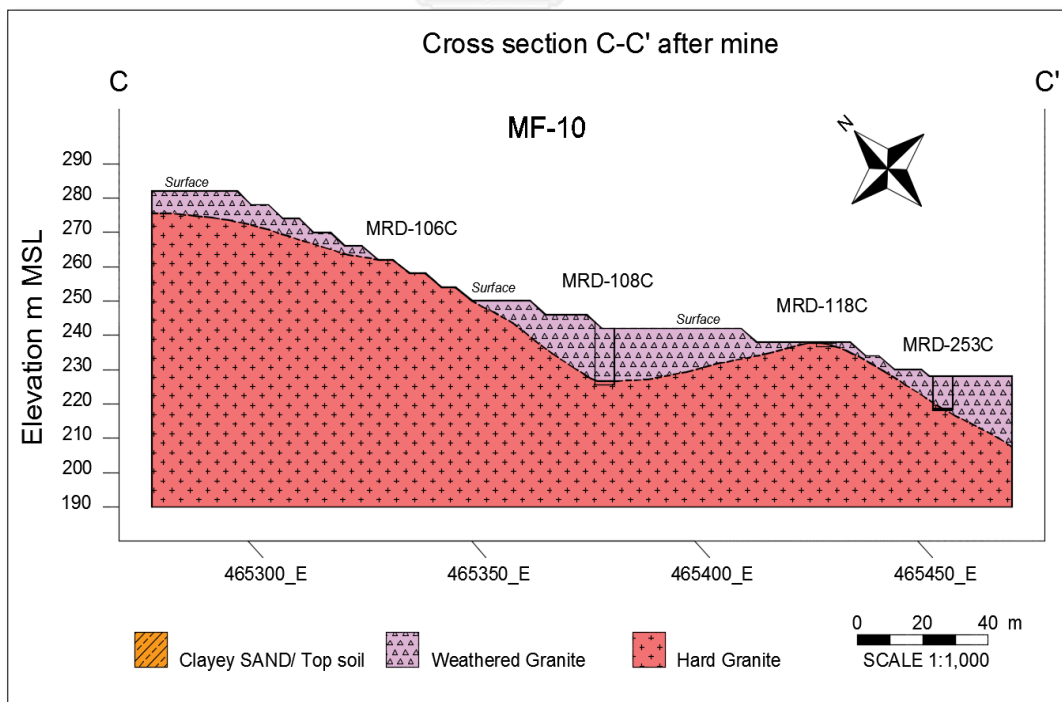


Figure 4. 29 Cross-section along C-C' after mining by Pit Ver.1

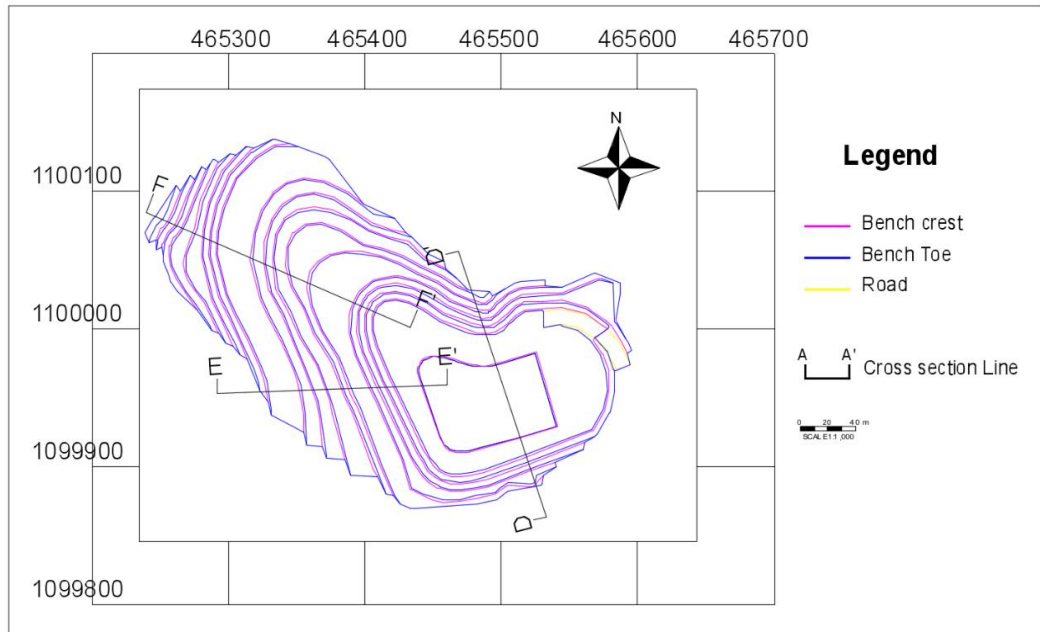


Figure 4. 30 Pit MF-10 after mining by Pit design Ver.2 and its cross-section line

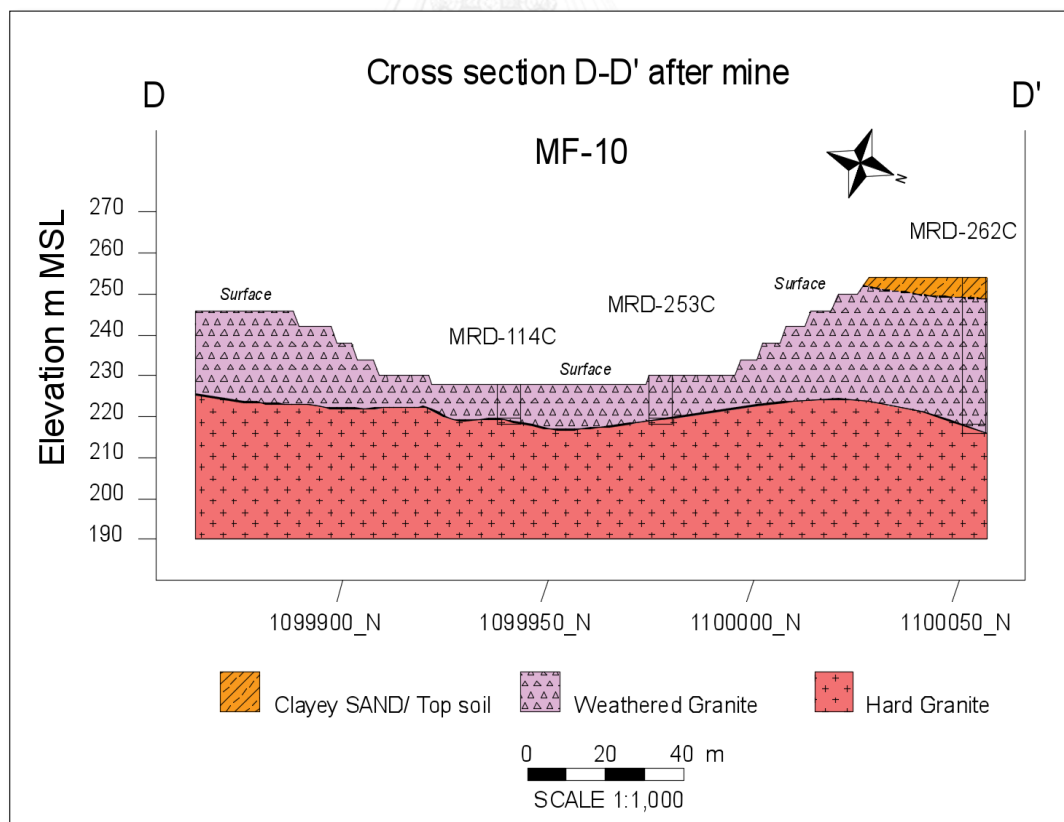


Figure 4. 31 Cross-section along D-D' of Pit Ver.2

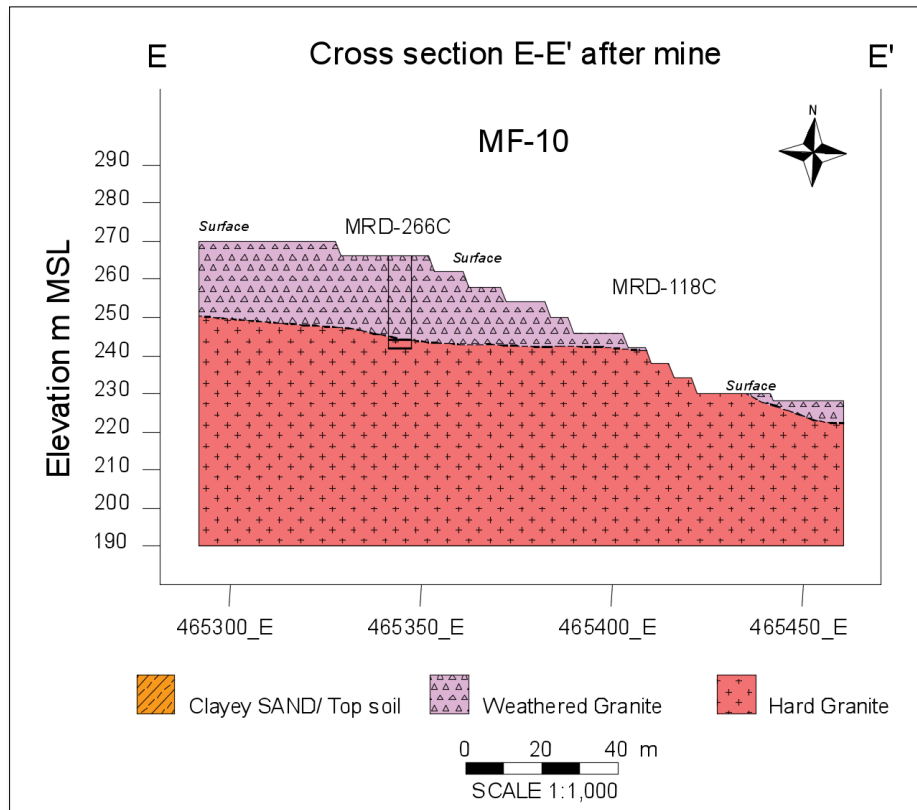


Figure 4. 32 Cross-section along E-E' of Pit Ver.2

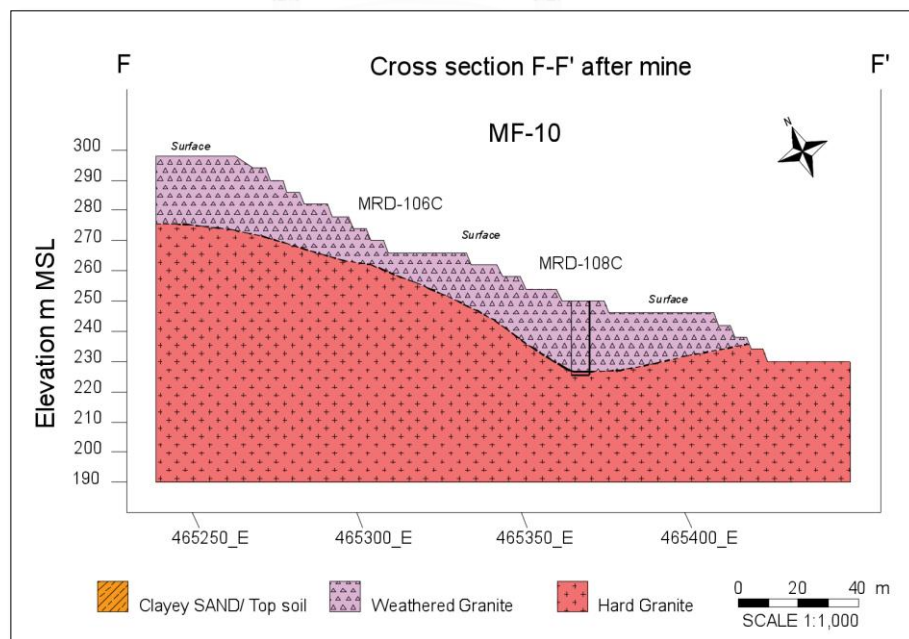


Figure 4. 33 Cross-section along F-F' of Pit Ver.2

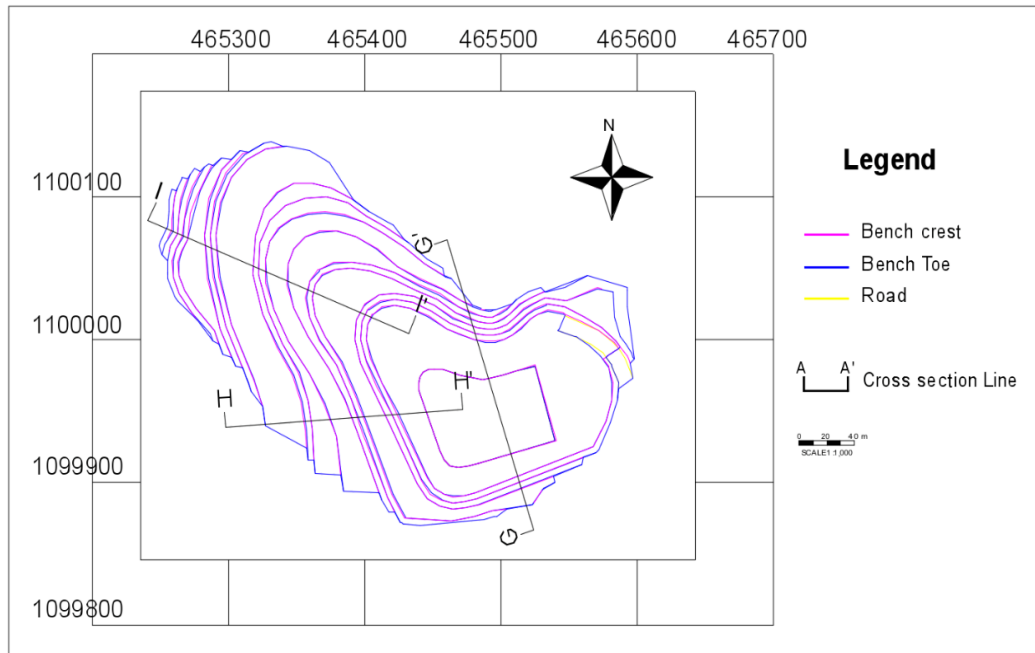


Figure 4. 34 Pit MF-10 after mining by Pit design Ver.3 and its cross-section line

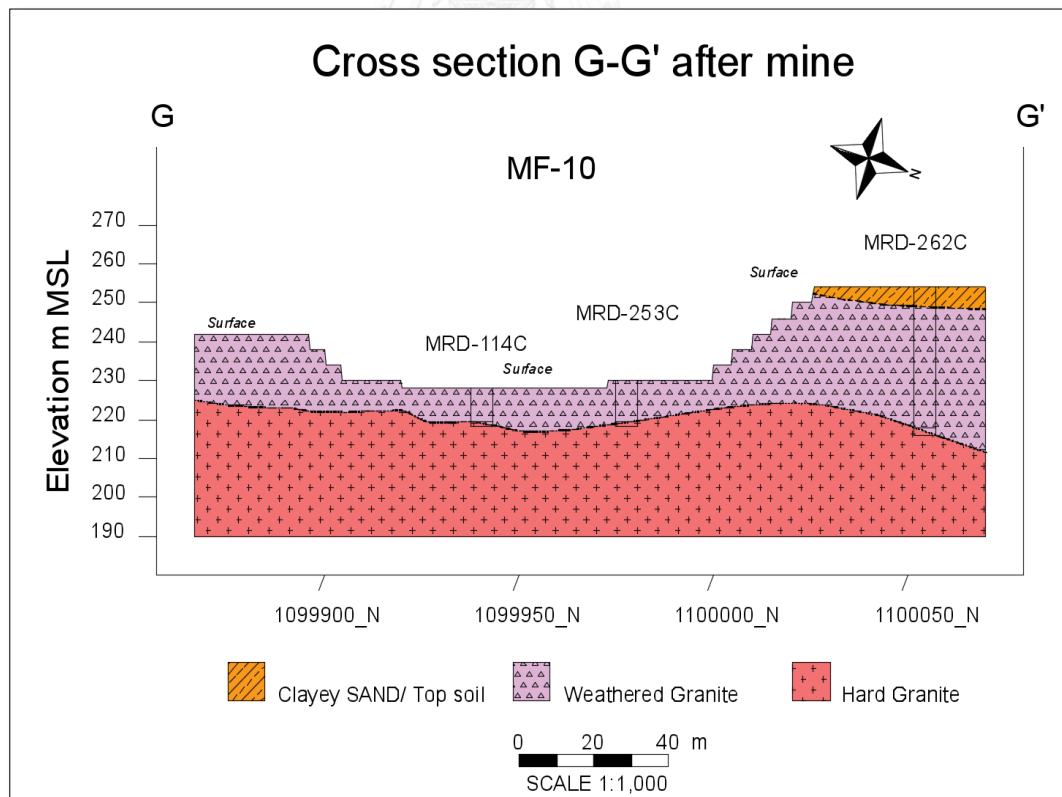


Figure 4. 35 Cross-section along G-G' of Pit Ver.3

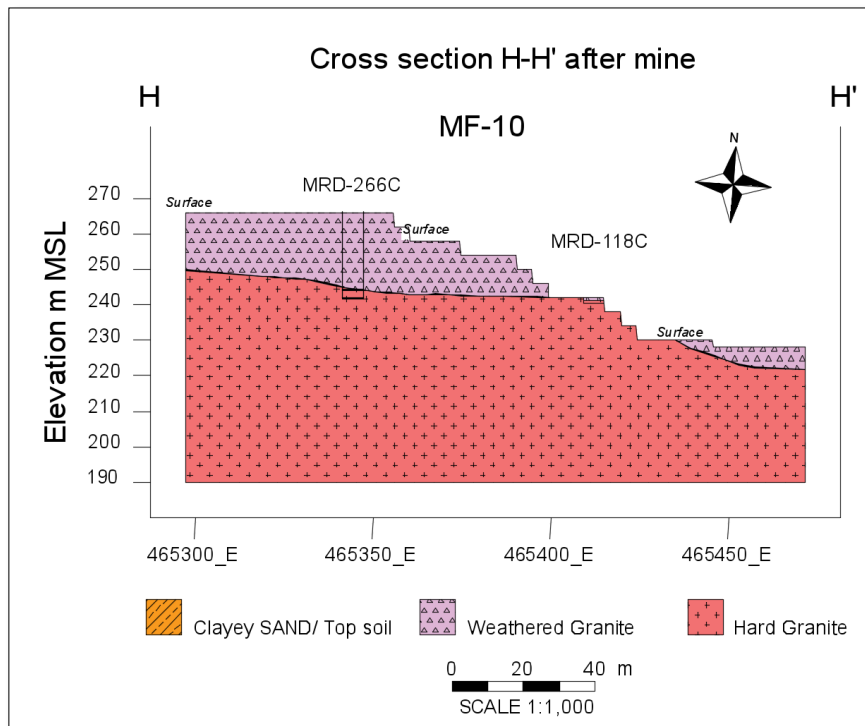


Figure 4. 36 Cross-section along H-H' of Pit Ver.3

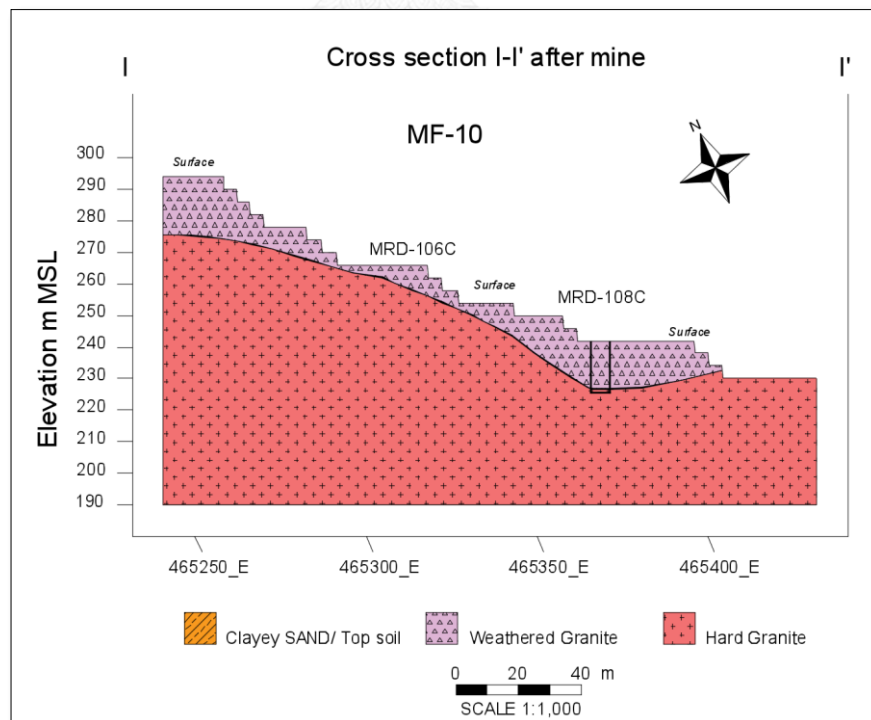


Figure 4. 37 Cross-section along I-I' of Pit Ver.3

Used the cross-section model of those pits above to build the slope geometry model (SGM) of analysis in FLAC3D. Then, assigning the geomaterials properties in Table 4.5 with a cohesion = 13.9 kPa and frictional angle = 28.5 deg. The results of analysis are tabulated in Table 4.7.

Table 4. 7 Summary the results of slope stability analysis of cross-section model of Pit Ver.1, 2, and 3

Case No.	Pit No.	Model	C (kPa)	ϕ (°)	FOS	Situation
1	Pit Ver.1	A	13.9	28.5	2.06	stable
2		A'			1.84	stable
3		BB'			1.79	stable
4		CC'			2.54	stable
5	Pit Ver.2	D	13.9	28.5	1.57	stable
6		D'			1.36	unstable
7		EE'			1.58	stable
8		FF'			1.42	unstable
9	Pit Ver.3	G	13.9	28.5	1.36	unstable
10		G'			1.21	unstable
11		HH'			1.46	unstable
12		II'			1.39	unstable

*Remark: given the situation of slope stability by $FOS \geq 1.50$ that slope model is "stable" and $FOS < 1.5$ is "unstable" or potential to failure.

The results detail of analytical model in this stages are demonstrated in Appendix III.

The resulting of cross-section model analysis, all model of Pit Ver.1 are stable. For Pit Ver.2, there are two (2) models stable and another two models is unstable. The last one is models of Pit Ver.3, all models are unstable as seen the graphs in Figure 4.38.

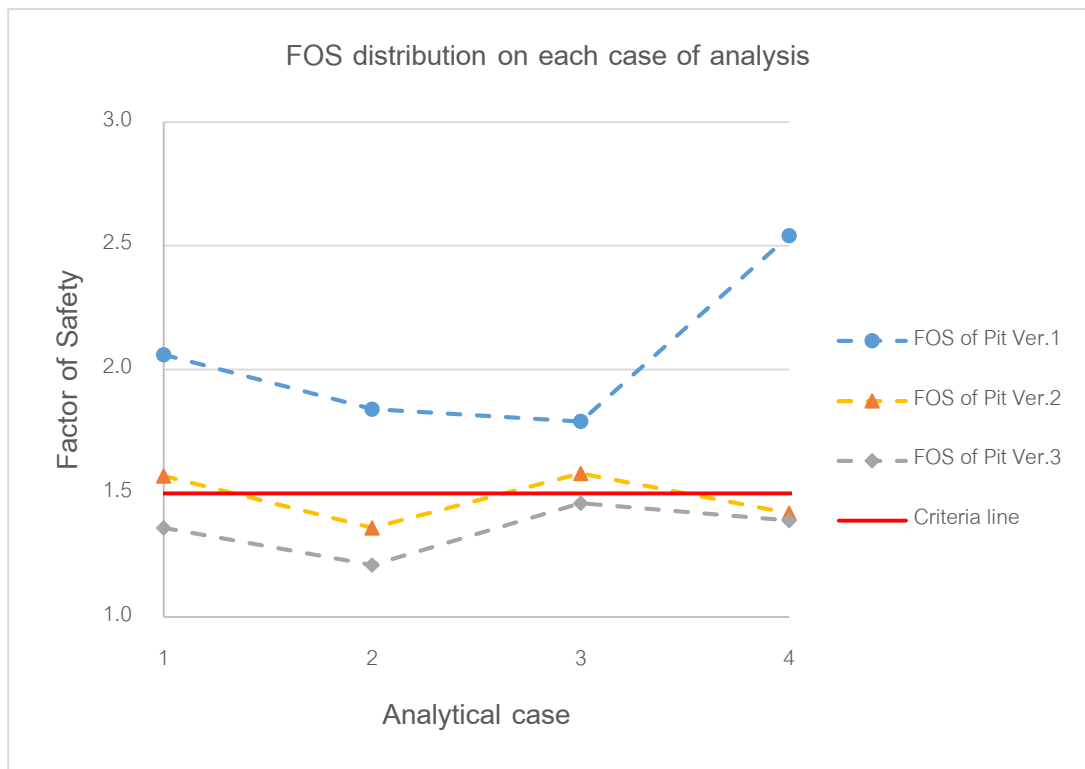


Figure 4. 38 Distribution curves of FOS value on cross-section model

To gain more understanding and clearly about the side of slopes are stable or potential to collapse, Figure 4.39, 4.40, and 4.41 will show the pit with results of analysis in each model for each pit design. Figure 4.39 is a result of cross-section analysis for Pit Ver.1, Figure 4.40 is a result of Pit Ver.2, and Figure 4.41 for Pit Ver.3.

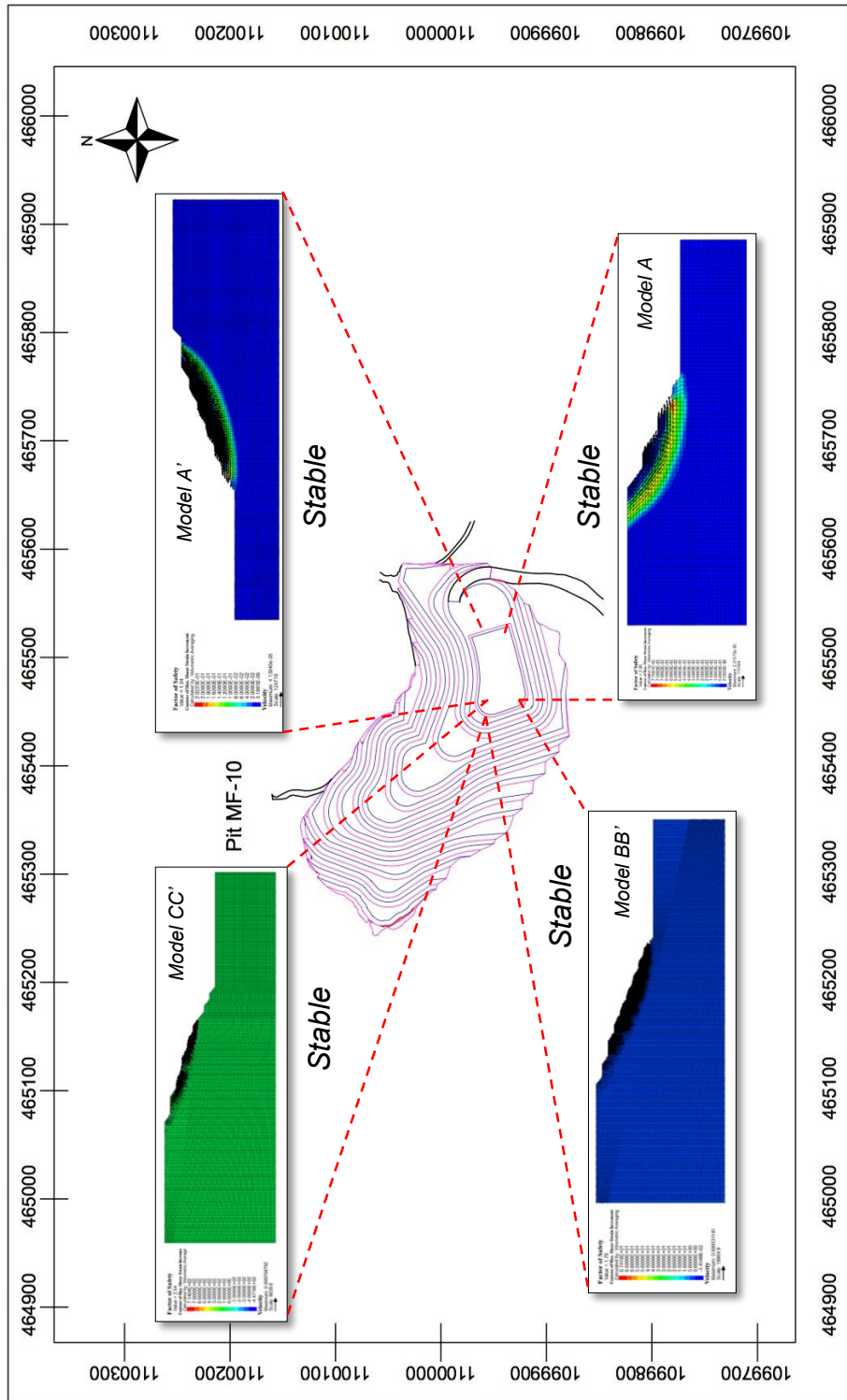


Figure 4. 39 The results of cross-section model analysis for Pit Ver. 1

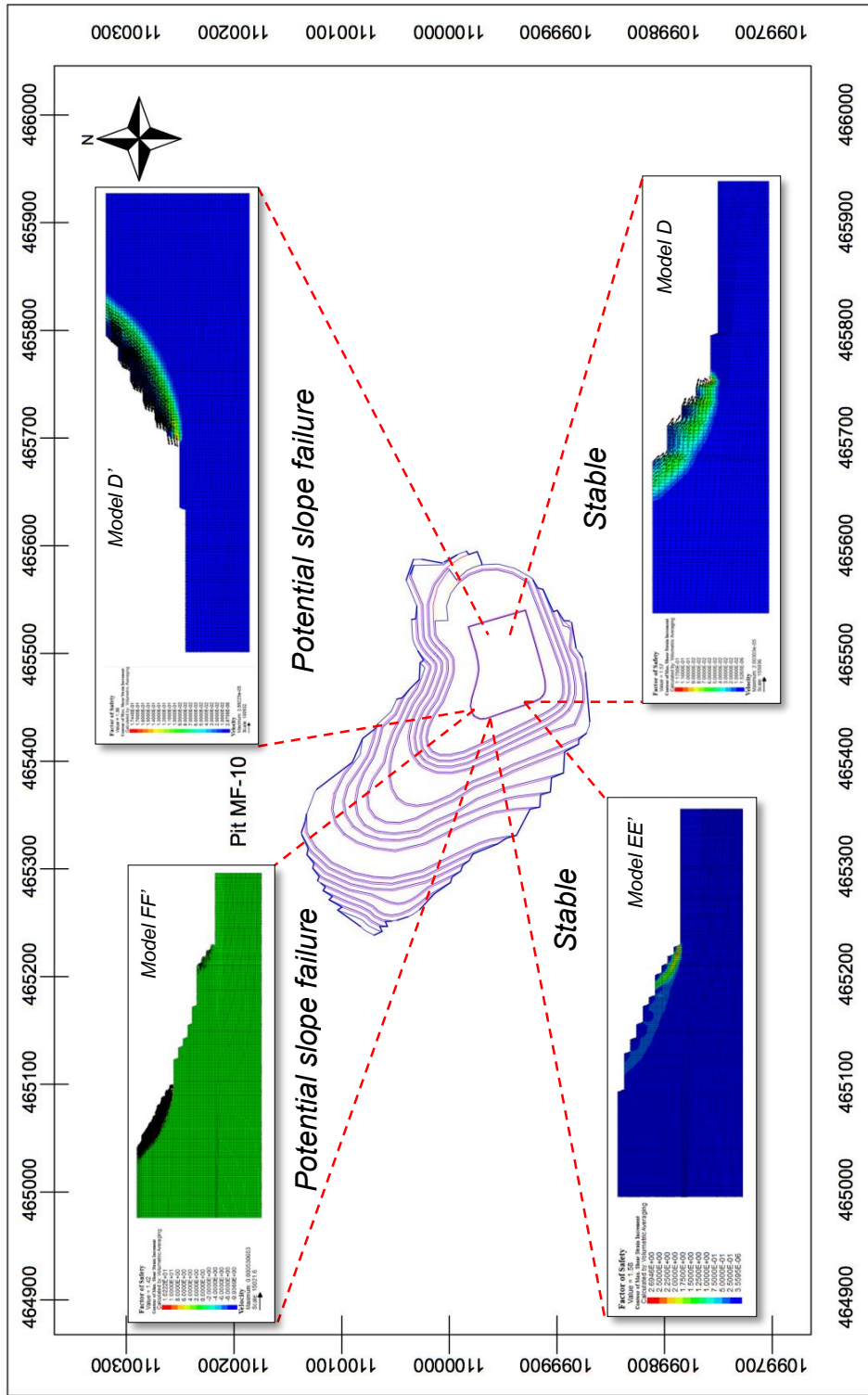


Figure 4. 40 The results of cross-section model analysis for Pit Ver.2

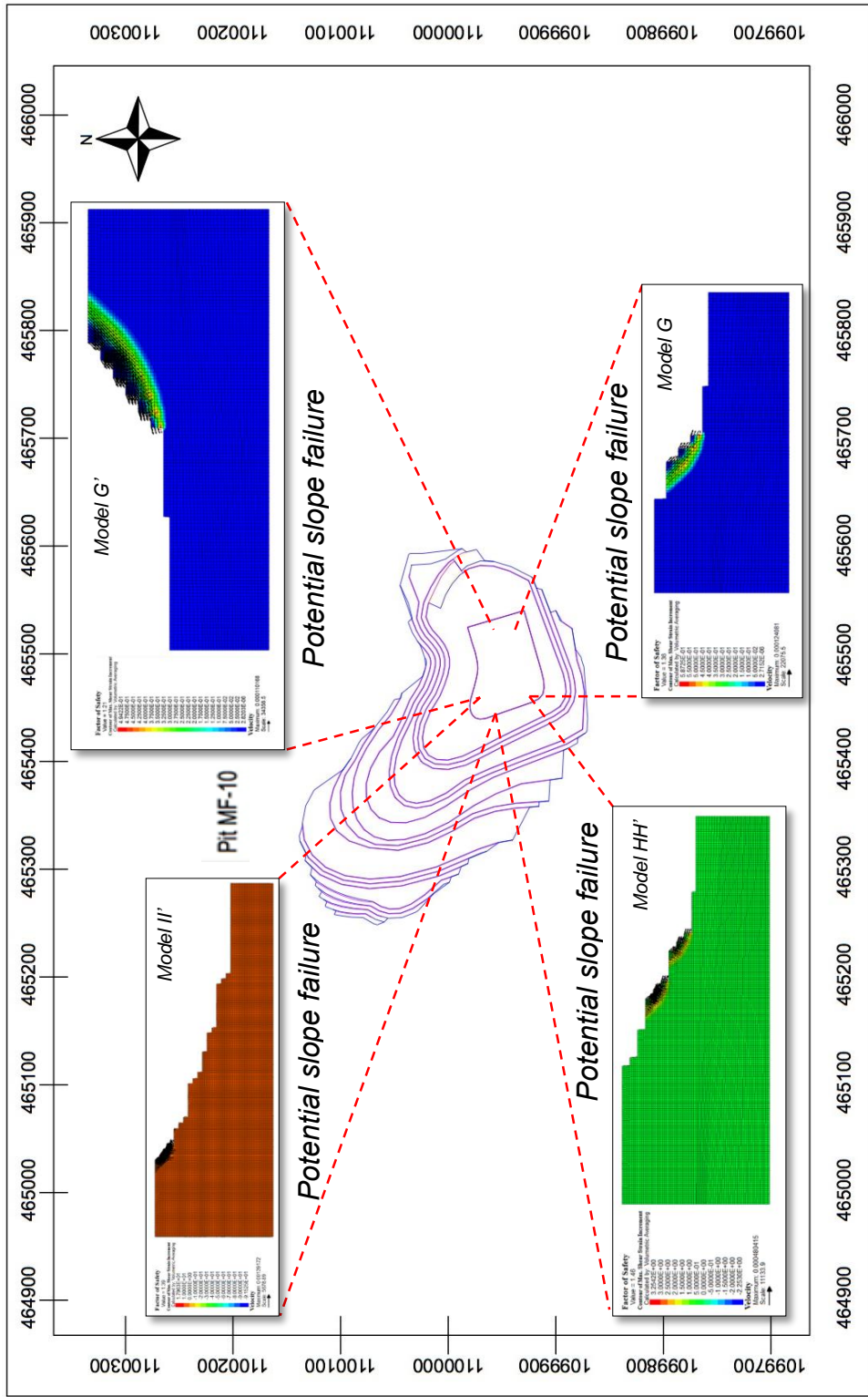


Figure 4. 41 The results of cross-section model analysis for Pit Ver.3

4.3.3 Pit slope stability analysis for the assuming bench height and face slope angle of trial pit slope (Short term mining slope)

In this stage, the slope stability analysis is to measure the ability of soil materials to hold slopes in Pit MF-10 area. The method is using various assuming numbers of bench height and face slope angle as described in the topic 3.6.3. For the assigned geomaterials properties, critical value of cohesion and frictional angle are used to make slope failure during the analysis

The results of this analysis have been tabulated in Table 4.8. According to those results, it can be guarantee that FOS's are reduced when the degree of face slope angle and bench height are increased as illustrated in Figure 4.42.

Table 4. 8 Summary the results of analysis for the models with various bench height

Case No.	Bench height (m)	Slope angle (°)	C (kPa)	ϕ (°)	FOS	Situation
1	4	20	13.9	28.5	4.03	stable
2	4	30	13.9	28.5	3.27	stable
3	4	40	13.9	28.5	2.82	stable
4	4	50	13.9	28.5	2.51	stable
5	4	60	13.9	28.5	2.32	stable
6	4	70	13.9	28.5	2.05	stable
7	4	80	13.9	28.5	1.83	stable
8	4	90	13.9	28.5	1.62	stable
9	8	20	13.9	28.5	3.13	stable
10	8	30	13.9	28.5	2.43	stable
11	8	40	13.9	28.5	1.98	stable
12	8	50	13.9	28.5	1.67	stable
13	8	60	13.9	28.5	1.47	unstable
14	8	70	13.9	28.5	1.25	unstable
15	8	80	13.9	28.5	1.11	unstable
16	8	90	13.9	28.5	0.96	unstable
17	12	20	13.9	28.5	2.95	stable
18	12	30	13.9	28.5	2.14	stable

Case No.	Bench height (m)	Slope angle (°)	C (kPa)	ϕ (°)	FOS	Situation
19	12	40	13.9	28.5	1.78	stable
20	12	50	13.9	28.5	1.46	unstable
21	12	60	13.9	28.5	1.2	unstable
22	12	70	13.9	28.5	1.03	unstable
23	12	80	13.9	28.5	0.87	unstable
24	12	90	13.9	28.5	0.75	unstable
25	16	20	13.9	28.5	2.87	stable
26	16	30	13.9	28.5	2.12	stable
27	16	40	13.9	28.5	1.68	stable
28	16	50	13.9	28.5	1.37	unstable
29	16	60	13.9	28.5	1.07	unstable
30	16	70	13.9	28.5	0.9	unstable
31	16	80	13.9	28.5	0.75	unstable
32	16	90	13.9	28.5	0.63	unstable
33	20	20	13.9	28.5	2.95	stable
34	20	30	13.9	28.5	2.16	stable
35	20	40	13.9	28.5	1.69	stable
36	20	50	13.9	28.5	1.35	unstable
37	20	60	13.9	28.5	1.06	unstable
38	20	70	13.9	28.5	0.88	unstable
39	20	80	13.9	28.5	0.69	unstable
40	20	90	13.9	28.5	0.57	unstable

*Remark: given the situation of slope stability by $FOS \geq 1.50$ that slope model is “stable” and $FOS < 1.5$ is “unstable” or potential to failure.

The dimension size of slope geometry model and its analysis from FLAC3D was illustrated in Appendix IV.

As observed, the plotting curve of FOS versus with face slope angle, can determined that, there is a only the curve along to bench height 4 metres still located above the criteria line, although the steep of face slope has increased until equal to 90 deg.

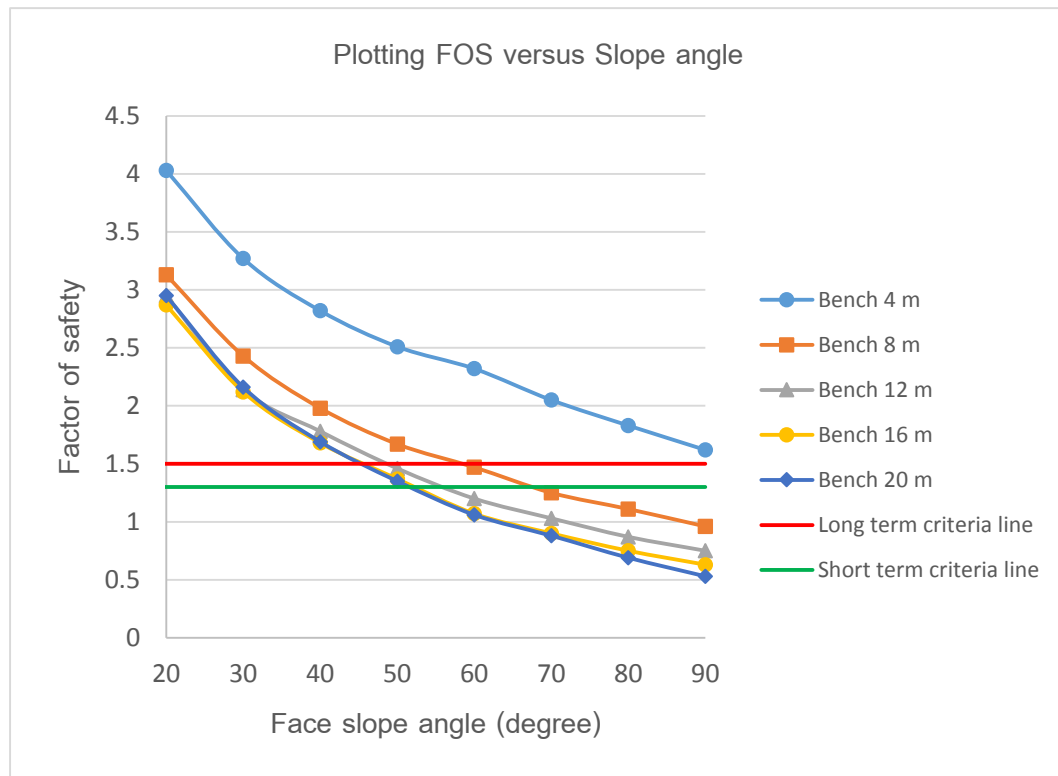


Figure 4. 42 The plotting curve of FOS versus slope angle

According to Figure 4.42 above, for the trial pit slope mining, there are many options to select the face slope angle and bench height as described in below:

- 1) *Case one*, if selected the bench height equal to 4 metres, the face slope of mining can be as steeper as possible, although the face slope equal to 90 deg. But it still stable.
- 2) *Case two*, if selected bench height equal to 8 metres, the maximum of face slope angle is equal to 60 – 65 deg.
- 3) *Case three*, if selected bench height equal to 12 metres, the maximum of face slope angle is 50 – 55 deg.
- 4) *Case four is the last*, if selected bench height equal to 16 or 20 metres, the maximum of face slope should be not over than 50 deg.

Note: Those options above are described as following the results of this study. In fact, there are many parameters need to be consider to make decision on this matter.

CHAPTER V

CONCLUSIONS AND RECOMMENDATIONS

5.1 Conclusions

In summary, this research has been done with a series of important works, such as the site investigation, geotechnical laboratory testing, 3 open pits design, and 3 major stages of slope stability analysis.

For the site investigation, it is to gain more understanding about the soils and rocks material properties located in the study area and slope failure process. One of the most important issue leading to slope failure is an erosional process occurred during rainy season. The slope erosion has started when the heavy raining arrived. The permeability of weathered granite is very low, hence, when raining the water cannot infiltrate fast enough, forming big runoff flowing from the crest to toe of the slope. Rapid runoff can erode these weak materials easily and then trigger slope failure (Pipat, 2016).

In this study, the laboratory testing has been done on four (4) block samples and a few soil samples had been also collected during the site investigation. The testing's have been completed with:

- 5 samples for gradation sieve analysis;
- 12 specimens for direct shear test;
- 6 specimens for unconfined compression test;
- 12 specimens for UU triaxial test;
- And the last, 12 specimens for CU triaxial testing.

The specimens used in unconfined compression test and triaxial test had been obtained from the remolded method. It might not represent the actual condition of weathered granite, but it is better to get the results from using those specimens in testing.

Pit slope design in this study has been separated into three (3) major pits configurations. The purpose of them is for simulation a different shapes of open pit, which they are containing different face slope and overall slope angles. The other objective is for a comparison among the resulting of those pits, which one gives a good reserve and

is suitable for mining operation at Pit MF-10. From the results, Pit Ver.3 is a steepest bench and also leads to the highest number of ore reserves, but in terms of safety factor, this pit is not suitable for mining in the area of weathered granite because it may have some risks occurs during the mining operation. Pit design Ver.1 and 2 are having more safety for mining in the weathered granite area. Pit Ver.1 is a one pit which give rise to minimum ore reserves but this pit design has proven acceptable in any steps of slope stability analysis. So this pit is suitable for long term mining in the area of Sub-Pit MF-10.

In slope stability analysis, there are total 55 slope geometry models and 88 analytical cases. That mean, it is required to build the slope geometry model within 55 models, and run the software FLAC3D by 88 times. The results of slope stability analysis are very satisfactory because it can determined the safe pit design and also determined the side of the pit slope which may occurs failure. In addition, it is to know the limit ability of pit slope design for the trial slope in this kaolin mine.

In terms of soil mechanics, the slope stability analysis for short term and long term mining slope should be considered. The parameters of geomaterials properties by using the results of cohesion and friction angle are obtained from laboratory testing. Those from undrained methods are assigned to the slope stability analysis of short term mining slope. The other one from the results of drained methods are assigned to the slope stability analysis of long term mining slope. But in this study, according to the results of previous studies and geotechnical investigation, the permeability of materials in the study area is low to very low, hence, the geomaterials parameters of drained and undrained cannot be used in simulation the actual condition of pit slope because almost all of the slope failure in this study area have been occurred from the erosional process. Therefore, the slope stability analysis in this study have been used the value of only cohesion and frictional angle that make the minimum factor of safety input to the step of slope stability analysis.

5.2 Recommendations

The results of this study can be used as part of making decision to selection the slope angle for mining in the kaolin mine. The resulting data was pointed out that Pit Ver.1 which have bench height equal 4 metres, face slope angle 40 deg., and overall slope

angle 28 deg. is the greatest safety pit. Hence, Pit Ver.1 is recommended for a mining operation in the Sub-Pit MF-10.

According to this research, during the site investigation the researcher can see a few sub-pits having occurred some small slope failures due to the effect from erosional process. So, that is another important issue which is needed to undertake further study and then find the appropriate measure to prevent or mitigate the slope failure due to erosion.

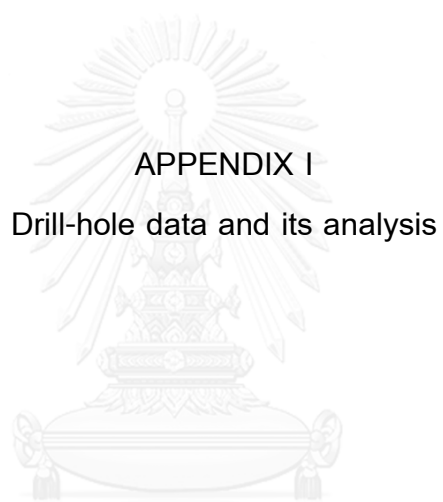


REFERENCES

- Appianing, E. J. A., & Mireku-Gyimah, D. (2015). Open Pit Optimisation and Design: A Stepwise Approach. *Ghana Mining Journal*, 15(2), 27-35.
- Carter, J., Desai, C., Potts, D., Schweiger, H., & Sloan, S. (2000). *Computing and computer modelling in geotechnical engineering*. Paper presented at the ISRM International Symposium.
- Crawford, J., & Davey, R. (1979). Case Study in Open Pit Limit Analysis. *Computer Methods for the 80's in the Mineral Industry*, 310-318.
- David, M. (2012). *Geostatistical Ore Reserve Estimation*: Elsevier Science.
- GDP. (2010a). Desk Study and Field Inspection Report for Slope Stability os Settling Pond Nos. 1-6, Haad Sompan Subdistrict, Muang District, Ranong Province. Mineral Resources Development Co., LTD.
- GDP. (2010b). Geotechnical Investigation at Existing Tailing Ponds, Haad Sompan Subdistrict, Muang Districc, Ranong Province *Final Report*. Mineral Resources Development Co., LTD.
- GDP. (2013). Final Report for Geotechnical Investigation Works and Slope Stability Analysis: Phase 1, Haad Sompan Subdistrict, Muang District, Ranong Province. Mineral Resources Development Co., LTD.
- Hustrulid, W. A., Kuchta, M., & Martin, R. K. (2013). *Open Pit Mine Planning and Design, Two Volume Set & CD-ROM Pack, Third Edition*: CRC Press.
- Hustrulid, W. A., McCarter, M. K., & Van Zyl, D. J. A. (2000). *Slope Stability in Surface Mining*: Society for Mining, Metallurgy, and Exploration.
- Itasca. (2005). *FLAC3D User Manual*.
- Jing, L., & Hudson, J. A. (2002). Numerical methods in rock mechanics. *International Journal of Rock Mechanics and Mining Sciences*, 39(4), 409-427. doi: Doi 10.1016/S1365-1609(02)00065-5

- Phairat, C. (2014). *The Safety Manual for Mining Activities*. Department of Primary Industry and Mine: Department of Primary Industry and Mine Retrieved from www.dpim.go.th/service/download?articleid=5838&F=10677.
- Philip, G., & Watson, D. (1987). *How ore deposits can be overestimated through computational methods*. Paper presented at the AIMM, RESOURCES AND RESERVES SYMPOSIUM, Melbourne, Proceedings.
- Pipat, L. (2016). Slope Stability Assessment at MRD's Kaolin Mine, Haad Sompan Subdistrict, Muang District, Ranong Province.
- Priest, S., & Brown, E. (1983). Probabilistic stability analysis of variable rock slopes.
- Read, J., & Stacey, P. (2009). Guidelines for open pit slope design.
- Soltani, A. (2015). ANALYSIS OF THE ARMP'S DATABASE USING FLAC3D; A PILLAR STABILITY COMPARISON FOR ROOM AND PILLAR COAL MINES DURING DEVELOPMENT.
- Soren, M. (2010). *EFFECTS OF FAULTS ON STABILITY OF SLOPES IN OPEN CAST MINES*. NATIONAL INSTITUTE OF TECHNOLOGY ROORKELA.
- Vermeer, P. A., & De Borst, R. (1984). Non-associated plasticity for soils, concrete and rock. *HERON*, 29 (3), 1984.
- Wenbing, W. (2008). *Three dimensional slope stability analysis and failure mechanism*. The Hong Kong Polytechnic University, <http://ira.lib.polyu.edu.hk/handle/10397/3829>.





APPENDIX I

Drill-hole data and its analysis

จุฬาลงกรณ์มหาวิทยาลัย
CHULALONGKORN UNIVERSITY

Assay File

Hole_id	From	To	Interval	KLN
MRD-106C	0	2.5	2.5	0
MRD-106C	2.5	5.5	3	0
MRD-106C	5.5	8	2.5	77.41
MRD-106C	8	10.5	2.5	82.97
MRD-106C	10.5	12	1.5	77.36
MRD-106C	12	14.5	2.5	88.5
MRD-106C	14.5	16.85	2.35	85.52
MRD-106C	16.85	18	1.15	79.87
MRD-106C	18	20.6	2.6	75.04
MRD-106C	20.6	22	1.4	53.84
MRD-106C	22	25.8	3.8	85.52
MRD-106C	25.8	27.8	2	79.87
MRD-106C	27.8	30.4	2.6	75.04
MRD-106C	30.4	33	2.6	0
MRD-108C	0	2	2	0
MRD-108C	2	4.5	2.5	0
MRD-108C	4.5	7.2	2.7	90.79
MRD-108C	7.2	9	1.8	78.29
MRD-108C	9	10.3	1.3	93.25
MRD-108C	10.3	12.8	2.5	91.99
MRD-108C	12.8	16	3.2	77.61
MRD-108C	16	18	2	79.09
MRD-108C	18	21	3	82.24
MRD-108C	21	23	2	88.62
MRD-108C	23	25	2	87.63
MRD-108C	25	26.2	1.2	91.03
MRD-108C	26.2	29	2.8	82.72
MRD-108C	29	32	3	90.05
MRD-108C	32	35	3	75.23

MRD-108C	35	37	2	91.99
MRD-108C	37	39	2	77.61
MRD-108C	39	41.5	2.5	79.09
MRD-108C	41.5	42.9	1.4	82.24
MRD-108C	42.9	43.5	0.6	0
MRD-114C	0	0.4	0.4	0
MRD-114C	0.4	3	2.6	79.97
MRD-114C	3	5.5	2.5	61.28
MRD-114C	5.5	7.6	2.1	50.85
MRD-114C	7.6	8.5	0.9	52.81
MRD-114C	8.5	10.2	1.7	86.35
MRD-114C	10.2	12	1.8	87.89
MRD-114C	12	13.5	1.5	74.67
MRD-114C	13.5	14.3	0.8	65.45
MRD-114C	14.3	16	1.7	56.93
MRD-114C	16	18.5	2.5	81.31
MRD-114C	18.5	19.3	0.8	87.08
MRD-114C	19.3	20.2	0.9	84.62
MRD-114C	20.2	22	1.8	87.97
MRD-114C	22	25.3	3.3	87.97
MRD-114C	25.3	27.3	2	84.45
MRD-114C	27.3	29	1.7	89.6
MRD-114C	29	31	2	90.07
MRD-114C	31	32.5	1.5	89.32
MRD-114C	32.5	34.9	2.4	87.97
MRD-114C	34.9	37	2.1	84.45
MRD-114C	37	38.7	1.7	89.6
MRD-114C	38.7	40	1.3	0
MRD-118C	0	3	3	0
MRD-118C	3	6	3	92.64
MRD-118C	6	9.7	3.7	92.61
MRD-118C	9.7	12	2.3	90

MRD-118C	12	15	3	91.67
MRD-118C	15	18	3	87.37
MRD-118C	18	20	2	78.05
MRD-118C	20	23	3	87.02
MRD-118C	23	26	3	84.78
MRD-118C	26	28	2	81.54
MRD-118C	28	30.1	2.1	81.54
MRD-118C	30.1	32.6	2.5	80.27
MRD-118C	32.6	35	2.4	91.67
MRD-118C	35	38	3	87.37
MRD-118C	38	41	3	78.05
MRD-118C	41	42	1	0
MRD-253C	0	2	2	92.74
MRD-253C	2	4	2	92.64
MRD-253C	4	6	2	92.61
MRD-253C	6	8	2	90
MRD-253C	8	10	2	91.67
MRD-253C	10	12	2	87.37
MRD-253C	12	14	2	78.05
MRD-253C	14	16	2	87.02
MRD-253C	16	18	2	84.78
MRD-253C	18	20	2	81.54
MRD-253C	20	22	2	81.54
MRD-253C	22	24	2	80.27
MRD-253C	24	26	2	78.73
MRD-253C	26	28	2	69.78
MRD-253C	28	30	2	63.3
MRD-253C	30	32	2	76.75
MRD-253C	32	34	2	86.76
MRD-253C	34	36	2	61.33
MRD-253C	36	38	2	63.25
MRD-253C	38	40	2	85.57

MRD-253C	40	42	2	0
MRD-256C	0	1	1	0
MRD-256C	1	2.6	1.6	90.62
MRD-256C	2.6	4	1.4	87.74
MRD-256C	4	5.65	1.65	88.61
MRD-256C	5.65	8	2.35	91.2
MRD-256C	8	10	2	91.42
MRD-256C	10	11.15	1.15	90.8
MRD-256C	11.15	13	1.85	93.9
MRD-256C	13	15	2	90.12
MRD-256C	15	17	2	90.79
MRD-256C	17	19	2	88
MRD-256C	19	19.5	0.5	0
MRD-256C	19.5	19.62	0.12	88
MRD-256C	19.62	23	3.38	83.6
MRD-256C	23	25	2	92.59
MRD-256C	25	25.3	0.3	0
MRD-256C	25.3	28	2.7	89.17
MRD-256C	28	30	2	88.44
MRD-256C	30	31	1	72.33
MRD-256C	31	33.1	2.1	0
MRD-257C	0	6.2	6.2	0
MRD-257C	6.2	8	1.8	91.63
MRD-257C	8	10	2	90.74
MRD-257C	10	12	2	67.26
MRD-257C	12	14.25	2.25	63.08
MRD-257C	14.25	16.1	1.85	61.55
MRD-257C	16.1	20	3.9	0
MRD-258C	0	3.6	3.6	0
MRD-258C	3.6	4.64	1.04	77.41
MRD-258C	4.64	4.8	0.16	0
MRD-258C	4.8	5	0.2	77.41

MRD-258C	5	7	2	82.97
MRD-258C	7	8.8	1.8	77.36
MRD-258C	8.8	9.05	0.25	0
MRD-258C	9.05	9.6	0.55	77.36
MRD-258C	9.6	10	0.4	85.09
MRD-258C	10	10.1	0.1	0
MRD-258C	10.1	11.8	1.7	85.09
MRD-258C	11.8	13.18	1.38	0
MRD-258C	13.18	15	1.82	88.5
MRD-258C	15	16.5	1.5	85.52
MRD-258C	16.5	17.9	1.4	79.87
MRD-258C	17.9	19	1.1	75.04
MRD-258C	19	21	2	53.84
MRD-258C	21	24	3	0
MRD-260C	0	0.9	0.9	0
MRD-260C	0.9	2.45	1.55	84.32
MRD-260C	2.45	4	1.55	83.53
MRD-260C	4	6	2	87.18
MRD-260C	6	8	2	86.27
MRD-260C	8	10	2	88.74
MRD-260C	10	11.4	1.4	86.35
MRD-260C	11.4	11.6	0.2	0
MRD-260C	11.6	12	0.4	86.35
MRD-260C	12	14	2	87.89
MRD-260C	14	16	2	74.67
MRD-260C	16	18	2	65.45
MRD-260C	18	19.85	1.85	56.93
MRD-260C	19.85	28	8.15	0
MRD-261C	0	2.87	2.87	0
MRD-261C	2.87	4.43	1.56	84.56
MRD-261C	4.43	5.73	1.3	0
MRD-261C	5.73	8	2.27	83.98

MRD-261C	8	10	2	79.97
MRD-261C	10	11.8	1.8	61.28
MRD-261C	11.8	13	1.2	50.85
MRD-261C	13	14	1	52.81
MRD-261C	14	14.2	0.2	53
MRD-261C	14.2	14.6	0.4	52.81
MRD-261C	14.6	18	3.4	0
MRD-262C	0	3.15	3.15	0
MRD-262C	3.15	5	1.85	81.31
MRD-262C	5	7	2	87.08
MRD-262C	7	9	2	84.62
MRD-262C	9	11	2	87.97
MRD-262C	11	13	2	87.97
MRD-262C	13	15	2	84.45
MRD-262C	15	17	2	89.6
MRD-262C	17	19	2	90.07
MRD-262C	19	20.9	1.9	89.32
MRD-262C	20.9	21.75	0.85	84.21
MRD-262C	21.75	24	2.25	68.21
MRD-262C	24	26	2	84.45
MRD-262C	26	28	2	86.77
MRD-262C	28	30	2	86.29
MRD-262C	30	32	2	83.55
MRD-262C	32	34	2	80.74
MRD-262C	34	36	2	78.38
MRD-262C	36	38	2	80.41
MRD-262C	38	40.75	2.75	88.57
MRD-262C	40.75	43	2.25	0
MRD-266C	0	2	2	90.22
MRD-266C	2	4	2	86.21
MRD-266C	4	5	1	85.39
MRD-266C	5	6.4	1.4	89.95

MRD-266C	6.4	7.95	1.55	89.16
MRD-266C	7.95	10.4	2.45	0
MRD-266C	10.4	12	1.6	90.79
MRD-266C	12	13.3	1.3	78.29
MRD-266C	13.3	15	1.7	93.25
MRD-266C	15	16.85	1.85	91.99
MRD-266C	16.85	18.6	1.75	77.61
MRD-266C	18.6	20	1.4	79.09
MRD-266C	20	22	2	82.24
MRD-266C	22	24	2	88.62
MRD-266C	24	26	2	87.63
MRD-266C	26	28.4	2.4	91.03
MRD-266C	28.4	30	1.6	82.72
MRD-266C	30	31.4	1.4	90.05
MRD-266C	31.4	32.8	1.4	75.23
MRD-266C	32.8	35	2.2	0

Collar File

Hole_id	X(m)	Y(m)	Z(m_MSL)	Max_Depth(m)
MRD-106C	465298.34	1100030.12	293.68	33
MRD-108C	465388.27	1100039.65	269.06	43.5
MRD-114C	465544.22	1099955.52	251.36	40
MRD-118C	465410.57	1099964.34	282.35	42
MRD-253C	465470.98	1099976.8	258.21	40
MRD-256C	465296.7	1100011.59	284.12	33.1
MRD-257C	465384.11	1100161.16	259.62	20
MRD-258C	465580.8	1100054.62	239.9	24
MRD-260C	465616.01	1100069.48	243.22	28
MRD-261C	465546.14	1100079.14	238.99	18
MRD-262C	465477.24	1100053.49	258.82	43
MRD-266C	465342.33	1099961.55	276.92	35

Survey File

Hole id.	From (m)	To (m)	Azimut	Dip
MRD-106C	0	33	0	-90
MRD-108C	0	43.5	0	-90
MRD-114C	0	40	0	-90
MRD-118C	0	42	0	-90
MRD-253C	0	40	0	-90
MRD-256C	0	33.1	0	-90
MRD-257C	0	20	0	-90
MRD-258C	0	24	0	-90
MRD-260C	0	28	0	-90
MRD-261C	0	18	0	-90
MRD-262C	0	43	0	-90
MRD-266C	0	35	0	-90

Lithology File

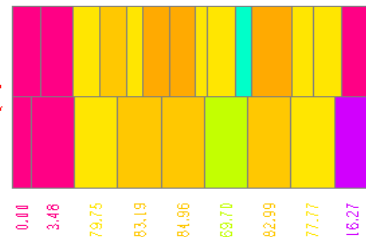
Hole_id	From (m)	To (m)	Rock_code	Rock_Type
MRD-106C	0	2.5	1	SAND
MRD-106C	2.5	30.4	2	KLN
MRD-106C	30.4	33	3	GRA
MRD-108C	0	4.5	1	SAND
MRD-108C	4.5	42.9	2	KLN
MRD-108C	42.9	43.5	3	GRA
MRD-114C	0	0.4	1	SAND
MRD-114C	0.4	38.7	2	KLN
MRD-114C	38.7	40	3	GRA
MRD-118C	0	3	1	SAND
MRD-118C	3	41	2	KLN
MRD-118C	41	42	3	GRA
MRD-253C	0	40	2	KLN

MRD-253C	40	42	3	GRA
MRD-256C	0	1	1	SAND
MRD-256C	1	31	2	KLN
MRD-256C	31	33	3	GRA
MRD-257C	0	6.2	1	SAND
MRD-257C	6.2	16.1	2	KLN
MRD-257C	16.1	20	3	GRA
MRD-258C	0	3.6	1	SAND
MRD-258C	3.6	21	2	KLN
MRD-258C	21	24	3	GRA
MRD-260C	0	0.9	1	SAND
MRD-260C	0.9	19.85	2	KLN
MRD-260C	19.85	28	3	GRA
MRD-261C	0	2.87	1	SAND
MRD-261C	2.87	14.6	2	KLN
MRD-261C	14.6	18	3	GRA
MRD-262C	0	3.15	1	SAND
MRD-262C	3.15	40.75	2	KLN
MRD-262C	40.75	43	3	GRA
MRD-266C	0	32.8	2	KLN
MRD-266C	32.8	35	3	GRA

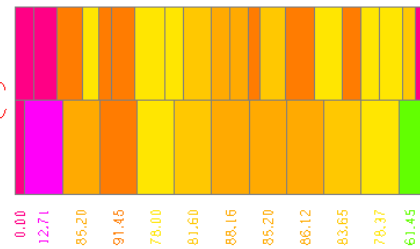
Drill-hole compositing Data and assay



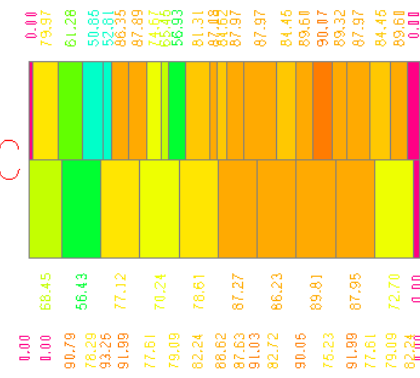
MRD-106C



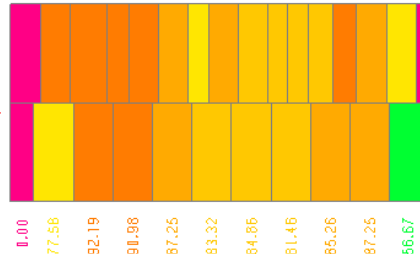
MRD-108C



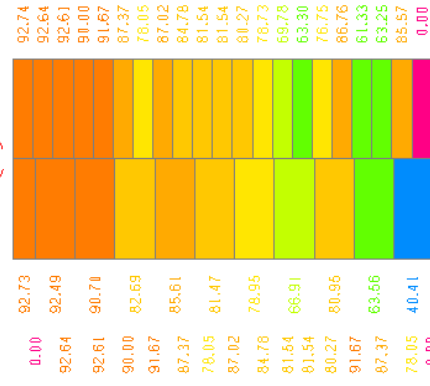
MRD-114C



MRD-118C



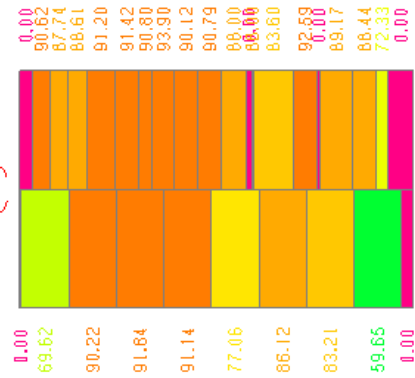
MRD-253C



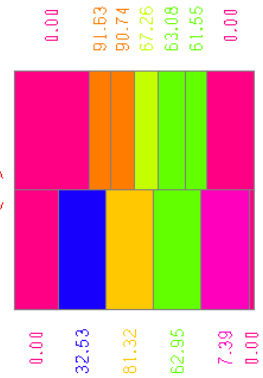
Drill-hole compositing Data and assay



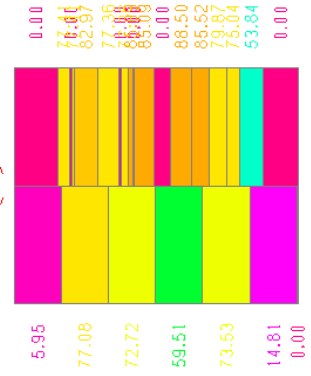
MRD-256C



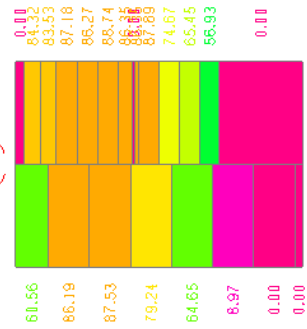
MRD-257C



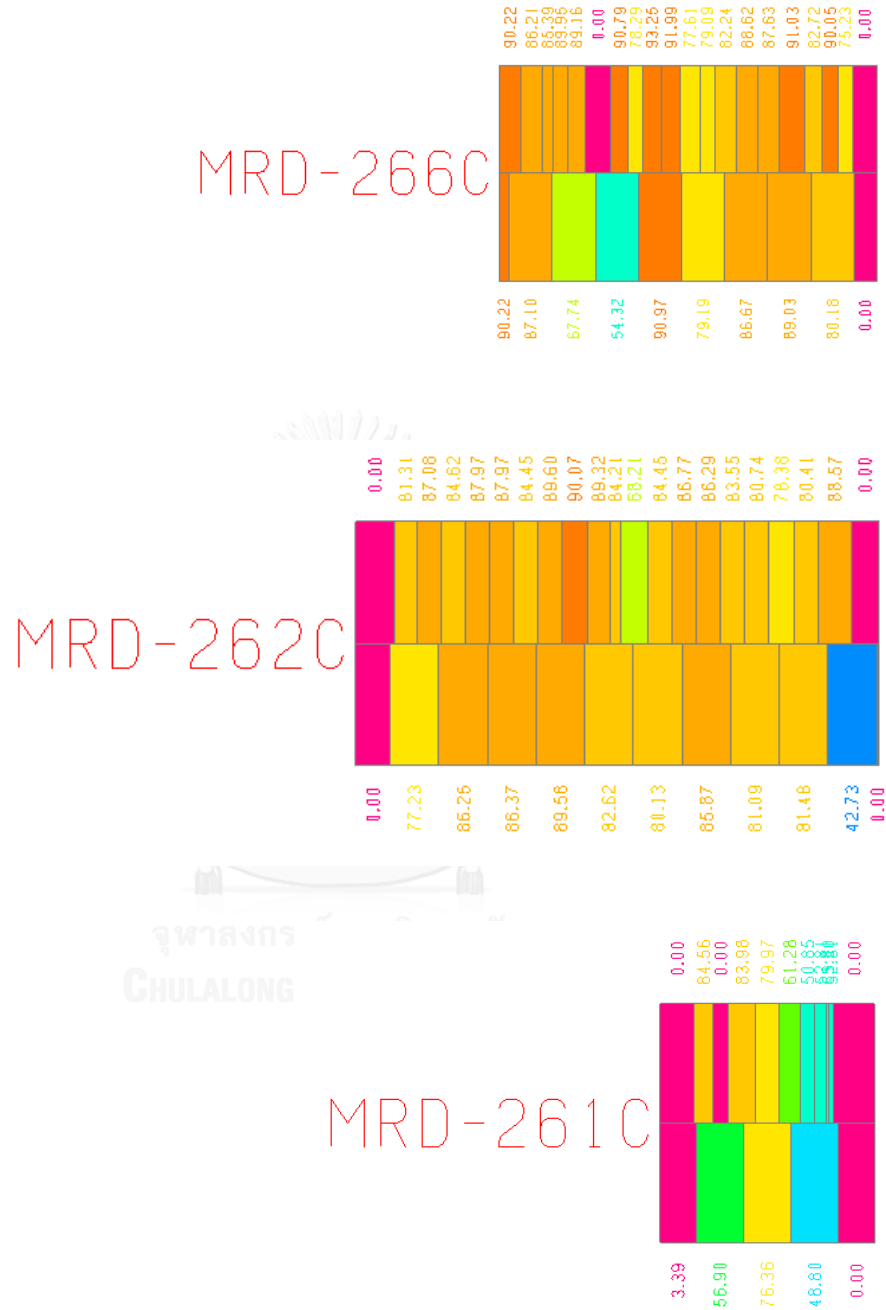
MRD-258C



MRD-260C



Drill-hole compositing Data and assay

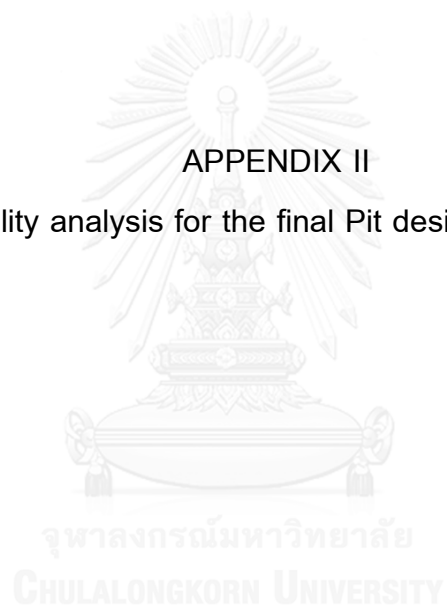


Total estimated blocks obtained from Inverse distance method

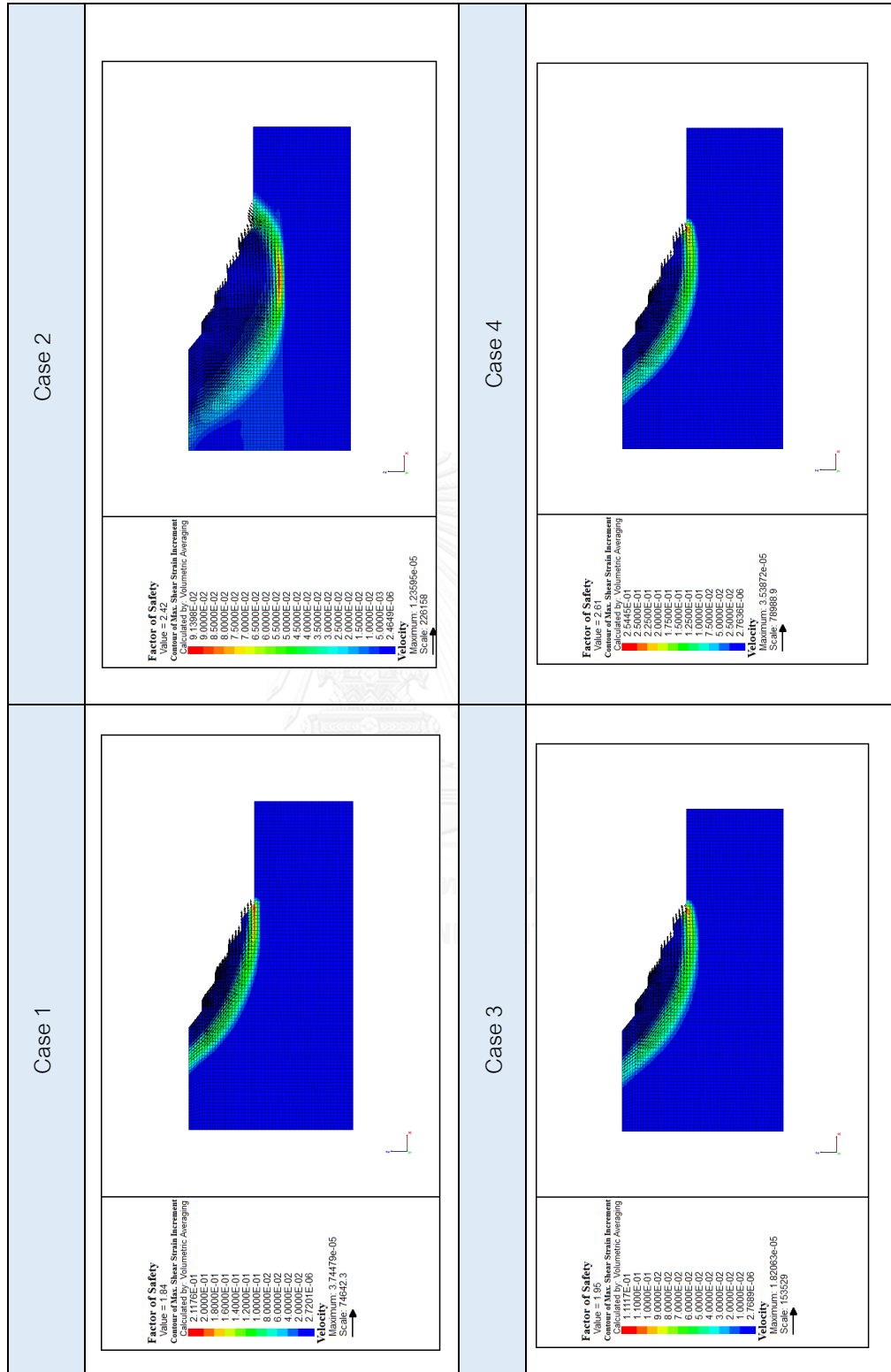
Bench no.	Elevation (m. MSL)	Total block in each bench
29	304	2
30	300	7
31	296	15
32	292	40
33	288	84
34	284	144
35	280	209
36	276	282
37	272	364
38	268	455
39	264	562
40	260	671
41	256	804
42	252	889
43	248	989
44	244	1066
45	240	1162
46	236	1267
47	232	1318
48	228	1252
49	224	1273
50	220	1123
51	216	969
52	212	967
53	208	966
54	204	824
55	200	795
56	196	723
57	192	305
Sum		19,527

APPENDIX II

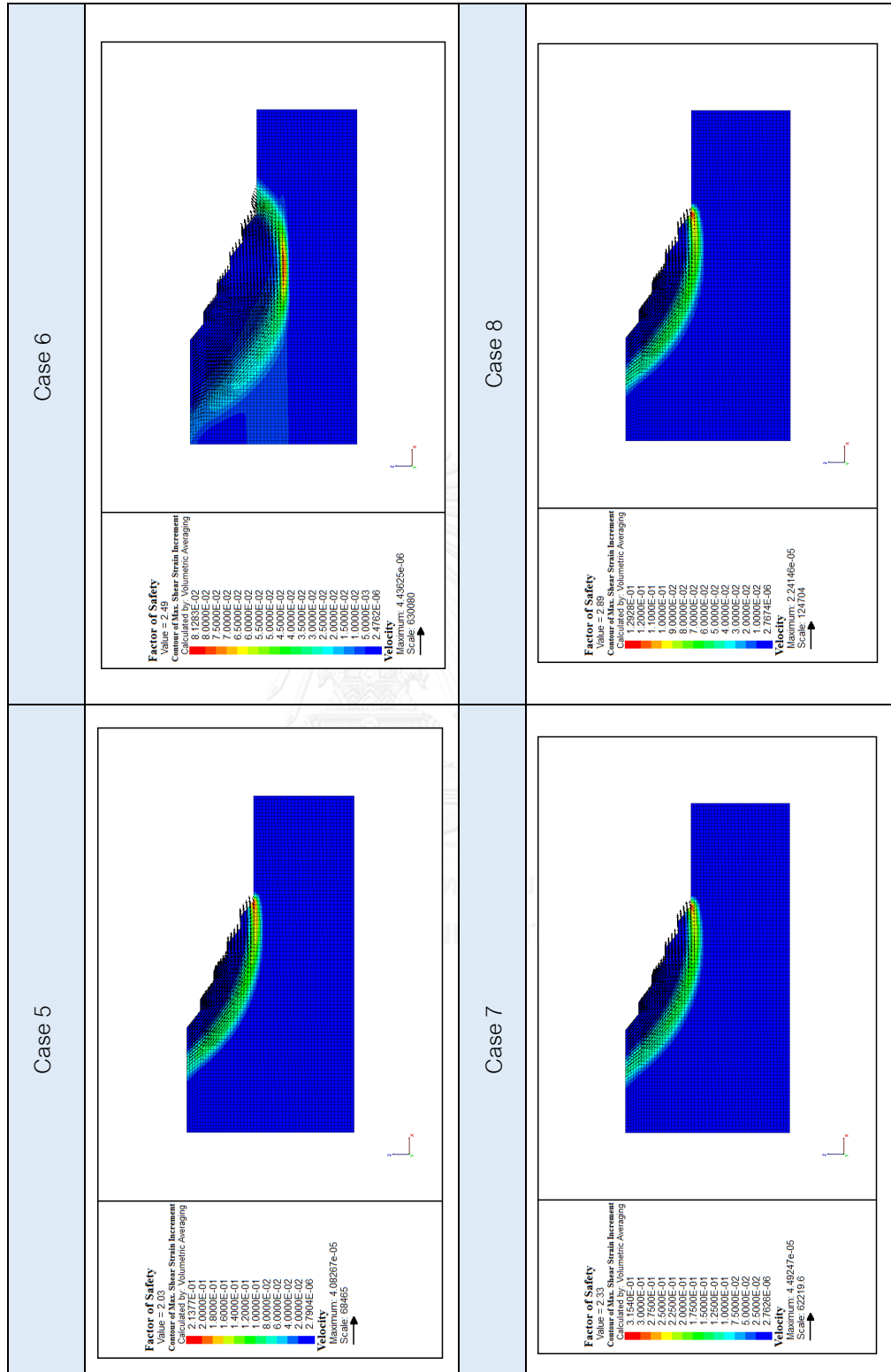
Slope stability analysis for the final Pit design Ver.1, 2, and 3



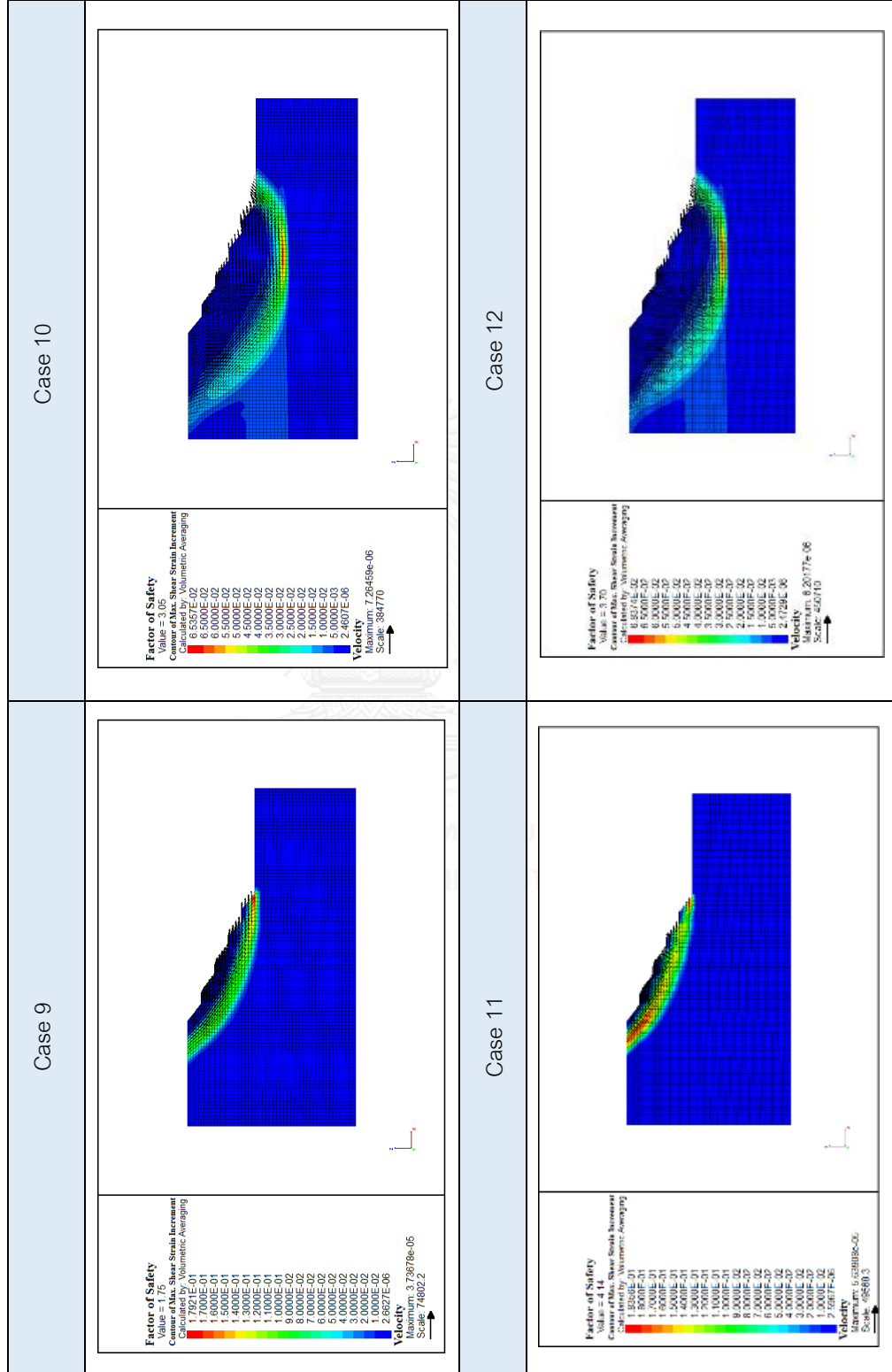
The results of slope stability analysis for final Pit design Ver.1



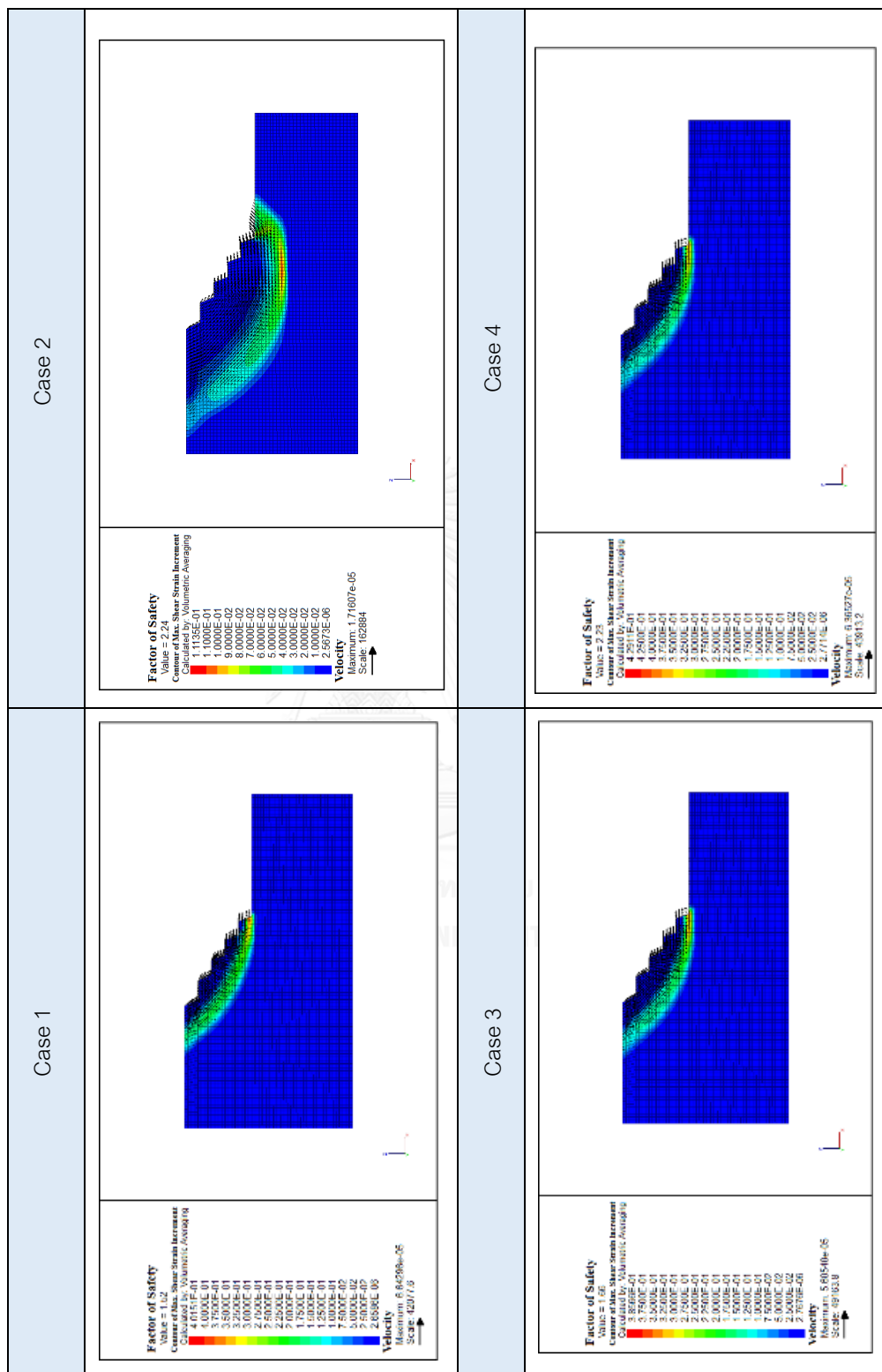
The results of slope stability analysis for final Pit design Ver.1



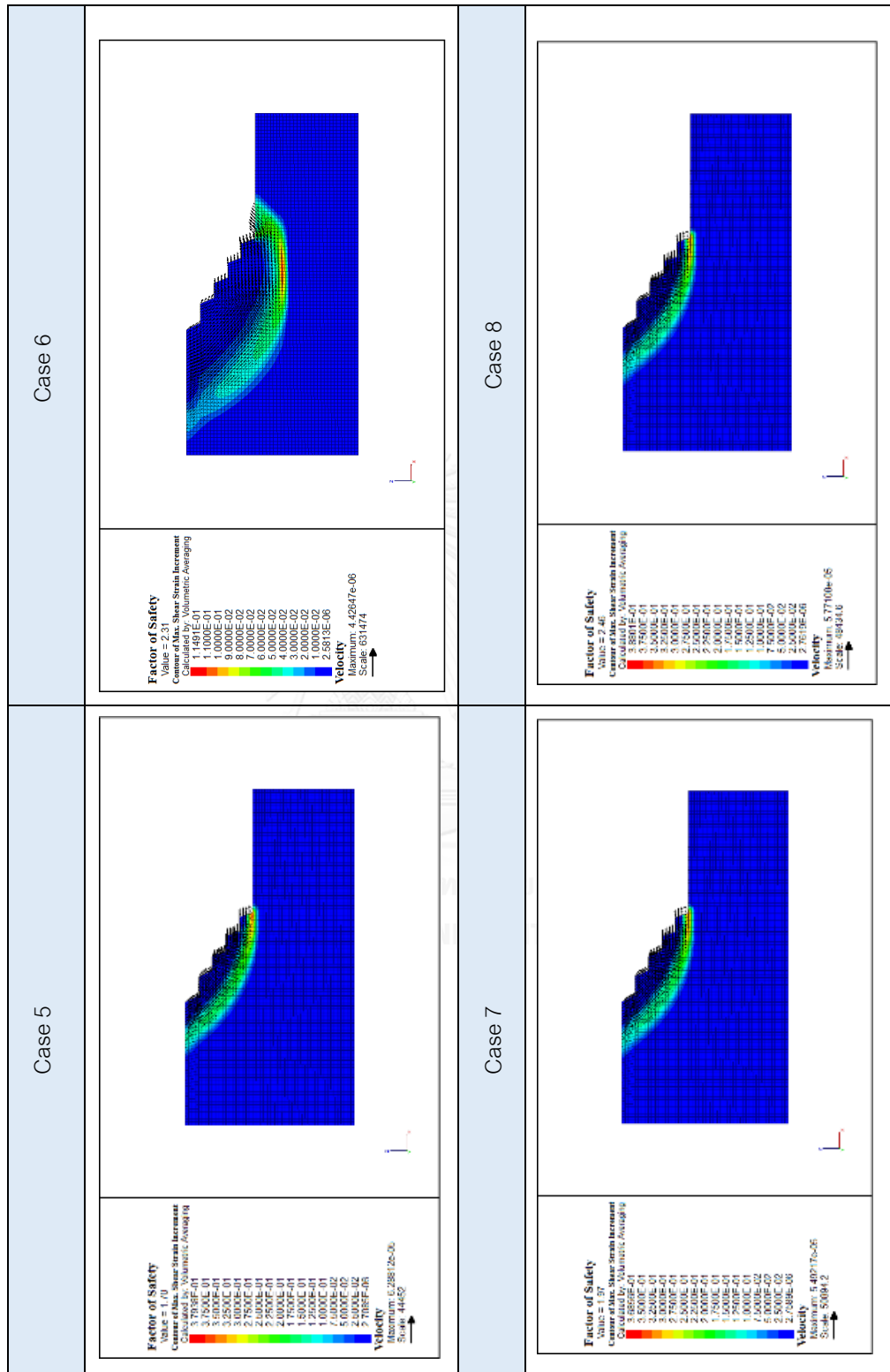
The results of slope stability analysis for final Pit design Ver.1



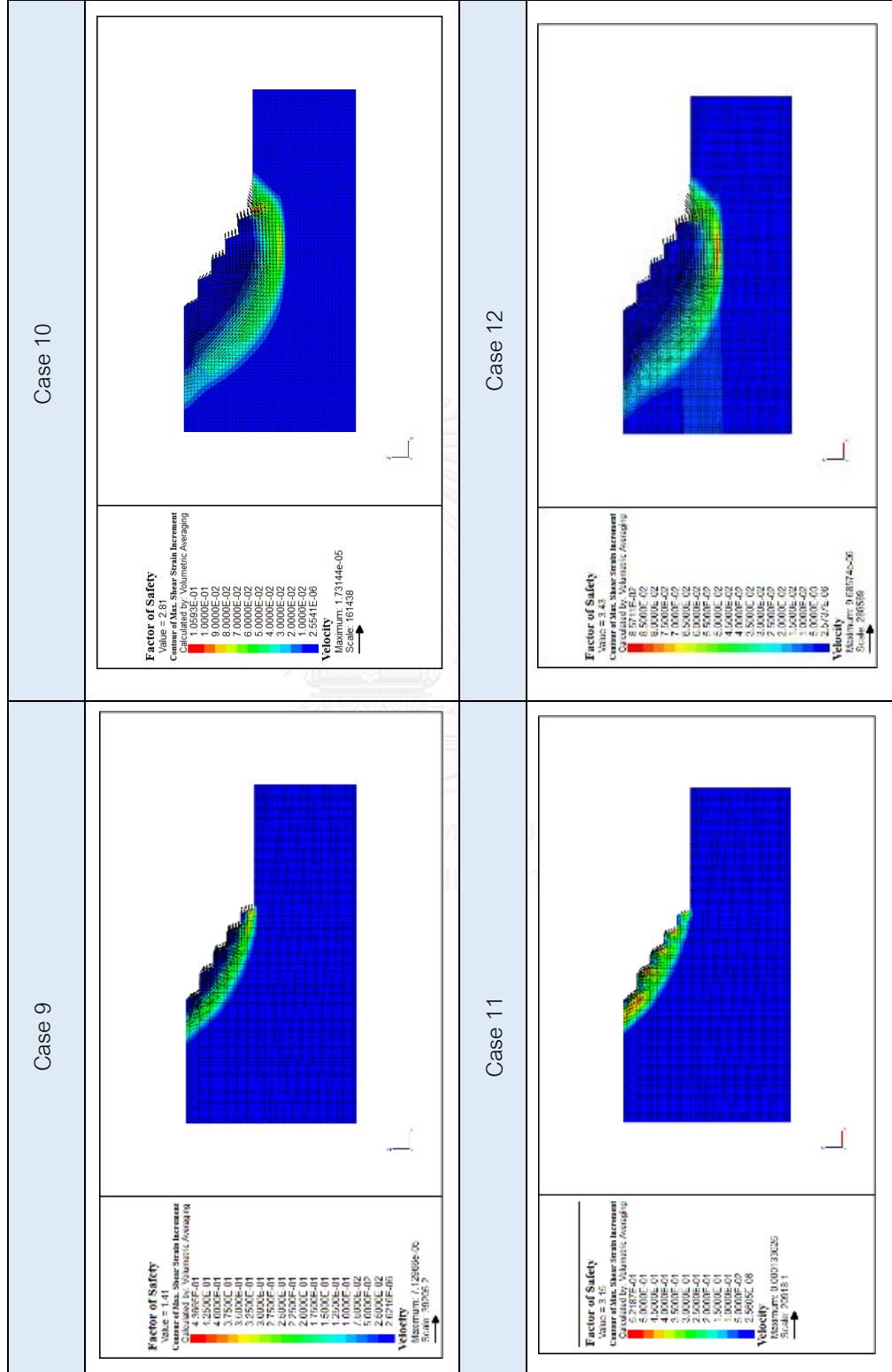
The results of slope stability analysis for final Pit design Ver.2



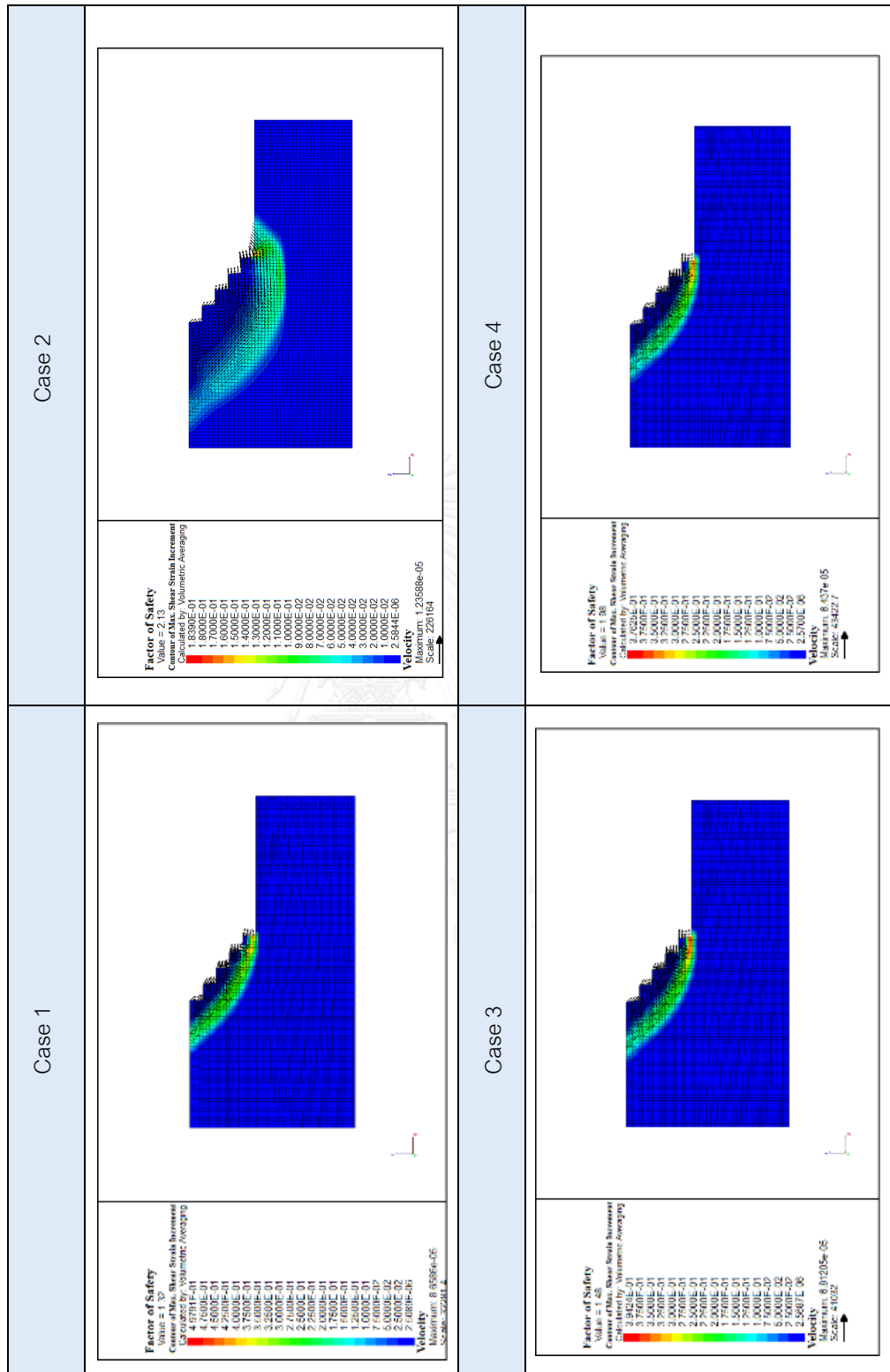
The results of slope stability analysis for final Pit design Ver.2



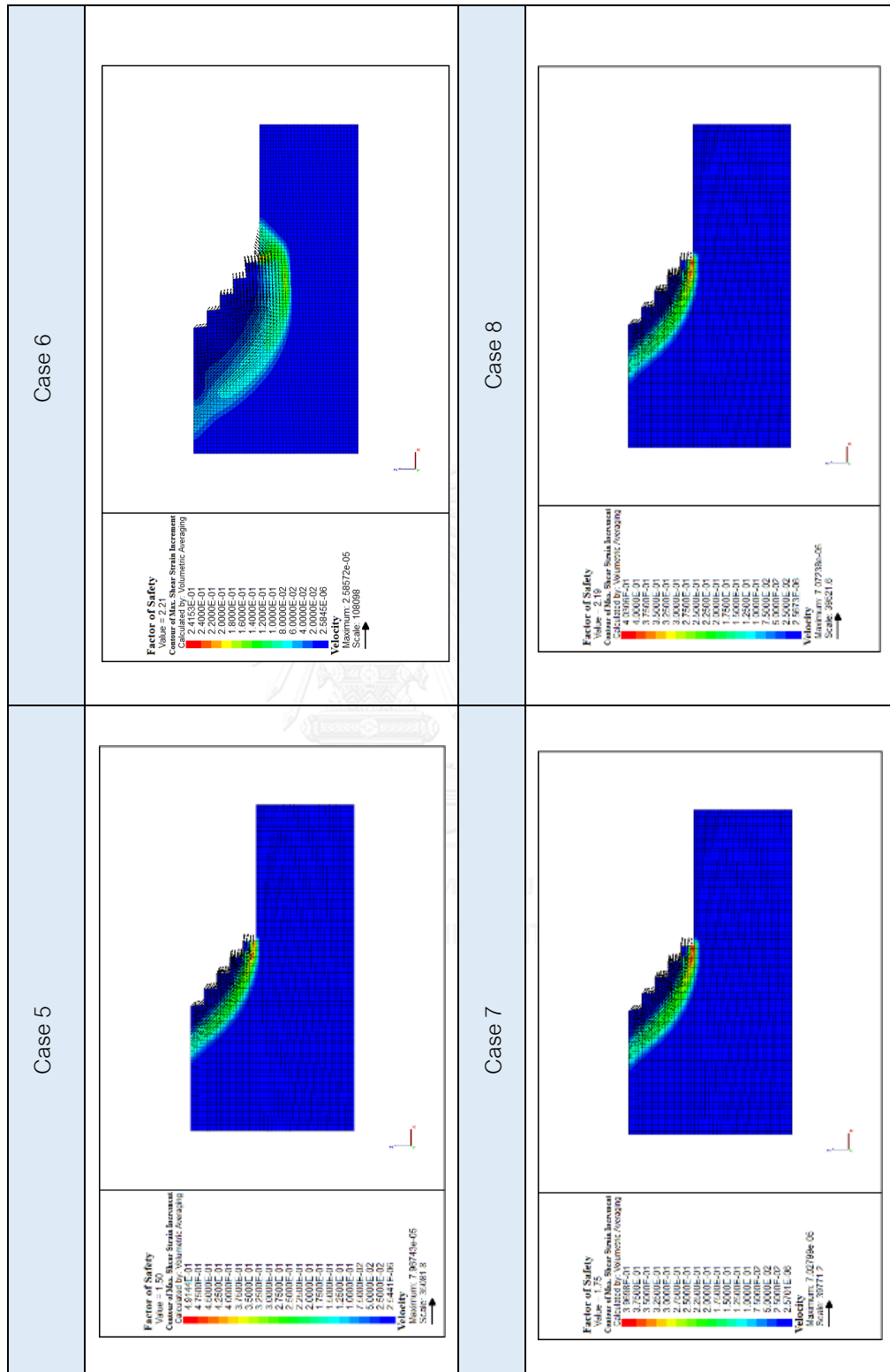
The results of slope stability analysis for final Pit design Ver.2



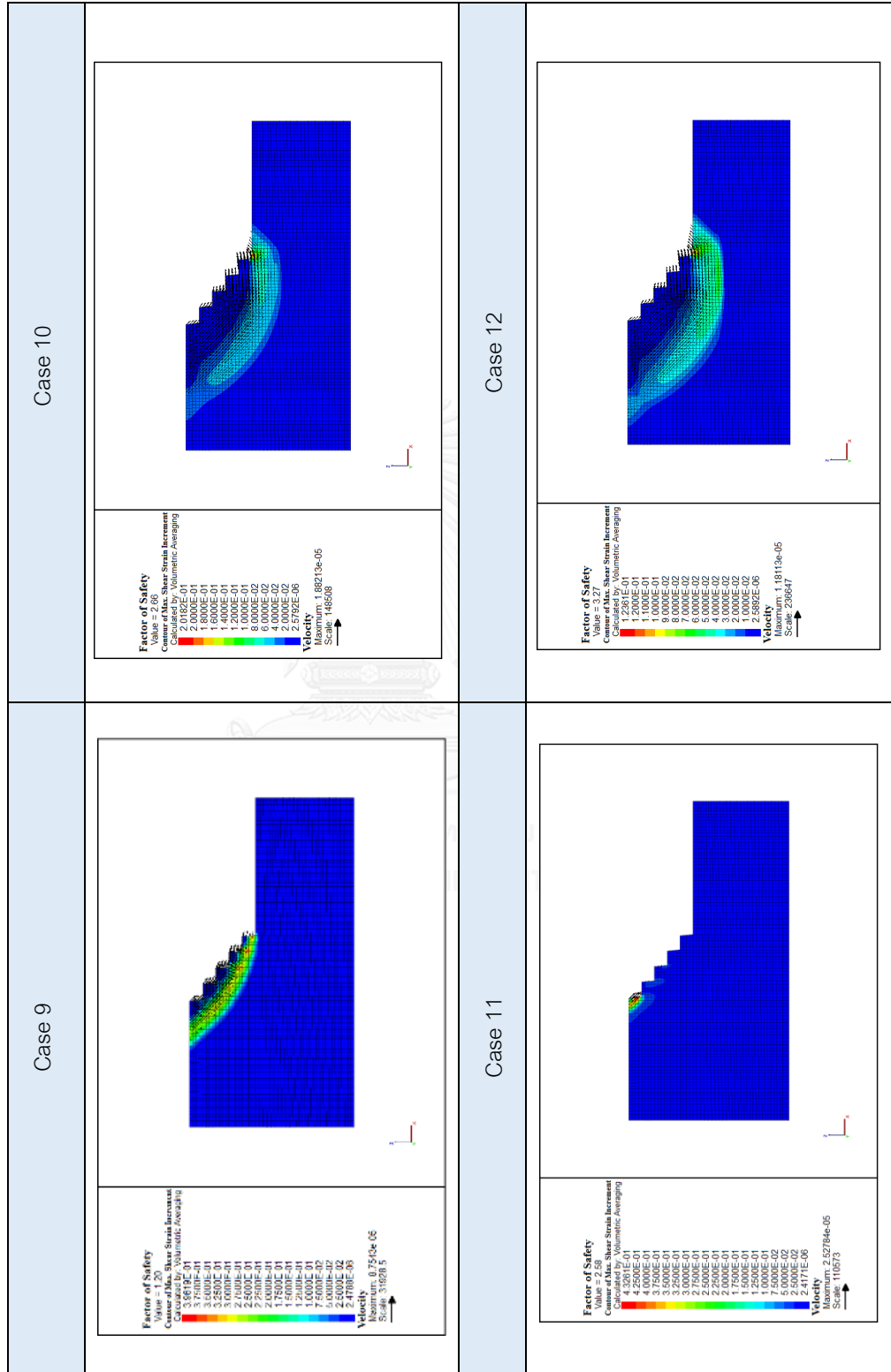
The results of slope stability analysis for final Pit design Ver.3



The results of slope stability analysis for final Pit design Ver.3

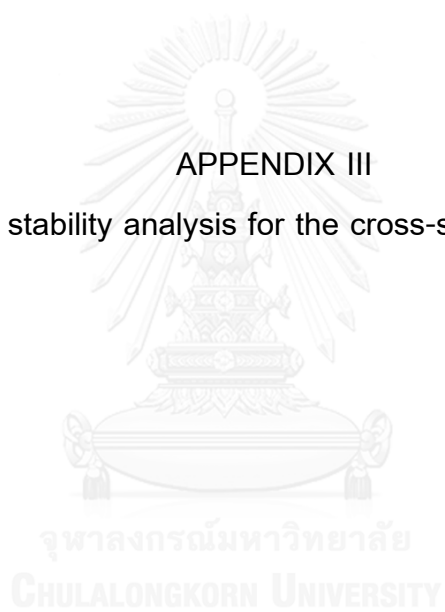


The results of slope stability analysis for final Pit design Ver.3

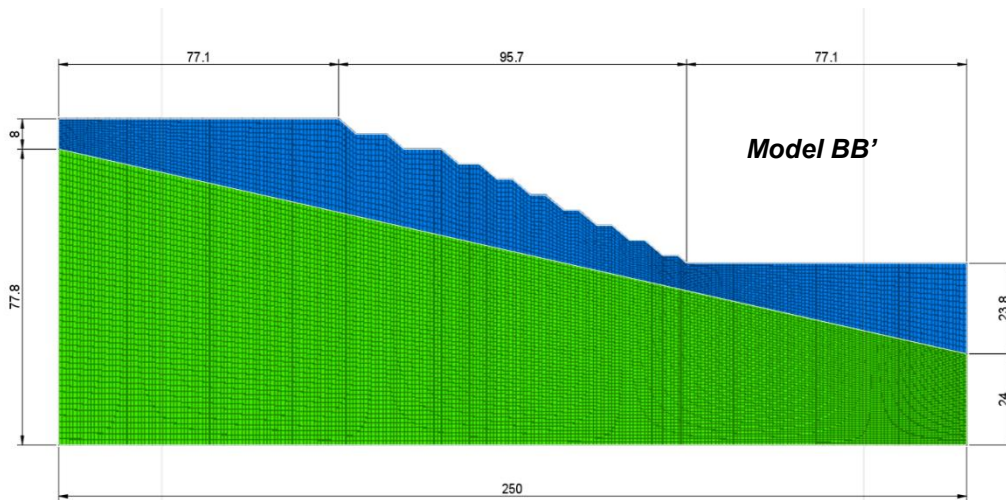
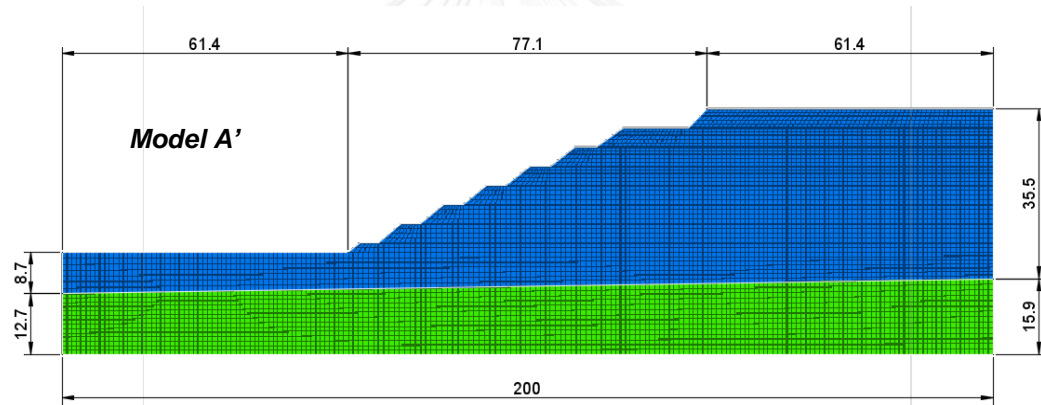
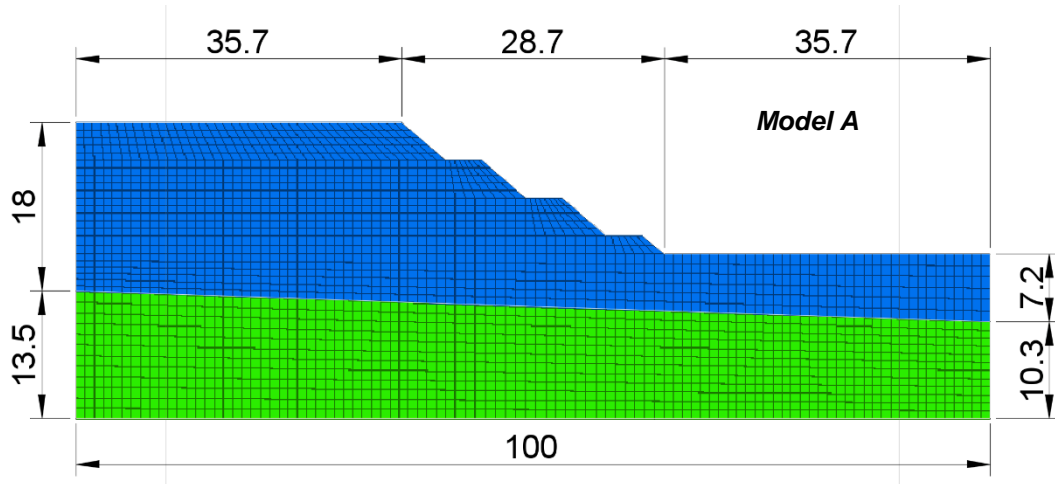


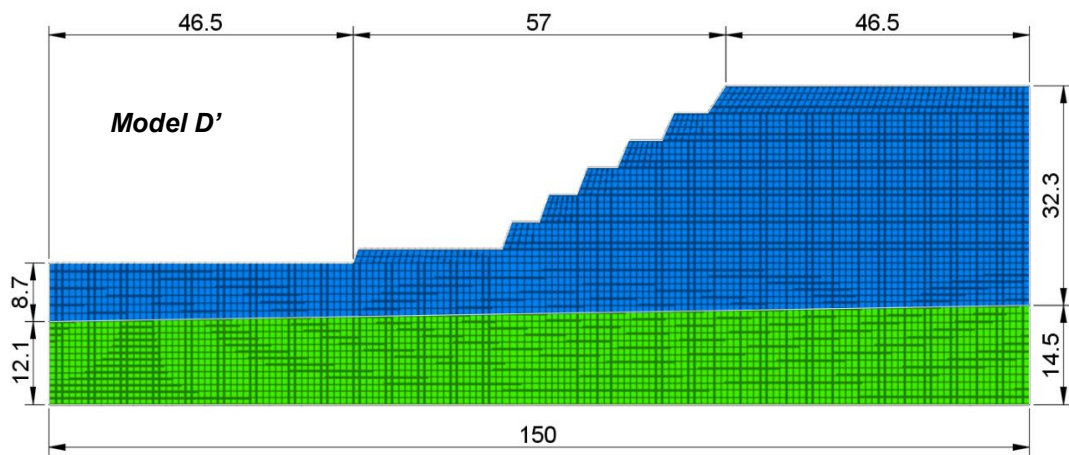
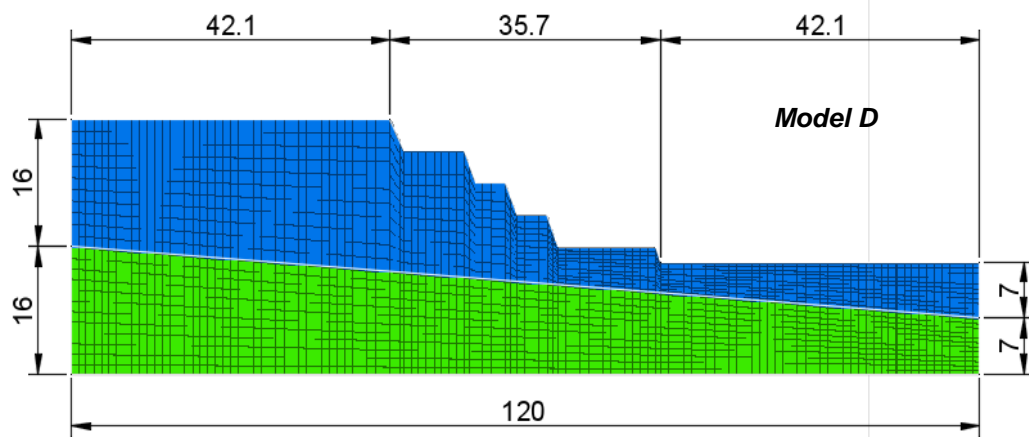
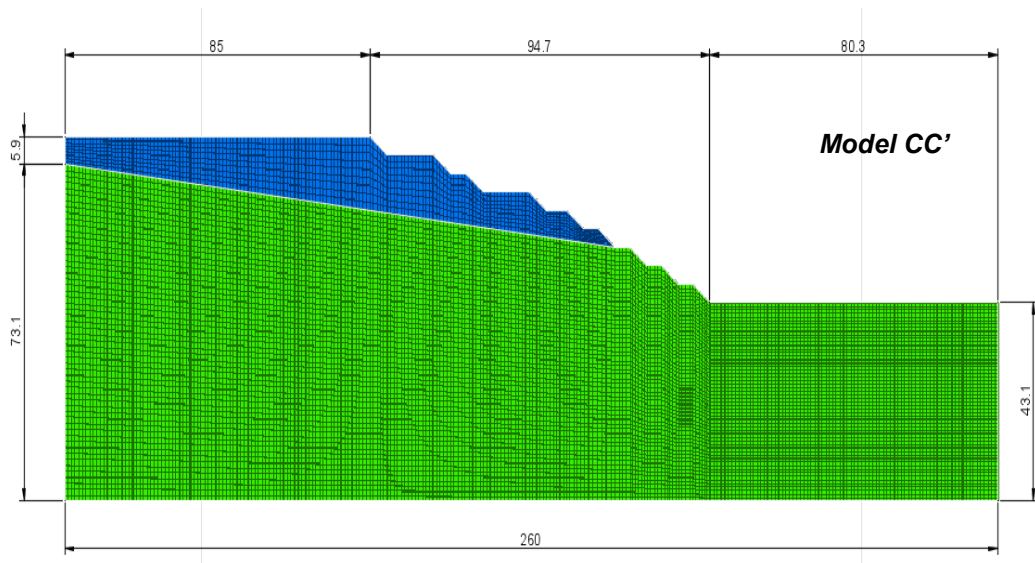
APPENDIX III

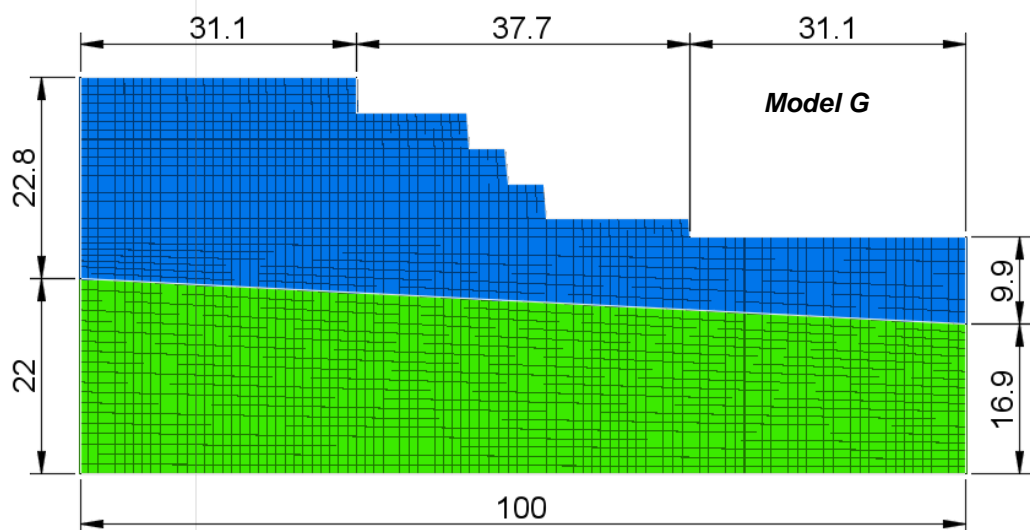
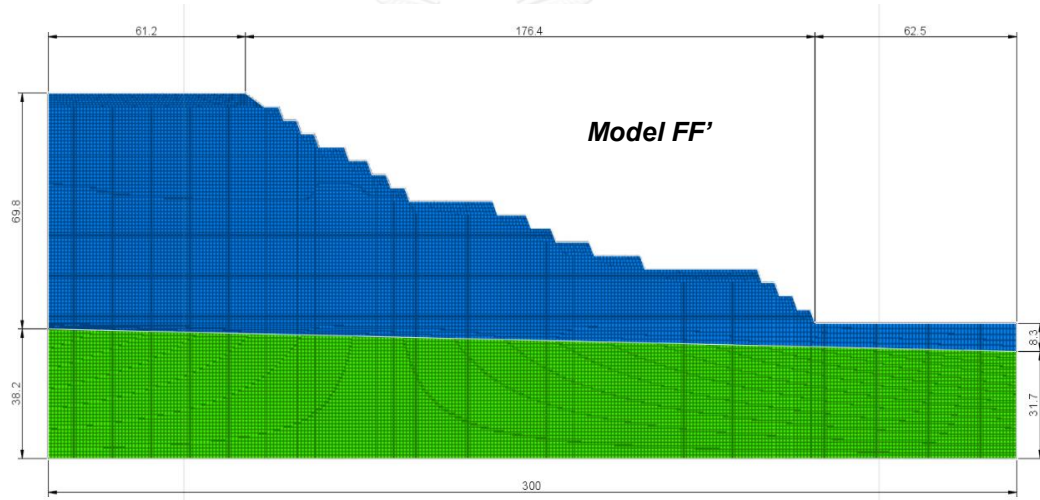
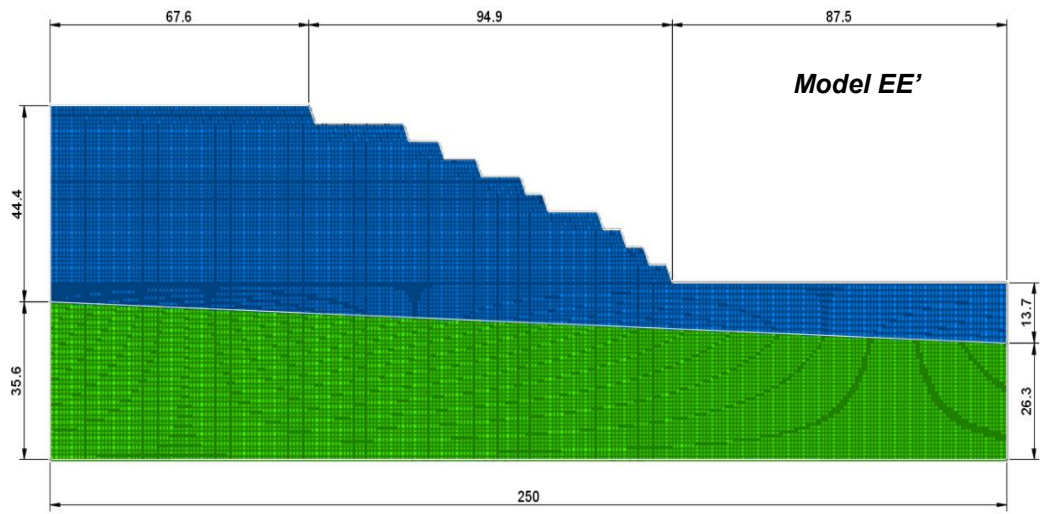
Slope stability analysis for the cross-section model

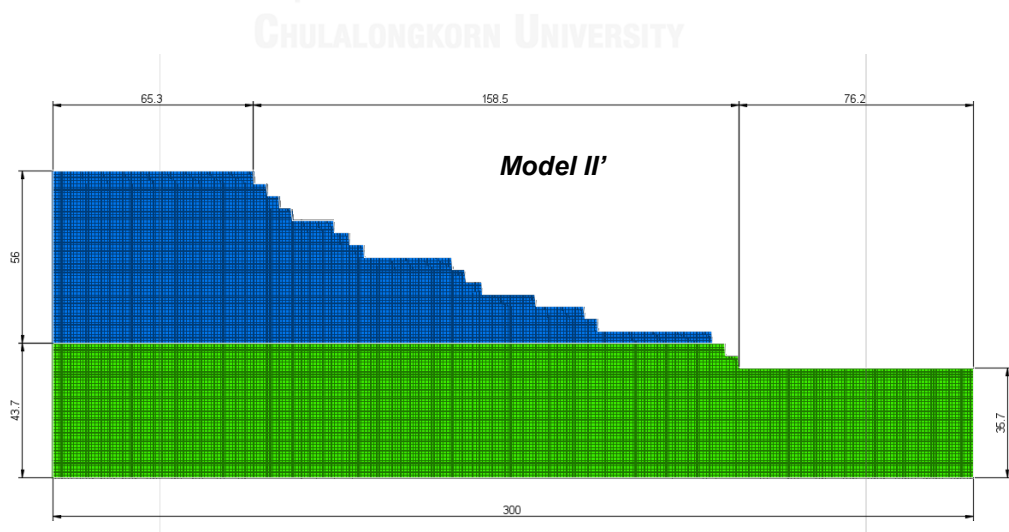
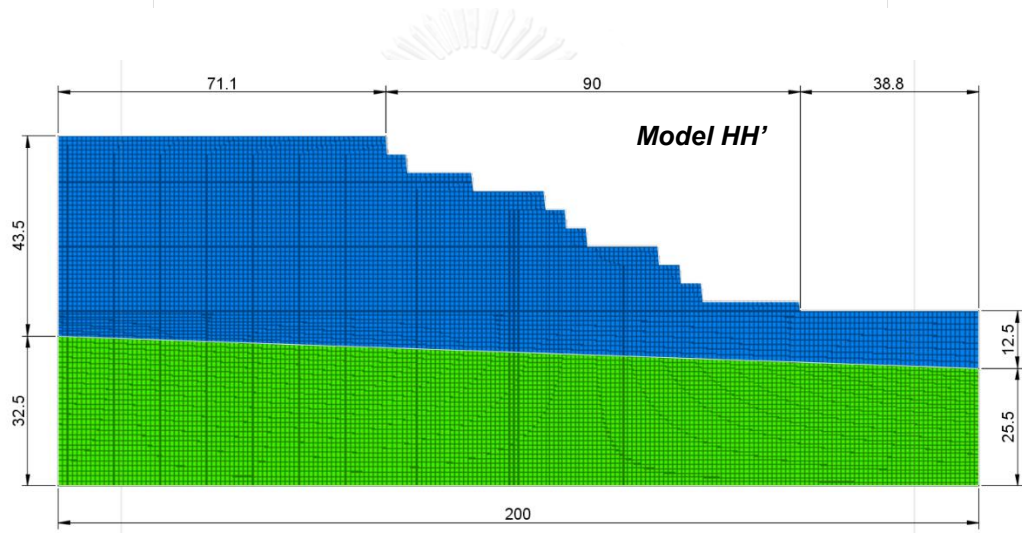
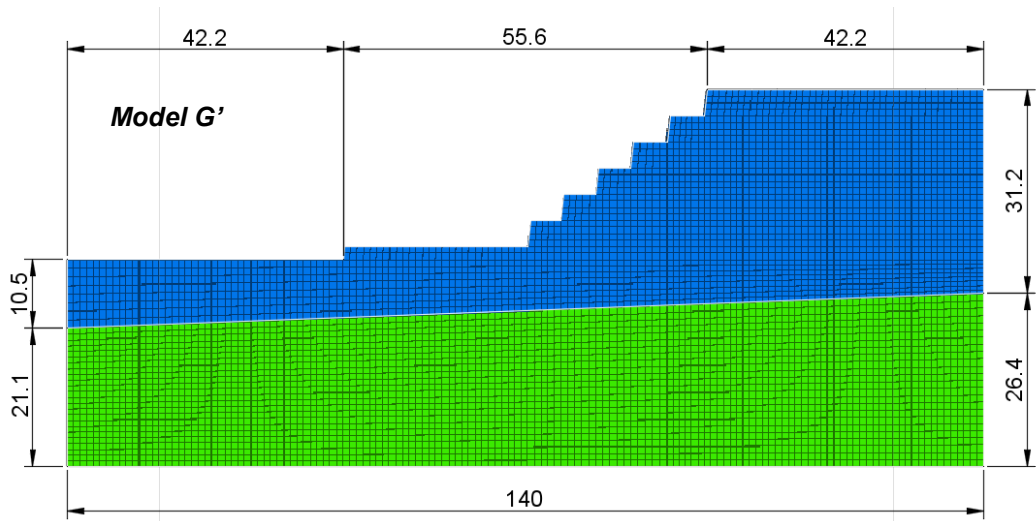


Slope geometry model of analysis for Pit Ver.1, 2, and 3



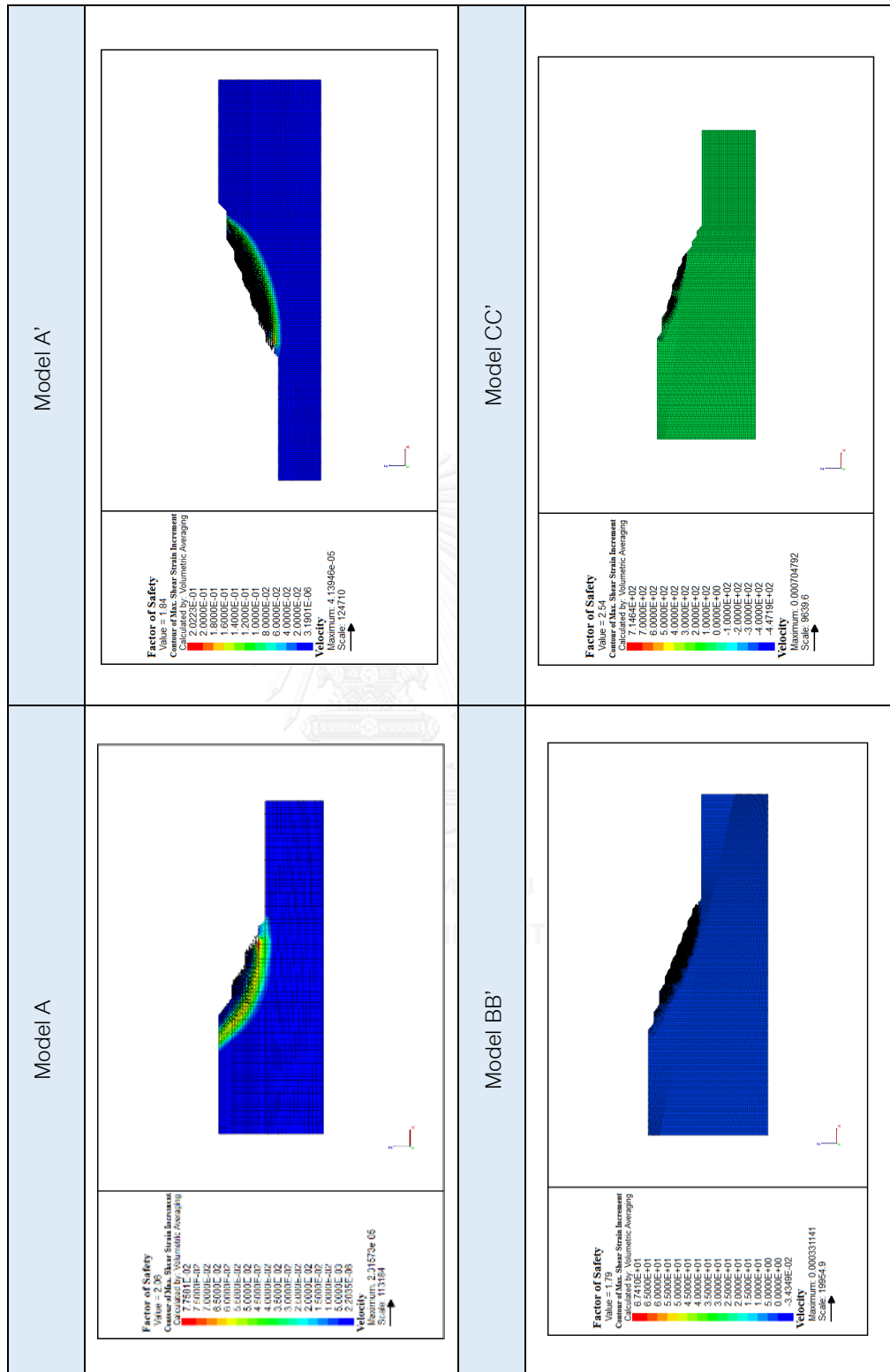




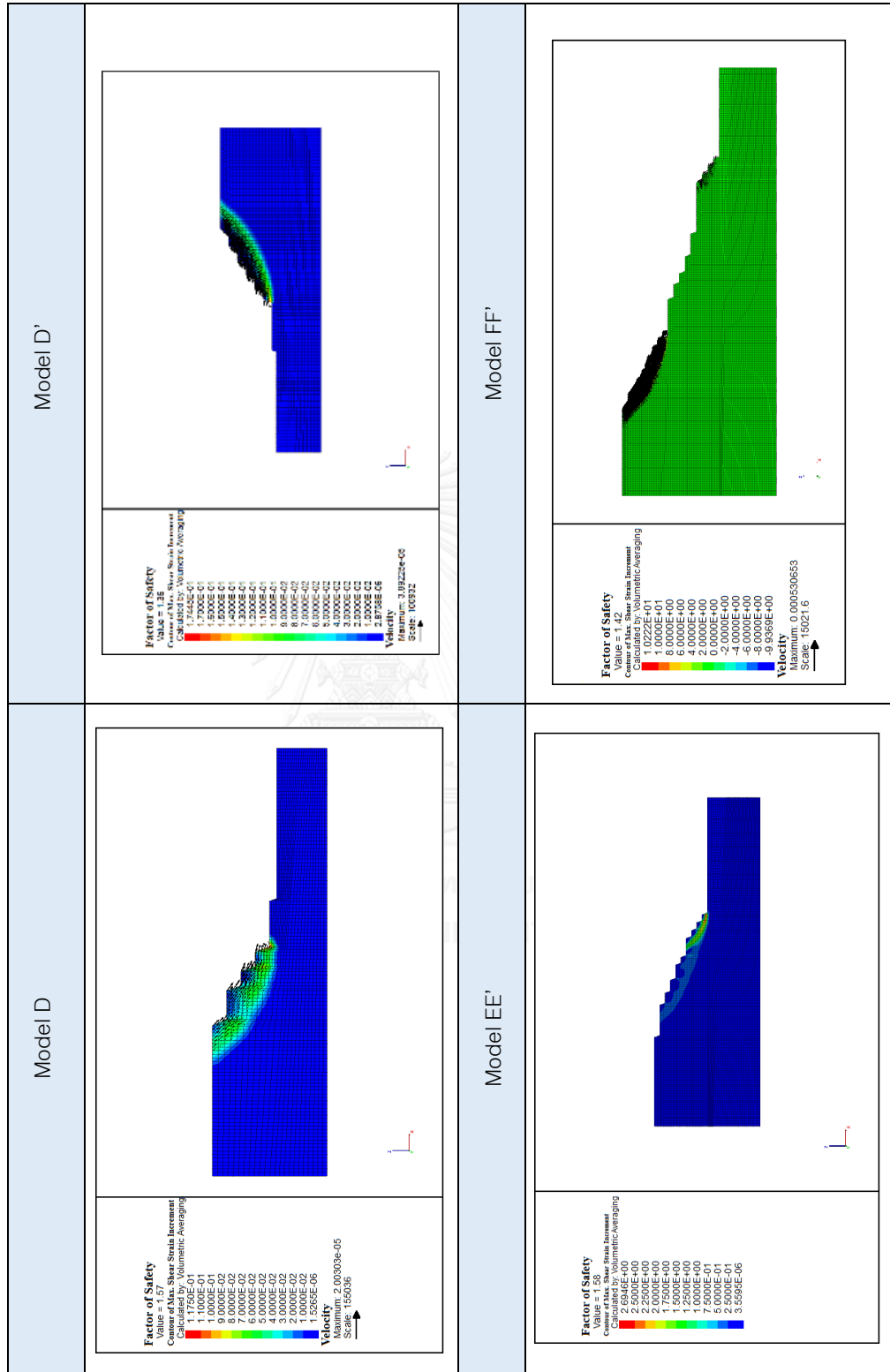


CHULALONGKORN UNIVERSITY

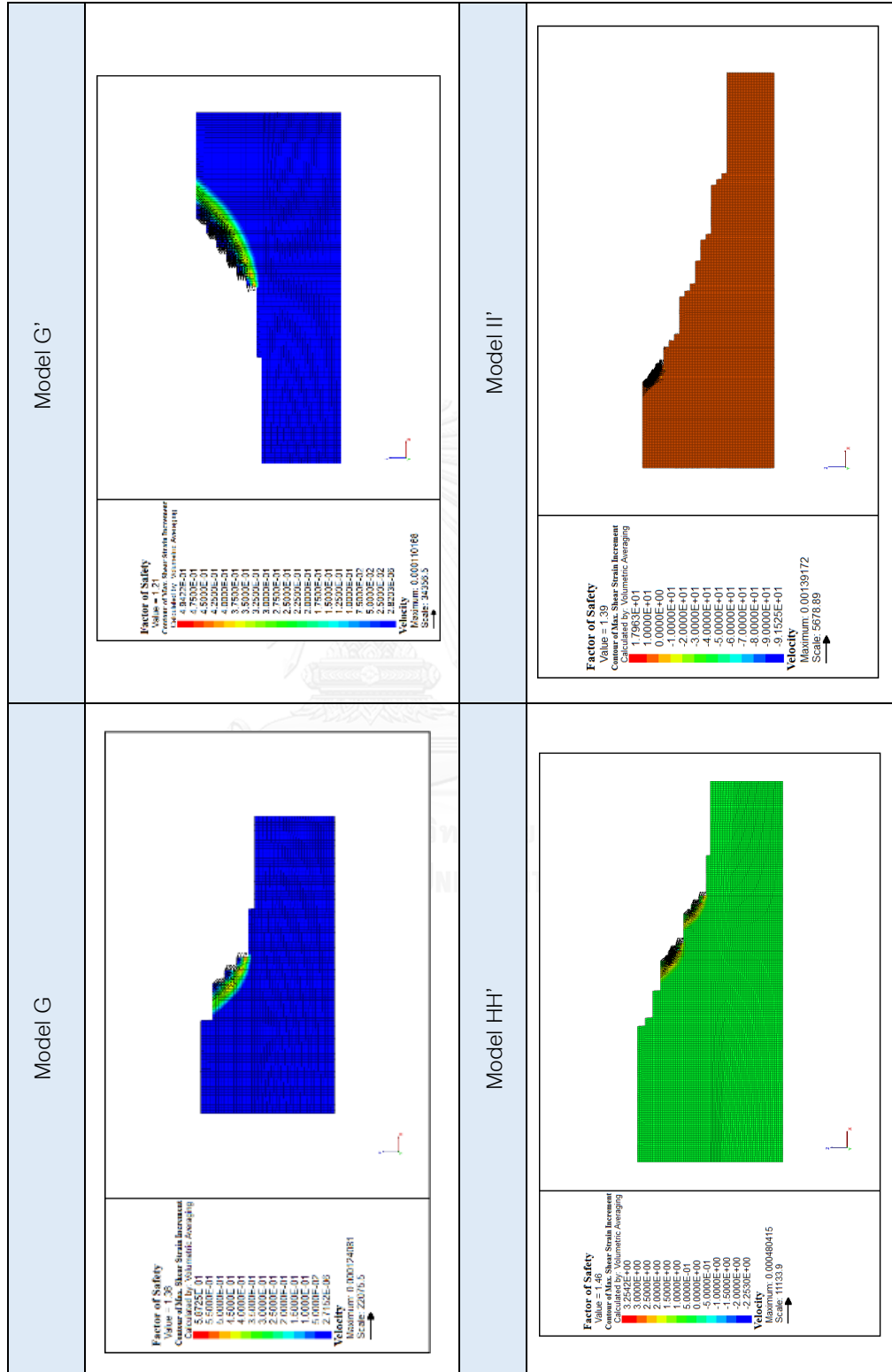
The results of slope stability analysis for cross-section model of Pit Ver.1



The results of slope stability analysis for cross-section model of Pit Ver.2

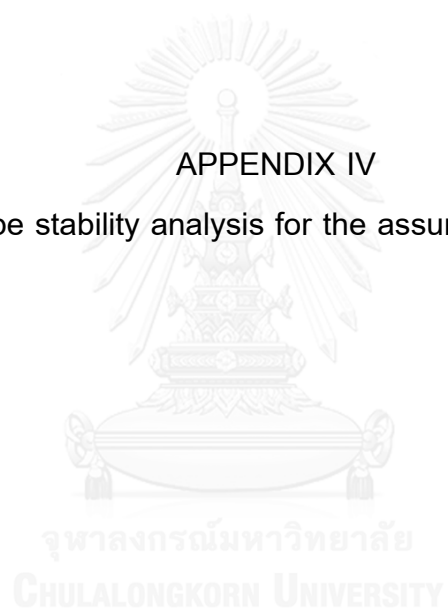


The results of slope stability analysis for cross-section model of Pit Ver.3

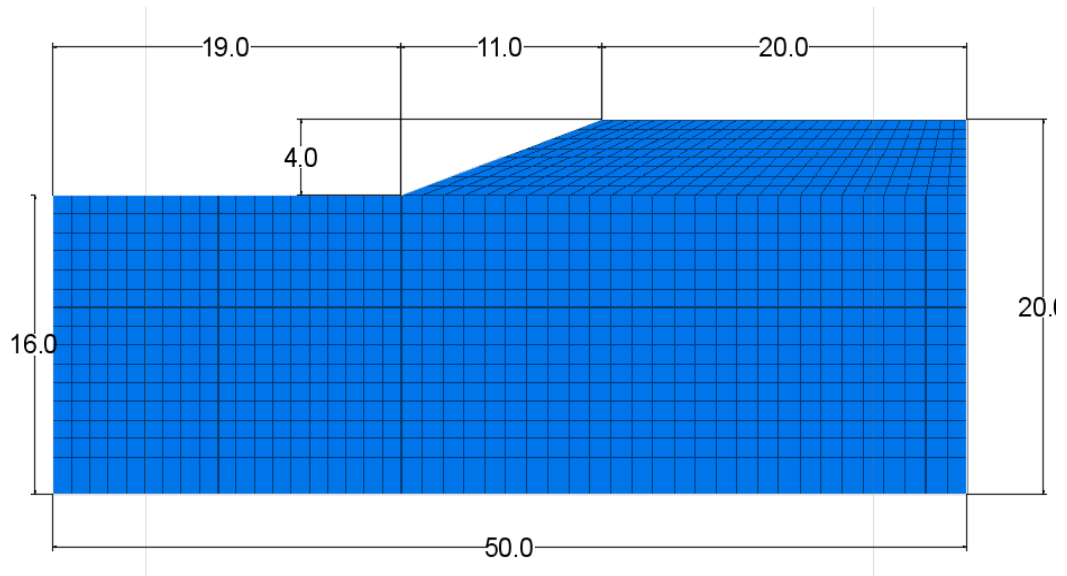


APPENDIX IV

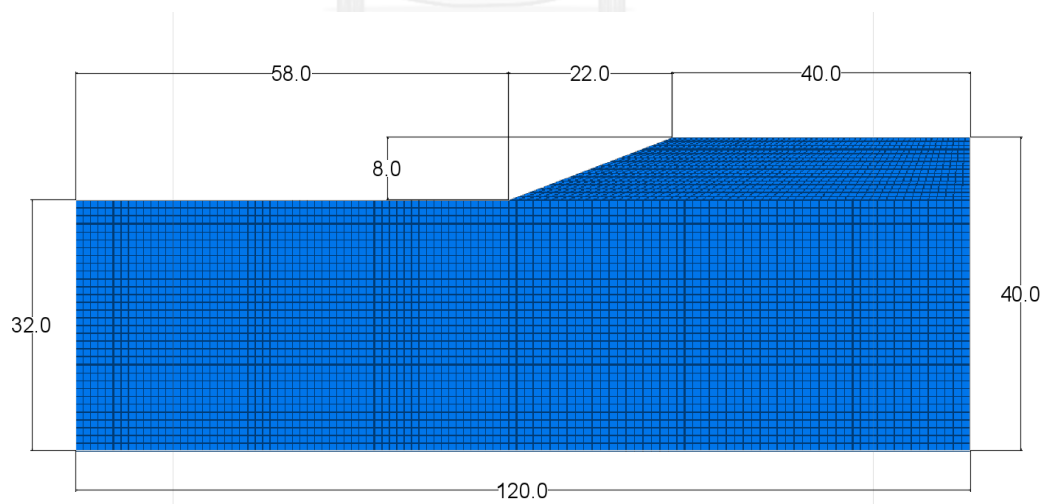
Slope stability analysis for the assuming model



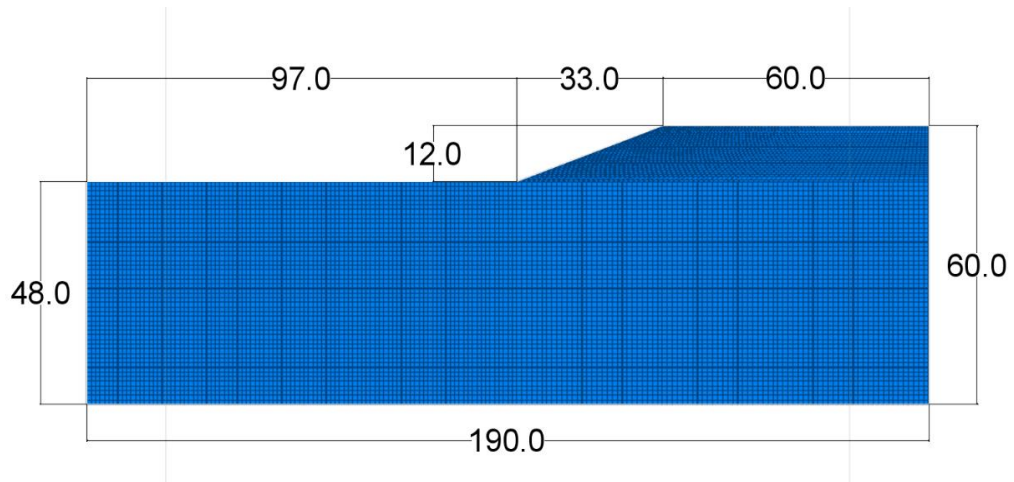
The model dimension shape of analysis for a geometry of bench height 4 metres



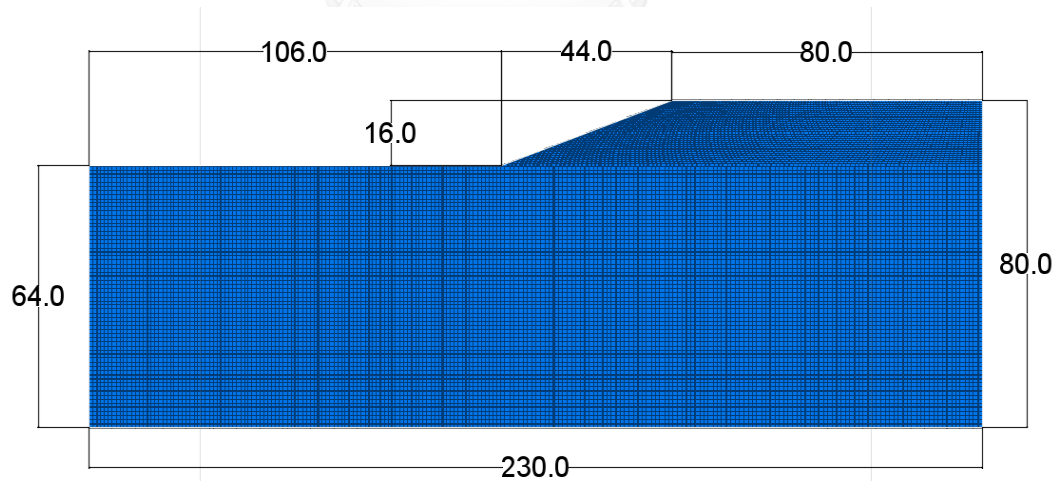
The model dimension shape of analysis for a geometry of bench height 8 metres



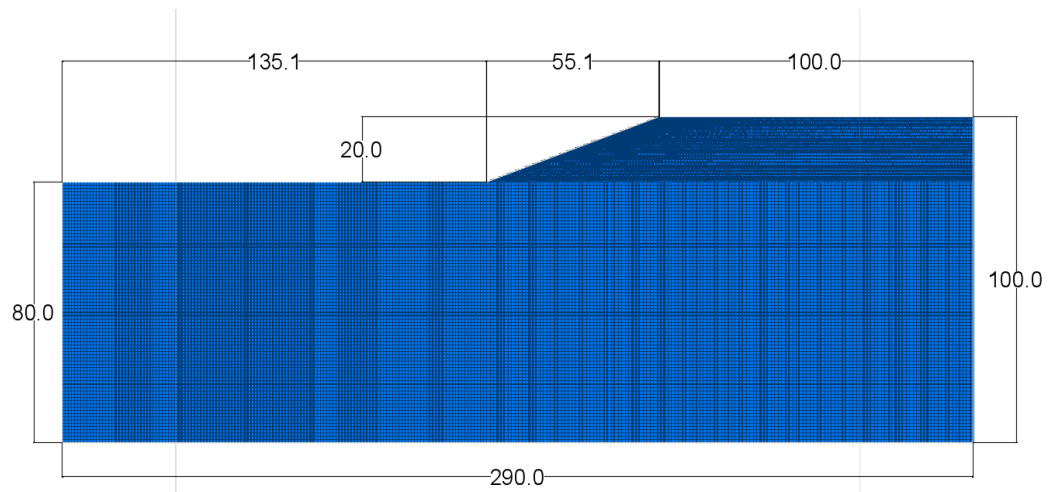
The model dimension shape of analysis for a geometry of bench height 12 metres



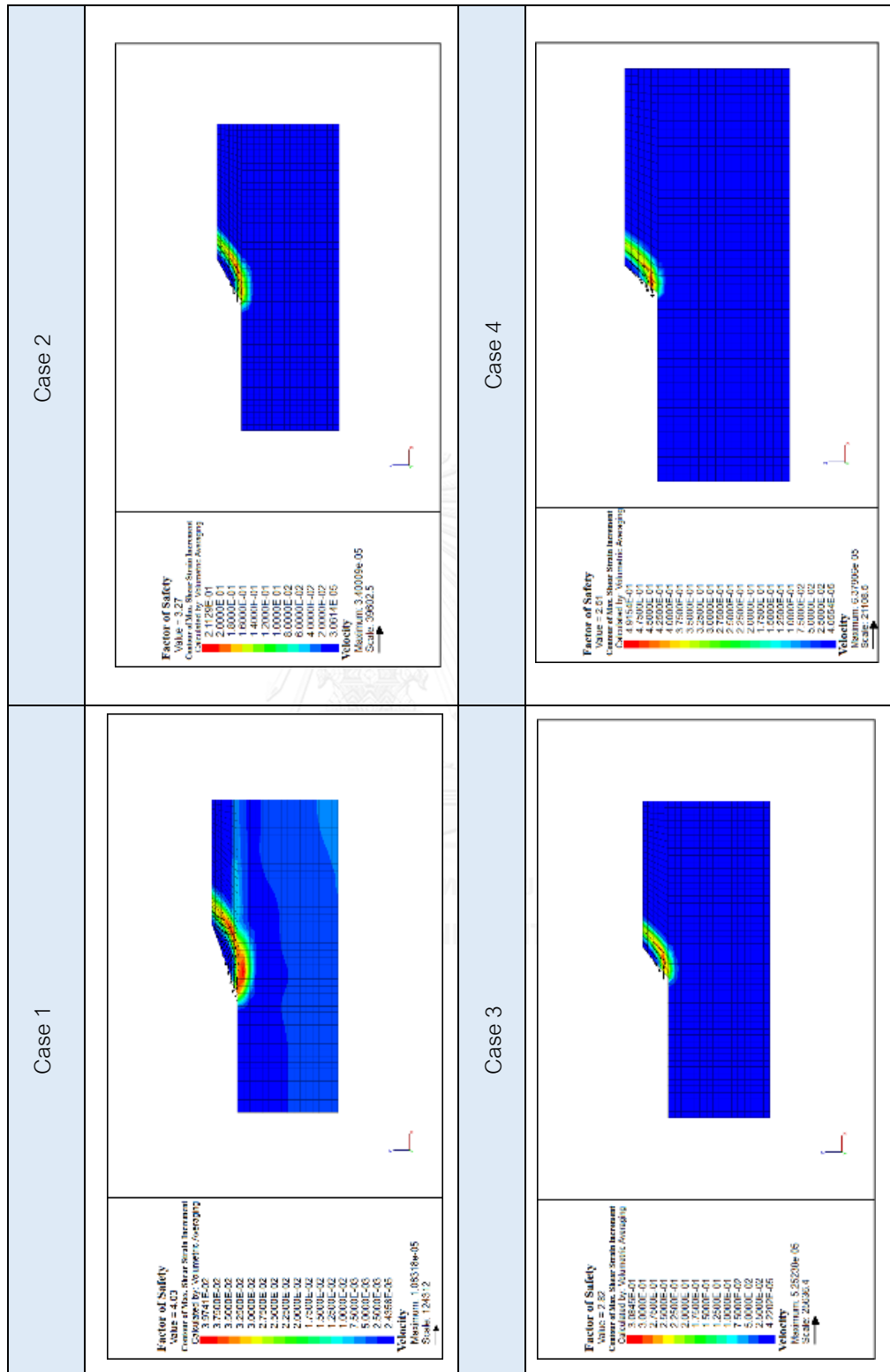
The model dimension shape of analysis for a geometry of bench height 16 metres



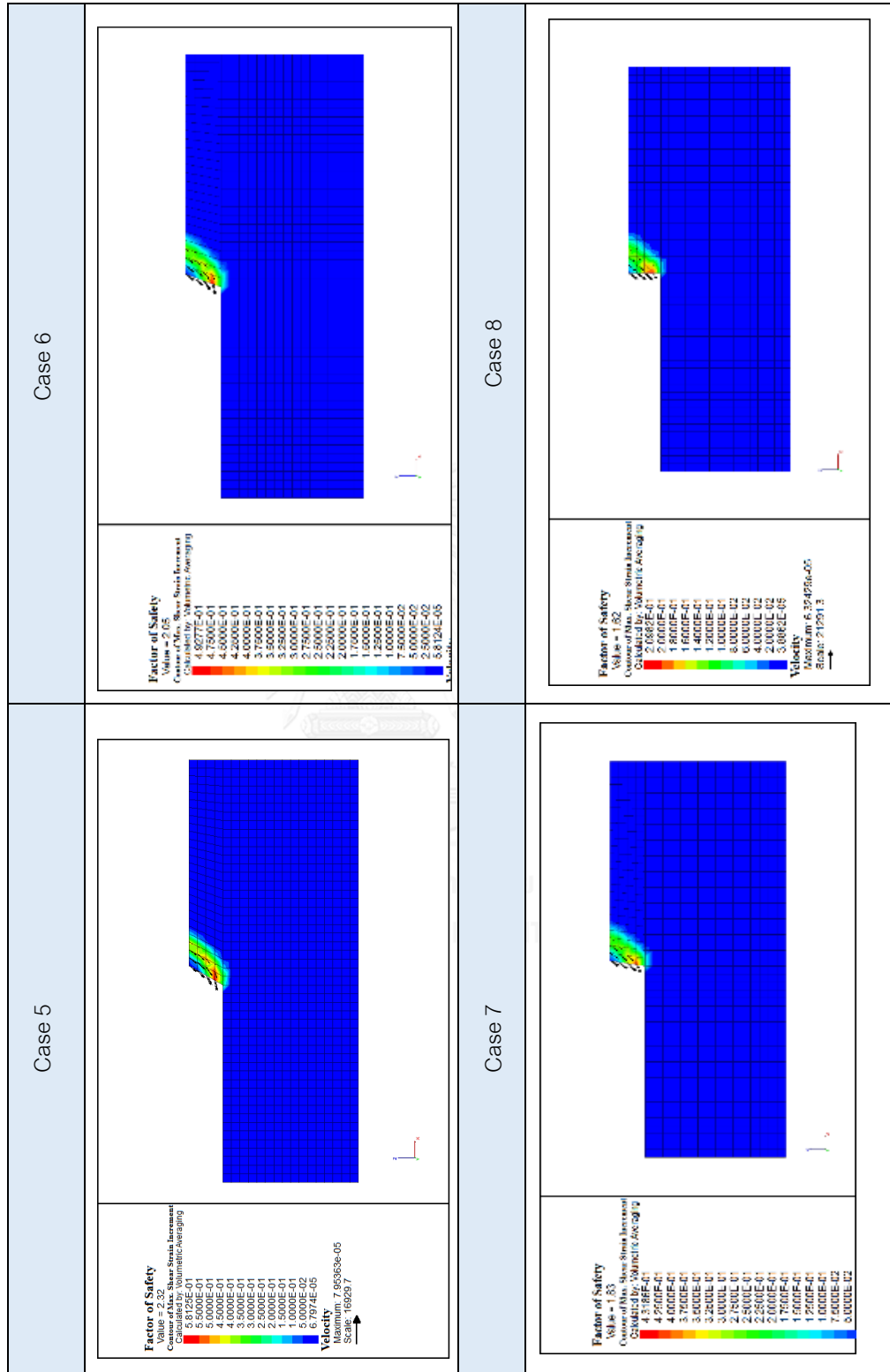
The model dimension shape of analysis for a geometry of bench height 20 metres



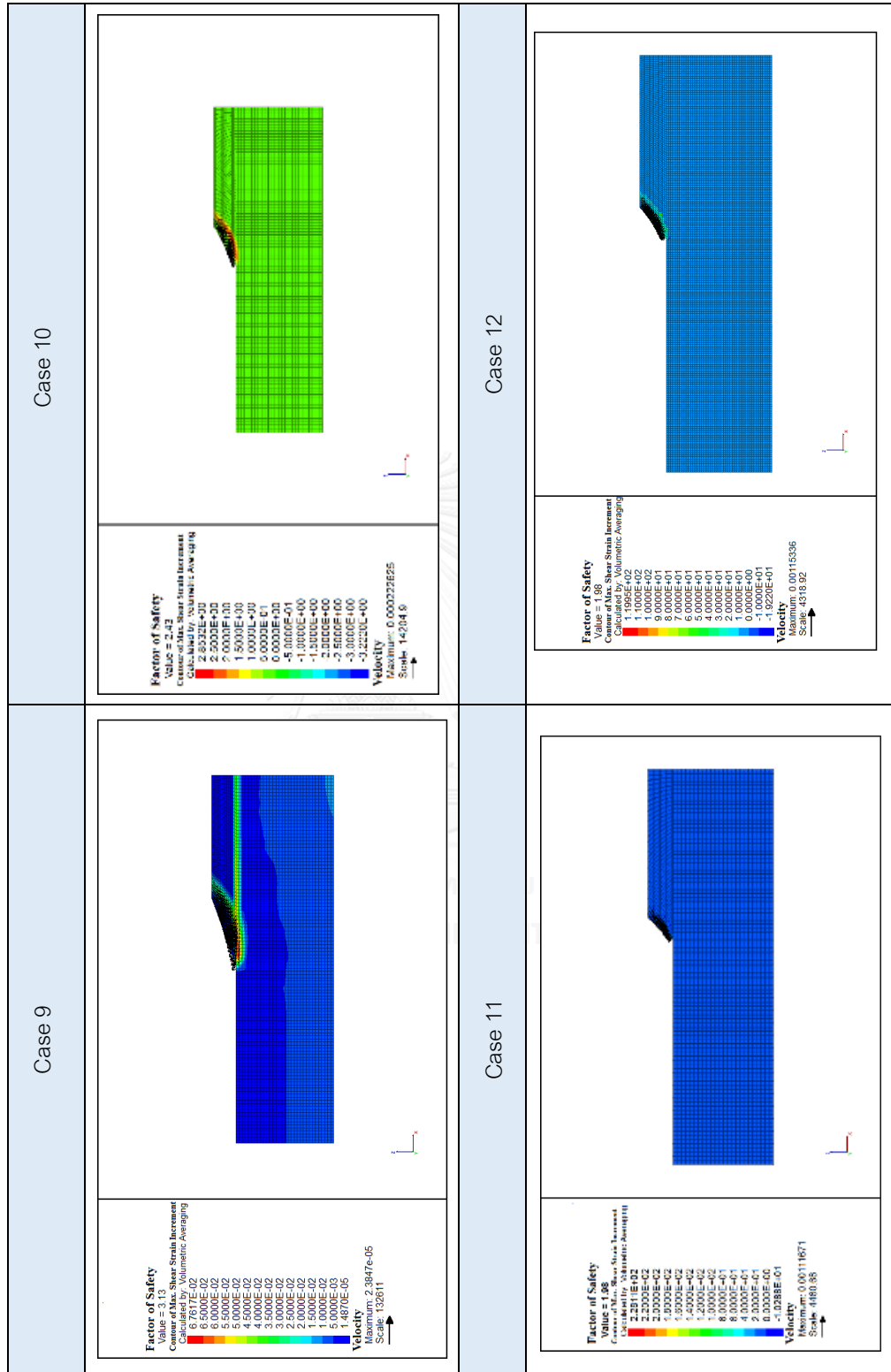
The results of slope stability analysis for the geometry of assuming bench height and face slope angle



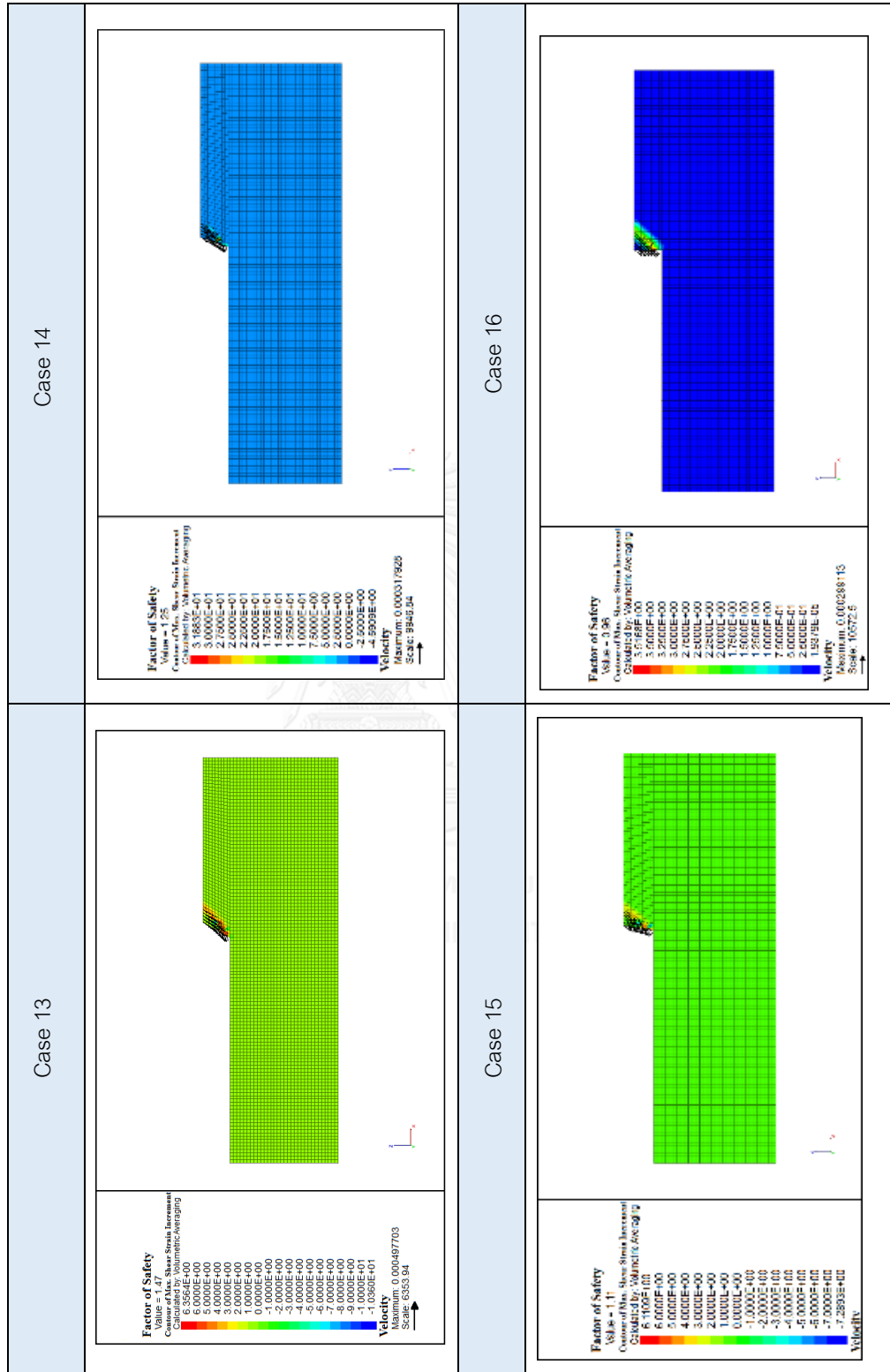
The results of slope stability analysis for the geometry of assuming bench height and face slope angle



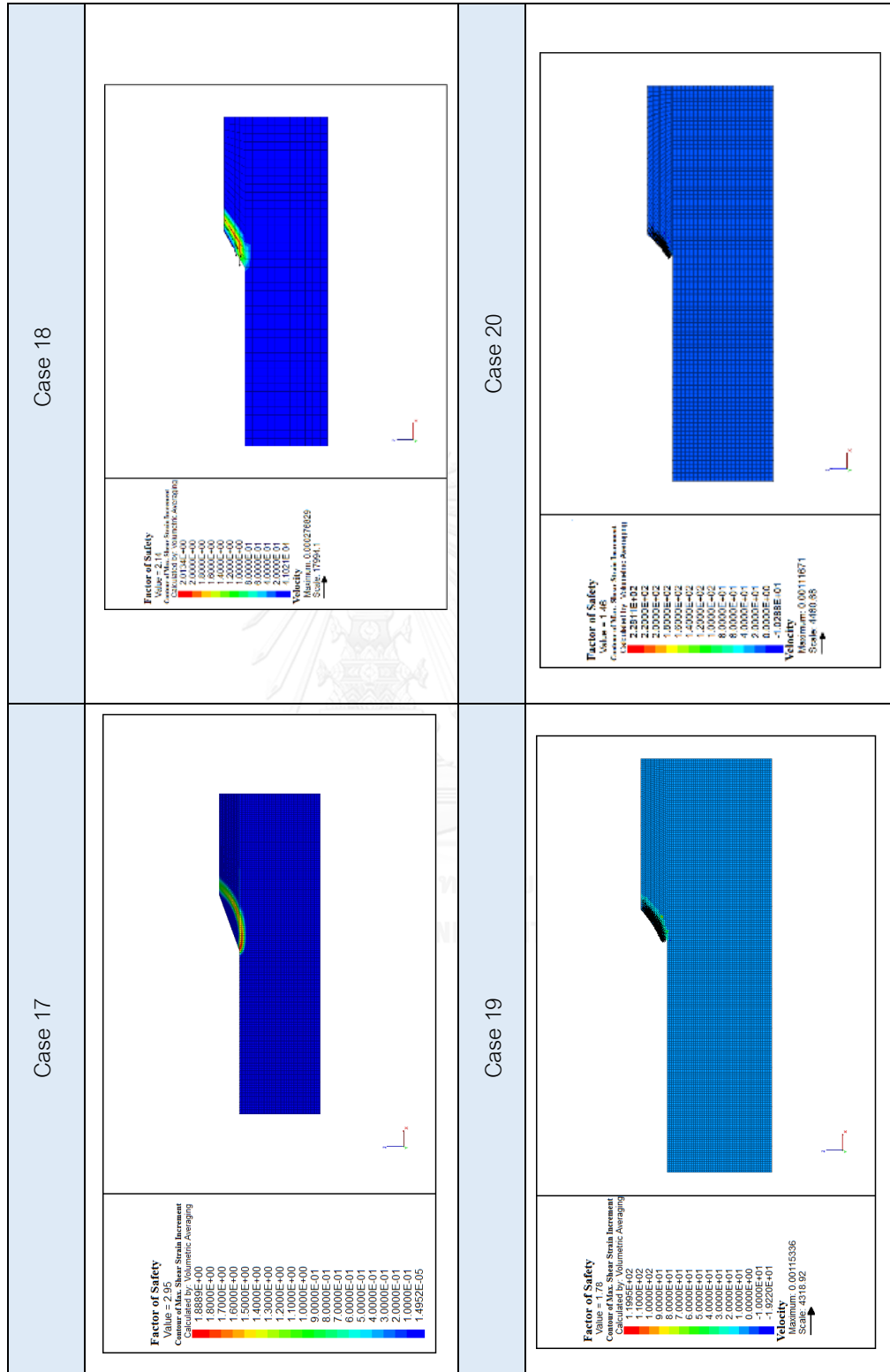
The result of slope stability analysis for the geometry of assuming bench height and face slope angle



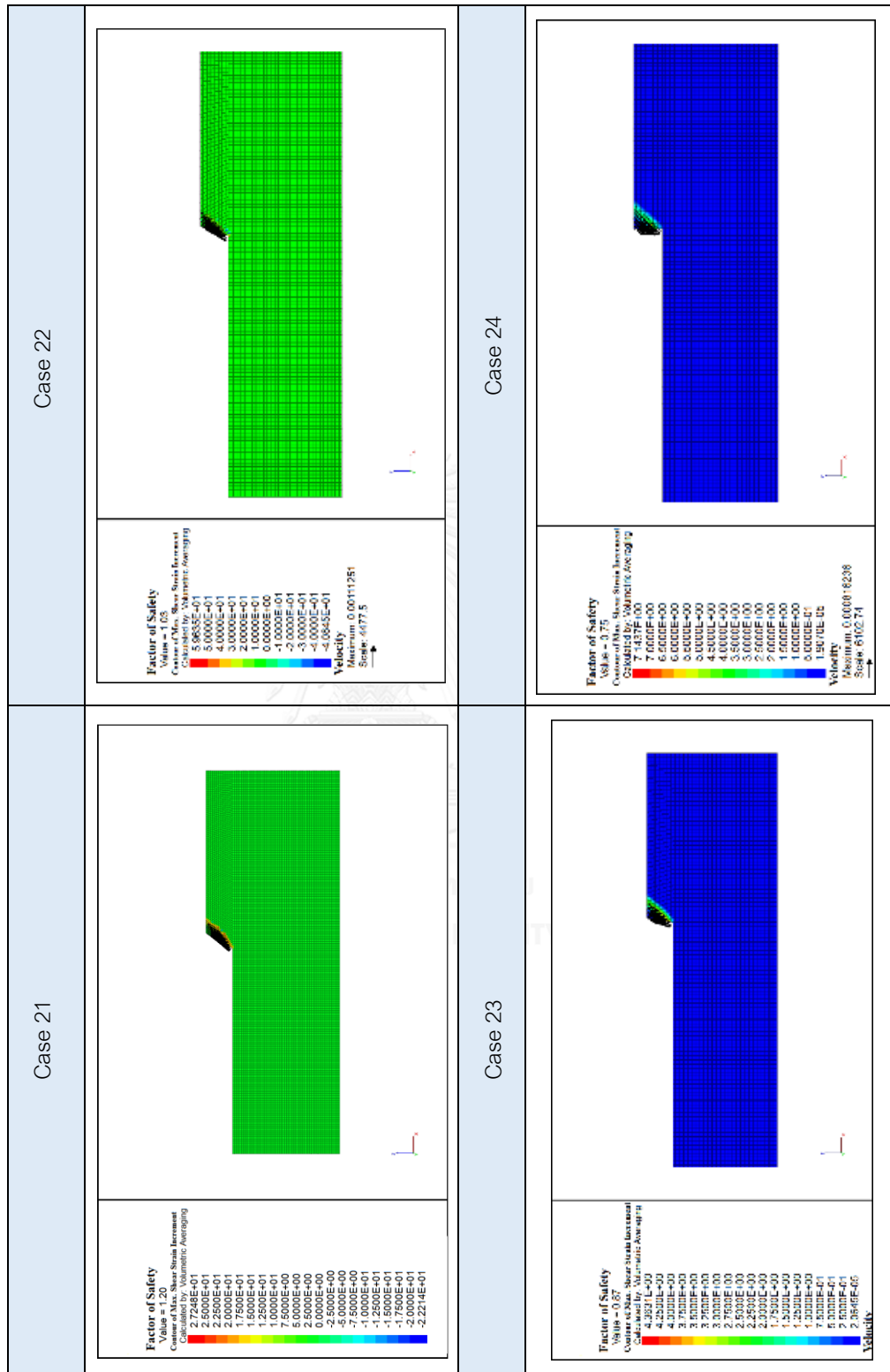
The result of slope stability analysis for the geometry of assuming bench height and face slope angle



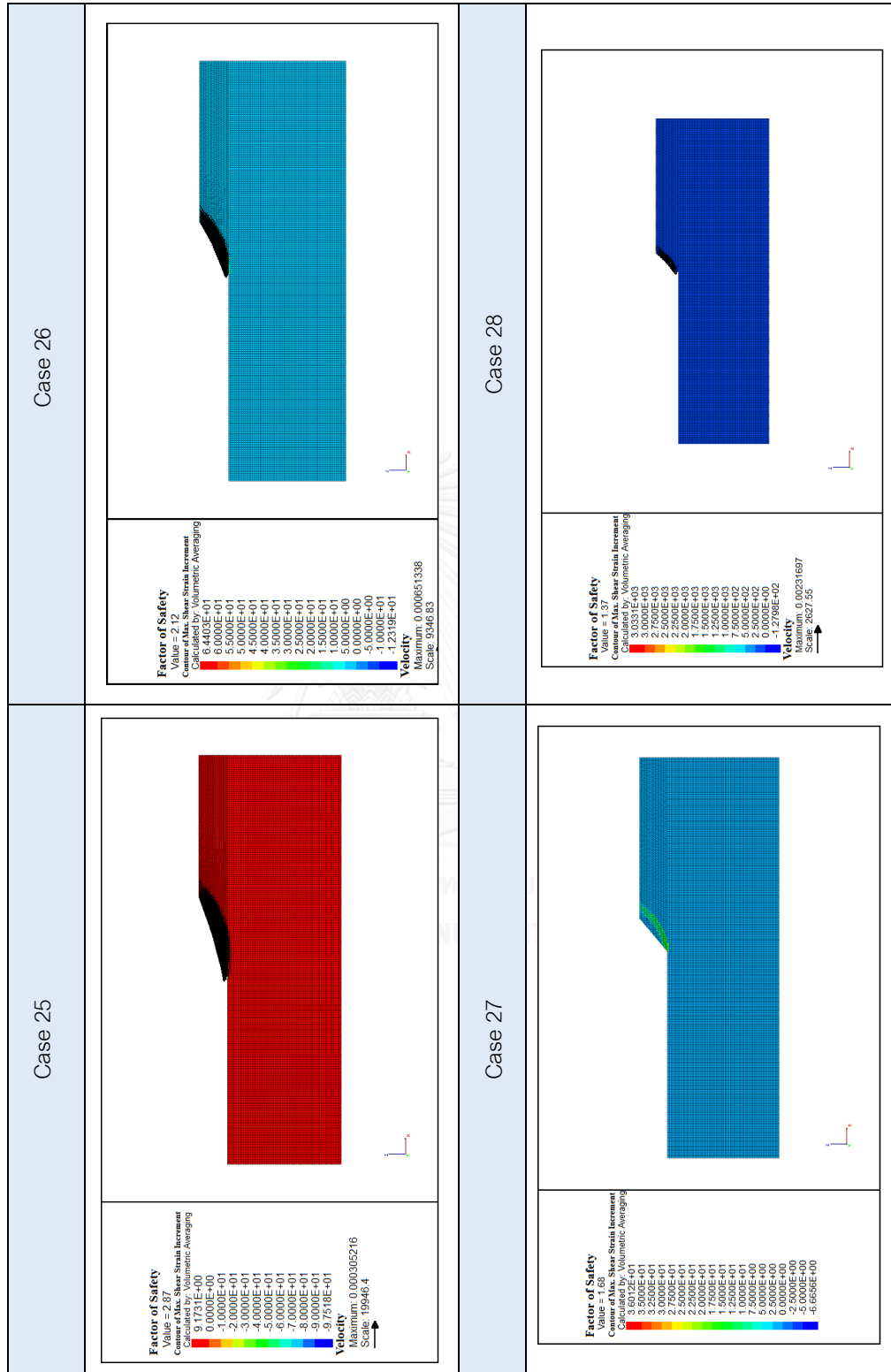
The result of slope stability analysis for the geometry of assuming bench height and face slope angle



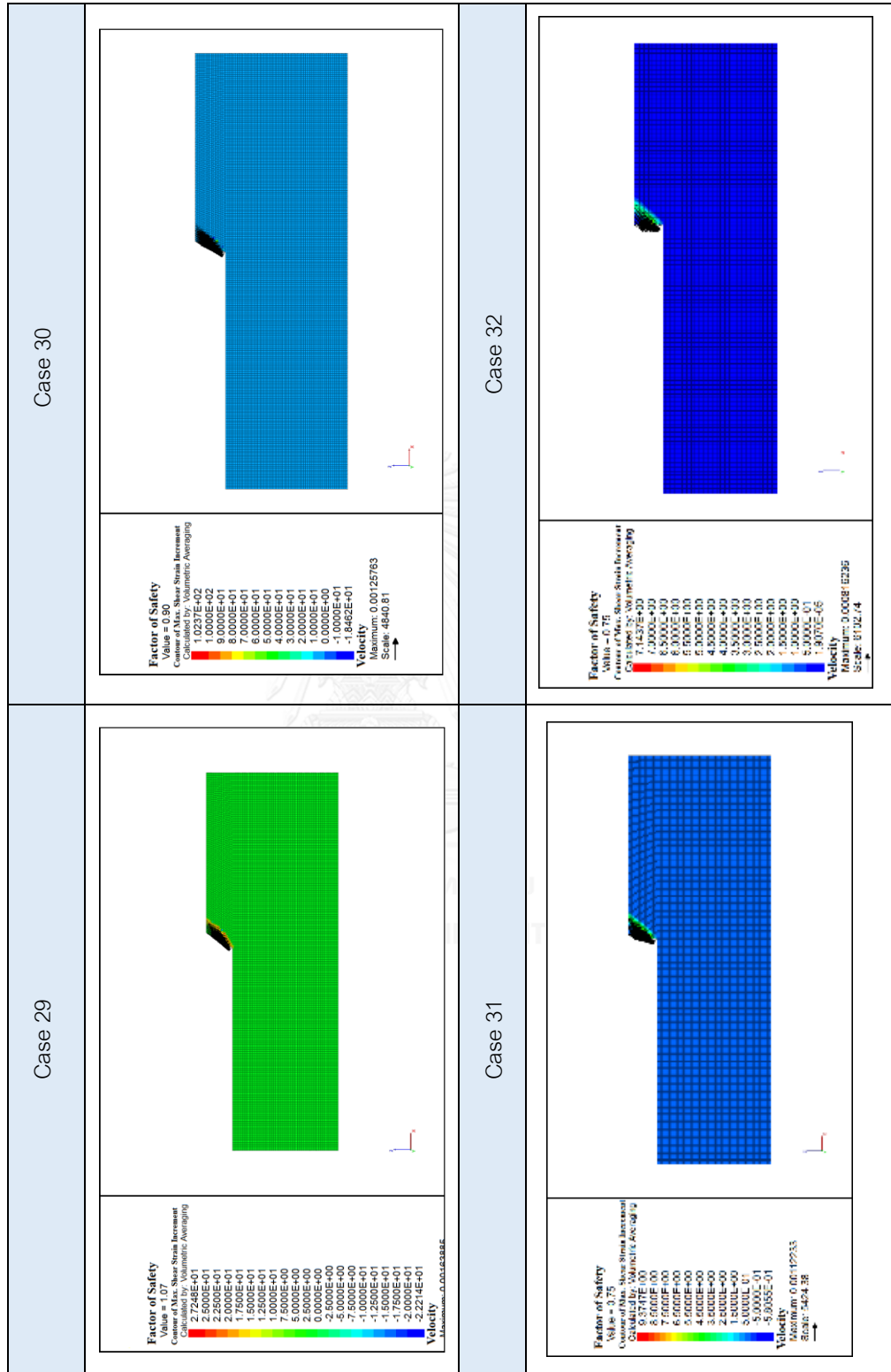
The result of slope stability analysis for the geometry of assuming bench height and face slope angle



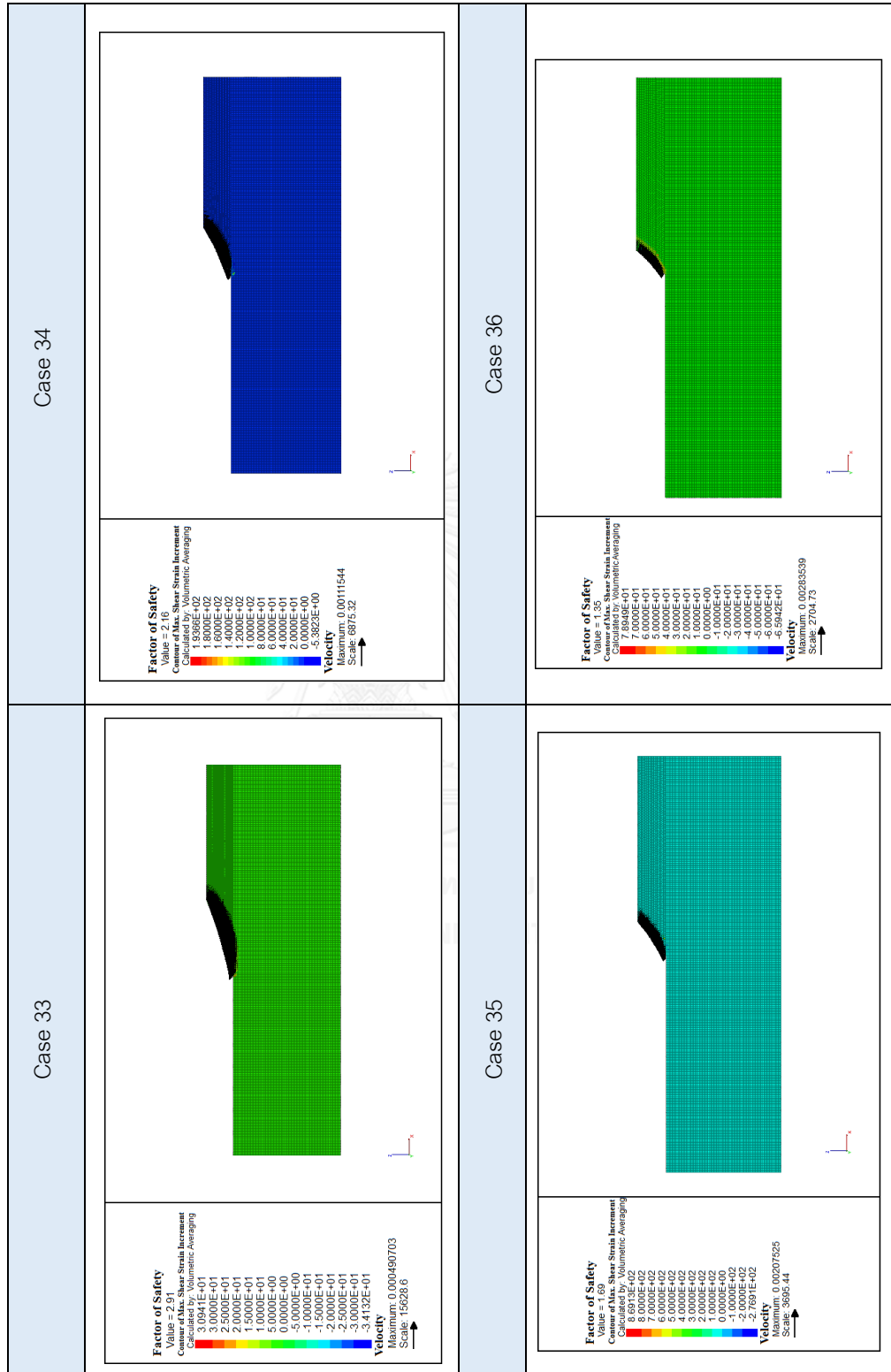
The result of slope stability analysis for the geometry of assuming bench height and face slope angle



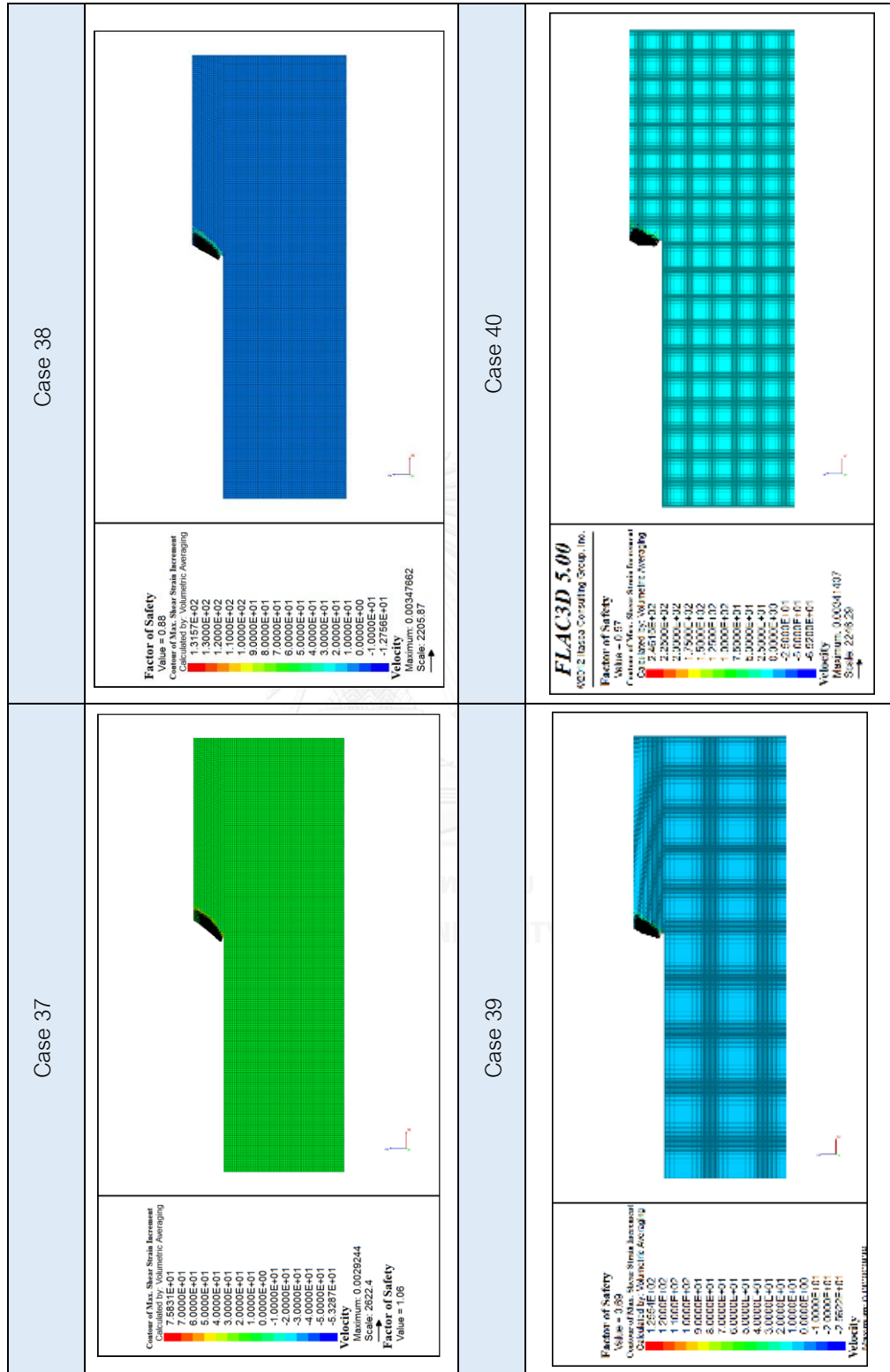
The result of slope stability analysis for the geometry of assuming bench height and face slope angle



The result of slope stability analysis for the geometry of assuming bench height and face slope angle



The result of slope stability analysis for the geometry of assuming bench height and face slope angle



APPENDIX V
Geotechnical laboratory testing results



Particle size gradation analysis

Project location: MRD's Kaolin mine, Pit MF-10

Sample No. SP1

Date test: 12/12/2015

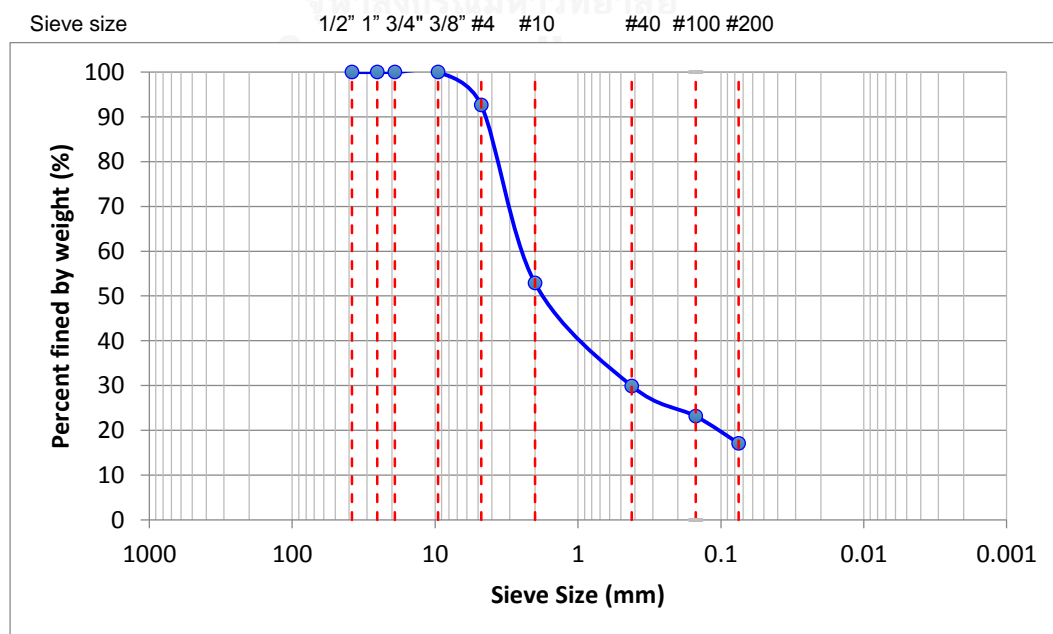
Can No. SP1

Wt. Can + Dry Soil: 353.03 g

Wt. Can: 32.93 g

Wt. Dry Soil: 320.1 g

Sieve No.	Sieve Opening (mm)	Wt. Sieve (gm)	Wt. Sieve + Soil Retained (gm)	Soil Retained (gm)	Soil Retained (%)	Cumulative Retained (%)	Percent Finer (%)
1 1/2"	38.10						100
1"	25.40						100
3/4"	19.10						100
3/8"	9.52						100
#4	4.76	503.6	527.2	23.6	7.4	7.4	92.6
#10	2.00	479	606.2	127.2	39.7	47.1	52.9
#40	0.42	365.5	439.2	73.7	23.0	70.1	29.9
#100	0.15	344.2	365.8	21.6	6.7	76.9	23.1
#200	0.08	274.3	293.6	19.3	6.0	82.9	17.1
Pan		250.6	304.9	54.3	17.0	99.9	



Project location: MRD's Kaolin mine, Pit MF-10

Sample No. SP2

Date test: 12/12/2015

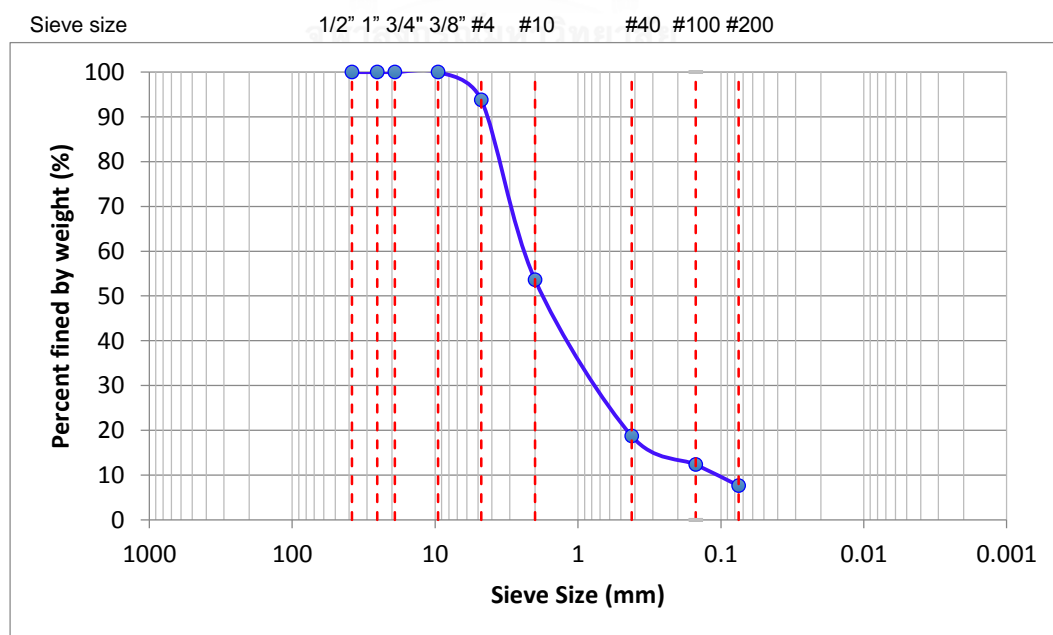
Can No. SP2

Wt. Can + Dry Soil: 395.47 g

Wt. Can: 31.87 g

Wt. Dry Soil: 363.6 g

Sieve No.	Sieve Opening (mm)	Wt. Sieve (gm)	Wt. Sieve + Soil Retained (gm)	Soil Retained (gm)	Soil Retained (%)	Cumulative Retained (%)	Percent Finer (%)
1 1/2"	38.10						100
1"	25.40						100
3/4"	19.10						100
3/8"	9.52						100
#4	4.76	503.6	526.1	22.5	6.2	6.2	93.8
#10	2.00	479.0	625.1	146.1	40.2	46.4	53.6
#40	0.42	365.5	492.6	127.1	35.0	81.3	18.7
#100	0.15	344.2	367.3	23.1	6.4	87.7	12.3
#200	0.08	274.3	291.5	17.2	4.7	92.4	7.6
Pan		250.6	277.1	26.5	7.3	99.7	



Project location: MRD's Kaolin mine, Pit MF-10

Sample No. SP3

Date test: 12/12/2015

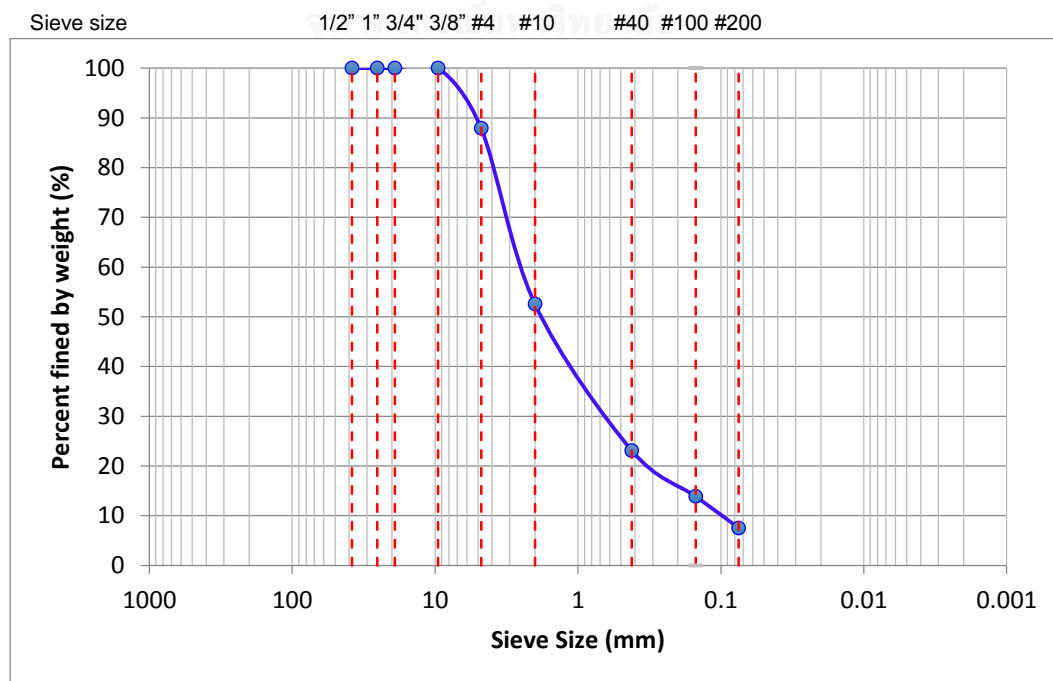
Can No. SP3

Wt. Can + Dry Soil: 368.1 g

Wt. Can: 33.5 g

Wt. Dry Soil: 334.6 g

Sieve No.	Sieve Opening (mm)	Wt. Sieve (gm)	Wt. Sieve + Soil Retained (gm)	Soil Retained (gm)	Soil Retained (%)	Cumulative Retained (%)	Percent Finer (%)
1 1/2"	38.10						100
1"	25.40						100
3/4"	19.10						100
3/8"	9.52						100
#4	4.76	503.6	544.1	40.5	12.1	12.1	87.9
#10	2.00	479	597.3	118.3	35.4	47.5	52.5
#40	0.42	365.5	464.1	98.6	29.5	76.9	23.1
#100	0.15	344.2	375	30.8	9.2	86.1	13.9
#200	0.08	274.3	295.5	21.2	6.3	92.5	7.5
Pan		250.6	279.1	28.5	8.5	101.0	



Project location: MRD's Kaolin mine, Pit MF-10

Sample No. MRD3

Date test: 12/12/2015

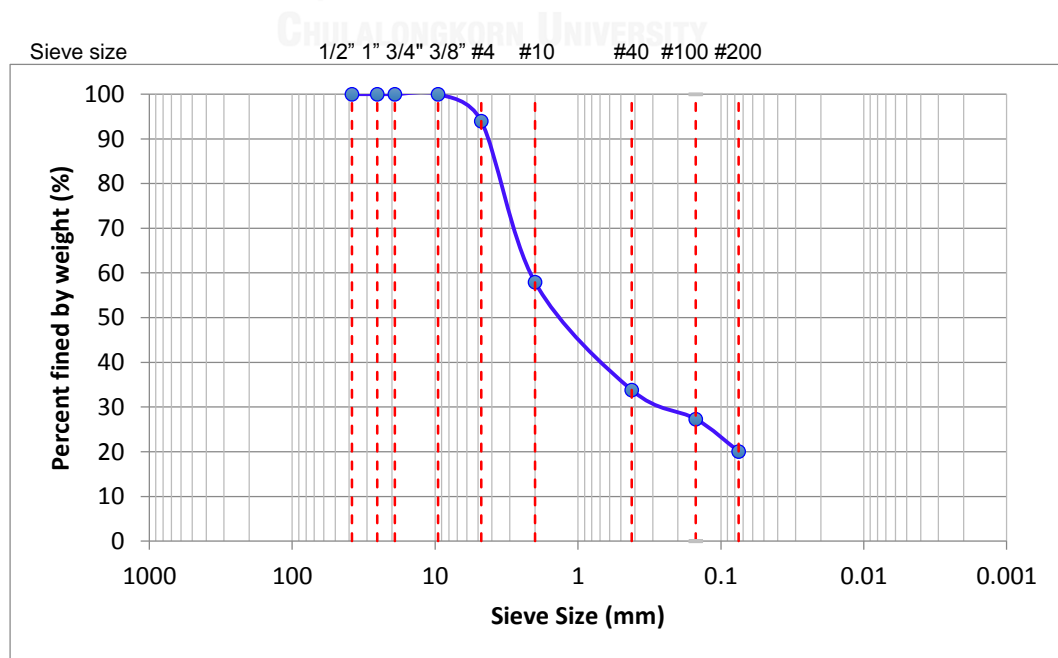
Can No. MRD3

Wt. Can + Dry Soil: 363.85 g

Wt. Can: 32.65 g

Wt. Dry Soil: 331.2 g

Sieve No.	Sieve Opening (mm)	Wt. Sieve (gm)	Wt. Sieve + Soil Retained (gm)	Soil Retained (gm)	Soil Retained (%)	Cumulative Retained (%)	Percent Finer (%)
1 1/2"	38.10						100
1"	25.40						100
3/4"	19.10						100
3/8"	9.52						100
#4	4.760	503.6	523.5	19.9	6.0	6.0	94.0
#10	2.000	479	598.4	119.4	36.1	42.1	57.9
#40	0.420	365.5	445.5	80.0	24.2	66.2	33.8
#100	0.150	344.2	365.6	21.4	6.5	72.7	27.3
#200	0.075	274.3	298.3	24.0	7.2	79.9	20.1
Pan		250.6	315.4	64.8	19.6	99.5	



Project location: MRD's Kaolin mine, Pit MF-10

Sample No. MRD4

Date test: 12/12/2015

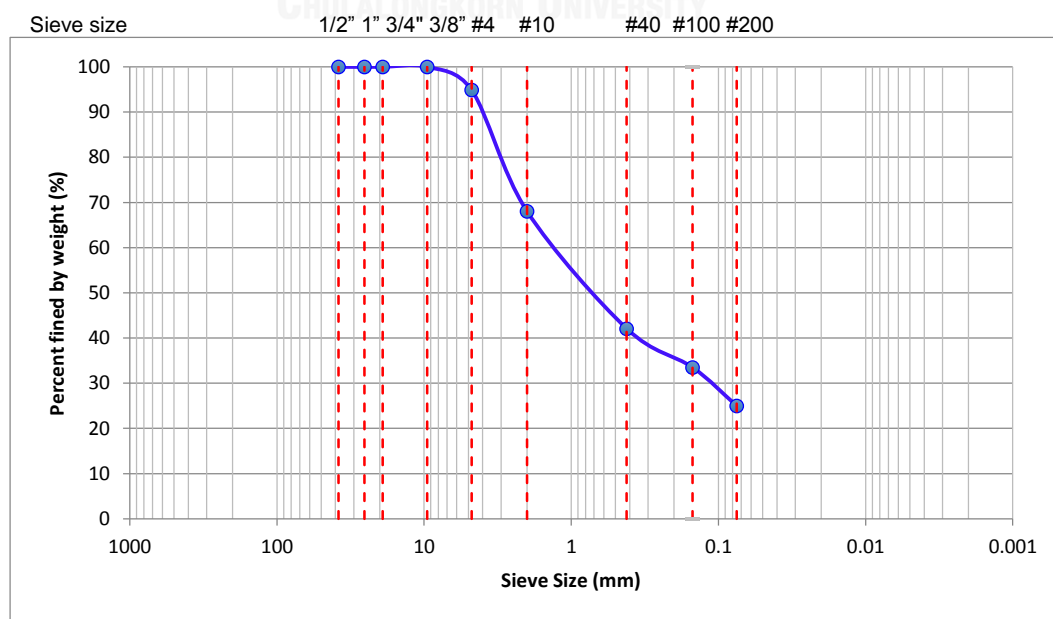
Can No. MRD4

Wt. Can + Dry Soil: 352.37 g

Wt. Can: 31.87 g

Wt. Dry Soil: 320.5 g

Sieve No.	Sieve Opening (mm)	Wt. Sieve (gm)	Wt. Sieve + Soil Retained (gm)	Soil Retained (gm)	Soil Retained (%)	Cumulative Retained (%)	Percent Finer (%)
1 1/2"	38.10						100
1"	25.40						100
3/4"	19.10						100
3/8"	9.52						100
#4	4.76	503.6	519.9	16.3	5.1	5.1	94.9
#10	2.00	479	565	86.0	26.8	31.9	68.1
#40	0.42	365.5	448.8	83.3	26.0	57.9	42.1
#100	0.15	344.2	371.7	27.5	8.6	66.5	33.5
#200	0.08	274.3	301.6	27.3	8.5	75.0	25.0
Pan		250.6	330.3	79.7	24.9	99.9	0.1



Direct shear test results

Sample No. *BMRD-03*

Boring No.....

Location: *HaadSompan Village, Ranong Province*

Depth: *Surface*

Description of sample: *Soft soil (weathered granite)*

Tested by: *Geotech lab, Civil department, CU*

Date: *Oct 20, 2015*

Specimen Data

Unit weight

	1	2	3
Mass of ring + Wet soil (g)	222.09	228.21	230.06
Mass of ring (g)	130.52	130.52	130.52
Mass of wet soil (g)	91.57	97.69	99.54
Unit weight (g/cm ³)	2.91	3.10	3.16
Average (g/cm ³)	3.06		
Average (kN/m ³)	30.02		

Normal load (Kg)

1	2	3
0.25	0.5	1

Weight of loading block ____ kN

Actual Normal Stress kN/m²

1	2	3
0.79	1.59	3.18

Soil Specimen Measurement

Diameter (cm)	6.33
Thickness (cm)	1.91
Area (cm ²)	31.47
Volume (cm ³)	60.11

Initial water content of specimen

Specimen	1			2			3		
	T	B	E	T	B	E	T	B	E
Container No.	C4	C5	C6	C7	C8	C9	C10	C11	C12
Mass container + wet soil (g)	24.94	42.61	32.16	34.65	32.11	39.84	47.19	43.42	41.09
Mass container + dry soil (g)	23.82	39.38	29.96	32.32	30.06	36.81	43.53	40.04	37.8
Mass of water (g)	1.12	3.23	2.20	2.33	2.05	3.03	3.66	3.38	3.29
Mass of container (g)	15.23	15.72	15.27	15.48	15.3	15.11	15.58	15.84	15.38
Mass of dry soil (g)	8.59	23.66	14.69	16.84	14.76	21.7	27.95	24.2	22.42
Water content (%)	13.04	13.65	14.98	13.84	13.89	13.96	13.09	13.97	14.67
Average water content (%)	13.89			13.90			13.91		

Final water content of specimen

Specimen	1	2	3
Container No.	MRD3.1	MRD3.2	MRD3.3
Mass container + entire wet soil (g)	128.43	134.55	137.06
Mass container + entire dry soil (g)	113.32	116.85	118.62
Mass of water (g)	15.11	17.70	18.44
Mass of container (g)	36.86	33.35	35.06
Mass of entire dry soil (g)	76.46	83.50	83.56
Water content (%)	19.76	21.20	22.07

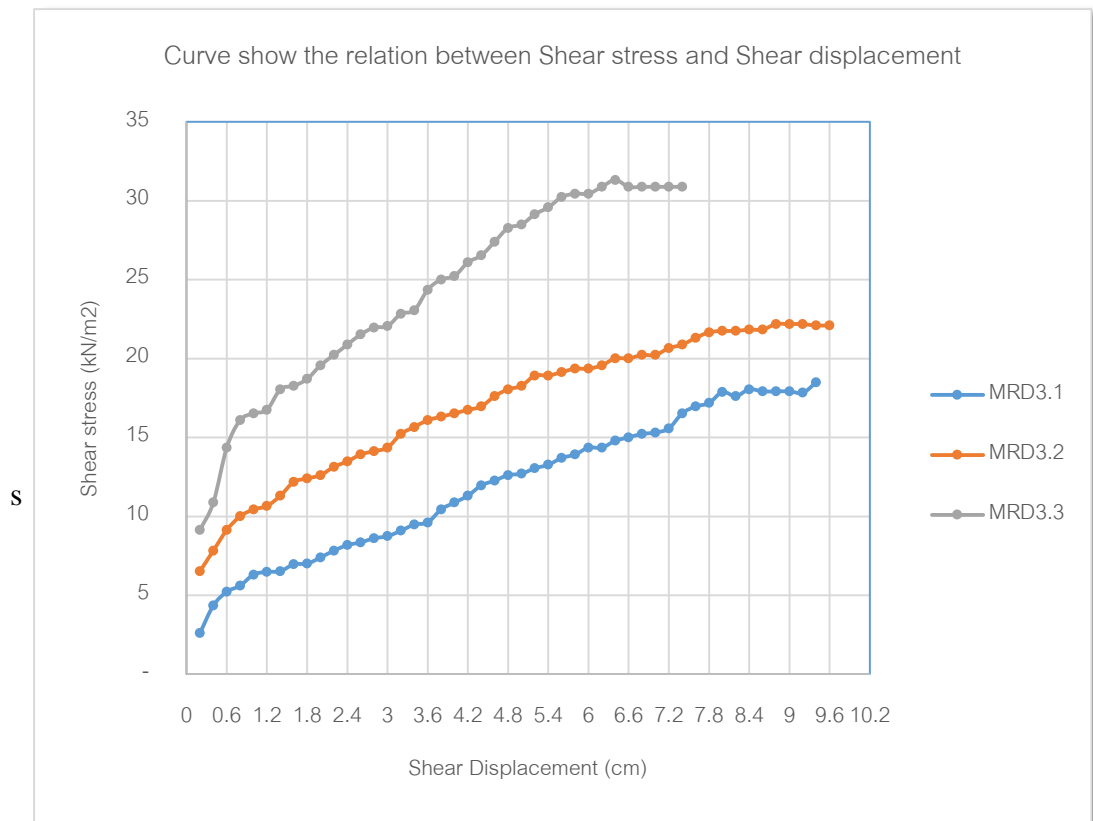
Shear Stress Data

Proving ring calibration: 0.001369 kN/division

Rate of shear: 1.75 mm/min

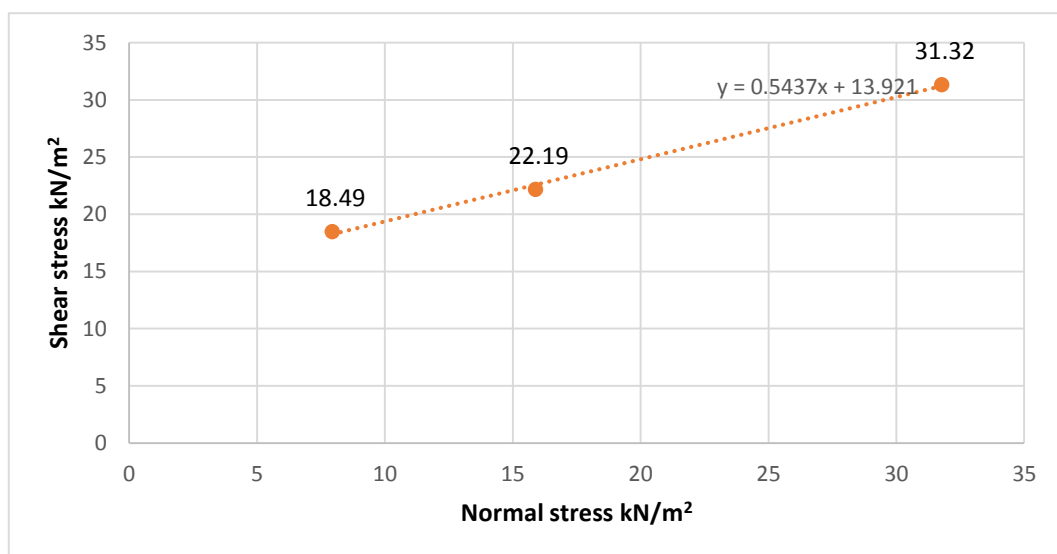
Shear Displacement (cm) x0.01			Normal Displacement (cm) x0.002			Proving Ring Dial in 0.0001"			Shear Force (kN)			S/A (kN/m ²)		
1	2	3	1	2	3	1	2	3	1	2	3	1	2	3
0.2	0.2	0.2			0.04	6	15	21	0.01	0.02	0.03	2.61	6.53	9.14
0.4	0.4	0.4			0.07	10	18	25	0.01	0.02	0.03	4.35	7.83	10.88
0.6	0.6	0.6			0.10	12	21	33	0.02	0.03	0.05	5.22	9.14	14.36
0.8	0.8	0.8			0.12	12.9	23	37	0.02	0.03	0.05	5.61	10.01	16.10
1	1	1			0.14	14.5	24	38	0.02	0.03	0.05	6.31	10.44	16.53
1.2	1.2	1.2			0.16	14.9	24.5	38.5	0.02	0.03	0.05	6.48	10.66	16.75
1.4	1.4	1.4			0.19	15	26	41.5	0.02	0.04	0.06	6.53	11.31	18.05
1.6	1.6	1.6			0.25	16	28	42	0.02	0.04	0.06	6.96	12.18	18.27
1.8	1.8	1.8			0.26	16.1	28.5	43	0.02	0.04	0.06	7.00	12.40	18.71
2	2	2			0.28	17	29	45	0.02	0.04	0.06	7.40	12.62	19.58
2.2	2.2	2.2			0.30	18	30.2	46.5	0.02	0.04	0.06	7.83	13.14	20.23
2.4	2.4	2.4			0.31	18.8	31	48	0.03	0.04	0.07	8.18	13.49	20.88
2.6	2.6	2.6			0.32	19.2	32	49.5	0.03	0.04	0.07	8.35	13.92	21.53
2.8	2.8	2.8			0.32	19.8	32.5	50.5	0.03	0.04	0.07	8.61	14.14	21.97
3	3	3			0.33	20.1	33	50.7	0.03	0.05	0.07	8.74	14.36	22.06
3.2	3.2	3.2			0.34	20.9	35	52.5	0.03	0.05	0.07	9.09	15.23	22.84
3.4	3.4	3.4			0.35	21.8	36	53	0.03	0.05	0.07	9.48	15.66	23.06
3.6	3.6	3.6			0.35	22.1	37	56	0.03	0.05	0.08	9.61	16.10	24.36
3.8	3.8	3.8			0.36	24	37.5	57.5	0.03	0.05	0.08	10.44	16.31	25.01
4	4	4			0.37	25	38	58	0.03	0.05	0.08	10.88	16.53	25.23
4.2	4.2	4.2			0.38	26	38.5	60	0.04	0.05	0.08	11.31	16.75	26.10
4.4	4.4	4.4			0.38	27.5	39	61	0.04	0.05	0.08	11.96	16.97	26.54
4.6	4.6	4.6			0.38	28.2	40.5	63	0.04	0.06	0.09	12.27	17.62	27.41
4.8	4.8	4.8			0.39	29	41.5	65	0.04	0.06	0.09	12.62	18.05	28.28
5	5	5			0.39	29.2	42	65.5	0.04	0.06	0.09	12.70	18.27	28.49
5.2	5.2	5.2			0.39	30	43.5	67	0.04	0.06	0.09	13.05	18.92	29.15
5.4	5.4	5.4			0.39	30.5	43.5	68	0.04	0.06	0.09	13.27	18.92	29.58
5.6	5.6	5.6			0.34	31.5	44	69.5	0.04	0.06	0.10	13.70	19.14	30.23

Shear Displacement (cm) x0.01			Normal Displacement (cm) x0.002		Proving Ring Dial in 0.0001"			Shear Force (kN)			S/A (kN/m ²)		
5.8	5.8	5.8		0.34	32	44.5	70	0.04	0.06	0.10	13.92	19.36	30.45
5.8	5.8	5.8		0.34	32	44.5	70	0.04	0.06	0.10	13.92	19.36	30.45
6	6	6		0.34	33	44.5	70	0.05	0.06	0.10	14.36	19.36	30.45
6.2	6.2	6.2		0.34	33	45	71	0.05	0.06	0.10	14.36	19.58	30.89
6.4	6.4	6.4		0.34	34	46	72	0.05	0.06	0.10	14.79	20.01	31.32
6.6	6.6	6.6		0.34	34.5	46	71	0.05	0.06	0.10	15.01	20.01	30.89
6.8	6.8	6.8		0.34	35	46.5	71	0.05	0.06	0.10	15.23	20.23	30.89
7	7	7		0.34	35.2	46.5	71	0.05	0.06	0.10	15.31	20.23	30.89
7.2	7.2	7.2		0.34	35.8	47.5	71	0.05	0.07	0.10	15.57	20.66	30.89
7.4	7.4	7.4		0.34	38	48	71	0.05	0.07	0.10	16.53	20.88	30.89
7.6	7.6	7.6			39	49		0.05	0.07		16.97	21.32	
7.8	7.8	7.8			39.5	49.8		0.05	0.07		17.18	21.66	
8	8	8			41.1	50		0.06	0.07		17.88	21.75	
8.2	8.2	8.2			40.5	50		0.06	0.07		17.62	21.75	
8.4	8.4	8.4			41.5	50.2		0.06	0.07		18.05	21.84	
8.6	8.6	8.6			41.2	50.2		0.06	0.07		17.92	21.84	
8.8	8.8	8.8			41.2	51		0.06	0.07		17.92	22.19	
9	9	9			41.2	51		0.06	0.07		17.92	22.19	
9.2	9.2	9.2			41	51		0.06	0.07		17.84	22.19	
9.4	9.4	9.4			42.5	50.8		0.06	0.07		18.49	22.10	
9.6	9.6	9.6				50.8		0.07				22.10	



Sample No.	Normal Stress (kN/m ²)	Shear Stress (kN/m ²)
BMRD3.1	0.79	18.49
BMRD3.2	1.59	22.19
BMRD3.3	3.18	31.32

c =	13.9
φ =	28.5



Direct shear test results

Sample No. *BMRD-04*

Boring No.....

Location: *HaadSompan Village, Ranong Province*

Depth: *Topsoil-surface*

Description of sample: *Soft soil (weathered granite)*

Tested by: *Geotech lab, Civil department, CU*

Date: *Oct 20, 2015*

Specimen Data

Unit weight

	1	2	3
Mass of ring + Wet soil (g)	240.46	245.57	240.65
Mass of ring (g)	130.52	130.52	130.52
Mass of wet soil (g)	109.94	115.05	110.13
Unit weight (g/cm ³)	3.49	3.66	3.50
Average (g/cm ³)	3.55		
Average (kN/m ³)	34.83		

Normal load (Kg)

1	2	3
0.25	0.5	1

Weight of loading block ____ kN

Actual Normal Stress kN/m²

1	2	3
0.79	1.59	3.18

Soil Specimen Measurement

Diameter (cm)	6.33
Thickness (cm)	1.91
Area (cm ²)	31.47
Volume (cm ³)	60.11

Initial water content of specimen

Specimen	1			2			3		
	T	B	E	T	B	E	T	B	E
Container No.	C13	C14	C15	C16	C17	C18	C19	C20	C21
Mass container + wet soil (g)	55.05	50.52	56.9	49.48	38.5	31.57	45.7	55.3	42.7
Mass container + dry soil (g)	50.85	47.59	52.35	46.39	35.94	29.51	40.9	52.93	39.57
Mass of water (g)	4.2	2.93	4.55	3.09	2.56	2.06	4.8	2.37	3.13
Mass of container (g)	15.16	15.26	14.8	15.7	15.34	15.47	15.95	15.98	15.35
Mass of dry soil (g)	35.69	32.33	37.55	30.69	20.6	14.04	24.95	36.95	24.22
Water content (%)	11.77	9.06	12.12	10.07	12.43	14.67	19.24	6.41	12.92
Average water content (%)	10.98			12.39			12.86		

Final water content of specimen

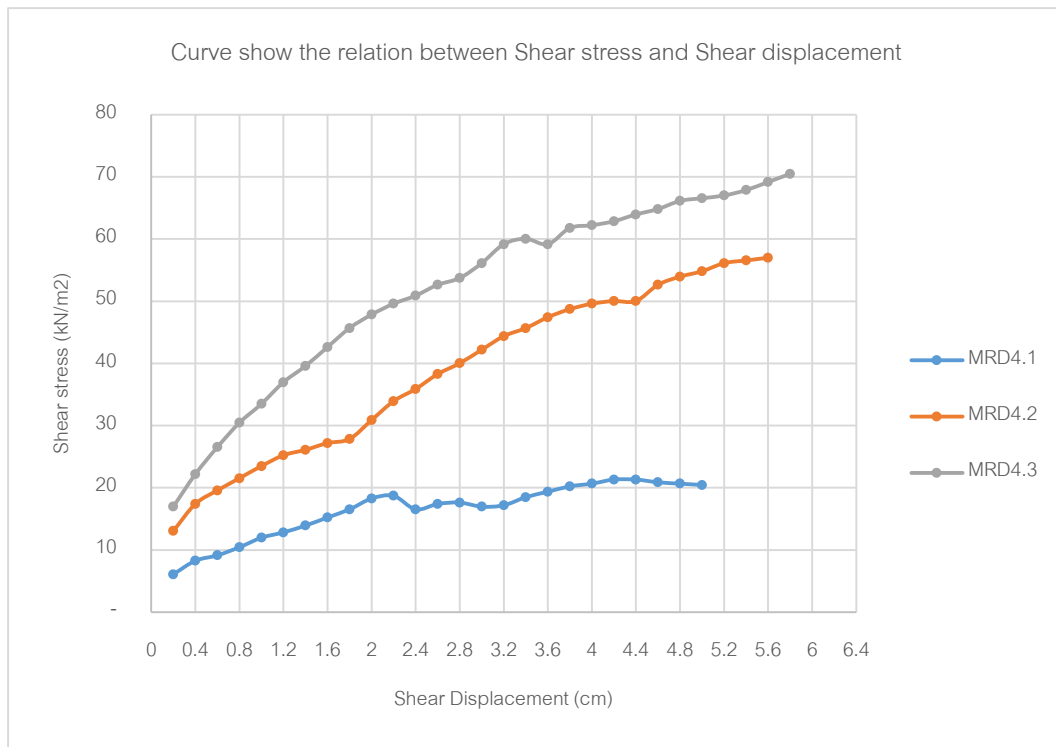
Specimen	1	2	3
Container No.	MRD4.1	MRD4.2	MRD4.3
Mass container + entire wet soil (g)	145.05	150.71	144.18
Mass container + entire dry soil (g)	134.48	136.95	131.51
Mass of water (g)	10.57	13.76	12.67
Mass of container (g)	35.11	36.58	35.09
Mass of entire dry soil (g)	99.37	100.37	96.42
Water content (%)	10.64	13.71	13.14

Shear Stress Data

Proving ring calibration: 0.001369 kN/division

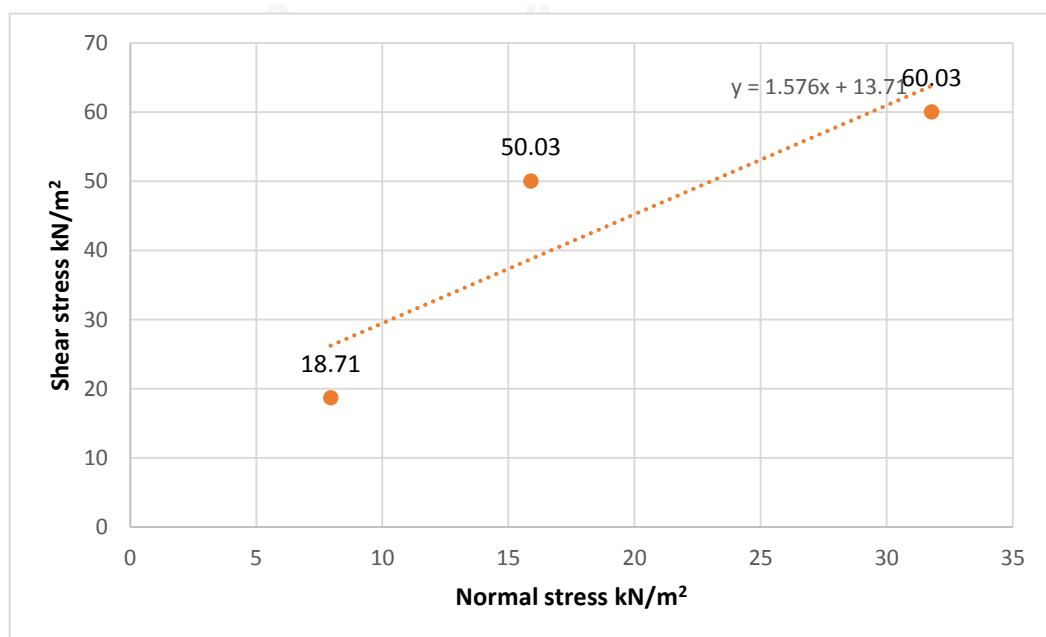
Rate of shear: 1.75 mm/min

Shear Displacement (cm), x0.01			Normal Displacement (cm), x0.002			Proving Ring Dial in 0.0001"			Shear Force (kN)			SIA (kN/m ²)		
1	2	3	1	2	3	1	2	3	1	2	3	1	2	3
20	0.2	0.2	0.01	0.03	-0.02	14	30	39	0.02	0.04	0.05	6.09	13.05	16.97
40	0.4	0.4	0.03	0.07	-0.02	19	40	51	0.03	0.05	0.07	8.27	17.40	22.19
60	0.6	0.6	0.07	0.10	-0.02	21	45	61	0.03	0.06	0.08	9.14	19.58	26.54
80	0.8	0.8	0.09	0.13	-0.01	24	49.5	70	0.03	0.07	0.10	10.44	21.53	30.45
100	1	1	0.13	0.18	-0.01	27.5	54	77	0.04	0.07	0.11	11.96	23.49	33.50
120	1.2	1.2	0.17	0.23	-0.01	29.5	58	85	0.04	0.08	0.12	12.83	25.23	36.96
140	1.4	1.4	0.22	0.29	-0.01	32	60	91	0.04	0.08	0.12	13.92	26.10	39.59
160	1.6	1.6	0.27	0.35	0.00	35	62.5	98	0.05	0.09	0.13	15.23	27.19	42.63
180	1.8	1.8	0.33	0.40	0.00	38	64	105	0.05	0.09	0.14	16.53	27.84	45.68
200	2	2	0.34	0.42	0.01	42	71	110	0.06	0.10	0.15	18.27	30.89	47.85
220	2.2	2.2	0.42	0.45	0.02	43	78	114	0.06	0.11	0.16	18.71	33.93	49.59
240	2.4	2.4	0.44	0.47	0.03	38	82.5	117	0.05	0.11	0.16	16.53	35.89	50.90
260	2.6	2.6	0.52	0.49	0.03	40	88	121	0.05	0.12	0.17	17.40	38.28	52.64
280	2.8	2.8	0.58	0.51	0.04	40.5	92	123.5	0.06	0.13	0.17	17.62	40.02	53.72
300	3	3	0.61	0.52	0.04	39	97	129	0.05	0.13	0.18	16.97	42.20	56.12
320	3.2	3.2	0.64	0.54	0.05	39.5	102	136	0.05	0.14	0.19	17.18	44.37	59.16
340	3.4	3.4	0.70	0.55	0.06	42.5	105	138	0.06	0.14	0.19	18.49	45.68	60.03
360	3.6	3.6	0.73	0.56	0.06	44.5	109	136	0.06	0.15	0.19	19.36	47.42	59.16
380	3.8	3.8	0.79	0.58	0.05	46.5	112	142	0.06	0.15	0.19	20.23	48.72	61.77
400	4	4	0.85	0.59	0.06	47.5	114	143	0.07	0.16	0.20	20.66	49.59	62.21
420	4.2	4.2	0.91	0.61	0.07	49	115	144.5	0.07	0.16	0.20	21.32	50.03	62.86
440	4.4	4.4	0.97	0.62	0.08	49	115	147	0.07	0.16	0.20	21.32	50.03	63.95
460	4.6	4.6	1.03	0.63	0.08	48	121	149	0.07	0.17	0.20	20.88	52.64	64.82
480	4.8	4.8	1.06	0.63	0.09	47.5	124	152	0.07	0.17	0.21	20.66	53.94	66.12
500	5	5	1.13	0.64	0.09	47	126	153	0.06	0.17	0.21	20.45	54.81	66.56
520	5.2	5.2		0.64	0.09		129	154		0.18	0.21		56.12	66.99
540	5.4	5.4		0.65	0.09		130	156		0.18	0.21		56.55	67.86
560	5.6	5.6		0.65	0.09		131	159		0.18	0.22		56.99	69.17
580	5.8	5.8			0.10			162			0.22			70.47



Sample No.	Normal Stress (kN/m ²)	Shear Stress (kN/m ²)
BMRD4.1	7.9	18.71
BMRD4.2	15.9	50.03
BMRD4.3	31.8	60.03

c =	13.7
φ =	57.6



Triaxial Compression Test (Unsolidated Undrained Test)

Sample No. *BMRD3.1-S4*

Boring No.

Location: *HaadSompan Village, Ranong Province*

Depth: *Topsoil-surface*

Description of sample: *Soft soil (weathered granite)*

Tested by: *Geotech lab, Civil department, CU*

Date: *Nov 3, 2015*

Specimen Data

At the beginning of test

1. Type of test performed	UU	
2. Type of specimen	Remold	
3. Diameter of specimen		
Top	3.33	cm
Middle	3.33	cm
Bottom	3.33	cm
4. Area of specimen	8.71	cm ²
5. Initial height of specimen	7.14	cm
6. Height to diameter ration	2.14	-
7. volume of specimen	62.18	cm ³
8. Mass of wet specimen	130.31	g
9. Unit weight of soil	2.10	g/ cm ³

Water content	Mass of container, g	Mass of wet soil, g	Mass of dried soil , g	Water content, %
Top		130.31	114.7	13.61
Bottom				
			Average	13.61

At the end of test

1. Final diameter of specimen		
Top		cm
Middle		cm
Bottom		cm
Average		
2. Final height of specimen	6.42	cm
3. Volume of specimen	0.00	cm ³
4. Water content of entire specimen		
a. Can no.	S4	
b. Mass of can	0	g
c. Mass of wet soil	130.31	g
d. Mass of dried soil	114.7	g
e. Mass of specimen	130.31	g
f. Mass of dried soil	114.7	g
g. Water content	13.6	%
5. Dry unit weight	1.84	g/cm ³
6. Specific gravity of soil (assumed)	2.66	g/cm ³
7. Void ratio	0.442	-
8. Degree of saturation	81.9	%

Triaxial Compression data

Cell pressure	100	kPa			
Rate of axial strain	0.064	mm/min			
Initial height of specimen	7.14	cm			
Area of specimen	8.71	cm ²			
Proving ring calibration	0.144	kg/div			
Deformation Dial, ΔL (cm)	Strain, ϵ %	Cross-section Area, A (cm ²)	Proving ring dial	Applied axial load, P (kg)	Stress, kPa
(1)			(4)	(5)=(4)x0.144	(6)=(5)/(3)
0	0	8.71	0	0	0
0.02	0.28	8.73	22	3.17	36.3
0.04	0.56	8.76	39	5.62	64.1
0.06	0.84	8.78	57	8.21	93.5

Deformation Dial, ΔL (cm)	Strain, ϵ %	Cross-section Area, A (cm ²)	Proving ring dial	Applied axial load, P (kg)	Stress, kPa
0.08	1.12	8.81	74	10.66	121.0
0.08	1.12	8.81	74	10.66	121.0
0.1	1.40	8.83	90	12.96	146.7
0.12	1.68	8.86	101	14.54	164.2
0.14	1.96	8.88	107	15.41	173.4
0.16	2.24	8.91	109	15.70	176.2
0.18	2.52	8.93	110	15.84	177.3
0.2	2.80	8.96	110.2	15.87	177.1
0.22	3.08	8.99	110	15.84	176.3
0.24	3.36	9.01	106	15.26	169.4
0.26	3.64	9.04	104.5	15.05	166.5
0.28	3.92	9.06	103	14.83	163.6

Minor principal

stress, s_3 100 kPa

Unit axial load at

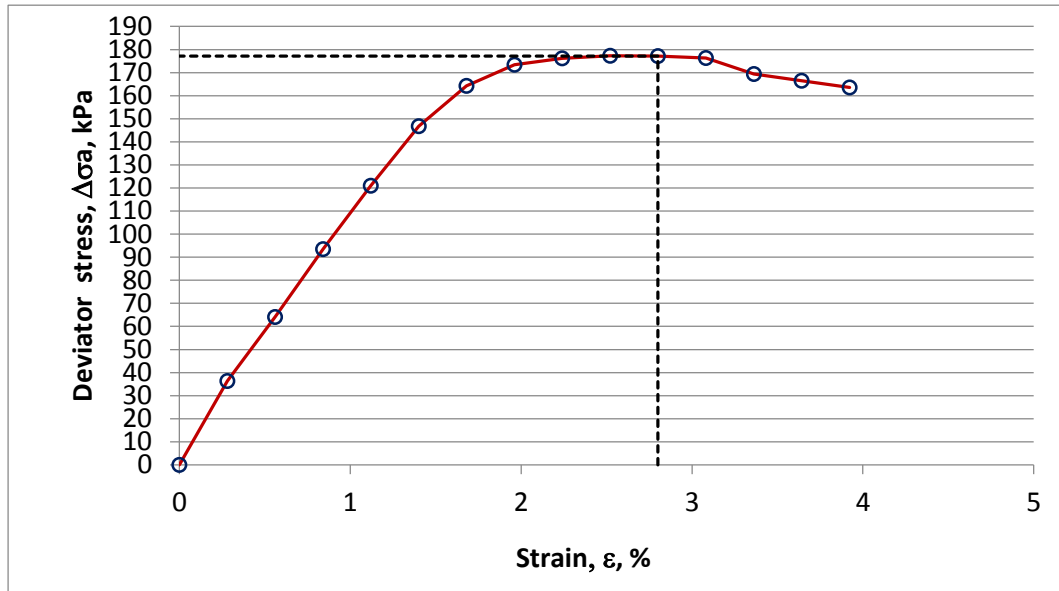
failure, D_{s1} 177.3 kPa

Major principal

stress, s_1 277.29 kPa

s_3 , kPa	s_1 , kPa	C_u , kPa	e , %
100	277.29	88.6	2.80

Curve shown the relation between Strain and stress of sample BMRD3.1S4



Triaxial Compression Test (Unsolidated Undrained Test)

Sample No. **BMRD3.2-S5**

Boring No.

Location: *HaadSompan Village, Ranong Province*

Depth: *Topsoil-surface*

Description of sample: *Soft soil (weathered granite)*

Tested by: *Geotech lab, Civil department, CU*

Date: *Nov 3, 2015*

Specimen Data

At the beginning of test

1. Type of test performed	UU	
2. Type of specimen	Remold	
3. Diameter of specimen		
Top	3.33	cm
Middle	3.33	cm
Bottom	3.33	cm
4. Area of specimen	8.71	cm ²
5. Initial height of specimen	7.14	cm
6. Height to diameter ration	2.14	-
7. volume of specimen	62.18	cm ³
8. Mass of wet specimen	130.34	g
9. Unit weight of soil	2.10	g/ cm ³

Water content	Mass of container, g	Mass of wet soil, g	Mass of dried soil , g	Water content, %
Top		130.34	114.7	13.6
Bottom				
			Average	13.6

At the end of the test

1. Final diameter of specimen		
Top		cm
Middle		cm
Bottom		cm
Average		
2. Final height of specimen	6.42	cm
3. Volume of specimen	0.00	cm ³
4. Water content of entire specimen		
a. Can no.	S5	
b. Mass of can	0	g
c. Mass of wet soil	130.34	g
d. Mass of dried soil	114.7	g
e. Mass of specimen	130.34	g
f. Mass of dried soil	114.7	g
g. Water content	13.6	%
5. Dry unit weight	1.84	g/cm ³
6. Specific gravity of soil (assumed)	2.66	g/cm ³
7. Void ratio	0.442	-
8. Degree of saturation	82.0	%

Triaxial compression data

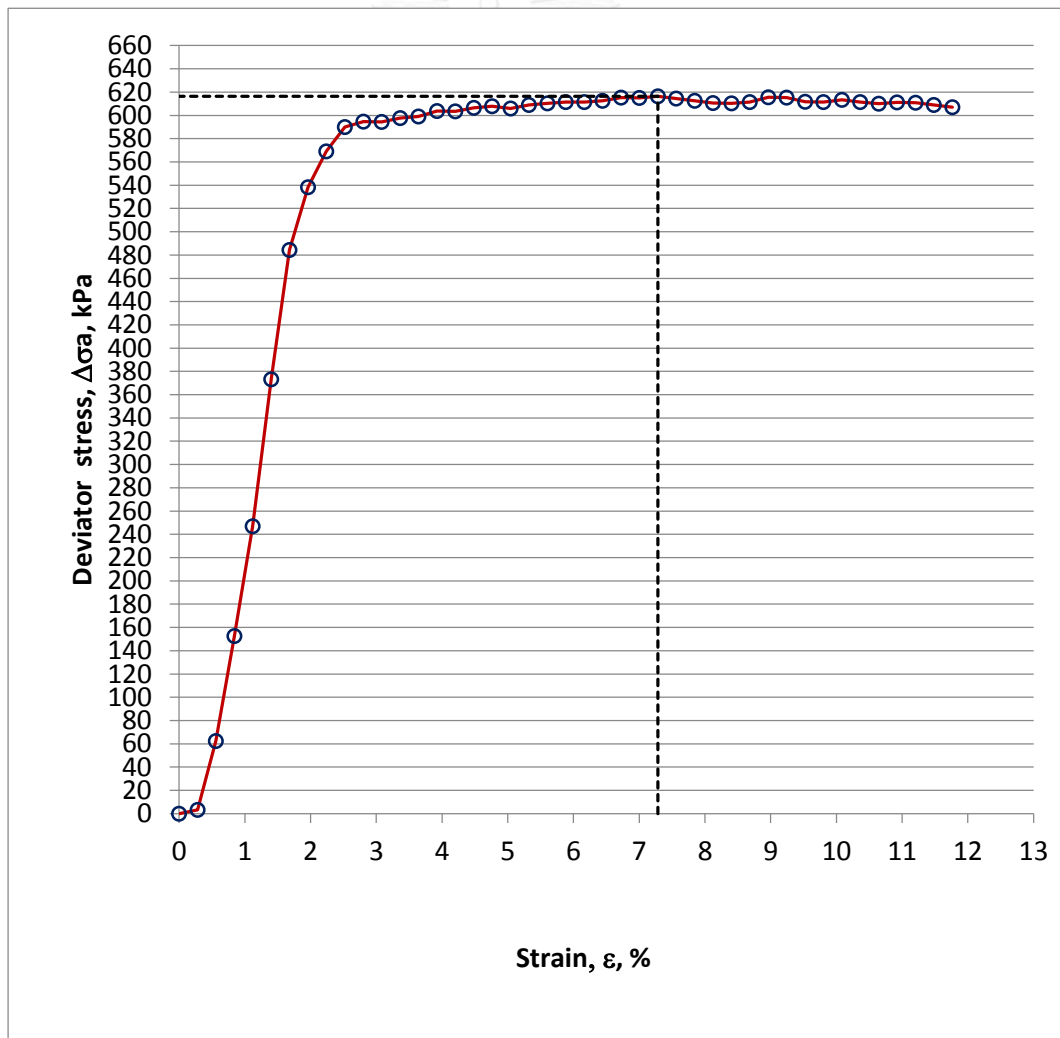
Cell pressure	200	kPa			
Rate of axial strain	0.064	mm/min			
Initial height of specimen	7.14	cm			
Area of specimen	8.71	cm ²			
Proving ring calibration	0.144	kg/div			
Deformation Dial, ΔL (cm)	Strain, ϵ %	Cross-section Area, A (cm ²)	Proving ring dial	Applied axial load, P (kg)	Stress, kPa
(1)			(4)	(5)=(4)x0.144	(6)=(5)/(3)
0	0	8.71	0	0	0
0.02	0.28	8.73	2	0.29	3.3
0.04	0.56	8.76	38	5.47	62.5
0.06	0.84	8.78	93	13.39	152.5
0.08	1.12	8.81	151	21.74	246.9

0.1	1.40	8.83	229	32.98	373.3
0.12	1.68	8.86	298	42.91	484.4
0.14	1.96	8.88	332	47.81	538.2
0.16	2.24	8.91	352	50.69	569.0
0.18	2.52	8.93	366	52.70	589.9
0.2	2.80	8.96	370	53.28	594.6
0.22	3.08	8.99	371	53.42	594.5
0.24	3.36	9.01	374	53.86	597.6
0.26	3.64	9.04	376	54.14	599.0
0.28	3.92	9.06	380	54.72	603.7
0.3	4.20	9.09	381	54.86	603.5
0.32	4.48	9.12	384	55.30	606.5
0.34	4.76	9.14	386	55.58	607.8
0.36	5.04	9.17	386	55.58	606.0
0.38	5.32	9.20	389	56.02	609.0
0.4	5.60	9.23	391	56.30	610.3
0.42	5.88	9.25	393	56.59	611.6
0.44	6.16	9.28	394	56.74	611.3
0.46	6.44	9.31	396	57.02	612.6
0.48	6.72	9.34	399	57.46	615.4
0.5	7.00	9.37	400	57.60	615.1
0.52	7.28	9.39	402	57.89	616.3
0.54	7.56	9.42	402	57.89	614.4
0.56	7.84	9.45	402	57.89	612.5
0.58	8.12	9.48	402	57.89	610.7
0.6	8.40	9.51	403	58.03	610.3
0.62	8.68	9.54	405	58.32	611.5
0.64	8.96	9.57	409	58.90	615.6
0.66	9.24	9.60	410	59.04	615.2
0.68	9.52	9.63	409	58.90	611.8
0.7	9.80	9.66	410	59.04	611.4
0.72	10.08	9.69	412.5	59.40	613.3
0.74	10.36	9.72	412.5	59.40	611.3
0.76	10.64	9.75	413	59.47	610.2
0.78	10.92	9.78	415	59.76	611.2
0.8	11.20	9.81	416	59.90	610.8
0.82	11.48	9.84	416	59.90	608.8
0.84	11.76	9.87	416	59.90	606.9

Minor principal
 stress, s_3 200 kPa
 Unit axial load at
 failure, Ds_1 616.3 kPa
 Major principal
 stress, s_1 816.27 kPa

s_3 , kPa	s_1 , kPa	C_u , kPa	e , %
200	816.27	308.1	7.28

Curve shown the relation between Strain and stress of sample BMRD3.2S5



Triaxial Compression Test (Unsolidated Undrained Test)

Sample No. **BMRD3.3-S7**

Boring No.

Location: *HaadSompan Village, Ranong Province*

Depth: *Topsoil-surface*

Description of sample: *Soft soil (weathered granite)*

Tested by: *Geotech lab, Civil department, CU*

Date: *Nov 3, 2015*

Specimen Data

At the beginning of test

1. Type of test performed	UU	
2. Type of specimen	Remold	
3. Diameter of specimen		
Top	3.33	cm
Middle	3.33	cm
Bottom	3.33	cm
4. Area of specimen	8.71	cm ²
5. Initial height of specimen	7.14	cm
6. Height to diameter ration	2.14	-
7. volume of specimen	62.18	cm ³
8. Mass of wet specimen	130.34	g
9. Unit weight of soil	2.10	g/cm ³

Water content	Mass of container, g	Mass of wet soil, g	Mass of dried soil , g	Water content, %
Top		130.31	115.12	13.19
Bottom				
			Average	13.19

At the end of test

1. Final diameter of specimen		
Top		cm
Middle		cm
Bottom		cm
Average		
2. Final height of specimen	6.42	cm
3. Volume of specimen	0.00	cm ³
4. Water content of entire specimen		
a. Can no.	S7	
b. Mass of can	0	g
c. Mass of wet soil	130.34	g
d. Mass of dried soil	115.12	g
e. Mass of specimen	130.34	g
f. Mass of dried soil	115.12	g
g. Water content	13.2	%
5. Dry unit weight	1.85	g/cm ³
6. Specific gravity of soil (assumed)	2.66	g/cm ³
7. Void ratio	0.437	-
8. Degree of saturation	80.5	%

Triaxial compression data

Cell pressure	300	kPa			
Rate of axial strain	0.064	mm/min			
Initial height of specimen	7.14	cm			
Area of specimen	8.71	cm ²			
Proving ring calibration	0.144	kg/div			
Deformation Dial, ΔL (cm)	Strain, ϵ %	Cross-section Area, A (cm ²)	Proving ring dial	Applied axial load, P (kg)	Stress, kPa
(1)			(4)	(5)=(4)x0.144	(6)=(5)/(3)
0	0	8.71	0	0	0
0.02	0.28	8.73	3	0.43	4.9
0.04	0.56	8.76	3	0.43	4.9
0.06	0.84	8.78	20	2.88	32.8
0.08	1.12	8.81	65	9.36	106.3

Deformation Dial, ΔL (cm)	Strain, ϵ %	Cross-section Area, A (cm ²)	Proving ring dial	Applied axial load, P (kg)	Stress, kPa
0.1	1.40	8.83	113	16.27	184.2
0.1	1.40	8.83	113	16.27	184.2
0.12	1.68	8.86	170	24.48	276.4
0.14	1.96	8.88	218	31.39	353.4
0.16	2.24	8.91	245	35.28	396.0
0.18	2.52	8.93	258	37.15	415.8
0.2	2.80	8.96	259	37.30	416.2
0.22	3.08	8.99	255	36.72	408.6
0.24	3.36	9.01	253	36.43	404.3
0.26	3.64	9.04	238	34.27	379.2
0.28	3.92	9.06	234	33.70	371.7
0.3	4.20	9.09	227	32.69	359.6
0.32	4.48	9.12	219	31.54	345.9
0.34	4.76	9.14	211	30.38	332.3
0.36	5.04	9.17	204	29.38	320.3

Minor principal

stress, s_3 300 kPa

Unit axial load at

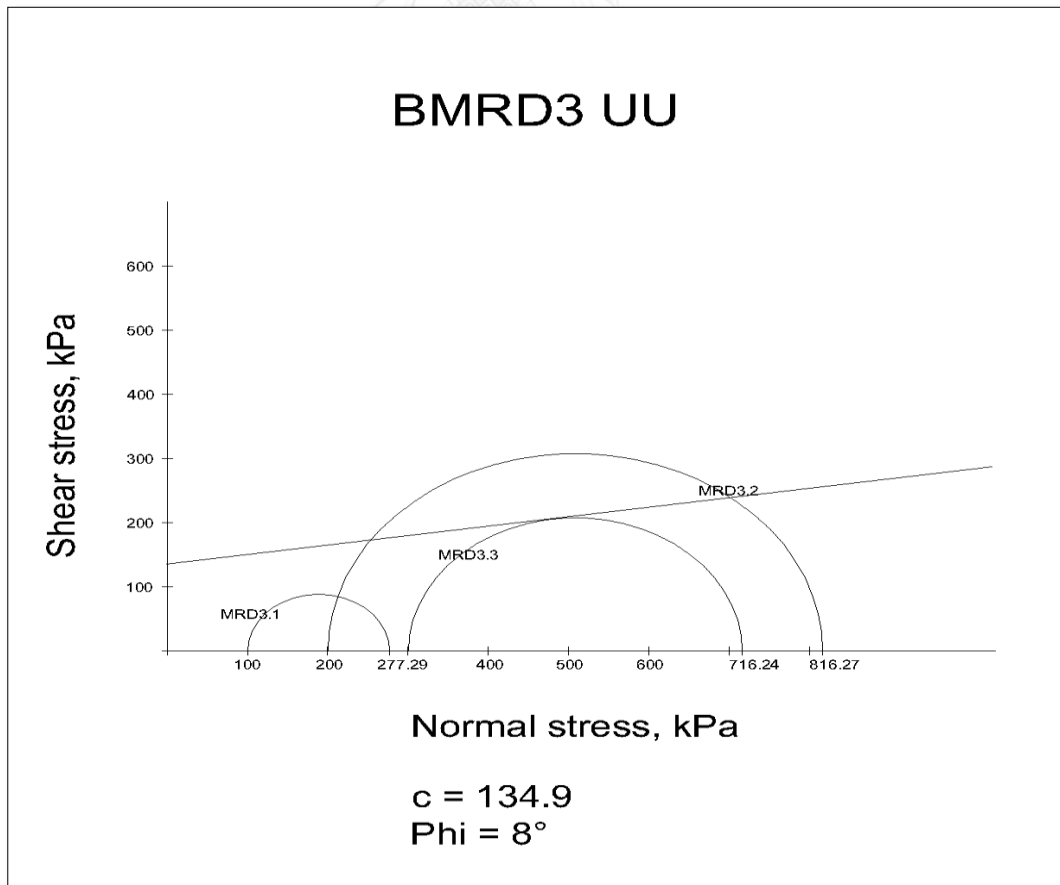
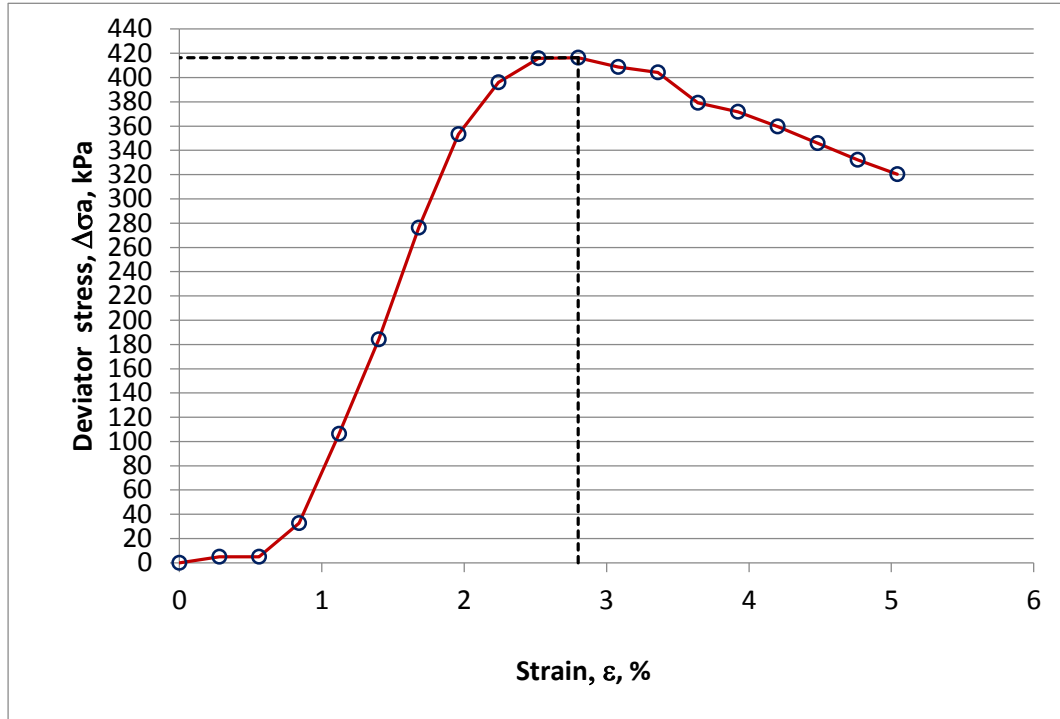
failure, D_{s1} 416.2 kPa

Major principal

stress, s_1 716.24 kPa

s_3 , kPa	s_1 , kPa	C_u , kPa	e , %
300	716.24	208.1	2.80

Curve shown the relation between Strain and stress of sample BMRD3.3S7



Triaxial Compression Test (Unsolidated Undrained Test)

Sample No. *BMRD4.1-S10*

Boring No.

Location: *HaadSompan Village, Ranong Province*

Depth: *Topsoil-surface*

Description of sample: *Soft soil (weathered granite)*

Tested by: *Geotech lab, Civil department, CU*

Date: *Nov 3, 2015*

Specimen Data

At the beginning of test

1. Type of test performed	UU	
2. Type of specimen	Remold	
3. Diameter of specimen		
Top	3.33	cm
Middle	3.33	cm
Bottom	3.33	cm
4. Area of specimen	8.71	cm ²
5. Initial height of specimen	7.14	cm
6. Height to diameter ration	2.14	-
7. volume of specimen	62.18	cm ³
8. Mass of wet specimen	130.31	g
9. Unit weight of soil	2.10	g/cm ³

Water content	Mass of container, g	Mass of wet soil, g	Mass of dried soil , g	Water content, %
Top		130.31	115.12	13.19
Bottom				
			Average	13.19

At the end of test

1. Final diameter of specimen		
Top		cm
Middle		cm
Bottom		cm
Average		
2. Final height of specimen	6.42	cm
3. Volume of specimen	0.00	cm ³
4. Water content of entire specimen		
a. Can no.	S10	
b. Mass of can	0	g
c. Mass of wet soil	130.31	g
d. Mass of dried soil	115.12	g
e. Mass of specimen	130.31	g
f. Mass of dried soil	115.12	g
g. Water content	13.2	%
5. Dry unit weight	1.85	g/cm ³
6. Specific gravity of soil (assumed)	2.66	g/cm ³
7. Void ratio	0.437	-
8. Degree of saturation	80.3	%

Triaxial compression data

Cell pressure	100	kPa			
Rate of axial strain	0.064	mm/min			
Initial height of specimen	7.14	cm			
Area of specimen	8.71	Cm ²			
Proving ring calibration	0.144	kg/div			
Deformation Dial, ΔL (cm)	Strain, ϵ %	Cross-section Area, A (cm ²)	Proving ring dial	Applied axial load, P (kg)	Stress, kPa
(1)			(4)	(5)=(4)x0.144	(6)=(5)/(3)
0	0	8.71	0	0	0
0.02	0.28	8.73	6	0.86	9.9
0.04	0.56	8.76	29	4.18	47.7
0.06	0.84	8.78	50	7.20	82.0
0.08	1.12	8.81	73	10.51	119.3

Deformation Dial, ΔL (cm)	Strain, ϵ %	Cross-section Area, A (cm ²)	Proving ring dial	Applied axial load, P (kg)	Stress, kPa
0.1	1.40	8.83	100	14.40	163.0
0.1	1.40	8.83	100	14.40	163.0
0.12	1.68	8.86	129	18.58	209.7
0.14	1.96	8.88	157	22.61	254.5
0.16	2.24	8.91	183	26.35	295.8
0.18	2.52	8.93	203	29.23	327.2
0.2	2.80	8.96	219	31.54	352.0
0.22	3.08	8.99	234	33.70	375.0
0.24	3.36	9.01	244	35.14	389.9
0.26	3.64	9.04	252	36.29	401.5
0.28	3.92	9.06	259.5	37.37	412.2
0.3	4.20	9.09	265	38.16	419.7
0.32	4.48	9.12	268	38.59	423.3
0.34	4.76	9.14	273	39.31	429.9
0.36	5.04	9.17	276	39.74	433.3
0.38	5.32	9.20	278	40.03	435.2
0.4	5.60	9.23	280.5	40.39	437.8
0.42	5.88	9.25	283.5	40.82	441.2
0.44	6.16	9.28	284.8	41.01	441.9
0.46	6.44	9.31	286	41.18	442.4
0.48	6.72	9.34	288	41.47	444.2
0.5	7.00	9.37	289.8	41.73	445.6
0.52	7.28	9.39	290.8	41.88	445.8
0.54	7.56	9.42	292	42.05	446.3
0.56	7.84	9.45	293.5	42.26	447.2
0.58	8.12	9.48	294.7	42.44	447.7
0.6	8.40	9.51	295.4	42.54	447.4
0.62	8.68	9.54	296.7	42.72	448.0
0.64	8.96	9.57	297	42.77	447.0
0.66	9.24	9.60	299	43.06	448.7
0.68	9.52	9.63	300	43.20	448.8

Unit axial load at

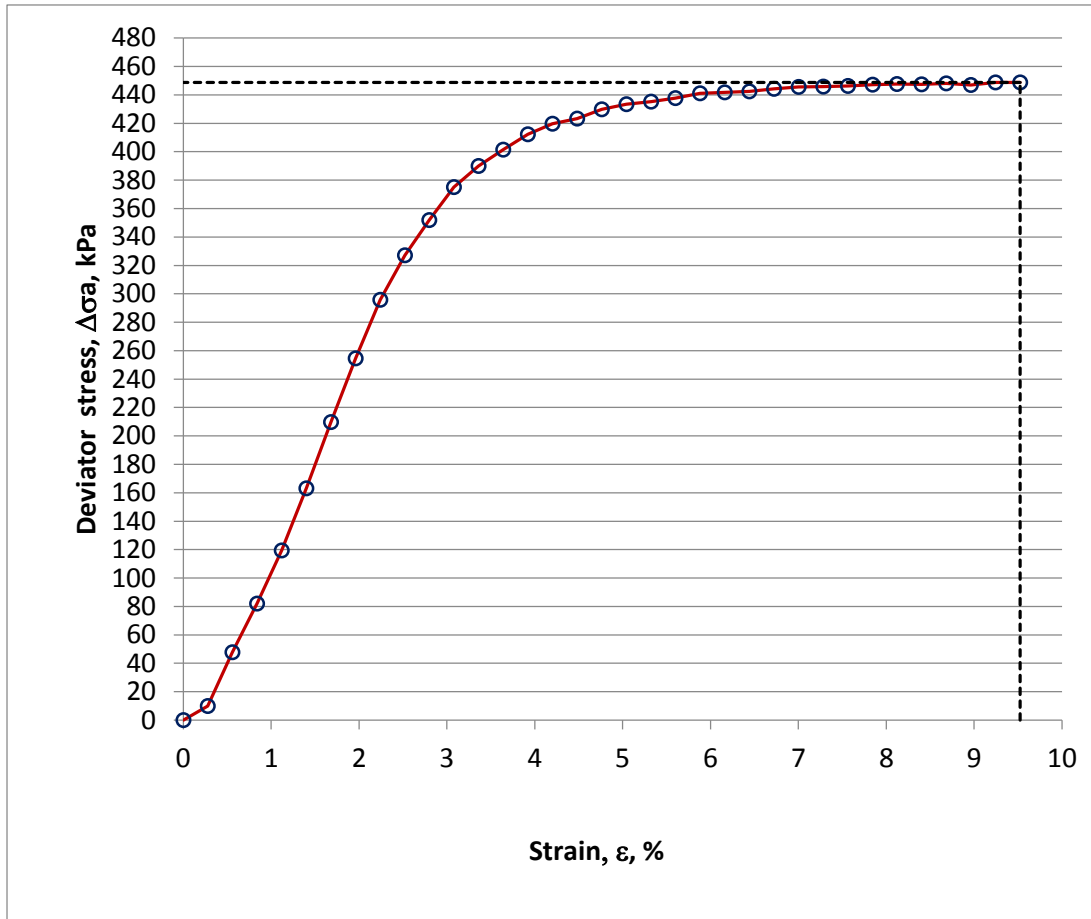
failure, Ds_1 448.8 kPa

Major principal

stress, s_1 548.79 kPa

s_3 , kPa	s_1 , kPa	C_u , kPa	e , %
100	548.79	224.4	9.52

Curve shown the relation between Strain and stress of sample BMRD4.1S10



Triaxial Compression Test (Unsolidated Undrained Test)

Sample No. *BMRD4.2-S11*

Boring No.

Location: *HaadSompan Village, Ranong Province*

Depth: *Topsoil-surface*

Description of sample: *Soft soil (weathered granite)*

Tested by: *Geotech lab, Civil department, CU*

Date: *Nov 3, 2015*

Specimen Data

At the beginning of test

1. Type of test performed	UU	
2. Type of specimen	Remold	
3. Diameter of specimen		
Top	3.33	cm
Middle	3.33	cm
Bottom	3.33	cm
4. Area of specimen	8.71	cm ²
5. Initial height of specimen	7.14	cm
6. Height to diameter ration	2.14	-
7. volume of specimen	62.18	cm ³
8. Mass of wet specimen	130.27	g
9. Unit weight of soil	2.09	g/cm ³

Water content	Mass of container, g	Mass of wet soil, g	Mass of dried soil , g	Water content, %
Top		130.31	112.19	16.15
Bottom				
			Average	16.15

At the end of test

1. Final diameter of specimen		
Top		cm
Middle		cm
Bottom		cm
Average		
2. Final height of specimen	6.42	cm
3. Volume of specimen	0.00	cm ³
4. Water content of entire specimen		
a. Can no.	S11	
b. Mass of can	0	g
c. Mass of wet soil	130.27	g
d. Mass of dried soil	112.19	g
e. Mass of specimen	130.27	g
f. Mass of dried soil	112.19	g
g. Water content	16.1	%
5. Dry unit weight	1.80	g/cm ³
6. Specific gravity of soil (assumed)	2.66	g/cm ³
7. Void ratio	0.474	-
8. Degree of saturation	90.4	%

Triaxial compression data

Cell pressure	200	kPa			
Rate of axial strain	0.064	mm/min			
Initial height of specimen	7.14	cm			
Area of specimen	8.71	cm ²			
Proving ring calibration	0.144	kg/div			
Deformation Dial, ΔL (cm)	Strain, ϵ %	Cross-section Area, A (cm ²)	Proving ring dial	Applied axial load, P (kg)	Stress, kPa
(1)			(4)	(5)=(4)x0.144	(6)=(5)/(3)
0	0	8.71	0	0	0
0.02	0.28	8.73	3	0.43	4.9
0.04	0.56	8.76	4	0.58	6.6
0.06	0.84	8.78	25	3.60	41.0

Deformation Dial, ΔL (cm)	Strain, ϵ %	Cross-section Area, A (cm ²)	Proving ring dial	Applied axial load, P (kg)	Stress, kPa
0.08	1.12	8.81	57	8.21	93.2
0.08	1.12	8.81	57	8.21	93.2
0.1	1.40	8.83	82	11.81	133.7
0.12	1.68	8.86	114	16.42	185.3
0.14	1.96	8.88	143	20.59	231.8
0.16	2.24	8.91	175	25.20	282.9
0.18	2.52	8.93	204	29.38	328.8
0.2	2.80	8.96	225	32.40	361.6
0.22	3.08	8.99	239	34.42	383.0
0.24	3.36	9.01	247	35.57	394.7
0.26	3.64	9.04	254	36.58	404.7
0.28	3.92	9.06	257	37.01	408.3
0.3	4.20	9.09	263	37.87	416.6
0.32	4.48	9.12	282	40.61	445.4
0.34	4.76	9.14	283	40.75	445.6
0.36	5.04	9.17	283	40.75	444.3
0.38	5.32	9.20	284	40.90	444.6
0.4	5.60	9.23	282	40.61	440.1
0.42	5.88	9.25	278	40.03	432.6
0.44	6.16	9.28	274	39.46	425.1
0.46	6.44	9.31	269	38.74	416.1

Minor principal

stress, s_3 200 kPa

Unit axial load at

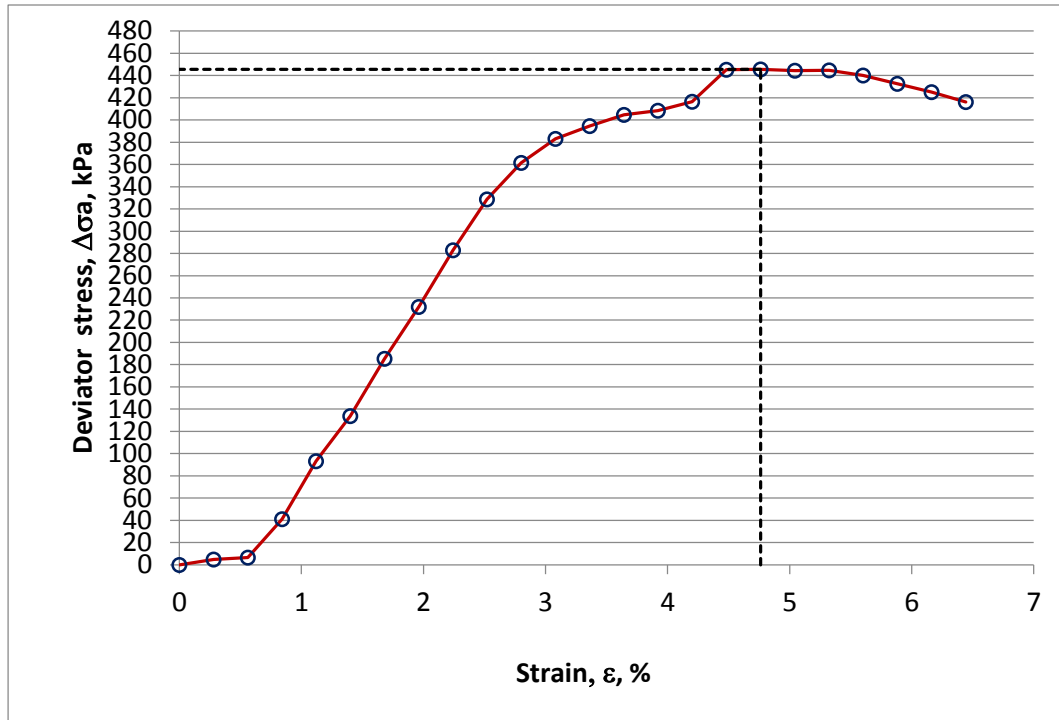
failure, Ds_1 445.6 kPa

Major principal

stress, s_1 645.64 kPa

s_3 , kPa	s_1 , kPa	C_u , kPa	e , %
200	645.64	222.8	4.76

Curve shown the relation between Strain and stress of sample BMRD4.2S11



Triaxial Compression Test (Unsolidated Undrained Test)

Sample No. *BMRD4.3-S12*

Boring No.

Location: *HaadSompan Village, Ranong Province*

Depth: *Topsoil-surface*

Description of sample: *Soft soil (weathered granite)*

Tested by: *Geotech lab, Civil department, CU*

Date: *Nov 3, 2015*

Specimen Data

At the beginning of test

1. Type of test performed	UU	
2. Type of specimen	Remold	
3. Diameter of specimen		
Top	3.33	cm
Middle	3.33	cm
Bottom	3.33	cm
4. Area of specimen	8.71	cm ²
5. Initial height of specimen	7.14	cm
6. Height to diameter ration	2.14	-
7. volume of specimen	62.18	cm ³
8. Mass of wet specimen	131.24	g
9. Unit weight of soil	2.11	g/cm ³

Water content	Mass of container, g	Mass of wet soil, g	Mass of dried soil , g	Water content, %
Top		130.31	116.88	11.49
Bottom				
			Average	11.49

At the end of test

1. Final diameter of specimen		
Top		cm
Middle		cm
Bottom		cm
Average		
2. Final height of specimen	6.42	cm
3. Volume of specimen	0.00	cm ³
4. Water content of entire specimen		
a. Can no.	S12	
b. Mass of can	0	g
c. Mass of wet soil	131.24	g
d. Mass of dried soil	116.88	g
e. Mass of specimen	131.24	g
f. Mass of dried soil	116.88	g
g. Water content	12.3	%
5. Dry unit weight	1.88	g/cm ³
6. Specific gravity of soil (assumed)	2.66	g/cm ³
7. Void ratio	0.415	-
8. Degree of saturation	78.7	%

Triaxial compression data

Cell pressure	300	kPa			
Rate of axial strain	0.064	mm/min			
Initial height of specimen	7.14	cm			
Area of specimen	8.71	cm ²			
Proving ring calibration	0.144	kg/div			
Deformation Dial, ΔL (cm)	Strain, ϵ %	Cross-section Area, A (cm ²)	Proving ring dial	Applied axial load, P (kg)	Stress, kPa
(1)			(4)	(5)=(4)x0.144	(6)=(5)/(3)
0	0	8.71	0	0	0
0.02	0.28	8.73	50	7.20	82.4
0.04	0.56	8.76	73	10.51	120.0
0.06	0.84	8.78	95	13.68	155.8
0.08	1.12	8.81	106	15.26	173.3

Deformation Dial, ΔL (cm)	Strain, ϵ %	Cross-section Area, A (cm ²)	Proving ring dial	Applied axial load, P (kg)	Stress, kPa
0.1	1.40	8.83	132	19.01	215.2
0.1	1.40	8.83	132	19.01	215.2
0.12	1.68	8.86	144	20.74	234.1
0.14	1.96	8.88	153	22.03	248.0
0.16	2.24	8.91	160	23.04	258.6
0.18	2.52	8.93	162	23.33	261.1
0.2	2.80	8.96	164	23.62	263.6
0.22	3.08	8.99	164	23.62	262.8
0.24	3.36	9.01	161	23.18	257.3
0.26	3.64	9.04	158.3	22.80	252.2
0.28	3.92	9.06	156	22.46	247.8
0.3	4.20	9.09	153.8	22.15	243.6
0.32	4.48	9.12	150	21.60	236.9
0.34	4.76	9.14	145	20.88	228.3
0.36	5.04	9.17	141	20.30	221.4
0.38	5.32	9.20	136.5	19.66	213.7

Unit axial load at

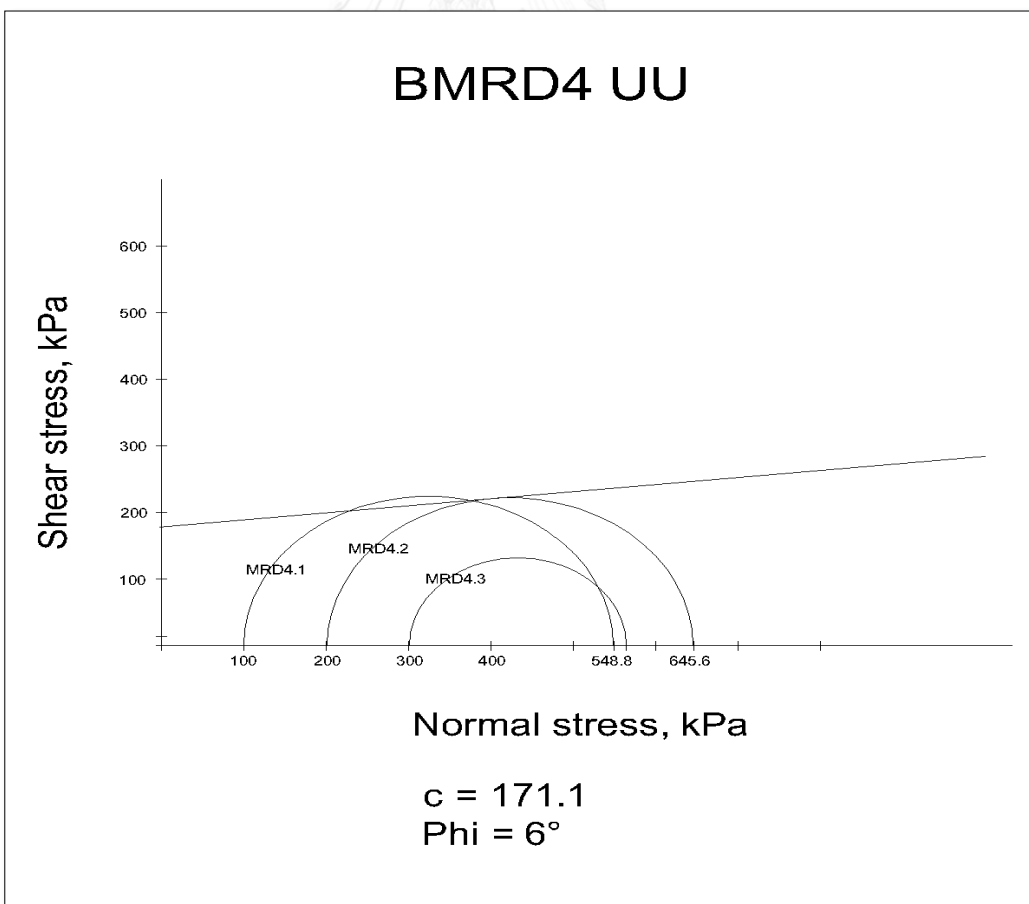
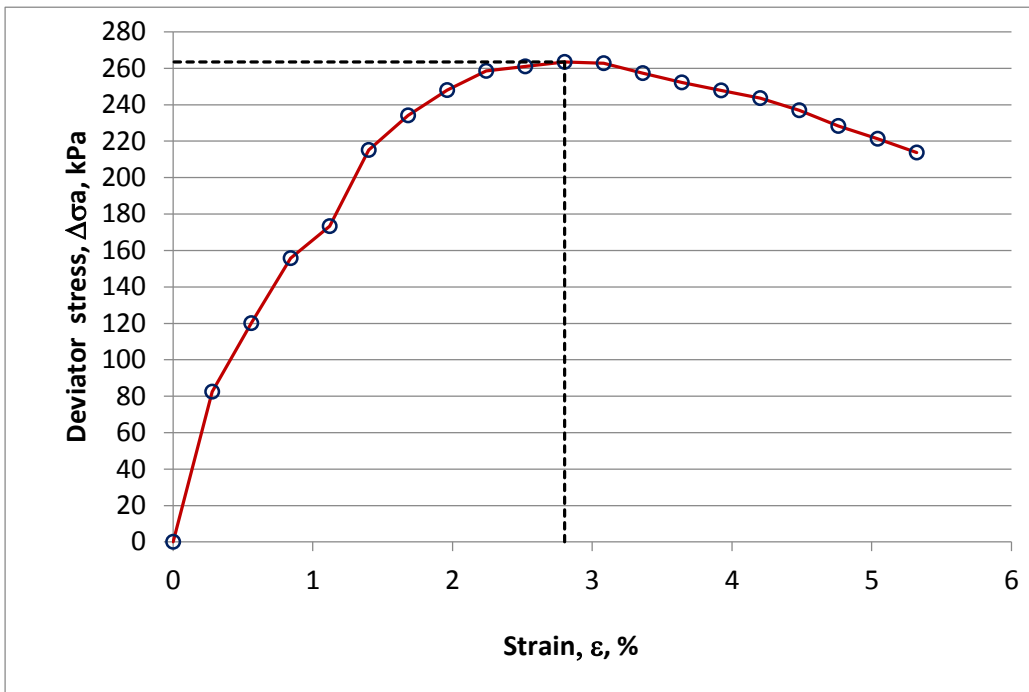
failure, Ds_1 263.6 kPa

Major principal

stress, s_1 563.57 kPa

s_3 , kPa	s_1 , kPa	C_u , kPa	e , %
300	563.57	131.8	2.80

Curve shown the relation between Strain and stress of sample BMRD4.23S12





APPENDIX VI

Command used in FLAC3D for solved FOS

จุฬาลงกรณ์มหาวิทยาลัย
CHULALONGKORN UNIVERSITY

Command used in Final Pit slope design analysis

```

; 1. Evaluate Fos for new geometry BMRD-01
model mech mohr
prop dens 1800 range group 'weathered granite'
prop dens 2650 range group 'Hard granite'
prop bulk 6e7 shear 3.3e8 ten 0.2e6 cohesion 21.2e3 friction 26.2 range
group 'weathered granite'
prop bulk 1.17e10 shear 4.38e10 ten 20e6 cohesion 1e7 friction 58.5 range
group 'Hard granite'
fix x range x 0
fix x range x 100
fix y range y 0
fix y range y 1
fix z range z 0
set gravity 0 0 -9.81
solve fos
; 2. Evaluate Fos for new geometry BMRD-01
model mech mohr
prop dens 1800 range group 'weathered granite'
prop dens 2650 range group 'Hard granite'
prop bulk 6e7 shear 3.3e8 ten 0.2e6 cohesion 116e3 friction 4 range group
'weathered granite'
prop bulk 1.17e10 shear 4.38e10 ten 20e6 cohesion 1e7 friction 58.5 range
group 'Hard granite'
fix x range x 0
fix x range x 100
fix y range y 0
fix y range y 1
fix z range z 0
set gravity 0 0 -9.81
solve fos
; 3. Evaluate Fos for new geometry BMRD-01
model mech mohr
prop dens 1800 range group 'weathered granite'
prop dens 2650 range group 'Hard granite'
prop bulk 6e7 shear 3.3e8 ten 0.2e6 cohesion 37e3 friction 21 range group
'weathered granite'
prop bulk 1.17e10 shear 4.38e10 ten 20e6 cohesion 1e7 friction 58.5 range
group 'Hard granite'
fix x range x 0
fix x range x 100
fix y range y 0
fix y range y 1
fix z range z 0
set gravity 0 0 -9.81
solve fos
; 4. Evaluate Fos for new geometry BMRD-01
model mech mohr
prop dens 1800 range group 'weathered granite'
prop dens 2650 range group 'Hard granite'
prop bulk 6e7 shear 3.3e8 ten 0.2e6 cohesion 50e3 friction 27 range group
'weathered granite'
prop bulk 1.17e10 shear 4.38e10 ten 20e6 cohesion 1e7 friction 58.5 range
group 'Hard granite'
fix x range x 0
fix x range x 100
fix y range y 0
fix y range y 1
fix z range z 0
set gravity 0 0 -9.81

```

```

solve fos
; 5. Evaluate FoS for new geometry BMRD-02
model mech mohr
prop dens 1800 range group 'weathered granite'
prop dens 2650 range group 'Hard granite'
prop bulk 6e7 shear 3.3e8 ten 0.2e6 cohesion 31.1e3 friction 24.8 range
group 'weathered granite'
prop bulk 1.17e10 shear 4.38e10 ten 20e6 cohesion 1e7 friction 58.5 range
group 'Hard granite'
fix x range x 0
fix x range x 100
fix y range y 0
fix y range y 1
fix z range z 0
set gravity 0 0 -9.81
solve fos
; 6. Evaluate FoS for new geometry BMRD-02
model mech mohr
prop dens 1800 range group 'weathered granite'
prop dens 2650 range group 'Hard granite'
prop bulk 6e7 shear 3.3e8 ten 0.2e6 cohesion 124e3 friction 3 range group
'weathered granite'
prop bulk 1.17e10 shear 4.38e10 ten 20e6 cohesion 1e7 friction 58.5 range
group 'Hard granite'
fix x range x 0
fix x range x 100
fix y range y 0
fix y range y 1
fix z range z 0
set gravity 0 0 -9.81
solve fos
; 7. Evaluate FoS for new geometry BMRD-02
model mech mohr
prop dens 1800 range group 'weathered granite'
prop dens 2650 range group 'Hard granite'
prop bulk 6e7 shear 3.3e8 ten 0.2e6 cohesion 43e3 friction 25 range group
'weathered granite'
prop bulk 1.17e10 shear 4.38e10 ten 20e6 cohesion 1e7 friction 58.5 range
group 'Hard granite'
fix x range x 0
fix x range x 100
fix y range y 0
fix y range y 1
fix z range z 0
set gravity 0 0 -9.81
solve fos
; 8. Evaluate FoS for new geometry BMRD-02
model mech mohr
prop dens 1800 range group 'weathered granite'
prop dens 2650 range group 'Hard granite'
prop bulk 6e7 shear 3.3e8 ten 0.2e6 cohesion 54e3 friction 30 range group
'weathered granite'
prop bulk 1.17e10 shear 4.38e10 ten 20e6 cohesion 1e7 friction 58.5 range
group 'Hard granite'
fix x range x 0
fix x range x 100
fix y range y 0
fix y range y 1
fix z range z 0
set gravity 0 0 -9.81
solve fos

```

```

; 9. Evaluate FoS for new geometry BMRD-03
model mech mohr
prop dens 1800 range group 'Weathered granite'
prop dens 2650 range group 'Hard granite'
prop bulk 6e7 shear 3.3e8 ten 0.2e6 cohesion 13.9e3 friction 28.5 range
group 'Weathered granite'
prop bulk 1.17e10 shear 4.38e10 ten 20e6 cohesion 1e7 friction 58.5 range
group 'Hard granite'
fix x range x 0
fix x range x 100
fix y range y 0
fix y range y 1
fix z range z 0
set gravity 0 0 -9.81
solve fos
; 10. Evaluate FoS for new geometry BMRD-03
model mech mohr
prop dens 1800 range group 'Weathered granite'
prop dens 2650 range group 'Hard granite'
prop bulk 6e7 shear 3.3e8 ten 0.2e6 cohesion 134.9e3 friction 8 range group
'Weathered granite'
prop bulk 1.17e10 shear 4.38e10 ten 20e6 cohesion 1e7 friction 58.5 range
group 'Hard granite'
fix x range x 0
fix x range x 100
fix y range y 0
fix y range y 1
fix z range z 0
set gravity 0 0 -9.81
solve fos
; 11. Evaluate FoS for new geometry BMRD-04
model mech mohr
prop dens 1800 range group 'Weathered granite'
prop dens 2650 range group 'Hard granite'
prop bulk 6e7 shear 3.3e8 ten 0.2e6 cohesion 13.7e3 friction 57.6 range
group 'Weathered granite'
prop bulk 1.17e10 shear 4.38e10 ten 20e6 cohesion 1e7 friction 58.5 range
group 'Hard granite'
fix x range x 0
fix x range x 100
fix y range y 0
fix y range y 1
fix z range z 0
set gravity 0 0 -9.81
solve fos
; 12. Evaluate FoS for new geometry BMRD-04
model mech mohr
prop dens 1800 range group 'Weathered granite'
prop dens 2650 range group 'Hard granite'
prop bulk 6e7 shear 3.3e8 ten 0.2e6 cohesion 178.1e3 friction 6 range group
'Weathered granite'
prop bulk 1.17e10 shear 4.38e10 ten 20e6 cohesion 1e7 friction 58.5 range
group 'Hard granite'
fix x range x 0
fix x range x 100
fix y range y 0
fix y range y 1
fix z range z 0
set gravity 0 0 -9.81
solve fos

```


→ The analysis of cross-section for each model used the same GMP, change only the dimension of model as show two case below

Command Used in Model A

```
; 9. Evaluate FoS for new geometry BMRD-03
model mech mohr
prop dens 1800 range group 'weathered granite'
prop dens 2650 range group 'Hard granite'
prop bulk 6e7 shear 3.3e8 ten 0.2e6 cohesion 13.9e3 friction 28.5 range
group 'weathered granite'
prop bulk 1.17e10 shear 4.38e10 ten 20e6 cohesion 1e7 friction 58.5 range
group 'Hard granite'
fix x range x 0
fix x range x 100
fix y range y 0
fix y range y 1
fix z range z 0
set gravity 0 0 -9.81
solve fos
```

Command Used in Model A'

```
; 9. Evaluate FoS for new geometry BMRD-03
model mech mohr
prop dens 1800 range group 'weathered granite'
prop dens 2650 range group 'Hard granite'
prop bulk 6e7 shear 3.3e8 ten 0.2e6 cohesion 13.9e3 friction 28.5 range
group 'weathered granite'
prop bulk 1.17e10 shear 4.38e10 ten 20e6 cohesion 1e7 friction 58.5 range
group 'Hard granite'
fix x range x 0
fix x range x 200
fix y range y 0
fix y range y 1
fix z range z 0
set gravity 0 0 -9.81
solve fos
```

→ The analysis of assuming bench height and slope angle used the same GMP,
change only the model dimension as two case example below:

Case 1

```
; 9. Evaluate FoS for new geometry BMRD-03
model mech mohr
prop dens 1800
prop bulk 6e7 shear 3.3e8 ten 0.2e6 cohesion 13.9e3 friction 28.5
fix x range x 0
fix x range x 50
fix y range y 0
fix y range y 1
fix z range z 0
set gravity 0 0 -9.81
solve fos
```

Case 2

```
; 9. Evaluate FoS for new geometry BMRD-03
model mech mohr
prop dens 1800
prop bulk 6e7 shear 3.3e8 ten 0.2e6 cohesion 13.9e3 friction 28.5
fix x range x 0
fix x range x 120
fix y range y 0
fix y range y 1
fix z range z 0
set gravity 0 0 -9.81
solve fos
```

VITA

Somboun Vang

Email: sbvang999@gmail.com

PERSONAL DATA:

Nationality : Lao

Marital Status : Married

Date of birth : 24 Nov 1987

Place of birth : Vientiane Province

EDUCATION/QUALIFICATION

2014 – Present: study Master degree of Georesources Engineering at Chulalongkorn University.

2009 – 2014: study Bachelor degree of Mining Engineering at National University of Laos.

จุฬาลงกรณ์มหาวิทยาลัย
CHULALONGKORN UNIVERSITY